SCHOOL OF ELECTRICAL AND ELECTRONIC ENGINEERING
ELECTRICAL POWER RESEARCH GROUP

EVALUATION OF ADVANCED VOLTAGE CONTROL ALGORITHMS FOR FUTURE SMART DISTRIBUTION NETWORKS

A THESIS PRESENTED FOR THE DEGREE OF DOCTOR OF PHILOSOPHY

PENGFEI WANG
December 2015

Abstract

The UK government aims to reduce the UK's carbon emission by at least 80% by 2050. To achieve this ambitious target, large quantities of renewable energy generation are being connected to UK power networks. Moreover, with the trend towards electrification of heat and transport, electric vehicles and heat pumps are expected to proliferate in future networks. These low carbon technologies (LCTs) are being connected to distribution networks, which results in voltage issues that cannot be catered for with the existing infrastructure.

Smart grid technologies provide a flexible, economic solution to facilitate the integration of LCTs. Advanced voltage control algorithms are required to fully utilize future smart distribution networks' capability to mitigate voltage problems and to enhance the network performance. In this PhD study, three different voltage control algorithms have been developed, evaluated and contrasted. A cost effective rule-based based voltage control algorithm is initially proposed to mitigate the voltage problems due to LCT integration. This algorithm is evaluated with simulation and power hardware-in-the-loop emulation. An algorithm from a state-of-the-art distribution management system (DMS) is accurately modelled and extended to solve more complicated voltage control problems. This algorithm is validated against the field trial results in the real distribution networks, in which the DMS is deployed. Finally, an algorithm based on a novel metaheuristic algorithm, Cuckoo Search via Lévy Flights, is developed. The last two algorithms are evaluated and compared with various test cases, which represent different, challenging network scenarios and control preferences for current and future distribution networks.

Evaluation results demonstrate that these algorithms can be utilized for voltage control in future smart distribution networks. Furthermore, these algorithms are compared and the salient characteristics of these developed algorithms are summarized. The findings from this research provide useful information when deploying advanced voltage control algorithms for future smart distribution networks.

Declaration

I hereby declare that this thesis is a record of work undertaken by myself, that it has not been the subject of any previous application for a degree, and that all sources of information have been duly acknowledged.

Acknowledgements

I would like to express my gratitude to my supervisors, Professor Phil Taylor and Dr Padraig Lyons, for giving me the chance to pursue a PhD, and for all their excellent support and inspiration during my PhD Study.

I would like to thank Northern Powergrid for funding my PhD study, and all the colleagues from the Customer-Led Network Revolution project. Special thanks to Ian Lloyd, Rosie Hetherington from Northern Powergrid.

I would like to thank Dr Neal Wade, Dr Mansoureh Zangiabadi, Dr Simon Blake and all the staff from the power system group, for their inspiration and advices on my research. I would like to thank all my friends. Specially, I would like to thank Dr Lorna Bang, Jialiang Yi, Dr Tianxiang Jiang, Lei Wang and Jin Chen, Zhiqiang Liao and Dr Zemin Chen for all the happy moments we shared together.

I would like to thank my parents, my mother in law and all the others from the family, for their support and patience, especially Pengyong Wang, who always takes care of my parents when I am abroad.

Above all, I want to thank my wife, Dr Yanchao Li, for her love and support during this long journey.

List of Publications

P. Wang, D. H. Liang, J. Yi, P. F. Lyons, P. J. Davison, P. C. Taylor, "Integrating Electrical Energy Storage Into Coordinated Voltage Control Schemes for Distribution Networks", in Smart Grid, IEEE Transactions on , vol.5, no.2, pp.1018-1032, March 2014

P. Wang, J. Yi, P. F. Lyons, D. H. Liang, P. C. Taylor, D. Miller, J. Baker, "Customer-led Network Revolution — Integrating renewable energy into LV networks using energy storage," in Integration of Renewables into the Distribution Grid, CIRED 2012 Workshop , vol., no., pp.1-4, 29-30 May 2012

J. Yi, **P. Wang**, P. C. Taylor, P. J. Davison, P. F. Lyons, D. H. Liang, S. Brown, D. Roberts, "Distribution network voltage control using energy storage and demand side response," in Innovative Smart Grid Technologies (ISGT Europe), 2012 3rd IEEE PES International Conference and Exhibition on , vol., no., pp.1-8, 14-17 Oct. 2012

J. Yi, P. F. Lyons, P. J. Davison, **P. Wang**, P. C. Taylor, "Robust Scheduling Scheme for Energy Storage to Facilitate High Penetration of Renewables", Sustainable Energy, IEEE Transactions on, (accepted for publication), 2015

P. Wang, T. Jiang, P. F. Lyons, J. Yi, "Tapchanging Secondary Transformer Autonomous and GUS Voltage Control", CLNR report, 2014

P. Wang, P. F. Lyons, "HV Regulator Autonomous and Single and GUS Voltage Control", CLNR report, 2014

P. Wang, P. F. Lyons, "CLNR Trial Analysis Capacitor Bank Autonomous and Single+GUS Voltage Control", CLNR report, 2014

P. F. Lyons, T. Jiang, **P. Wang**, J. Yi, "Analysis of Collaborative Voltage Control on HV and LV networks", CLNR report, 2014

T. Jiang, P. F. Lyons, **P. Wang**, J. Yi, "Electrical Energy Storage 2 (100kVA/200kWh) Powerflow Management CLNR Trial Analysis", CLNR report, 2014

T. Jiang, S. Blake, P. F. Lyons, **P. Wang**, J. Yi, "CLNR Post Trial Analysis EES2 and EES3 GUS Powerflow Management", CLNR report, 2014

Acronyms

Acronym	Definition
ASHP	Air source heat pump
AVC	Automatic voltage control
CBR	Case based reasoning
CLNR	Customer-led network revolution
CLASS	Customer load active system services
COP	Coefficient of performance
CS	Cuckoo search
CTC	Conventional test case
DC	Direct current
DG	Distributed generation
DMS	Distribution management system
DNO	Distribution network operator
DSSE	Distribution system state estimator
D-STATCOM	Distribution static synchronous compensator
EES	Electrical energy storage
EPSO	Evolutionary particle swarm optimisation
EV	Electric vehicle
FACTS	Flexible alternating current transmission system
FTC	Future test case
FVDF	Feeder voltage divergence factor
GA	Genetic algorithm
GUS	Grand unified scheme
ICT	Information and communication technology
LCT	Low carbon technology
LV	Low-voltage
MINLP	Mixed integer nonlinear programming
MOCS	Multi-objective cuckoo search algorithm
MSC	Mechanically switched capacitor
MV	Medium voltage
NPG	Northern powergrid
NSGA-II	Non-dominated sorting genetic algorithm ii
ODCDM	Oriented discrete coordinate descent method
Ofgem	Office of gas and electricity markets
OLTC	On load tap changer
OPF	Optimal power flow
PDIP	Primal-dual interior point algorithm
PHIL	Power hardware in the loop
PSO	Particle swarm optimisation
PV	Photovoltaics
RRPF	Ratio of the reference point found
RTDS	Real time digital simulator
RTU	Remote terminal unit
SCADA	Supervisory control and data acquisition
SOC	State of charge

SOCS	Single-objective cuckoo search algorithm
SP	Starting point
STATCOM	Static synchronous compensator
UK	United kingdom
VCSF	Voltage cost sensitivity factor
VSF	Voltage sensitivity factors
VUF	Voltage unbalance factor
VVC	Voltage var control

Nomenclature

Symbol	Definition	Unit
$\underline{I}$	Current flowing from the sending end to the receiving end	(A)
$\underline{V}_1$	Voltage at the sending end	(V)
$\underline{V}_2$	Voltage at the receiving end	(V)
R	Resistance of the branch between the sending end and the load	(Ω)
X	Reactance of the branch between the sending end and the load	(Ω)
$\underline{\hat{S}}$	Complex conjugate of the apparent power of the load	(VA)
$\underline{\hat{V}}_2$	Complex conjugate of the load voltage	(V)
P_L	Real power of the load	(W)
Q_L	Reactive power of the load	(VAr)
ΔV	Voltage change from the sending end voltage to the receiving end voltage	(V)
δ	Voltage angle between the sending end voltage to the receiving end voltage	(Radian)
P_G	Real power injected by the DG	(W)
Q_G	Reactive power injected by the DG	(VAr)
V_{pri}	Voltage at the primary side of OLTC	(V)
V_{Sec}	Voltage at the secondary side of OLTC	(V)
N_{pri}	Transformer winding number at the primary side	(no unit)
N_{Sec}	Transformer winding number at the primary side	(no unit)
k	Winding number change of the OLTC	(%)
Q_{MSC}	Reactive power injected by the MSC	(VAr)
f	Network frequency	(Hz)
C_{MSC}	Capacitance of the MSC capacitor	(F)
V_{MSC}	Voltage at the MSC	(V)
$\mathbf{x}$	Vector of state variables	(no unit)
$\mathbf{u}$	Vector of control variables	(no unit)
$\boldsymbol{f}(\bullet)$	Optimisation objective function(s)	(no unit)
$\boldsymbol{g}(\bullet)$	Equality constraints	(no unit)
$\boldsymbol{h}(\bullet)$	Inequality constraints	(no unit)
T	Time for control scheduling	(h)
%VUF	Percentage voltage unbalance factor	(%)
$\Delta\theta_i$	Voltage phase angle change of busbar i	(Radian)
ΔV_i	Voltage magnitude change of busbar i	(V)
$\boldsymbol{J}^{\boldsymbol{1}}$	Jacobian matrix	(no unit)
ΔP_i	Real power change of busbar i	(W)

ΔQ_i	Reactive power change of busbar i	(VAr)
$C_{P,\,EES}$	Cost of operating EES real power	(£/kW)
$C_{Capital,\,EES}$	Capital cost of EES	(£)
N_{EES}	Total charge and discharge cycles of EES	(no unit)
$P_{Rating,\,EES}$	Real power rating of EES	(kW)
SOC_T	Target state-of-charge (SOC) of battery	(%)
SOC	State-of-charge (SOC) of battery	(%)
$C_{Q,\,EES}$	Cost of operating the EES reactive power	(£/kVAr)
$C_{Capital,\,Converter}$	Capital cost of converter system of the EES	(£)
$Q_{Rating,\,EES}$	Reactive power rating of EES	(kVAr)
$T_{Lifespan}$	Expected lifespan of converter	(min)
$T_{Control\ cycle}$	Control cycle	(min)
$N_{\mathrm{OLTC,\,Remaining}}$	Remaining operation times of the tapchanger	(no unit)
$N_{\mathrm{OLTC,\,Total}}$	Estimated total operation times of the tapchanger	(no unit)
$LS_{\mathrm{OLTC,\,Remaining}}$	Remaining lifespan of the tapchanger	(min)
$LS_{\mathrm{OLTC,\,Total}}$	Total lifespan of the tapchanger	(min)
C_{OLTC}	Cost of OLTC tap operation	(£)
$C_{\mathrm{OLTC\ Replacement}}$	Cost of replacing the tapchanger	(£)
$VCSF_{ij}$	Voltage cost sensitivity factor of device *j* to node *i*	(pu/£)
ΔV_{ij}	Voltage change at node *i* caused by device *j*	(V)
C_j	Cost to operate device *j*	(£)
$V_{Highest}$	Highest feeder voltage	(pu)
V_{Lowest}	Lowest feeder voltage	(pu)
V_-	RMW values of the negative sequence component	(no unit)
V_+	RMW values of the positive sequence component of the voltage	(no unit)
Va	Voltage at phase A	(V)
Vb	Voltage at phase B	(V)
Vc	voltage at phase C	(V)
V_{avg}	average value of the three-phase voltages	(V)
ΔV_{isoln}	Change in the voltage due to the deployment of the FVDF solution	(V)
ΔV_i	Voltage excursion at node *i*	(V)
$\Delta V_i'$	Updated voltage excursion at node *i*	(V)
ΔP_{EES}	Required real power change from EES	(kW)
ΔQ_{EES}	Required reactive power change from EES	(KVAr)
$\Delta V_{i,required}$	Required voltage change at node *i*	(pu)
$VSF_{i\_P,EES}$	Voltage sensitivity factor of node *i* for the	(pu/kW)

	real power of EES	
$VSF_{i\_Q,EES}$	Voltage sensitivity factor of node *i* for the reactive power of EES	(pu/kVAr)
ΔTap	Required tap position change	(%)
$VSF_{i,OLTC}$	Voltage sensitivity factor of node *i* for OLTC tap position change	(pu/%)
$\underline{V}_i$	Voltage at bus *i*	(V)
$\underline{V}_j$	Voltage at bus *j*	(V)
$\underline{Y}_{ij}$	Element of admittance matrix **Y**	(no unit)
P_i	Net injected real power at busbar *i*	(W)
Q_i	Net injected reactive power at busbar *i*	(VAr)
u_i	Control variable *i*	(no unit)
$u_i^{\min}$	Lowest value of control variable *i*	(no unit)
$u_i^{\max}$	Highest value of control variable *i*	(no unit)
$V_i^{\min}$	Lower limit of busbar voltage *i*	(pu)
$V_i^{\max}$	Upper limit of busbar voltage *i*	(pu)
fi	ith objective function	(no unit)
N_{obj}	Number of optimisation objective functions	(no unit)
F^k	Objective function values before the control variable change	(no unit)
F^{k+1}	Objective function values after the control variable change	(no unit)
X_i^k	Control variable value before the control variable change	(no unit)
X_i^{k+1}	Control variable value after the control variable change	(no unit)
f_{obj}	Optimisation objective function	(no unit)
$f_{penalty}$	Penalty function	(no unit)
F	Optimisation objective function added by penalty function	(no unit)
x_i	State variable *i*	(no unit)
$x_i^{\max}$	Lower limit of state variable *i*	(no unit)
$x_i^{\min}$	Upper limit of state variable *i*	(no unit)
s_i	Penalty coefficient	(no unit)
N_{branch}	Number of network branches	(no unit)
g_{ij}	Conductance of the branch between busbar i and j	(S)
V_i	Voltage magnitude of busbar *i*	(V)
V_j	Voltage magnitude of busbar *j*	(V)
δ_{ij}	The phase angle between the voltages of busbar *i* and busbar *j*	(Radian)
$\mathbf{x}_i^{t+1}$	New solution generated for CS	(no unit)
$\mathbf{x}_i^{t}$	Current solution for CS	(no unit)

$\mathbf{X}$	A set of solutions in CS	(no unit)
$\mathbf{x}_b$	Current best solution	(no unit)
p_a	Nest abandon probability	(no unit)
$stepsize_i$	Step size generated by Lévy flights for the ith solution	(no unit)
Γ	Gamma function	(no unit)
β	Scale factor for CS	(no unit)
$TapPosition_{OLTC}$	Tap position of the OLTC transformer	(%)
Tap^{min}	Minimum tap position of the OLTC transformer	(%)
$Stepsize^{OLTC}$	Step size of the OLTC transformer	(%)
N_{Tap}	Total number of the tap positions	(no unit)
$\mathrm{StagePosition}_{\mathrm{MSC}}$	Stage position of MSC	(no unit)
$\mathrm{Stepsize}^{\mathrm{MSC}}$	The step size of the MSC	(no unit)
N_{Stage}	The total number of the MSC stage positions	(no unit)
σ	Standard deviation	(no unit)
N	Number of runs	(no unit)
$result_i$	Result of the ith run	(no unit)
$result_{average}$	Average value of the results from the N runs	(no unit)
N_{CS}	Number of fitness function evaluations	(no unit)
N_{GA}	Numbers of fitness function evaluations for GA	(no unit)
N_{PSO}	Numbers of fitness function evaluations for PSO	(no unit)
$V_i^{reference}$	Reference voltage for busbar *i*	(V)
$CR(A)$	Ratio of the reference point found for solution A	(%)
A	Solution set A	(no unit)
R	Reference set	(no unit)
B	Solution set B	(no unit)
$C(A, B)$	Coverage metric of solution set A to solution set B	(%)
$SolutionSet^{before}$	Solution set achieved before increasing the maximum iteration number	(no unit)
$SolutionSet^{after}$	Solution set achieved after increasing the maximum iteration number	(no unit)
$N_{Switching}^{Total}$	Total number of switching operations for all OLTCs and MSCs	(no unit)
$SwitchingNumber_i^{OLTC}$	Numbers of the switching operations for OLTC *i*	(no unit)
$SwitchingNumber_i^{MSC}$	Numbers of the switching operations for MSC *i*	(no unit)
$Position$	Position of the voltage control device after control	(no unit)
$Position^0$	Position of the voltage control device before control	(no unit)

$StepSize$	Step size of the voltage control device	(no unit)
Tap_i	Tap position of OLTC *i*	(%)
Tap_i^{min}	Lowest tap position of OLTC *i*	(%)
Tap_i^{max}	Highest tap position of OLTC *i*	(%)
N_{OLTC}	Number of OLTCs	(no unit)
Cap_i	Stage position of MSC *i*	(no unit)
Cap_i^{min}	Lowest stage position of MSC *i*	(no unit)
Cap_i^{max}	Highest stage position of MSC *i*	(no unit)
N_{MSC}	Number of MSCs	(no unit)
$N_{DG}^{PControl}$	Total number of DGs with real power control	(no unit)
$P_{DGi}^{available}$	Available real power output of DG *i*	(W)
P_{DGi}^{output}	Real power output of DG *i*	(W)
$N_{DG}^{QControl}$	Total number of DGs with reactive power control	(no unit)
$Q_{DGi}^{reference}$	Reference value for the reactive power from DG *i*	(VAr)
Q_{DGi}^{output}	Reactive power output of DG *i*	(VAr)
P_{DGi}^{min}	Lower limit of the real power output of DG *i*;	(W)
P_{DGi}^{max}	Upper limit of the real power output of DG *i*;	(W)
Q_{DGi}^{min}	Lower limit of the reactive power output of DG *i*;	(VAr)
Q_{DGi}^{max}	Upper limit of the reactive power output of DG *i*;	(VAr)
$P_{DGi}^{Capacity}$	Installed capacity of DG i	(W)
φ	Power factor of DG output	(no unit)
S_{EES}^{Max}	Limit of the EES apparent power	(VA)
P_{EES}	EES real power outputs	(W)
Q_{EES}	EES reactive power outputs	(VAr)
I_{ij}	Current flow for the branch between busbar i and busbar j	(A)
I_{ij}^{max}	Capacity of the branch between busbar i and busbar j	(A)

Table of Contents

List of Figures

List of Tables

Chapter 1 Introduction

1.1 Background

To protect the environment and to achieve a sustainable economy, many countries have set demanding carbon reduction targets. The United Kingdom (UK) government aims to reduce the UK's carbon emission by at least 80%, with respect to the baseline from 1990, by 2050 [1]. To achieve this ambitious target, large quantities of renewable energy generation are being connected to UK power systems. Meanwhile, with the trend towards electrification of heat and transport, electric vehicles (EVs) and heat pumps are also expected to proliferate in future power systems [2].

Generally power systems can be divided into three different areas: power generation, power transmission and power distribution. Conventionally, electrical power is generated from large scale power plants, and transmitted to customer areas by interconnected transmission networks. Supplied by transmission networks, distribution networks deliver electricity to the domestic and commercial customers. In the UK, distribution networks are operated and maintained by fourteen licensed distribution network operators (DNOs) [3]. Each of these DNOs covers a separate geographical region of Great Britain. These DNOs need to ensure the electricity delivery meets the requirements of the Office of Gas and Electricity Markets (Ofgem), which is an independent national regulatory authority of the UK government. One of the essential tasks for DNOs is to maintain network voltages within their statutory limits. Any voltage violating the limits, especially the upper limits, can pose a hazard to apparatus in the network, and could damage the customer's equipment [4]. In the UK, the steady-state voltage should be maintained within ±6% of the nominal voltage in systems between 1kV and 132kV, and within between +10% and -6% for 400V low-voltage (LV) networks [5].

Distribution networks are conventionally planned and operated by DNOs to cope with voltage problems under varying load conditions, using the assumption that power flow is unidirectional. Renewable energy resources are commonly connected to distribution networks, in the form of distributed generation (DG) [6, 7]. Large penetrations of DGs can cause reverse power flow and voltage problems, which are seen as one of the key challenges for DG connection, especially for rural distribution networks [4, 7, 8]. The significant new demand from electric vehicles and heat pumps, also connected to distribution networks, could also result in voltage problems [2, 9-11]. The connection of single-phase DGs may also cause voltage unbalance problems, especially in LV networks [12]. Conventional voltage control

schemes may not be able to cost-effectively solve these voltage problems, which could then restrict the connection of low carbon technologies (LCTs) [6, 7], and therefore hinder progress towards decarbonisation.

In the rest of this chapter, the fundamental theories of steady-state voltage problems and voltage unbalance problems are introduced. Conventional voltage control techniques and schemes are described. The impacts of smart grid approaches to voltage control are introduced. The research objectives are proposed, followed by the contributions to knowledge. Finally, the thesis outlines are introduced.

1.2 Theoretical analysis of voltage changes and voltage unbalance in distribution networks

1.2.1 Steady-state voltage changes in distribution networks

The principle of steady-state voltage changes in conventional distribution networks can be explained with the diagram shown in Fig. 1, which represents the equivalent circuit of electricity delivery from the sending end to the load end. Here the sending end represents the upstream network.

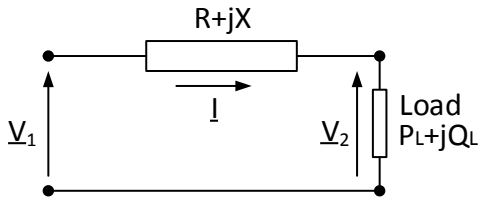

Fig. 1 Equivalent circuit for voltage change analysis for conventional distribution networks

The relationship between the voltage at the sending end, $\underline{V}_1$, and the voltage at the load, $\underline{V}_2$, can be represented by (1).

$$\underline{V}_1-\underline{V}_2=\underline{I}\times(R+jX) \tag{1}$$

where $\underline{I}$ is the current flowing from the sending end to the load. R and X are the resistance and reactance of the branch between the sending end and the load.

The current $\underline{I}$ can be represented by (2) with the load power and voltage.

$$\underline{I}=\frac{\hat{\underline{S}}}{\hat{\underline{V}}_2}=\frac{P_L-jQ_L}{\hat{\underline{V}}_2} \tag{2}$$

where,

$\hat{\underline{S}}$ complex conjugate of the apparent power of the load

$\hat{\underline{V}}_2$ complex conjugate of the load voltage

P_L real power of the load

Q_L reactive power of the load

If the load voltage is taken as the reference voltage, $\underline{V}_2 = V\angle 0$. The voltage change between the sending end and load can be represented by (3).

$$\Delta\underline{V} = \underline{V}_1 - \underline{V}_2 = \underline{I}(R+jX) = \frac{(RP_L+XQ_L)+j(XP_L-RQ_L)}{\hat{\underline{V}}_2} = \frac{RP_L+XQ_L}{V_2} + j\frac{XP_L-RQ_L}{V_2} \quad (3)$$

The phasor diagram representing the relationship between $\underline{V}_1$ and $\underline{V}_2$ is shown in Fig. 2. It should be noted that this diagram is purely qualitative, since in real networks the large voltage change depicted in this diagram would not be acceptable [6].

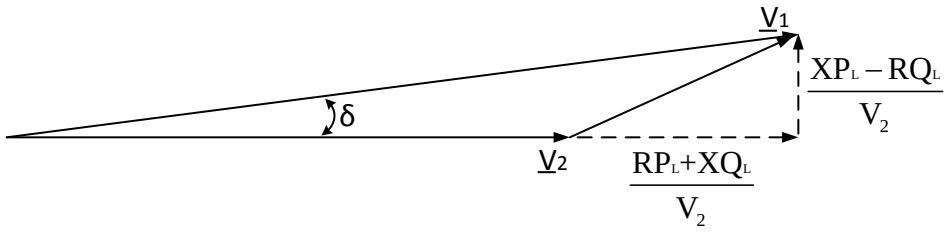

Fig. 2 Phasor diagram of sending-end voltage and load voltage for conventional distribution networks

In practice, the voltage angle δ between $\underline{V}_1$ and $\underline{V}_2$ is actually small, and the voltage change can be approximated by (4).

$$\Delta V \approx \frac{RP_L+XQ_L}{V_2} \quad (4)$$

In distribution networks, the X/R ratio of the branch is small. In other words, X and R are usually of similar magnitude. Therefore neither RP_L nor XQ_L are negligible. The voltage at the load end depends on the network resistance and reactance, the real and reactive powers of the load, and the voltage at the sending end [13]. If the load is too heavy, the voltage change could be too large and the voltage at the load end could be lower than its statutory lower limit, leading to an undervoltage problem.

The connection of DG will also affect the power flow and the voltage change, as explained in the following. In this example, DG is connected in parallel with the load, as shown in Fig. 3.

P_G is the real power injected by the DG, and Q_G is the reactive power injected or absorbed by the DG.

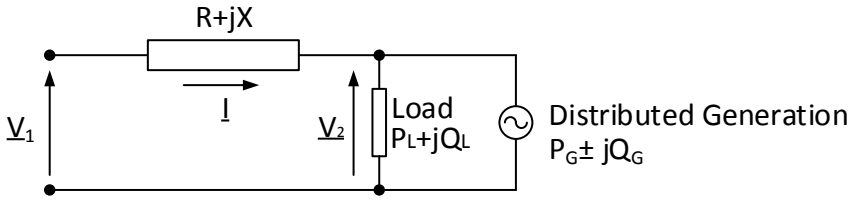

Fig. 3 Equivalent circuit for voltage change analysis for distribution networks with DG connection

In this case, the voltage change between the sending end and the load, which was represented by (4) for conventional distribution networks, can now be represented by (5).

$$\Delta \underline{V} = \frac{R(P_L - P_G) + X(Q_L \pm Q_G)}{V_2} + j\frac{X(P_L - P_G) - R(Q_L \pm Q_G)}{V_2} \tag{5}$$

If the real power injected by the DG is larger than the load, and $|P_G - P_L|$ is significantly larger than $|Q_L \pm Q_G|$, the phasor diagrams of the voltages $\underline{V}_1$ and $\underline{V}_2$ can be represented by Fig. 4.

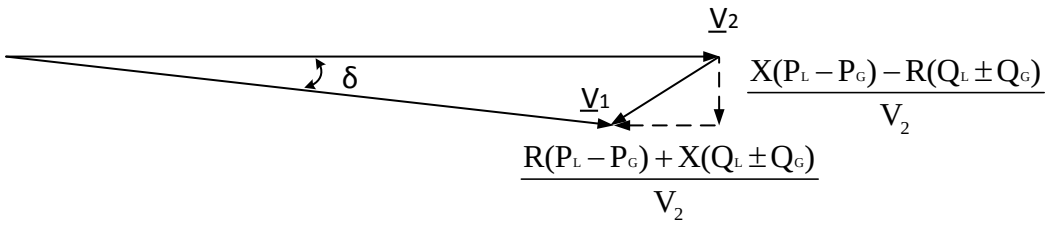

Fig. 4 Phasor diagram of sending end voltage and load voltage for the distribution networks with DG connection

As before, in practice, the voltage angle δ between $\underline{V}_1$ and $\underline{V}_2$ is small and thus the voltage change can be approximated by (6).

$$\Delta V \approx \frac{R(P_L - P_G) + X(Q_L \pm Q_G)}{V_2} \tag{6}$$

It can be seen therefore that if DG real power export is large enough may result in voltages that rise above the statutory upper limit.

It should be noted that in real distribution networks the voltage problems are more complicated, especially when DGs are connected, as the network topologies are far more complex than the two-node systems shown earlier [4, 8, 14]. Moreover, the load's real and reactive powers, and the DG real power output, are not constant but are continuously varying.

1.2.2 Voltage unbalance in distribution networks

Voltage unbalance is a condition in which the three-phase voltages differ in amplitude or are displaced from their normal 120° phase relationship or both [15]. In the UK and Europe, the percentage voltage unbalance factor, %VUF, is used to represent the level of voltage unbalance in a system [16, 17]. It is defined as the ratio (in percent) between the root mean square (RMS) values of the negative sequence component V_- and the positive sequence component of the voltage V_+, as shown by (7).

$$\%VUF = \frac{V_-}{V_+} \times 100\% \tag{7}$$

V- and V+ can be calculated from three phase voltages by (8).

$$\begin{bmatrix} V_0 \\ V_+ \\ V_- \end{bmatrix} = \frac{1}{3} \begin{bmatrix} 1 & 1 & 1 \\ 1 & 1\angle 120^o & 1\angle -120^o \\ 1 & 1\angle -120^o & 1\angle 120^o \end{bmatrix} \begin{bmatrix} V_a \\ V_b \\ V_c \end{bmatrix} \tag{8}$$

where V_a, V_b and V_c are the three-phase voltages. The %VUF can also be approximated by (9) (for values of voltage unbalance of a few percent), as the maximum deviation from the average of the three-phase voltages, divided by the average of the three-phase voltages.

$$\%VUF = \frac{Max\left\{\left|V_a - V_{avg}\right|, \left|V_b - V_{avg}\right|, \left|V_c - V_{avg}\right|\right\}}{V_{avg}} \times 100\% \tag{9}$$

where V_{avg} is the average value of the three-phase voltages.

Unbalanced voltages can have adverse effects on the power system and on equipment. Voltage unbalance may cause unbalance in the phase currents, leading to increased network losses and heating effects [18]. Also, voltage unbalance can reduce the efficiencies and decrease lifespans of induction machines, and power electronic converters and drives [18]. Therefore, voltage unbalance needs to be maintained below defined limit. The %VUF has a regulatory limit of 1.3% in the UK, although short-term deviations (less than one minute) may be allowed up to 2%, which is the standard limit used for the maximum steady-state %VUF allowed in European networks [16, 17].

Conventionally, the uneven distribution of single-phase loads and asymmetrical impedances of the network are the major cause of voltage unbalance. When single-phase generations are connected to distribution networks, they may also result in unbalanced voltages [12, 19, 20].

It is worth noting that in LV networks, voltage rise has been determined as the first technical constraint to be encountered as penetrations of generation increase [20]. However, it is anticipated that voltage unbalance may also become a constraint as overvoltage problems could be mitigated by three-phase balanced voltage control techniques such as the secondary on load tap changer (OLTC) [21]. However these approaches are unable to reduce voltage unbalance on these networks.

1.3 Conventional distribution network voltage control

To maintain network voltages within their statutory limits, various voltage control techniques have been developed and applied in distribution networks. In this work, the term "control technique" is used to describe different types of voltage control equipment, and "control device" is used to describe individual control equipment of infrastructure. Conventionally, OLTC transformers, in-line voltage regulators and mechanically switched capacitor banks (MSCs) are used in distribution networks for voltage control.

1.3.1 On load tap changer

OLTC is a classic voltage control technique used in distribution networks. The secondary side voltage of the transformer can be adjusted by changing the OLTC tap ratio when the transformer is energized. The simplified structure of an OLTC transformer is shown in Fig. 5.

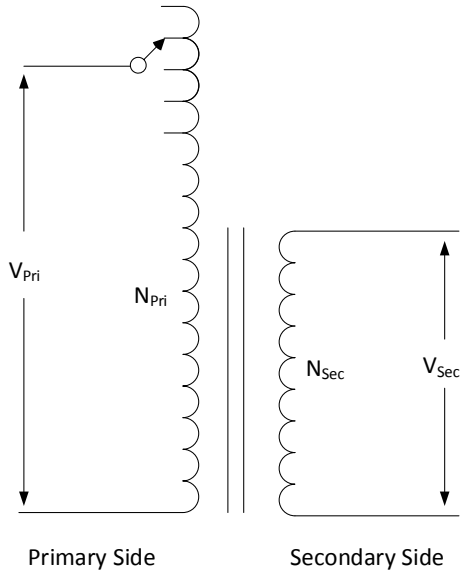

Fig. 5 Simplified structure of a transformer with OLTC

The basic principle of OLTC is explained in the following. For a transformer, the voltage at the primary side and the secondary side follows the following relationship represented by (10), if the voltage drop across the transformer is neglected.

$$\frac{V_{Pri}}{V_{Sec}} = \frac{N_{Pri}}{N_{Sec}} \tag{10}$$

where V_{Pri}, V_{Sec} are the voltages at the primary and secondary side, and N_{Pri} and N_{Sec} are the transformer winding numbers at the primary and secondary side.

The secondary side voltage V_{Sec} can be seen as a function of primary side voltage V_{Pri}, and the winding numbers N_{Pri} and N_{Sec}. Normally, the winding number at the high voltage side of the transformer is adjustable. This is because the current on the primary side is normally smaller than the current on the secondary side, thereforea more cost-effective design is to change the tap position on the high voltage side. If the winding number change for N_{Pri} is defined as k (%), the relationship can be represented by (11).

$$\frac{V_{Pri}}{V_{Sec}} = \frac{N_{Pri}(1+k)}{N_{Sec}} \tag{11}$$

Therefore, the secondary voltage can be increased or decreased by varying the tap ratio of OLTC. In conventional distribution network design, a transformer with OLTC is only used at primary substations. At secondary substations, off load tap changers are used. However, OLTCs are beginning to be used at secondary substations, to facilitate the integration of renewable energy generation [21].

1.3.2 Mechanically switched capacitor bank

MSCs are also used in distribution networks, to correct power factors, to support network voltages, and to reduce network losses. MSC can be located at primary substations for power factor correction, and can also be located along long feeders to support voltages. Here the MSCs, which are located along feeders and used for voltage control, are studied. A simplified MSC, including a capacitor bank and a circuit breaker (CB), is shown in Fig. 6. The reactive power injected by the capacitor bank can be controlled by switching the CB on/off.

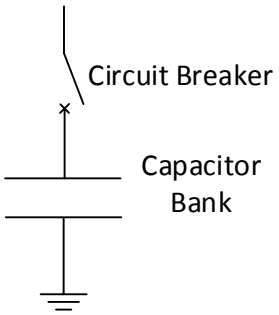

Fig. 6 Simple structure of mechanically switched capacitor bank

The amount of reactive power injected by the MSC depends on the capacitance of the capacitor bank, the network frequency and the voltage of the busbar, to which the MSC is connected, as represented by (12).

$$Q_{MSC} = 2\pi f C_{MSC} V_{MSC}^2 \tag{12}$$

where:

Q_{MSC}	reactive power injected by the MSC
f	network frequency
C_{MSC}	capacitance of the MSC capacitor
V_{MSC}	voltage at the MSC

As indicated in section 1.2.1, the reactive power affects the voltage magnitude in distribution networks. The MSC is able to affect the reactive power flow in distribution networks, which in turn affects the network voltages. In practice, a MSC could include multiple capacitor banks and CBs, and the reactive power injected by this MSC has multiple stages. An illustration of a simple multi-stage MSC is shown in Fig. 7.

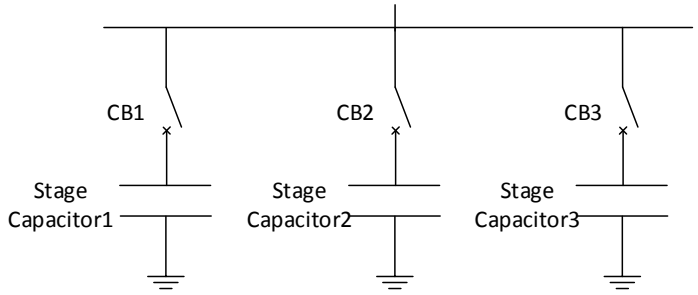

Fig. 7 Structure of a simple multi-stage MSC

This multi-stage MSC shown in Fig. 7 has three CBs and three capacitors. Using the CBs different combinations can be connected to distribution networks resulting in different amounts of reactive power injection. These three capacitor banks can have the same or different sizes. Normally, the size of the capacitor bank is defined as the reactive power provided by the capacitor bank at its rated voltage and at the normal network frequency. It should be noted that these reactive power values are only used to represent the stages of the MSC. The reactive power injected by the MSC is also affected by the MSC voltage and the network frequency, as indicated by (12). These three capacitor banks could also have different sizes. For example, the sizes could be 1MVAr, 2MVAr and 4MVAr. In this case, the MSC

could provide eight different stages of reactive power, as shown in Table 1. The relationships shown in Table 1 are from a real set of MSC from Northern Powergrid, which has been trialled in the CLNR project.

Table 1 The relationships between MSC stage positions and circuit breaker status

MSC Stage Position	**Total MVAr**	**CB Status**		
		1MVAr	2MVAr	4MVAr
1	0MVAr	off	off	off
2	1MVAr	on	off	off
3	2MVAr	off	on	off
4	3MVAr	on	on	off
5	4MVAr	off	off	on
6	5MVAr	on	off	on
7	6MVAr	off	on	on
8	7MVAr	on	on	on

1.3.3 In-line voltage regulator

In-line voltage regulators, also known as step voltage regulators, are sometimes used in rural networks to help support network voltages for load customers towards the end of a long feeder. A typical configuration of the in-line voltage regulator application is illustrated in Fig. 8. The in-line voltage regulator affects the voltages of the downstream network section.

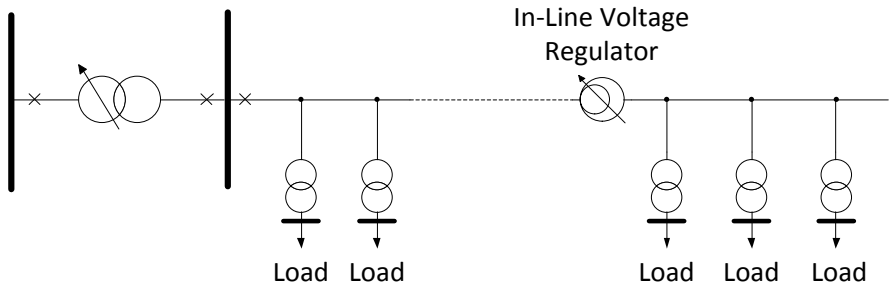

Fig. 8 Configuration of in-line voltage regulator

Voltage regulators are normally autotransformers with an adjustable transformer ratio. They share the same principle as OLTC transformers in terms of voltage control, but only affect voltages on a single feeder.

1.3.4 Conventional distribution network voltage control architecture

Voltage control devices, such as OLTC and MSCs, are typically controlled by local controllers, which operate on the basis of local measurement only. The configuration of the conventional voltage control architecture is illustrated in Fig. 9. As shown in Fig. 9, there is no communication infrastructure between these controllers. These voltage control devices could be coordinated by setting the target voltages and time delays of their controllers. For conventional distribution networks, this local control architecture often provides an acceptable solution, if the local controllers are configured appropriately [22]. However, it has been shown previously that this conventional voltage control architecture can have limitations when large penetrations of DGs are connected [8, 13, 23].

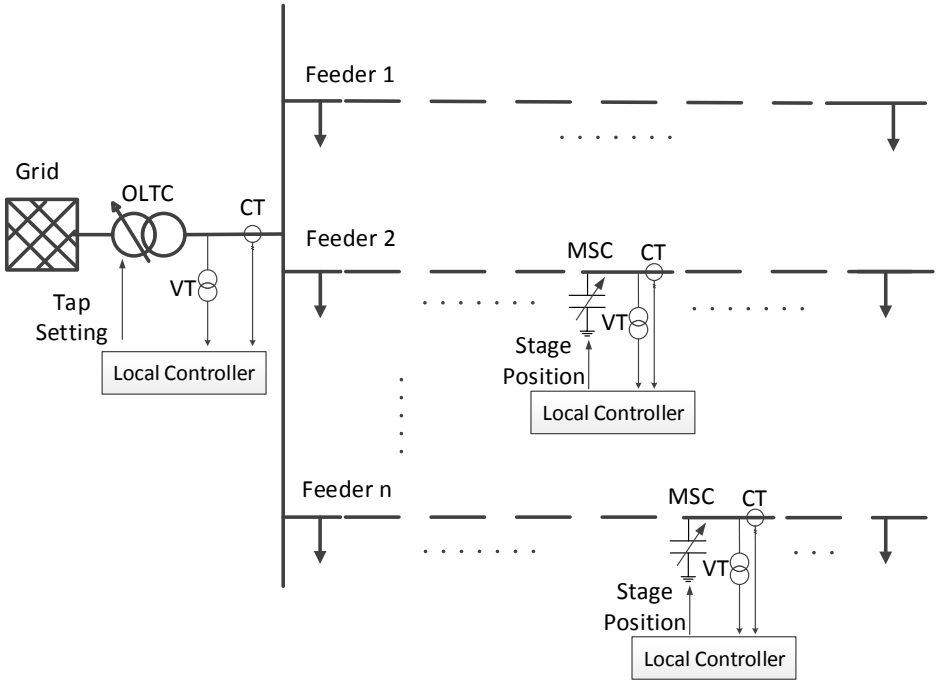

Fig. 9 Configuration of conventional voltage control architecture

1.4 Smart grid

Smart grid technologies have the potential to provide a flexible, economic solution to facilitate the integration of LCTs [10, 24, 25]. For example, novel control techniques, such as DG with real and reactive power controllability and electrical energy storage (EES), could be introduced to mitigate the problems caused by the connection of LCTs [26-29]. Information and communication technologies (ICTs) enable the application of advanced voltage control architectures and algorithms, with which the voltage problems could be mitigated by operating voltage control devices cooperatively [30, 31]. Voltage control is expected to deliver a broad range of benefits to power systems [24, 27, 31-34]. For example, the smart grid devices, such as controllable DG and EES, should be accommodated in voltage control

effectively [27]. Also, besides maintaining network voltages within their limits, it is expected to achieve various additional objectives with voltage control, which are related to energy efficiency improvement, and operational cost reduction [31]. For example, in two recent smart grid projects, customer-led network revolution (CLNR) and customer load active system services (CLASS), advanced voltage control algorithms are applied and trialled to facilitate the connection of LCTs and to manage electricity demand without any discernible impacts on customers [35, 36].

Therefore, voltage control problems are expected to be more complicated in future smart distribution networks, because of the more complex flow of energy across the distribution network caused by LCTs, new voltage control devices and various secondary control objectives. Advanced voltage control architectures and algorithms are required to solve the future voltage control problems, to which conventional voltage control architectures and algorithms struggle to provide adequate solutions [27]. Various advanced architectures and algorithms have been proposed for voltage control previously [30]. Generally, these architectures can be categorized as centralized and distributed control architectures, both of which could potentially provide solutions for future voltage control problems [30]. This PhD study concentrates on centralized voltage control architecture, with which secondary control objectives could be easily considered at the system level, and potentially optimal solutions could be achieved with respect to the secondary control objectives. Numerous algorithms have been proposed in previous studies based on the centralized voltage control architecture. These algorithms have been categorized into three different groups in this PhD study:

- Rule-based control algorithm;
- Deterministic optimisation algorithm;
- Metaheuristic optimisation algorithm;

For each group, numerous algorithms have been developed and successfully applied for distribution network voltage control. However, many of these algorithms were developed and evaluated only for conventional distribution networks. The algorithms from these three groups have not been evaluated comparatively in terms of voltage control in distribution networks before. It is important to develop and evaluate these algorithms regarding the voltage control problems in the context of future smart distribution networks. In this thesis, advanced algorithms from each algorithm group have been developed, evaluated and compared, to develop guidelines when deploying advanced voltage control algorithms for future smart distribution networks.

1.5 Research objectives

The primary aim of the research presented in this thesis is to develop and evaluate advanced voltage control algorithms for future smart distribution networks. The main research objectives are:

- To investigate the voltage control problems in future smart distribution networks;
- To develop and evaluate advanced voltage control algorithms from each algorithm group regarding voltage control problems in future smart distribution networks;
- To summarize the salient characteristics of these algorithms by comparing the voltage control algorithms from different groups in terms of solving potential voltage control problems in future smart distribution networks;
- To provide guidance to distribution network management product manufactures and DNOs, for voltage control algorithm design by understanding the links between algorithms and voltage control problems.

1.6 Contributions to knowledge

This thesis presents the following contributions to knowledge:

- A novel rule-based voltage control algorithm has been proposed to solve voltage problems and voltage unbalanced problems in future distribution networks. Voltage cost sensitivity factor has been defined to represent the cost-effectiveness of network interventions in terms of voltage control. Feeder voltage divergence factor has been introduced as a network voltage metric for networks with large, clustered distributions of LCTs;
- Representing two different types of optimisation algorithms, ODCDM and CS algorithms have been extended and applied to solve mixed integer and multi-objective voltage optimisation problems in future smart distribution networks. A novel test methodology has been proposed to test, evaluate and compare two different types of voltage optimisation algorithms, regarding voltage control problems in conventional and future smart distribution networks;
- The rule-based voltage control algorithm and the two different voltage optimisation algorithms have been comparatively evaluated, regarding various aspects of potential voltage control problems in future smart distribution networks. The salient characteristics of these three algorithms have been summarized and guidelines have been proposed to distribution network management product manufactures and DNOs, regarding voltage control algorithm selection for future smart distribution networks.

The algorithms and findings from this study could provide useful information for practical distribution network voltage control algorithm design, and the theoretical studies of voltage optimisation.

1.7 Thesis outline

The remainder of this thesis is structured as follows: Chapter 2 reviews advanced voltage control techniques, architectures and algorithms for distribution networks. Novel voltage control techniques, such as EES, are introduced. The voltage control problems for conventional and future distribution networks are discussed. Different voltage control architectures are reviewed. Typical algorithms based on the centralized voltage control architecture are reviewed.

Chapter 3 proposes a rule-based voltage control algorithm, which could be used to mitigate the voltage problems and voltage unbalance problems, caused by the clustered distributions of LCTs in terms of both feeder and phase location. Feeder voltage divergence factor and percentage voltage unbalance factor are utilized as network voltage metrics for networks with large, clustered distributions of LCTs. Voltage cost sensitivity factor is defined to represent how cost effective each network intervention is, in terms of voltage control. Voltage sensitivity factor is used to determine the required response from each network intervention. These metrics and factors are then used in the proposed control algorithm to provide a cost effective solution to mitigate voltage problems and voltage unbalance problems. The algorithm is evaluated with steady-state simulation and in a laboratory using real time power hardware in the loop (PHIL) emulation.

Chapter 4 introduces a deterministic voltage optimisation algorithm, based on oriented discrete coordinate descent method (ODCDM). The implementation of the original ODCDM based voltage control algorithm is introduced, and the extensions of this algorithm to solve mixed integer nonlinear programming (MINLP) problems and multi-objective problems are discussed. A case study is presented to demonstrate the basic mechanism of the developed algorithm. The algorithm is then further validated with field trial results from the Customer-led Network Revolution project, in which the ODCDM based control algorithm is implemented in real distribution networks in north east England.

Chapter 5 proposes novel voltage optimisation algorithms, based on a metaheuristic algorithm, Cuckoo Search via Lévy Flights, which is normally referred to as Cuckoo Search (CS). The principle of CS is introduced. Single-objective cuckoo search algorithm (SOCS) and multi-

objective cuckoo search algorithm (MOCS) are developed and applied for voltage optimisation. The voltage optimisation algorithm, based on SOCS, is evaluated and compared with genetic algorithm (GA) and particle swarm optimisation algorithm (PSO), regarding the single-objective test case from Chapter 4. The MOCS based voltage optimisation algorithm is also evaluated and compared with non-dominated sorting genetic algorithm ii (NSGA-II), regarding a multi-objective test case.

In Chapter 6 and Chapter 7, the voltage optimisation algorithms are evaluated with respect to single-objective and multi-objective voltage optimisation. Evaluation methods are proposed based on the analysis of the problem formulation for voltage optimisation, and the voltage control problems in conventional and future distribution networks. Test results demonstrating this evaluation method are also presented.

In Chapter 8, these three types of voltage control algorithms are compared based on the literature reviewed and the algorithm evaluation results. Based on this evaluation, guidelines are proposed to distribution network management product manufactures and DNOs regarding voltage control algorithm selection for future distribution networks. Finally, Chapter 9 summarises the key findings with respect to the research objectives set out in Chapter 1. Future work is also proposed.

Chapter 2 Advanced Distribution Network Voltage Control

2.1 Introduction

As discussed in Chapter 1, the conventional voltage control techniques and architectures may not be sufficient to solve these voltage problems and voltage unbalance problems in future distribution networks. Novel voltage control techniques, such as EES and DG, have been introduced to support voltage control. Advanced voltage control architectures and algorithms have been proposed to maintain the distribution network voltages with the application of ICTs. In this study, the control architecture is generally seen as the infrastructure of the control system (hardware), whereas the control algorithm is seen as the specific method adopted within the control architecture (software). Secondary control objectives, such as network loss reduction, could also be achieved by these architectures and algorithms.

In the rest of this chapter, novel voltage control techniques are introduced, followed by the introduction of voltage unbalance control techniques. The voltage control problems for conventional distribution networks and future distribution networks are discussed. Different advanced voltage control architectures and algorithms are reviewed. Conclusions are drawn on the basis of this review.

2.2 Advanced voltage control techniques

2.2.1 Electrical energy storage

EES has been introduced to distribution networks for voltage control [23, 37-40]. In [23, 37], it has been applied to solve the overvoltage problems caused by PV generation. In [38], a distribution network voltage support operation strategy for EES has been proposed, so that the real and reactive powers of the EES are operated with reactive power priority. EES is also used to solve the undervoltage problems with demand side response in [10]. EES is able to inject/absorb both real and reactive power. In other words, it can be operated in all four quadrants.

Besides voltage control, EES has been applied for many other purposes. A comprehensive review of the possible benefits of EES has been presented previously [29]. As indicated by [29], EES can be used to support a heavily loaded feeder, provide power factor correction, reduce the need to constrain DG, minimise OLTC operations and mitigate flicker, sags and swells.

2.2.2 Distributed generation control

DG connection could cause voltage problems in distribution networks, which is one of the main issues restricting allowable DG penetration, especially in rural distribution networks [7, 8, 41-43]. This is because the rural distribution networks have long feeders, with high impedance, which could lead to large voltage deviation. It is possible to mitigate the voltage problems without introducing the DG control. For example, in [44], an advanced voltage controller is introduced to control the OLTC at the primary substation and to keep the network busbar voltages within their statutory limits. Additional voltage control equipment could be installed to mitigate the voltage problems caused by DG connection, such as in-line voltage regulators [45] and electrical energy storage [46]. Also, line re-conductoring or building a dedicated line is a potential way to facilitate DG integration, although the cost could be high [47]. However, the existing voltage control techniques may not be sufficient when the DG penetration is significant. Controlling DG can further increase the allowable DG penetration without introducing additional voltage control equipment or carrying out network reinforcement. Many previous research and projects demonstrate the methods and benefits of utilizing DG for voltage control [6, 13, 48]. Different DG control techniques have been proposed before, including DG real power control, DG reactive power control, DG power factor control and DG busbar voltage control.

As shown in section 1.2.1, the real power injected by DG is the reason for overvoltage problems. Reducing the DG real power, normally named as DG curtailment, could mitigate the overvoltage problems. As shown in [49], it is often beneficial to accommodate a larger DG capacity and curtail it during extreme situations (such as the coincidence of minimum load with maximum generation), the probability of which is generally low. DG curtailment can also be used to support distribution network voltage control, when other voltage control devices are not available [42].

DG reactive power injection can also be used for voltage control. As shown by (5), the reactive power from DG can affect the voltage change, and the effectiveness of DG reactive power is strongly related to the line reactance X. In [50], the reactive power from DG was controlled to mitigate the voltage problems caused by DG connection. DG reactive power can be used to control the voltages across the network, and to improve the network control performance. For example, the switching operation numbers of OLTC and MSC can be reduced by introducing DG reactive power control [51]. In some studies, both the DG real power and reactive powers are controlled. The real power reduction is not beneficial for the

DG owner, so reactive power is preferable in some studies [52, 53]. In these studies, normally the reactive power is controlled first and the real power is controlled when the reactive power control is not available.

Instead of controlling their real and reactive powers directly, we can also control DGs by controlling their power factors and terminal voltages. In [54], the DG power factor is controlled, while in [55, 56], the DG terminal voltage is controlled. Basically, the DG power factor control and DG bus voltage control are also realized by controlling the DG's real and reactive powers. It should also be noted that the control capabilities of DGs depend on the DG technology [13, 47, 57]. For example, for synchronous generator-based DGs, real power control is achieved by controlling the prime mover of the synchronous generator and reactive power control is achieved by controlling the excitation system. For power electronic converter-based DGs, the real and reactive powers can be controlled by controlling the switching angles of the power electronic converters [6].

2.3 Voltage unbalance control techniques

Voltage unbalance problems can be solved with different techniques. Distribution networks can be balanced by changing the network configuration through feeder switching operations to transfer loads among circuits [18].

Some power electronic devices, such as the static synchronous compensator (STATCOM), can be used to compensate for voltage unbalance. For example, as shown in [58], voltage unbalance can be almost fully compensated by the STATCOM, with two novel control strategies: voltage-controlled current source strategy and modified voltage-controlled voltage source strategy.

The power electronic device of EES can be controlled to mitigate voltage unbalance like STATCOM. Three-phase EES is applied to mitigate voltage unbalance with an improved fuzzy controller in [59]. Furthermore, EES can be placed at the phase where the generation and load are connected, to reduce the voltage unbalance by absorbing the generation or compensating the load, as shown in [60].

Coordinated control of generation and controllable load could also be used for voltage unbalance control in LV networks [12]. However, this method may not be suitable for medium voltage (MV) networks, as the vast majority of generation load and generation connected to MV networks is three-phase.

2.4 Voltage control problems in future smart distribution networks

Normally, multiple devices, using the same or different voltage control techniques, are connected to distribution networks for voltage control. The voltage control devices are operated to maintain the network voltages within their statutory limits under all network load and generation conditions [27].

In conventional distribution networks, different network conditions are mainly driven by the load variation. Classic distribution network voltage control techniques, including OLTC, MSCs and in-line voltage regulators, are used. In future distribution networks, more significant load variation is expected, because of the additional load from the electrification of transport and heat. More importantly, the DG generation variation will also lead to different network conditions. Besides classic voltage control techniques, novel voltage control techniques are also expected to be applied, such as DG and EES. Some of these novel voltage control techniques could be multifunctional. For example, EES can be applied to mitigate both the voltage problem and the voltage unbalance problem. One key requirement for voltage control in future smart distribution networks is to accommodate these novel techniques effectively [27, 32, 34].

Besides maintaining the networks within the limits, voltage control could achieve secondary control objectives. In the smart grid era, it is becoming more and more essential to pursue various objectives, which are related to different aspects, such as energy efficiency improvement, operation cost reduction and so on [27, 31, 33]. For conventional distribution networks, some control objectives have been proposed, such as network loss reduction [61]. For future distribution networks, new control objectives, such as maximizing the DG real power output, could also be considered.

Therefore, in future distribution networks, voltage control problems are expected to be more challenging, with more network load and generation conditions, more voltage control devices and more control objectives.

2.5 Voltage control architectures and algorithms

To solve the distribution network voltage control problems, different voltage control architectures and algorithms have been proposed. Conventional voltage control architecture has been introduced in Chapter 1. Based on the conventional control architecture, advanced control algorithms can be implemented in the local controllers to mitigate the voltage problems caused by the DG connection. For example, a control method, which is

implemented in the SuperTAPP n+ relay [62], has been introduced to control the OLTC to facilitate the DG connection [63]. This cost-effective method could solve the voltage problems caused by DG integration, with local measurements only. However, this method only focuses on controlling the OLTC. Generally, it is difficult to achieve secondary control objectives with the conventional voltage control architecture [27].

Advanced voltage control architectures and algorithms have been proposed with the application of ICTs [32, 64, 65]. These advanced architectures and algorithms could provide many benefits which the conventional voltage control architecture cannot provide. For example, they are able to mitigate voltage problems which cannot be mitigated by the conventional voltage control architecture. The distribution network's hosting capacity for DG can also be increased significantly, with these advanced control architectures and algorithms [13, 66]. Also, secondary control objectives can easily be achieved and could even be optimised. In the following, advanced voltage control architectures and algorithms are reviewed.

2.5.1 Advanced voltage control architectures

New voltage control architectures are enabled by the application of ICTs. In the new control architectures, the controller can receive the measurements across the network, and if there is more than one controller, data can be exchanged between the different controllers. The control architectures can be generally divided into distributed control architecture and centralized control architecture [67, 68]. The configurations of these two control architectures can be found in Fig. 10 and Fig. 11. One of the key differences between the distributed control architecture and the centralized control architecture is how the control decisions are made for all the voltage control devices. For the distributed control architecture shown in Fig. 10, the voltage control devices are controlled by their own distributed controllers. These distributed controllers make their own control decisions not only with the local measurement, but also with the information from the other distributed controllers. For centralized control architecture shown in Fig. 11, the control decisions for all the voltage control devices are made by a centralized controller. The central controller dispatches the control decisions to the remote terminal units (RTUs), and the RTUs operate the voltage control devices depending on the received control decisions. Normally, the central controller collects the measurements from the network.

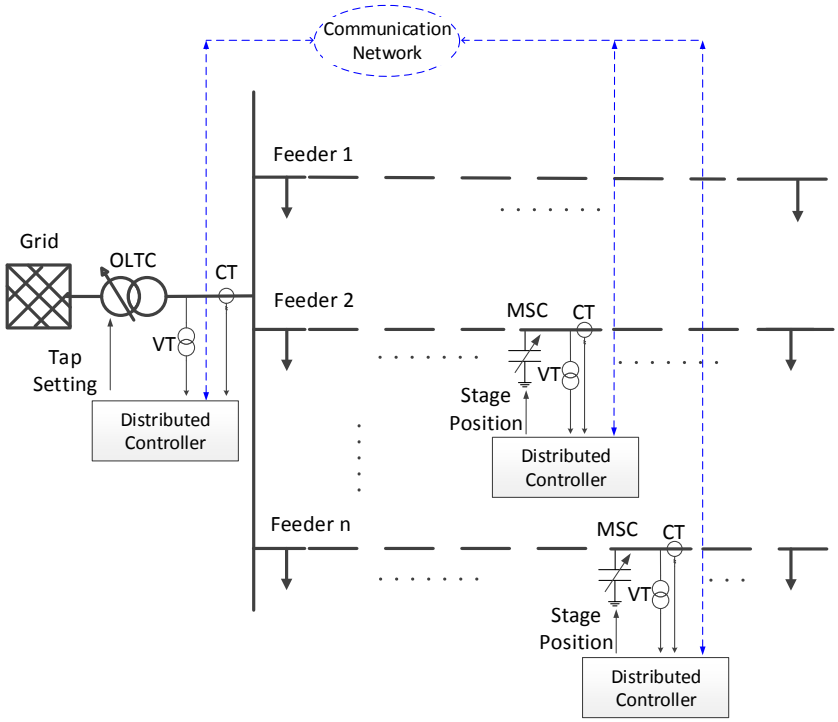

Fig. 10 Configuration of distributed voltage control architecture

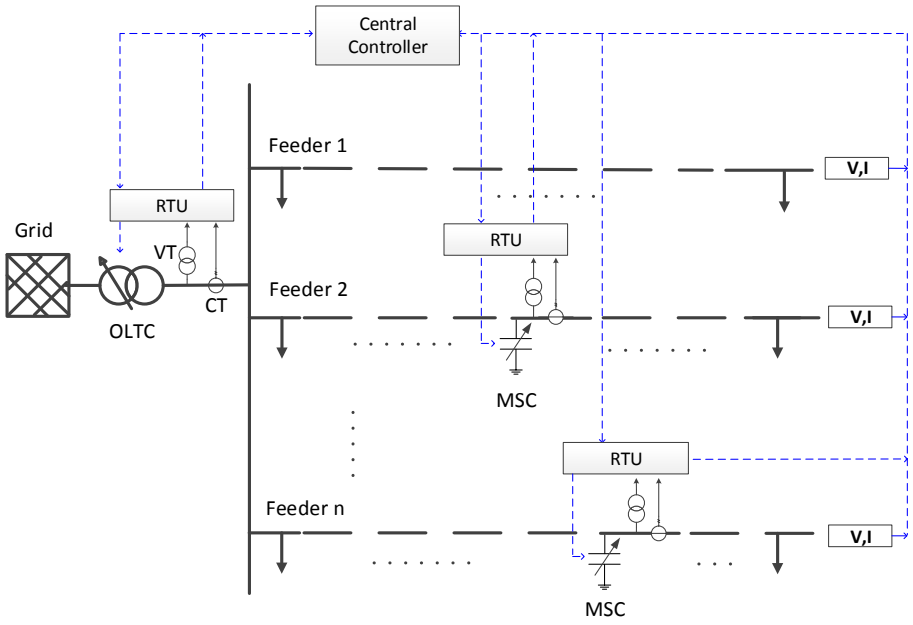

Fig. 11 Configuration of centralized voltage control architecture

Both of these architectures have their own advantages and disadvantages, which have been investigated in previous studies [12, 67]. Generally speaking, the communication infrastructure requirement for the distributed control architecture is not as high as that for the centralized control architecture. If the communication infrastructure fails, the distributed controllers in the distributed control architecture could still operate with local information, whereas the centralized controller may fail completely. Also, greater flexibility could be

gained by integrating more control devices, without changing the existing distributed controllers. The centralized controller needs to be updated if new control devices are integrated. On the other hand, the centralized control architecture could easily achieve secondary control objectives at the system level, not just at the local level [61]. Potentially, the centralized control architecture could provide full network transparency, and optimal control solutions, which could not be achieved by the distributed control architecture [67]. Local controllers can always be added within the centralized control architecture, as the backup solution when the communication infrastructure fails [69, 70]. In addition, as shown by recent smart grid projects, DNOs prefer centralized control to distributed control [35, 36]. In this study, centralized control architecture is investigated.

Numerous algorithms have been proposed for the centralized voltage control architecture, and they can be classified in different ways. In this PhD study, these algorithms are categorized into three different groups: rule-based control algorithms, deterministic optimisation algorithms and metaheuristic optimisation algorithms, as shown in Fig. 12.

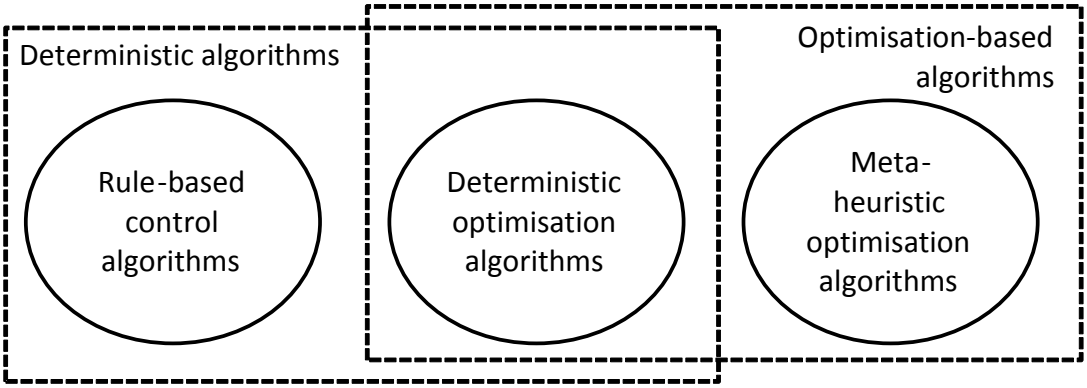

Fig. 12 Categorization of voltage control algorithms for centralized control architecture

Optimisation-based voltage control algorithms are also referred to as voltage optimisation algorithms or Volt/VAR optimisation algorithms [61]. In this study, the term voltage optimisation algorithm is used. In the following, some typical algorithms from these three algorithm groups are reviewed.

2.5.2 Rule-based voltage control algorithms

In this study, algorithms which are not based on optimisation but on control rules are generally seen as rule-based algorithms [68].

In [14], an algorithm is proposed to control the OLTC at the primary substation. The algorithm compares the maximum and minimum voltages within the network with the

network upper and lower voltage limits respectively. The maximum and minimum voltages in the network are determined by a network state estimator, which estimates the network voltages supplied by the primary substation, using real-time measurement, network data and load data. If any voltage violation is found, the algorithm will decide a new target voltage value, and send this value to the automatic voltage control (AVC) relay of the OLTC. The AVC relay can be seen as the RTU in this case. This algorithm was designed for a single OLTC device only, and could not be used to control multiple devices cooperatively. In [71], the DG reactive power is also controlled with the OLTC and more sophisticated rules are implemented. However, the algorithm is still based on specific combinations of voltage control devices.

In [72], a sensitivity factor-based voltage control algorithm is introduced for voltage profile improvement by controlling OLTCs, shunt elements and generator voltages. The control devices are ranked with regard to their efficiency, which is measured according to the voltage sensitivities, current voltage profile and reserve margin of control variables. The most efficient control devices are selected to correct the voltage violations. This algorithm is flexible in terms of integrating different voltage control devices. However, it only considers the efficiency of the voltage control devices from the technical point of view, which may not provide the most cost-efficient solutions in practice.

In [73], a case based reasoning (CBR) technique is used to mitigate the voltage problems in the distribution networks with DG connections by controlling OLTC and the DG's real and reactive powers. The CBR determines the control decisions by comparing the network voltage problems with the cases in its case base library. The case base library is populated by simulation and can be updated according to the feedback from implementation. Potentially, this CBR based algorithm has the chance to provide an optimal or a near-optimal solution without running online optimisation calculation. However, building a sufficient case base library could be time consuming.

In [23], an algorithm is proposed to control EESs and OLTCs and mitigate the voltage problems caused by PV generation. The following rules are defined within this algorithm. During off-peak load time, the OLTC will respond to the voltage rise first and the EES will charge to lessen the OLTC operation stress. During peak load time, the EES will discharge to shave the peak load. It is shown in [23] that the voltage problems can be mitigated and the number of the OLTC tap operations can be expected to be reduced. However, in this paper, only the EES real power capability has been utilized.

The rule-based voltage control algorithms are normally simple, fast and without any non-convergence problems. Normally, it is easy to understand the operational principles behind these algorithms. However, most of these algorithms are designed for networks with only a few control variables. When the number of control variables increases, the determination of control rules can become a complex task [13]. If multiple control objectives are considered, the rules could also become too complex in practical applications. In addition, when optimal solutions are required, rule-based algorithms are not suitable, since they could only guarantee feasible solutions. In these cases, voltage optimisation algorithms could be used.

2.5.3 Voltage optimisation algorithms – problem formulation

The basic idea of voltage algorithms is to formulate and solve voltage control problems as an optimisation problem, which is a subgroup of Optimal Power Flow (OPF) problems [74, 75]. As shown in Fig. 13, a voltage optimisation algorithm includes two essential parts: a problem formulation and an optimisation algorithm.

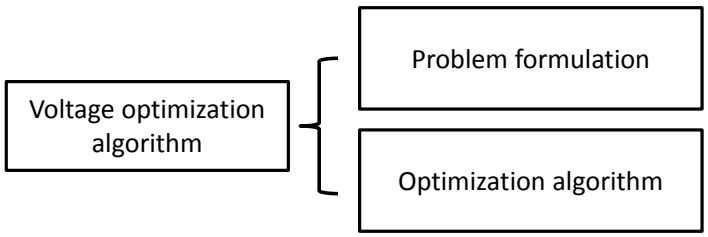

Fig. 13 Structure of voltage optimisation algorithm

Different problem formulations have been proposed for voltage optimisation. These problem formulations can be categorized into the formulations for snapshot control and control scheduling, according to the timescale of the voltage control. For snapshot control, the problem is formulated from a snapshot of the network load and generation condition. As a sub-problem of the optimal power flow problem [74, 75], the problem formulation can be represented by (13) - (15):

$$\min_{\mathbf{u}} f(\mathbf{x},\mathbf{u}) \tag{13}$$

subject to

$$g(\mathbf{x},\mathbf{u}) = 0 \tag{14}$$

$$h(\mathbf{x},\mathbf{u}) \leq 0 \tag{15}$$

where **x** is the vector of state variables (e.g. the magnitude of busbar voltages), whereas **u** is the vector of control variables (e.g. OLTC tap ratios); $\boldsymbol{f}(\bullet)$ is the optimisation objective function(s), $\boldsymbol{g}(\bullet)$ and $\boldsymbol{h}(\bullet)$ are vectors of functions which represent equality and inequality constraints.

The fundamental control objective, maintaining the network voltages within their limits, is always considered as a set of inequality constraints. The other control objectives can be considered as an optimisation objective function, or as a constraint. For example, the control objective, reducing the network losses, is normally formulated as the objective function.

For control scheduling, the problem formulation is based on the forecast load and generation profile for a certain period of time *T*. The problem formulation of control scheduling can be represented by (16) - (18).

$$\min_{\mathbf{u}} \sum_{t=t_0}^{T} f(\mathbf{x},\mathbf{u},t) \tag{16}$$

subject to

$$g(\mathbf{x},\mathbf{u},t) = 0, \forall t \tag{17}$$

$$h(\mathbf{x},\mathbf{u},t) \le 0, \forall t \tag{18}$$

where t is the time point within T; t_0 is the starting time point of T. This control period T (normally, T=24hour) is divided into a set of time points, with a fixed time interval (normally one hour) [76] or using analysis of the forecast load profile [77].

With control scheduling formulation, the time-related control objectives and constraints can be considered. For example, the maximum allowable daily switching operation numbers of the OLTC and MSCs are considered in [76-78]. However, the computation burden of the control scheduling formulation is much heavier than that for the snapshot formulation, although longer computation time can be allowed for control scheduling. The strategy used in [77], which determines the time point by decomposing a daily load forecast into several sequential load levels, could potentially reduce the computation burden. However, when DGs are connected, it may be difficult to determine the time point with this strategy, since various generation levels of DGs may also need to be considered. Also, the voltage control devices can only be operated at the pre-determined time points, and the capability of the voltage

control devices may not be fully used. Moreover, it could be a demanding task to obtain accurate load and generation forecasts [13].

This thesis concentrates on voltage control algorithms that operate in real time and for which the snapshot control formulation is normally adopted.

2.5.4 Deterministic optimisation-based voltage control algorithms

Since the reduced gradient method was proposed in 1968 [79], a number of different deterministic optimisation algorithms have been applied to solve the OPF problems. These algorithms, with different characteristics, have been designed for different OPF applications [74, 80, 81]. Distribution network voltage optimisation has its own characteristics, which need to be considered for the optimisation algorithm selection. As summarized in [61], distribution system voltage control is different from transmission system control regarding the following two aspects. The problem size, in terms of both the network size and the number of control variables, is relatively small. This is because distribution system is divided into electrically subnetworks and the voltage control optimisation is applied to a subnetwork. Also, the number of control variables in the subnetwork is normally less than transmission networks. Most controls in distribution systems are discrete controls and the step sizes of these discrete controls are relatively large, which indicates the necessity of treating the control variables in distribution systems explicitly as discrete variables.

In [82], the voltage control problem is formulated as a linear optimisation problem, which is then solved with a dual linear programming technique. The network loss is minimised, and the network voltages are held within the statutory limits. Linearized sensitivity relationships are employed to model the power flow for distribution networks. The original nonlinear voltage control problem is simplified as a linear problem, which can then be solved with well-developed linear optimisation algorithms, such as the simplex method. These linear algorithms normally have many advantages, such as short computation speed, high reliability and excellent convergence properties [74]. In addition, a global optimal solution can be found for the simplified linear problem. However, this global optimal solution is not guaranteed to be the global optimum of the original nonlinear voltage control problem. In some cases, it may not even be a feasible solution for the original voltage control problem.

In [61], the voltage control problem is formulated as a combinatorial problem, which only includes discrete control variables. This is based on the fact that most of the voltage control variables in conventional distribution networks are discrete. Network loss minimisation is

defined as the optimisation objective. Oriented discrete coordinate descent method is applied to solve this combinatorial problem. The centralized control system, in which the ODCDM is used, has been applied in real distribution networks [83, 84]. ODCDM is efficient in terms of solving combinatorial problems. However, in future distribution networks, not only discrete control variables, but also continuous control variables need to be considered.

In [75], the problem is formulated as a MINLP problem, in which both discrete and continuous control variables are included. Network loss minimisation is defined as the optimisation objective. A primal-dual interior point algorithm (PDIP) is used to solve the optimisation problem. Discrete control variables are treated as continuous variables in the optimisation, and a penalty function is applied to force the discrete control variables to converge at their feasible points. However, the optimisation may get trapped in a local optimum because of the penalty function [85].

Deterministic optimisation algorithms have been successfully applied in voltage control. Additional control objectives can be easily addressed and optimal solutions can be guaranteed. However, these deterministic optimisation algorithms have some common drawbacks, as summarized in previous studies [61, 74, 80, 81, 86-88].

- Deterministic algorithms can only guarantee a local optimal solution, when they are applied to solve non-convex voltage optimisation problems.
- Deterministic algorithms usually treat control variables as either continuous or discrete variables. They cannot be used to solve MINLP problems directly. Certain methods are required to facilitate the application of deterministic algorithms to MINLP problems, such as those in [75].
- Deterministic algorithms can only consider one optimisation objective. If they are used to solve multi-objective optimisation algorithms, these optimisation objectives need to be combined into a single objective function [87], or to be converted to a single objective function and some additional constraints [88]. Multiple runs are required to find results for multi-objective optimisation problems, which is normally time-consuming.

2.5.5 Metaheuristic algorithm-based voltage control algorithm

To address the issues of deterministic algorithms, non-deterministic optimisation algorithms, which are normally referred to as metaheuristic algorithms, have been developed and applied in voltage control. Metaheuristic algorithms can be seen as an iterative process which looks for the optimal solution by intelligently exploring and exploiting the search space [89].

Exploring the search space means the progress to search in a local solution region to find a current good solution in this region. Exploiting the search space means to generate diverse solutions to explore the search space globally. Theoretically, metaheuristic algorithms could find global optimal solutions. At least, they have the chance to escape from local optimal solutions, because of their stochastic nature. Many metaheuristic algorithms can solve MINLP optimisation problems directly. As population-based algorithms, metaheuristic algorithms could solve multi-objective optimisation problems in a single run [86, 90]. It is worth noting here that metaheuristic algorithms are also called as heuristic algorithms in some previous studies. However, the idea that metaheuristic algorithms are developed from heuristic algorithms is becoming more and more popular. The differences between heuristic algorithms and metaheuristic algorithms are discussed in previous studies [91, 92]. A heuristic algorithm is seen as a technique (consisting of a rule or a set of rules), which seeks (and hopefully finds) good solutions at a reasonable computational cost [92]. Heuristic algorithms could provide a good solution but it does not guarantee optimality [92]. Metaheuristic is seen as a top-level strategy that guides an underlying heuristic to looks for optimal solutions [92]. Therefore, metaheuristic is used in this study.

In [70], a genetic algorithm is applied to control the OLTC, step voltage regulator and different shunt components, and to minimise the network losses and the voltage deviation. Imitating the evolution of organisms, a GA employs different operators, such as crossover and mutation, to improve the solution as per the calculated fitness function value. Test results demonstrate that the network voltages can be kept within their limits with the proposed algorithm, and the network loss and voltage deviation can be minimised. In this paper, all the control variables were considered as discrete variables by GA. However, for some shunt components studied in this paper, such as SVC, the control variables are actually continuous.

In [93], the voltage control problem for the distribution networks with DG and microgrids is formulated as a MINLP problem. An evolutionary particle swarm optimisation (EPSO) algorithm is applied to solve this problem. EPSO is a combination of particle swarm optimisation algorithm and evolutionary algorithm. The reactive power from DG, active power and reactive power from microgrids, and the OLTC tap positions are controlled, to minimise the network loss and microgeneration shedding. In this paper, the total real power generation of microgrids have been considered. However, the total real power generation of microgrids was simply added with the network active power losses to create the optimisation objective function.

In [94], the voltage control problem is formulated as a multi-objective optimisation problem, with two objectives, network loss minimisation and voltage deviation minimisation. The OLTCs are adopted as the control variables. Multi-objective metaheuristic algorithms based on the Pareto archived evolution strategy are applied to solve this multi-objective optimisation problem directly. In [95], a three-objective optimisation problem is formulated for voltage control. Network loss minimisation, voltage deviation minimisation and voltage stability index minimisation are considered simultaneously. The generator active power and reactive powers, the stage positions of the compensator capacitors, and the tap ratios of the OLTCs are considered as the control variables. This problem is solved with the opposition-based self-adaptive modified gravitational search algorithm.

The metaheuristic algorithms are normally computationally intensive [90]. Their stochastic nature makes them less predictable, compared with deterministic algorithms. In addition, normally metaheuristic algorithms contain parameters which may need to be adjusted for different problems.

It should be noted that a few hybrid voltage optimisation algorithms have been proposed before [90] and [96], which are combinations of deterministic and metaheuristic optimisation algorithms. These hybrid algorithms have the advantages of both deterministic and metaheuristic optimisation algorithms. Here these hybrid algorithms are not studied separately, because once the stochastic nature from the metaheuristic algorithm is included in the hybrid algorithm, it can also be seen as a metaheuristic algorithm.

2.5.6 Algorithm comparison

As shown in section 2.5.2, 2.5.4 and 2.5.5, the algorithms from these three algorithm groups have their own advantages and disadvantages. Although numerous algorithms have been proposed, these algorithms are normally compared with those from the same group. Only a few studies compare algorithms from different groups [13, 68, 97].

In [97], two deterministic optimisation algorithms are compared with two metaheuristic algorithms regarding general optimal power flow (OPF) problems. Total generation cost minimisation is used as the optimisation objective. It was found that deterministic optimisation algorithms are robust and reliable for medium-size systems (up to 708 buses), even for MINLP problems, offering a theoretical advantage over metaheuristics. Test results in [97] suggested that, metaheuristics have shown satisfactory behaviour in small scale systems, but failed to provide robust solutions in medium-size systems.

In [13, 68], one rule-based algorithm from [71] and one optimisation algorithm from MATLAB Optimisation Toolbox are proposed for voltage control and compared. These two algorithms are evaluated with time domain simulation and long-term evaluation using a distribution network planning procedure. Test results suggest that generally both algorithms can be used for distribution networks with several distributed energy resources, and the most suitable voltage control strategy can be selected by means of statistical distribution network planning. A general deterministic optimisation algorithm is used in [13, 68], but is only able to deal with continuous control variables. However, in distribution networks, many of the control variables are discrete. Although a simple procedure is proposed in [13, 68] to consider the tap ratio of the OLTC at the primary substation, this optimisation algorithm is not suitable for voltage optimisation problems including multiple discrete control variables. In addition, in [13, 68] the optimisation objective is simply defined as the sum of the costs related to network losses and DG curtailment. However, there are more optimisation objectives which should be considered for distribution network voltage control. Sometimes, more than one objective needs to be optimised and these objectives cannot be simply summed together.

In this PhD, the algorithms are categorized into three different groups, and they are evaluated and compared in terms of the voltage control problems discussed in section 2.4.

2.6 Conclusions

In this chapter, novel voltage control techniques, such as EES, are introduced, followed by the discussion of voltage control problems in conventional and future smart distribution networks. Generally, voltage control problems are expected to be more challenging in future distribution networks, with more network load and generation conditions, and more control objectives. More voltage control techniques could introduce more control combinations, from which optimised control solutions could be achieved.

The conventional voltage control architecture, in which only the local measurement is used, may not be sufficient to solve the voltage control problems in future distribution networks. Advanced control architectures and algorithms, enabled by ICTs, have been proposed. In this study, centralized control architecture is investigated. The algorithms proposed can be categorized into three different groups: rule-based algorithms, deterministic voltage optimisation algorithms and metaheuristic voltage optimisation algorithms. These three algorithms have their own advantages and disadvantages, but potentially they could all be used to solve the voltage control problems in future distribution networks.

In this PhD study, the algorithms from these three groups are developed, evaluated and compared in relation to the voltage control problems in future distribution networks. A contribution to knowledge on the design of centralized voltage control algorithms for future smart distribution networks is made.

Chapter 3 Development and Evaluation of Voltage Cost Sensitivity Factor based Voltage Control Algorithm

3.1 Introduction

As shown in Chapter 2, different rule based voltage control algorithms have been developed before [14, 23, 72, 73]. In this chapter, a novel rule based algorithm is proposed, which integrates the control of the primary and secondary transformer OLTCs and EES units located at different voltage levels. This algorithm provides a cost-optimised voltage control solution for the distribution networks with both generation LCTs and load LCTs. In addition, the algorithm provides a holistic solution not only to voltage problems on medium-voltage (MV) and low-voltage networks[98, 99], but also to voltage unbalance problems in LV networks.

Voltage cost sensitivity factor (VCSF) is defined for this algorithm to represent how cost effective each network intervention is, in terms of voltage control. Feeder voltage divergence factor (FVDF) is defined and used, together with percentage voltage unbalance factor (%VUF), as network voltage metrics for networks with large, clustered distributions of LCTs. Voltage sensitivity factors (VSFs) are used to determine the required response from each network intervention. These metrics and factors are then used in the proposed control algorithm to fully realize the capabilities of EES in the system. In the rest of this thesis, this algorithm will be referred to as the VCSF based voltage control algorithm.

This VCSF based voltage control algorithm is evaluated with a real, smart grid enabled case study network. Multiple LCT clusters are connected to both the 20kV MV feeders and the 0.4kV LV feeders of the case study network, to create a case study. Simulation and Power hardware in the loop emulation are utilized to test the operation of the proposed control algorithm.

In the rest of this chapter, the essential definitions used in the VCSF based voltage control algorithm are introduced. The flow chart of this algorithm is presented, followed by the introduction of a case study network and the implementation of the proposed control algorithm in the case study network. The simulation and evaluation results from the application of the control algorithm in the case study are presented. Finally, conclusions are drawn.

3.2 Essential definitions in the VCSF based algorithm

3.2.1 Voltage sensitivity factor

VSF describes the sensitivity of network voltage to the real power P or reactive power Q injection at a certain network busbar, which can be analysed through the use of the Jacobian Matrix [100], as shown by (19).

$$\begin{bmatrix} \Delta\theta_1 \\ \Delta\theta_2 \\ \vdots \\ \Delta\theta_n \\ \Delta V_1 \\ \Delta V_2 \\ \vdots \\ \Delta V_n \end{bmatrix} = \boldsymbol{J}^{-1} \begin{bmatrix} \Delta P_1 \\ \Delta P_2 \\ \vdots \\ \Delta P_n \\ \Delta Q_1 \\ \Delta Q_2 \\ \vdots \\ \Delta Q_n \end{bmatrix} = \begin{bmatrix} \frac{\partial\theta_1}{\partial P_1} & \frac{\partial\theta_1}{\partial P_2} & \cdots & \frac{\partial\theta_1}{\partial P_n} & \frac{\partial\theta_1}{\partial Q_1} & \frac{\partial\theta_1}{\partial Q_2} & \cdots & \frac{\partial\theta_1}{\partial Q_n} \\ \frac{\partial\theta_2}{\partial P_1} & \frac{\partial\theta_2}{\partial P_2} & \cdots & \frac{\partial\theta_2}{\partial P_n} & \frac{\partial\theta_2}{\partial Q_1} & \frac{\partial\theta_2}{\partial Q_2} & \cdots & \frac{\partial\theta_2}{\partial Q_n} \\ \vdots & \vdots & \vdots & \vdots & \vdots & \vdots & \vdots & \vdots \\ \frac{\partial\theta_n}{\partial P_1} & \frac{\partial\theta_n}{\partial P_2} & \cdots & \frac{\partial\theta_n}{\partial P_n} & \frac{\partial\theta_n}{\partial Q_1} & \frac{\partial\theta_n}{\partial Q_2} & \cdots & \frac{\partial\theta_n}{\partial Q_n} \\ \frac{\partial V_1}{\partial P_1} & \frac{\partial V_1}{\partial P_2} & \cdots & \frac{\partial V_1}{\partial P_n} & \frac{\partial V_1}{\partial Q_1} & \frac{\partial V_1}{\partial Q_2} & \cdots & \frac{\partial V_1}{\partial Q_n} \\ \frac{\partial V_2}{\partial P_1} & \frac{\partial V_2}{\partial P_2} & \cdots & \frac{\partial V_2}{\partial P_n} & \frac{\partial V_2}{\partial Q_1} & \frac{\partial V_2}{\partial Q_2} & \cdots & \frac{\partial V_2}{\partial Q_n} \\ \vdots & \vdots & \vdots & \vdots & \vdots & \vdots & \vdots & \vdots \\ \frac{\partial V_n}{\partial P_1} & \frac{\partial V_n}{\partial P_2} & \cdots & \frac{\partial V_n}{\partial P_n} & \frac{\partial V_n}{\partial Q_1} & \frac{\partial V_n}{\partial Q_2} & \cdots & \frac{\partial V_n}{\partial Q_n} \end{bmatrix} \times \begin{bmatrix} \Delta P_1 \\ \Delta P_2 \\ \vdots \\ \Delta P_n \\ \Delta Q_1 \\ \Delta Q_2 \\ \vdots \\ \Delta Q_n \end{bmatrix} \quad (19)$$

where,

$\Delta\theta_i$ change of voltage phase angle of busbar i

ΔV_i change of voltage magnitude of busbar i

$\boldsymbol{J^{-1}}$ inverse of Jacobian matrix

ΔP_i change of real power injection of busbar i

ΔQ_i change of reactive power injection of busbar i

As shown by (19), voltage sensitivity factors relate the change in voltage at a network node due to a change in real or reactive power at the same node, or a particular load or generation node elsewhere in the network. A large voltage sensitivity factor indicates that a variation in nodal real or reactive power leads to a large change in voltage at a specified network location.

The network voltage changes arising from single tap operation of a tapchanger are defined as voltage sensitivity factors of the tapchanger. The voltage sensitivity factor of a single tap operation depends on multiple parameters, such as the voltage at the primary side, load condition, and the tapchanger position before the tap operation. It has been demonstrated by simulation that the tapchanger position before the tap operation has a much larger effect on

the voltage sensitivity factors of a tapchanger than the other parameters. Thus, a lookup table of voltage sensitivity factors based on the tapchanger tap position is used in this voltage control algorithm.

3.2.2 Cost functions

The cost functions are defined to represent the cost of operating the voltage control devices. Here, the cost function of the EES is defined by the capital investment and the cost related to the state of charge (SOC). EES has a time limit if the real power is used for voltage control, due to the finite energy capacity of the energy storage. A target SOC is defined for future application and other functions. Therefore, the cost of the real power for the EES can be calculated by (20).

$$C_{P,EES} = \frac{C_{Capital,EES}}{N_{EES} \times P_{Rating,EES}} + k_{EES} \times \left(SOC_T - SOC\right) \tag{20}$$

where,

$C_{P,\,EES}$	cost of operating EES real power (£/kW)
$C_{Capital,\,EES}$	capital cost of EES (£)
N_{EES}	total charge and discharge cycles of EES
$P_{Rating,\,EES}$	real power rating of EES(kW)
SOC_T	target state-of-charge (SOC) of battery (%)
SOC	state-of-charge (SOC) of battery (%)

And k_{EES} is a factor relating the deviation of SOC from the target SOC to the cost of charging/discharging the EES. The cost becomes larger when the SOC approaches 100% during charging of the EES and also when the SOC approaches 0% during discharging.

Thus, the cost function for real power in an EES is a combination of capital investment and an offset to account for a changing SOC. It is assumed that the net power consumption of the EES is zero and that the cost of exporting and importing are equal. An approximate cost function for the cost of using the reactive power capability of the EES is defined by (21).

$$C_{Q,EES} = \frac{C_{Capital,Converter}}{T_{Lifespan}} \times \frac{T_{Control\ cycle}}{Q_{Rating,EES}} \tag{21}$$

where,

$C_{Q,\ EES}$	cost of operating the EES reactive power (£/kVAr)
$C_{Capital,\ Converter}$	capital cost of converter system of the EES (£)
$Q_{Rating,\ EES}$	reactive power rating of EES(kVAr)
$T_{Lifespan}$	expected lifespan of converter (min)
$T_{Control\ cycle}$	control cycle (min)

In (20) and (21), it is assumed that the EES is operated in full power for both real and reactive power operation cost calculation. It should be noted that the EES is a multifunction network intervention, which means it may be used to provide services in addition to voltage control. Therefore, other control functions, such as power flow management, could also be considered when evaluating the capability of EES to contribute to the network operation in distribution network control systems.

The cost of tapchanger operation is calculated based on the total and remaining lifespan of the tapchanger equipped transformer, the estimated lifetime number of operations and the total cost of replacing the OLTC transformer. The remaining number of tapchanger operations is defined to be a function of the remaining and total lifespan of the transformer and the estimated total number of tapchanger operations, as indicated by (22).

$$N_{\text{OLTC, Remaining}} = \frac{LS_{\text{OLTC, Remaining}}}{LS_{\text{OLTC, Total}}} \times N_{\text{OLTC, Total}} \tag{22}$$

where,

$N_{\text{OLTC, Remaining}}$	remaining operation times of the tapchanger
$N_{\text{OLTC, Total}}$	estimated total operation times of the tapchanger
$LS_{\text{OLTC, Remaining}}$	remaining lifespan of the tapchanger (min)
$LS_{\text{OLTC, Total}}$	total lifespan of the tapchanger (min)

The cost of each OLTC tap operation can be represented by (23).

$$C_{\text{OLTC}} = \frac{C_{\text{OLTC Replacement}}}{N_{\text{OLTC, Remaining}}} \tag{23}$$

where,

C_{OLTC} cost of OLTC tap operation (£)

$C_{OLTC\ Replacement}$ cost of replacing the tapchanger (£)

Different cost functions can be utilized to represent the costs of operating EES and OLTC, based on the control preference of distribution network operators. In addition, the cost functions of other voltage control techniques can be defined and this VCSF based algorithm can be extended by including these voltage control techniques.

3.2.3 Voltage-cost sensitivity factor

VCSF is used to account for the cost associated with the utilization or deployment of a network solution within the proposed control algorithm. The VCSF is derived as a function of the voltage sensitivities and network intervention operating costs. For example, the VCSF of device *j* to node *i*, $VCSF_{ij}$ is defined by (24).

$$VCSF_{ij} = \frac{\Delta V_{ij}}{C_j} \tag{24}$$

where $VCSF_{ij}$ quantifies the voltage change ΔV_{ij} at node *i* with a cost of C_j to operate device *j* to achieve the voltage change $_{\Delta V_{ij}}$ at node *i*.

3.2.4 Feeder voltage divergence factor

In distribution networks, the loads are normally not evenly distributed, and the voltage change varies with the electrical distance. This may create a network voltage condition, in which there are large voltage divergences between the busbars from different feeders, which are downstream of a common mode controlled busbar. The connection of DGs may make the load distribution more uneven. This is explained with an example network shown in Fig. 14. Two MV feeders, Feeder1 and Feeder2, are connected to the same busbar, the voltage of which could be controlled by the primary OLTC transformer. One DG is connected to Feeder1. It is assumed that Feeder1 is lightly loaded and the DG injects a large amount of power into the network, while Feeder2 is heavily loaded.

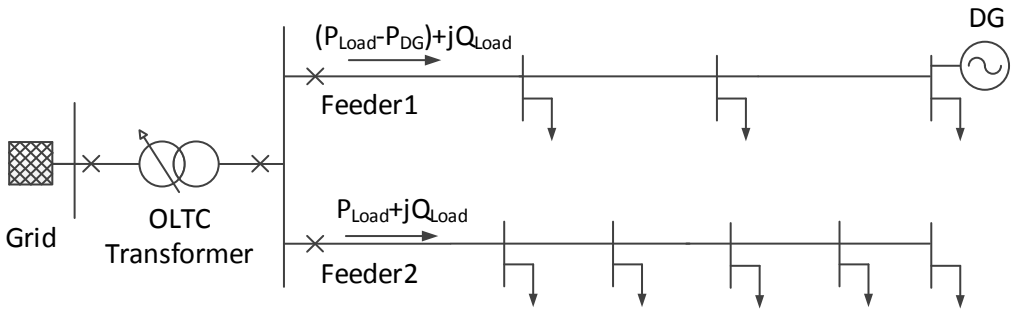

Fig. 14 An example network with uneven distribution of load and generation

Based on the assumptions made for this example network, the voltage profiles of these two feeders are shown in Fig. 15.

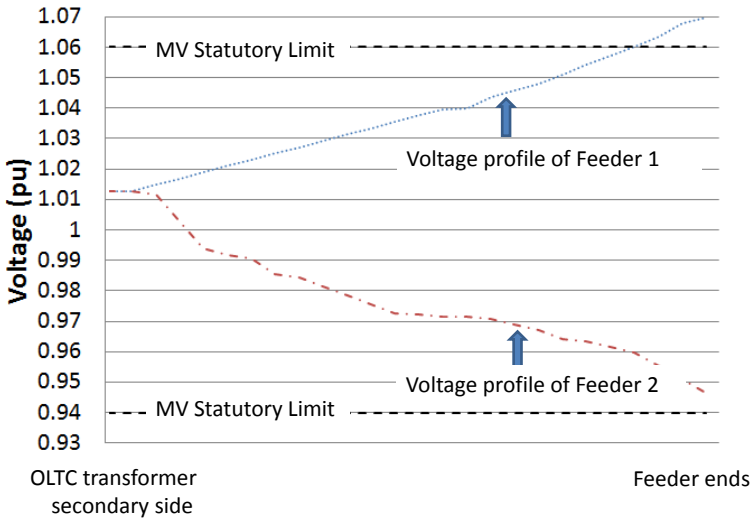

Fig. 15 Voltage profiles of Feeder1 and Feeder2 in the example network

As shown in Fig. 15, there is a large divergence between the busbar voltages at the ends of Feeder1 and Feeder2. Potentially, the voltage at the end of Feeder2 may be reduced below the lower statutory limit, if the primary OLTC transformer tries to mitigate the overvoltage problem at the end of Feeder1 by reducing the voltage at the primary substation.

FVDF is defined by (25), as the maximum feeder voltage divergence among the voltages (pu value) of different feeders, which are downstream of a common mode controlled busbar.

$$FVDF = V_{Highest} - V_{Lowest} \tag{25}$$

where,

$V_{Highest}$ Highest feeder voltage (pu)

V_{Lowest} Lowest feeder voltage (pu)

As illustrated in Fig. 16, the threshold of FVDF is determined with the statutory voltage limits, the maximum voltage variation at the remote ends of the feeders following the upstream tapchanger tap operation and the maximum voltage change at the remote ends of the feeders in a control cycle due to load or generation change. Here it is assumed that both the highest and lowest feeder voltages are found at the remote ends of the feeders. In practice, offline load flow analysis should be utilized to find the locations where the highest and lowest voltages exist, and to derive the maximum voltage changes at these locations.

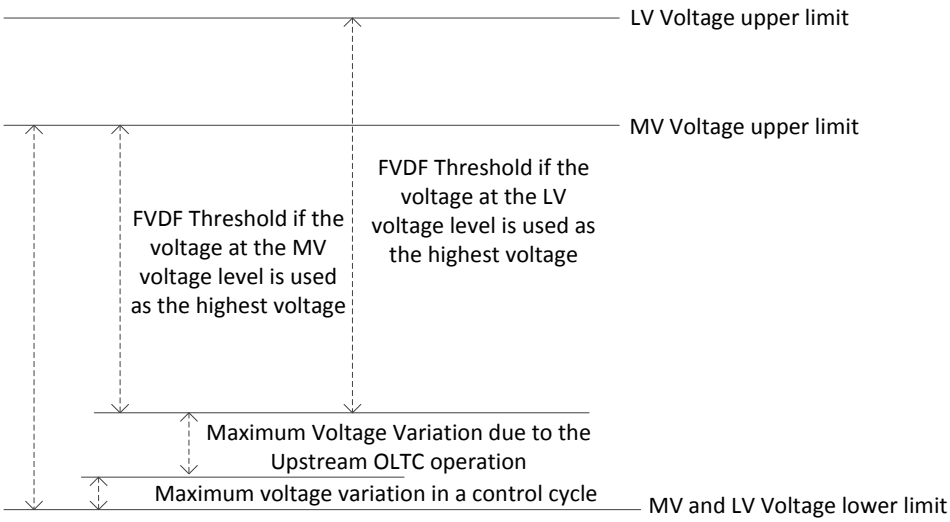

Fig. 16 FVDF threshold determination

3.2.5 Voltage unbalance factor

As introduced in Chapter 1, %VUF is used to represent the unbalance conditions in networks. Here, it is approximated by (9), and also used as a metric in the VCSF based algorithm.

3.3 Development of voltage cost sensitivity factor based voltage control algorithm

Based on the concepts discussed in section 3.2, the control algorithm is now proposed. The control methods for EES and OLTC are then introduced.

3.3.1 Control flow chart

This algorithm monitors and mitigates voltage problems and voltage unbalance problems of the key locations or ‘critical nodes’ of the network. The critical nodes are identified in advance using offline load flow analysis, which utilizes the network model and data. The flow chart of the proposed control algorithm is illustrated in Fig. 17.

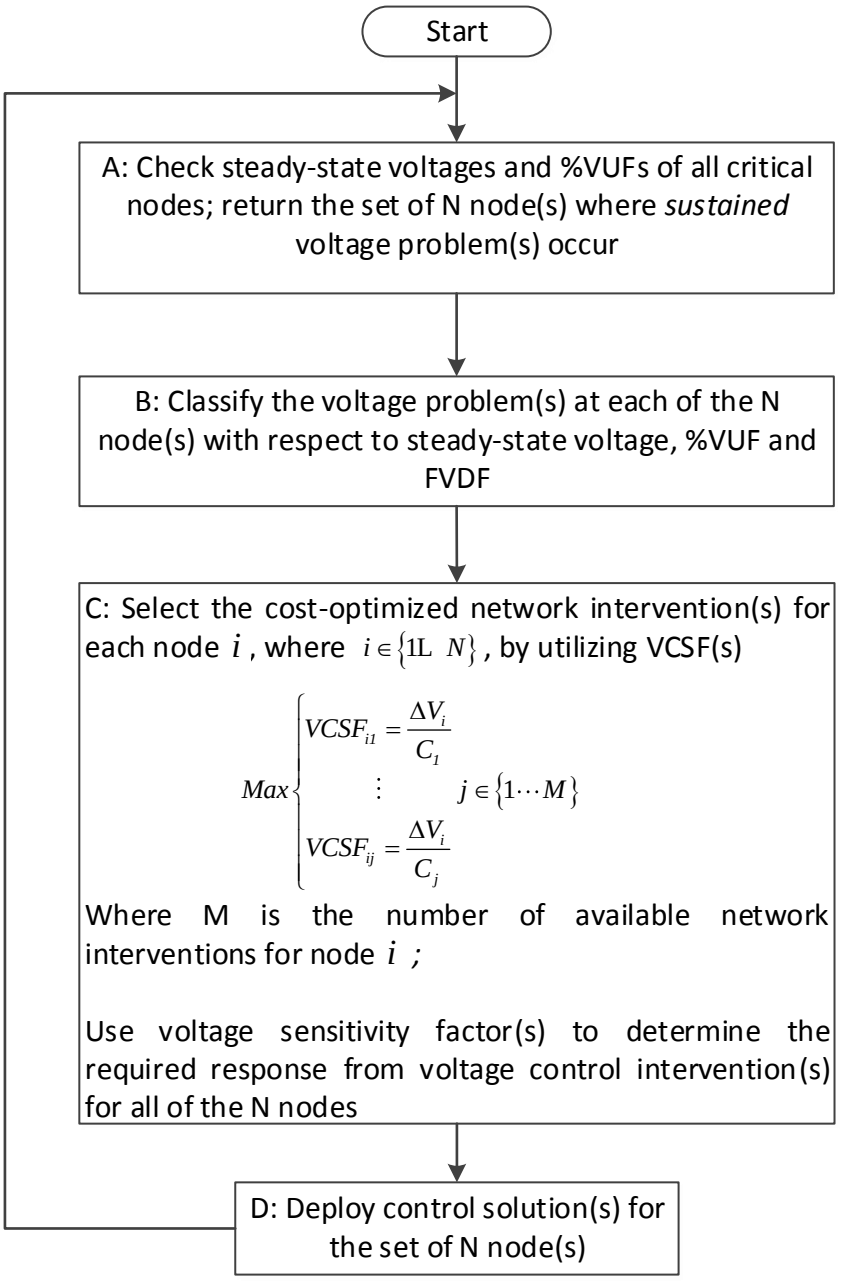

Fig. 17 Flow chart of the VCSF based voltage control algorithm

The following sections describe in further detail the operation of each of the phases in the VCSF based voltage control algorithm.

Phase A: The critical voltage nodes of the network are monitored. A set of N critical nodes, where sustained voltage problems occur, are identified in this phase.

Phase B: The voltage problems at each of the N nodes identified in the previous phase are classified as per Table 2.

Table 2 Voltage Problem Classification

Node *i*, *i*∈N	
Steady-state voltage excursion	None/Overvoltage/Undervoltage
FVDF > Threshold	Yes/No
%VUF > Regulatory Limit	Yes/No

Phase C: The cost-optimised voltage control solutions for voltage problems at each node are identified in this phase. The solutions available to solve each of these problems are determined using the classifications defined in Phase B. The required response from the network solution is determined using voltage sensitivity factors.

For example, if a sustained overvoltage has been detected at node *i* and the FVDF is above the threshold, the set of network solutions available are defined to be those that are located on the feeders with the highest and lowest voltages fed from the common mode controlled busbar. The solution with the largest VCSF in this set will be selected to decrease the FVDF within the threshold. Voltage sensitivity factors will be used to compute the required response from the networks solution to reduce the FVDF.

The change in the voltage ΔV_{isoln}, due to the deployment of the FVDF solution is computed, using voltage sensitivity factors, and is added arithmetically to the voltage excursion ΔV_i to give $\Delta V_i'$. The network solution with the largest VCSF is selected to mitigate the overvoltage. Voltage sensitivity factor is again used to calculate the required response from the second network solution deployed which would reduce $\Delta V_i'$ to zero. If more than one solution is required then the solution available with the next highest VCSF is also selected and the required response calculated using voltage sensitivity factors.

Phase D: Deploy voltage control solutions for the set of N nodes.

This voltage control algorithm has been designed to be particularly appropriate for networks with large, clustered distributions of LCTs, in terms of feeder and phase location. Moreover, it is likely that these clusters become more prevalent, especially in liberalized, unbundled electricity markets, due to the consumer-driven and non-centrally planned connection of LCTs.

3.3.2 EES and OLTC control

Both real power and reactive power of EES can be controlled. Here the real power and reactive power are selected as per the VCSFs, which are based on charging/discharging command, the SOC and the predefined target SOC. The import/export power change of the EES required is determined with the VSF by using (26) and (27).

$$\Delta P_{EES} = (\Delta V_{i,required}) / VSF_{i\_P,EES} \tag{26}$$

$$\Delta Q_{EES} = (\Delta V_{i,required}) / VSF_{i\_Q,EES} \tag{27}$$

where,

ΔP_{EES} required real power change from EES (kW)

ΔQ_{EES} required reactive power change from EES (kVAr)

$\Delta V_{i,required}$ required voltage change at node *i* (pu)

$VSF_{i\_P,EES}$ voltage sensitivity factor of node *i* for the real power of EES (pu/kW)

$VSF_{i\_Q,EES}$ voltage sensitivity factor of node *i* for the reactive power of EES (pu/kVAr)

The required tap position change of OLTC is also determined based on the magnitude of voltage excursion and the VSFs of the OLTC, as represented by (28).

$$\Delta Tap = (\Delta V_{i,required}) / VSF_{i,OLTC} \tag{28}$$

where,

ΔTap required tap position change

$VSF_{i,OLTC}$ voltage sensitivity factor of node *i* for OLTC tap position change

It should be noted that the calculated value for tap position change should be rounded up to the nearest multiple of OLTC step size, since the OLTC tap position is not continuous.

3.4 Case study

3.4.1 Case study network

A rural network, which is located in the northeast of England, and owned by Northern Powergrid, is adopted as the case study network to evaluate the VCSF based algorithm. A

single line diagram of this case study network is illustrated in Fig. 18. A central control infrastructure has been installed on this network.

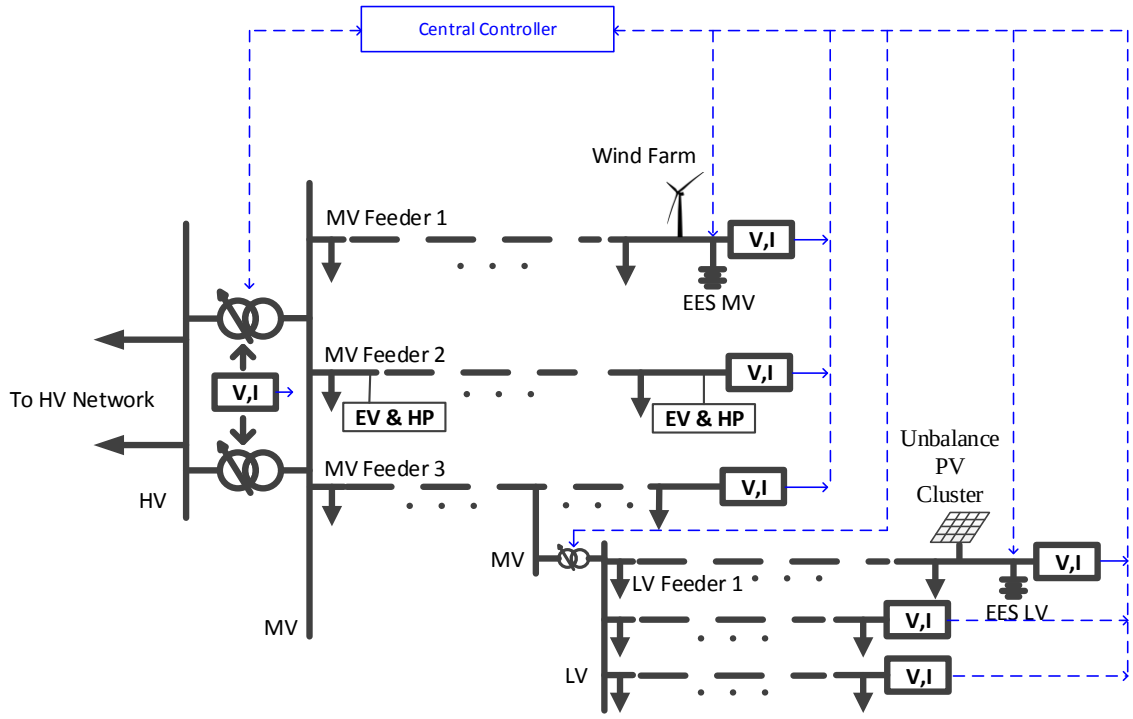

Fig. 18 Case study network and coordinated voltage control algorithm

In order to create a future network test case, a 5MW windfarm has been connected to MV Feeder 1, while a 10% domestic penetration rate of EVs and air source heat pumps (ASHPs) has been evenly distributed along MV Feeder 2. Furthermore, it has been assumed that a PV cluster has been developed on LV Feeder 1, which is one of the LV network feeders connected to MV Feeder 3. The distribution of PV generations across this cluster is uneven across the phases of the feeder. Specifically, PV penetration rates of 38%, 77% and 33% are used for phase A, B and C respectively. The details of the LCT penetrations, which are used to create future network test case, can be found in Table 3.

Table 3 Details of the LCT Penetrations in the Future Network Test Case

Low Carbon Technologies	**Location**	**Penetration level**	**Number of LCT customers**
EV	MV Feeder 2	10%	212
ASHP	MV Feeder 2	10%	212
PV	LV Feeder 1 Phase A	38%	9
	LV Feeder 1 Phase B	77%	17
	LV Feeder 1 Phase C	33%	8

Furthermore, demand profiles of each MV feeder, windfarm generation data, profiles of domestic load and multiple domestic LCTs are used to create the future network test case.

3.4.2 Windfarm generation profile and demand profile

Wind data from 30 windfarms connected to the Northern Powergrid distribution network have been analysed to generate a set of windfarm daily profiles for this work. A typical daily generation profile for the windfarm connected to MV Feeder 1 is derived from this data, as illustrated in Fig. 19.

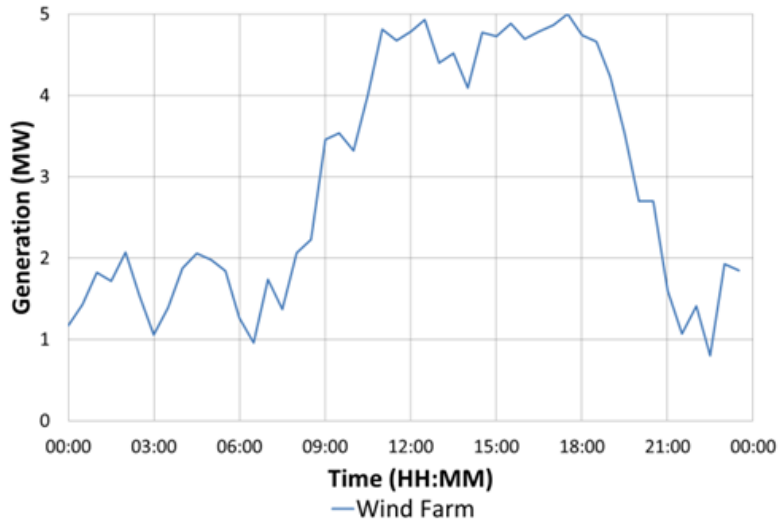

Fig. 19 Daily generation profile of a 5MW windfarm

Typical winter weekday daily demand profiles, from supervisory control and data acquisition (SCADA) data on the case study network, of the MV feeders are illustrated in Fig. 20.

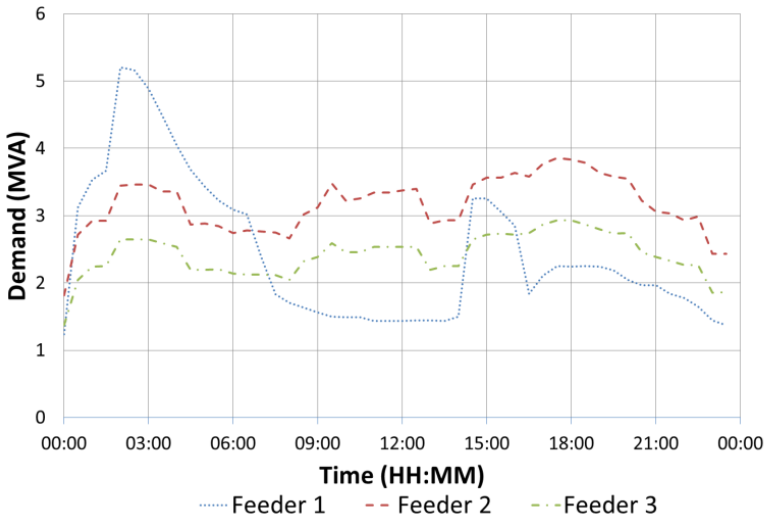

Fig. 20. Demand profiles of MV feeders

It can be seen from Fig. 20 that there are already significant differences between the demands of the three MV feeders, especially between the demand of MV Feeder 1 and that of MV Feeder 2. This is due to the distribution of customers supplied by each feeder. The customer details of each MV feeder are shown in Table 4. It can be seen that 90% of the customers on MV Feeder 1 are domestic customers, and 47% of these domestic customers are Super Tariff Customers. Super Tariff, which gives cheap-rate electricity for 5-6 hours overnight and 2 hours at lunchtime, is popular with customers in the case study area due to the prevalence of electric storage heating.

Table 4 Customer Details of the Case Study Network

MV Feeder	Domestic Customer (%)	Super Tariff Domestic Customer (%)
Feeder 1	90.00%	46.86%
Feeder 2	76.24%	24.68%
Feeder 3	84.59%	26.38%

3.4.3 Smart meter surveys and profile development

Historical data from over 5000 domestic customers, covering the period May 2011 to May 2012 was used to derive typical domestic profiles in the CLNR project. A typical domestic demand profile is used here, as shown in Fig. 21 [101].

The PV generation profile, load profiles of electrical vehicles and heat pumps are also shown in Fig. 21. The PV generation profile is derived from disaggregated enhanced metering data available from CLNR project. The electrical profiles of ASHPs in detached and semi-detached houses are generated based on the thermal profiles, which are derived and aggregated in previous work [102]. A coefficient of performance (COP) value of 2.5 has been assumed. This value has been selected to be in the middle of the range of COP values, which are from 2 to 3, as per previous work [11, 103, 104]. The EV consumer model used in this work was based on profiles developed and reported previously [105].

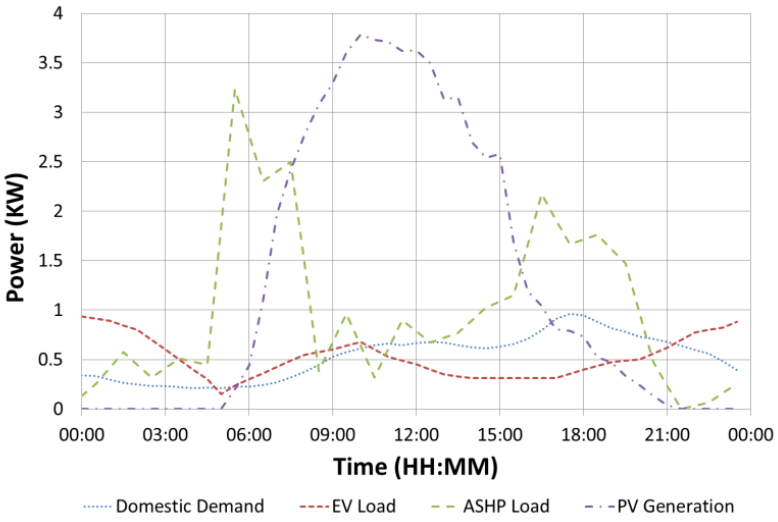

Fig. 21 Profiles of domestic demand, EV, ASHP and PV

It should be noted that the profiles illustrated in Fig. 21 are for individual customers. These profiles are utilized together with the customer numbers from Table 3 and the current demand profiles from Fig. 20 to create the total demand profiles for the case study network shown in Fig. 18.

3.4.4 Control algorithm implementation

As shown in Fig. 18, the central controller, in which this VCSF based algorithm is implemented, monitors the voltages at the ends of MV feeders and critical LV feeders, and sends control commands to network interventions. In this case study, the network solutions include the tapchangers located at the primary substation and the secondary substation to which the PV cluster is connected, as well as the EES units located at the end of MV Feeder 1 and at the end of LV Feeder 1, MV EES and LV EES respectively. The rated power and capacity are 2.5MW and 5MWh for MV EES, and 0.05MW and 0.1MWh for LV EES. It should be noted here that the maximum reactive power of each EES is 0.8 times of the rated power, as per the EES units, which have been installed for the CLNR project.

The VSFs of the EESs and tapchangers were calculated by running an offline load flow analysis with IPSA on a validated network model. The VSFs for critical nodes due to the operation of multiple network interventions are expressed in Table 5. The VSFs of EES are expressed in 1×10^{-3}pu/50kVA. The VSFs of tapchangers are expressed in 1×10^{-3}pu/tap step and are calculated by increasing one tap step from the middle tap position.

Table 5 Voltage sensitivity factors of EES and tapchanger

	MV Feeder 1 End	MV Feeder 2 End	LV Feeder 1 End
MV EES (1x10-3pu/50kVA)	1.092	0.110	0.115
LV EES (1x10-3pu/50kVA)	0.106	0.106	36.577
Primary tapchanger (1x10-3 pu/tap step)	15.000	15.700	16.900
Secondary tapchanger (1x10-3 pu/tap step)	N/A	N/A	21.300

The cost of different network interventions are calculated based on the real information from the case study network in the CLNR project [35], with the approach specified in previous sections. In this case study network, the transformers at the primary substation have been in service for 46 years since their installation in 1966. Therefore, the estimated remaining number of tap change operations is substantially less than that of the new on load tapchanger transformer, which has been recently installed at the secondary substation. In this work, it is assumed that the lifespan and the total estimated number of tap change operations of each transformer are 50 years and 80,000 operations, respectively. Furthermore, the indicative cost of replacing the current primary on load tapchanger equipped transformer is composed of the capital costs of two transformers and all other enabling works, including the costs of civil, installation, commission and protection. The cost of replacing the secondary transformer tapchanger is assumed to be its capital investment. The capital investments and total charge discharge cycles for the storage systems are also from the CLNR project. Therefore, the cost of operating EES and using the tapchanger are detailed in Table 6. The cost of EES real power is based on 50kW and when SOC is at target SOC.

It can be seen from Table 6 that the cost per kW of the MV EES is much smaller than that of the LV EES. That is because the cost per kW of the EES is decreasing with the increasing size. It can also be found that the cost per operation of the primary tapchanger is much greater than that of the secondary tapchanger. This is due to the primary tapchanger being in service for 46 years, while the secondary tapchanger has been recently installed. Therefore the secondary tapchanger has larger numbers of tap change operations remaining than the primary

tapchanger. Additionally, the capital cost of the primary transformer tapchanger is much greater than that of the secondary tapchanger.

Table 6 Cost of EES and tapchanger

Network intervention	**Cost**
MV EES (£/50kW)	18.31
LV EES (£/50kW)	102.90
Primary tapchanger (£/tap step operation)	218.75
Secondary tapchanger (£/tap step operation)	0.33

The VCSFs in this case study were calculated using (24) and the values in Table 5 and Table 6. The resultant VCSFs are detailed in Table 7.

Table 7 Voltage-cost sensitivity factor

	MV Feeder 1 End	MV Feeder 2 End	LV Feeder 1 End
	(1×10^{-6} pu/£)		
MV EES	59.62	5.98	6.29
LV EES	1.03	1.03	355.47
Primary tapchanger	68.79	71.68	77.18
Secondary tapchanger	0.36	0.72	64,212.00

All loads in the case study area are assumed to be constant power loads. Changes in load have been found to have minimal effect on voltage sensitivities [106]. Therefore, the use of offline analysis for calculation of the VCSFs was thought to be valid.

3.5 Algorithm evaluation results

3.5.1 *Voltage control algorithm evaluation approaches*

In order to evaluate this voltage control algorithm comprehensively, two approaches, IPSA2 simulation and network in the loop emulation, have been adopted.

A detailed model of the case study MV network has been developed in IPSA2 and validated against the field trial results from the CLNR project. Annual load flow, which can be performed by scripting in Python, provides the flexibility of long term evaluation. The long term benefits of the EES and this proposed control algorithm can be evaluated by running

annual load flow, using the annual SCADA load data and windfarm generation data from Northern Powergrid.

This voltage control algorithm is also verified and evaluated with the PHIL emulation platform at a smart grid laboratory. With its features of real-time simulation and real LV network, this evaluation approach is able to address many practical issues of the control algorithm, such as tolerance of communication delay or loss. Additionally, the three-phase four wire network representation of the PHIL system can provide a more realistic representation of LV networks than the three-phase representation in IPSA2.

3.5.2 Baseline of future network test case

The simulation results shown in Fig. 22 and the laboratory emulation results in Fig. 23 and Fig. 24, represent the baseline of the future network test case. In this baseline study, two sustained voltage problems and a voltage unbalance problem can be observed to occur concurrently on the network. As shown in Fig. 22, an overvoltage problem, caused by the wind farm, is found on MV Feeder1. This overvoltage problem cannot be solved by the primary transformer tapchanger, without causing undervoltage problem on MV Feeder2. An overvoltage problem and a voltage unbalance problem are found on LV Feeder1, as shown in Fig. 23. The overvoltage and voltage unbalance problems are caused by the high concentrations of unevenly distributed PV generation.

It can be seen from Fig. 22 that during the period where the voltage at the end of MV Feeder 1 is exceeding the upper voltage limit because of the windfarm generation, the voltage at the end of MV Feeder 2 is also close to the lower limit due to the heavy load on this feeder. If a conventional tapchanger based control algorithm with remote end measurements is applied, the primary substation tapchanger will be actuated to mitigate the overvoltage at the end of MV Feeder 1, resulting in voltage violation of the lower limit at the end of MV Feeder 2.

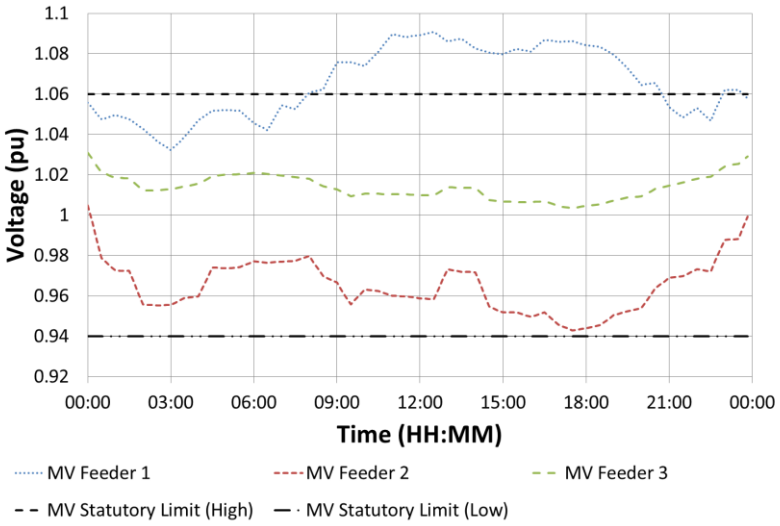

Fig. 22 Voltage profiles at the remote end of MV Feeders – Baseline

Concurrently, in the laboratory, voltage rise and voltage unbalance problems are occurring at the end of LV Feeder 1, where the unbalanced PV cluster is connected, as illustrated in Fig. 23 and Fig. 24. The tapchanger could be operated to mitigate the overvoltage problem at the end of LV Feeder1, but it could not mitigate the voltage unbalance problems.

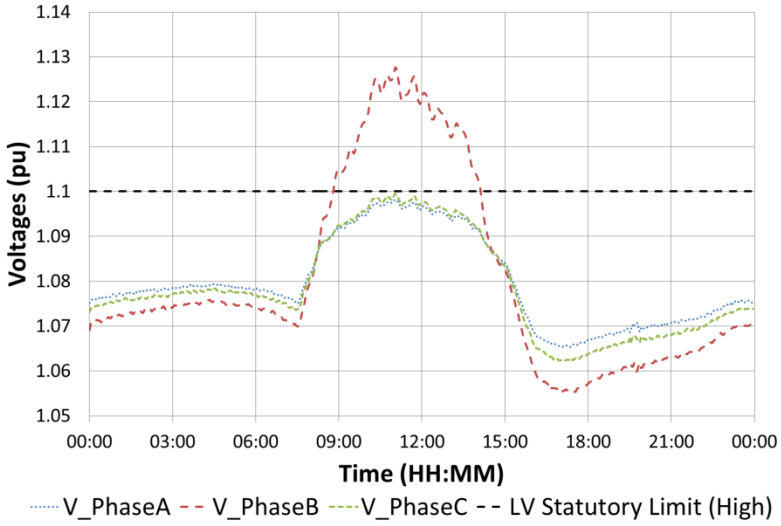

Fig. 23 Three-phase voltage profiles at the end of LV Feeder 1 (Laboratory LV Network) - Baseline

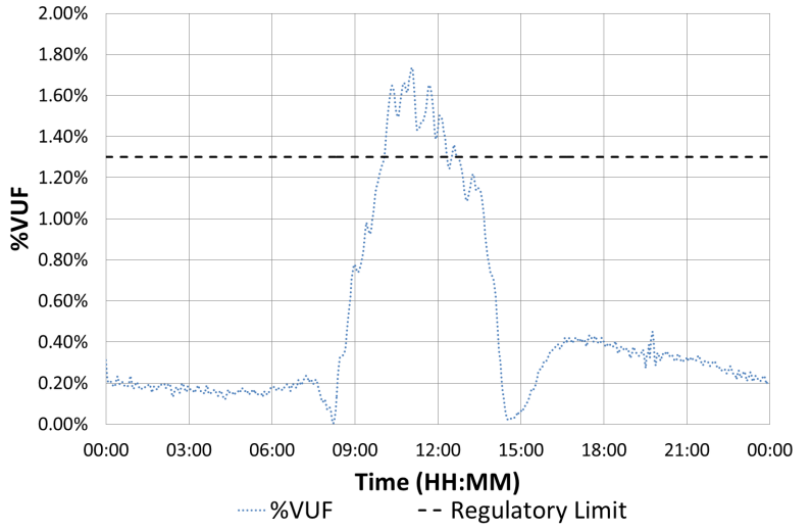

Fig. 24 %VUF at the remote end of LV Feeder 1 (Laboratory LV Network) - Baseline

3.5.3 Desktop implementation and evaluation of the control algorithm

The proposed control algorithm was realized in Python script in conjunction with the validated network model of the case study network in IPSA2. It should be noted here that in IPSA2, the simulation is three-phase balanced, which means the %VUF is not considered in the simulation approach. The simulation results of the proposed control algorithm are shown in Fig. 25, Fig. 26 and Fig. 27. The MV feeder end voltages are illustrated in Fig. 25. The tap position of the primary transformer tapchanger and the power import/export of the MV EES are shown in Fig. 26 and Fig. 27 respectively.

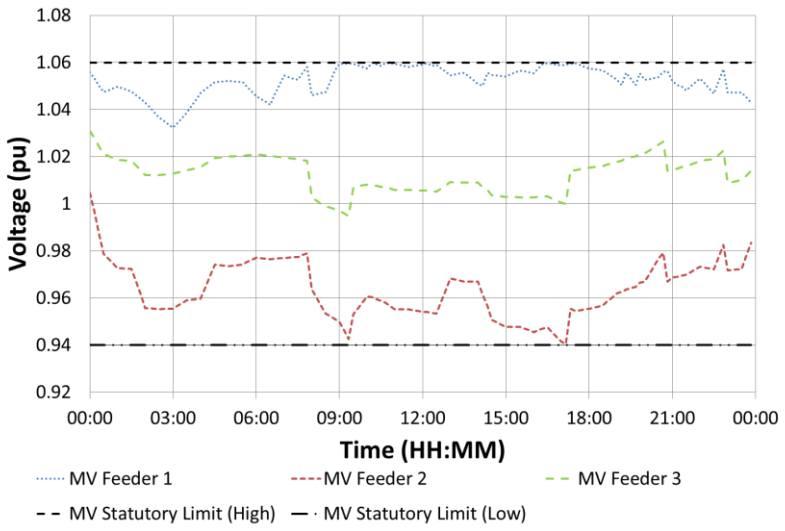

Fig. 25 Voltage profiles at the remote end of MV feeders

It can be seen from Fig. 25 that at 08:00, the voltage at the end of MV Feeder 1 reaches the MV upper statutory voltage limit. This voltage problem is classified, and all the voltage control solutions are available since the FVDF is less than the threshold. Then the voltage

control solution with the largest VCSF is selected, which is the primary tapchanger in this case. The tap position of the primary tapchanger against time is shown in Fig. 26.

At 09:00, the voltage at the end of MV Feeder 1 rises above the MV upper statutory voltage limit. This voltage problem is classified by FVDF being greater than the threshold. As per the control algorithm flowchart in Fig. 17, the MV EES is operated to decrease the FVDF. The overvoltage problem is mitigated at the same time when reducing the FVDF.

At 09:10, the voltage at the end of MV Feeder 2 falls below the MV lower statutory voltage limit. This voltage problem is classified by the FVDF being greater than the threshold. As per the control algorithm flowchart in Fig. 17 the MV EES is operated to decrease the FVDF. The primary transformer tapchanger is used to increase the voltage at the end of MV Feeder 2 as it has the largest VCSF. It should be noted here that this undervoltage at the end of MV Feeder 2 does not happen in the baseline, due to the windfarm generation. If the windfarm generation reduces or is compensated by the EES, an undervoltage is likely to occur.

At 17:10, a similar undervoltage issue is solved. However, between 17:10 and 19:00, the real power is also required as the MV EES is no longer able to reduce FVDF using reactive power only.

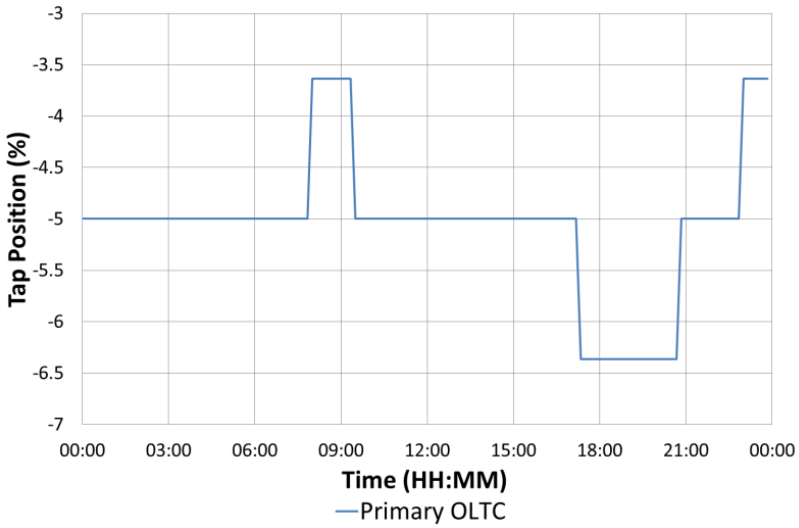

Fig. 26 Tap position of primary transformer tapchanger

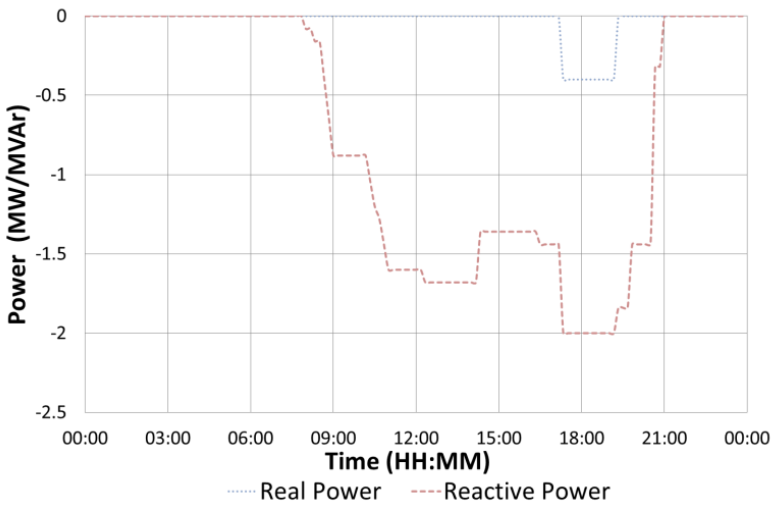

Fig. 27 Real and reactive power import of MV EES

In this test case, the target SOC and the initial SOC of the MV EES are both set to 50%. Therefore the VCSF of reactive power is larger than the VCSF of real power in the test case. As a result, reactive power is selected more frequently than real power, which is illustrated in Fig. 27. This is because the cost of operating the reactive power will not charge/discharge the batteries in the EES, which is cheaper than operating the real power.

At 20:30, the FVDF drops below the threshold. The primary tapchanger lowers the voltage across the feeders, since the primary tapchanger has the largest VCSF at this stage, and thus MV EES is not required.

At 22:50, the voltage at the end of MV Feeder 1 reaches the limit again. At this time, the FVDF is smaller than the FVDF threshold and all the voltage control solutions are available. Then the primary tapchanger is selected to control the voltage.

3.5.4 Laboratory implementation and evaluation of control algorithm

Smart Grid Laboratory Facility

The network diagram of the smart grid laboratory used in this work is shown in Fig. 28. This laboratory hosts an experimental LV network and a Real Time Digital Simulator (RTDS). The experimental network includes multiple LCTs and smart grid technologies. Specifically, a PV generation emulator, a wind generation emulator, an EES unit, a Mitsubishi i-MIEV EV, a Mitsubishi Ecodan ASHP, and controllable load banks are connected to the four wire three-phase experimental network. In addition, the RTDS is connected to the experimental network via a three-phase power amplifier. This arrangement provides the PHIL emulation platform, which enables the real experimental LV network to interact with the large scale network

model simulated by RTDS in real-time. Furthermore, the system is fully instrumented with precise measurement boards, high-speed data communication network, and human-machine graphical interface.

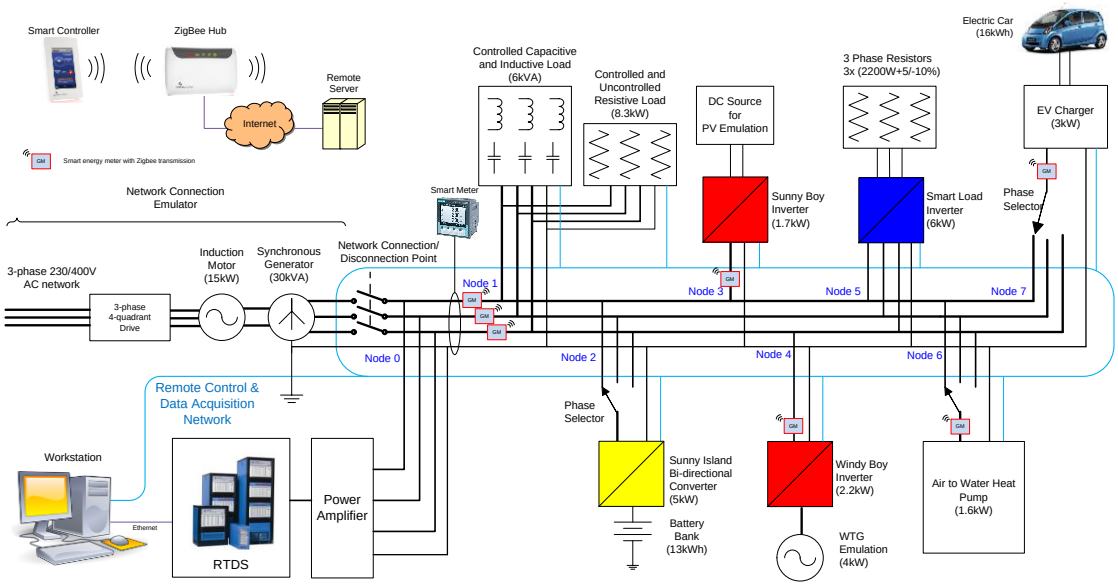

Fig. 28 Smart Grid Laboratory network diagram

Implementation of Power Hardware in the Loop Emulation

The layout of the PHIL emulation platform for this work is shown in Fig. 29. It consists of the PV emulator, the EES unit, the power amplifier, the LV network, the RTDS and the computer.

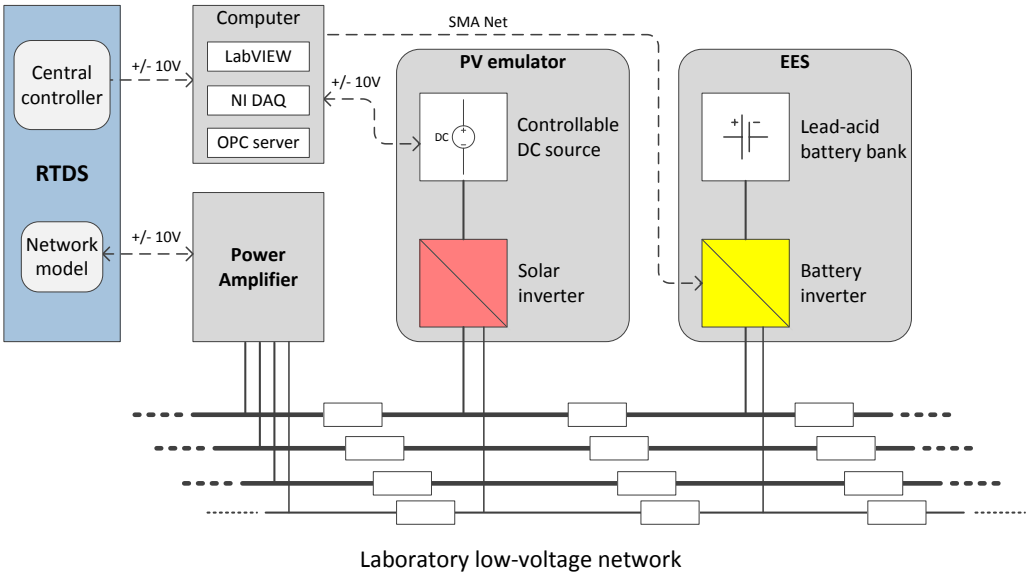

Fig. 29 Layout of PHIL emulation of case study

To realize the interaction between the network model in RTDS and the real LV network, the RTDS transmits ±10V signals, which reflect the instantaneous voltages of the real-time network model, to the three-phase power amplifier. Then the three-phase power powers up the experimental LV network. Simultaneously, instantaneous current monitoring signals from the amplifier are fed back to the RTDS. These current signals are used as inputs of the controllable current source in the RTDS model, to reflect the power exchange between the experimental LV network and the network model in RTDS.

To represent the case study network, the simplified MV network are modelled in RSCAD and validated against the IPSA2 model used in desktop simulation. The majority of the PV cluster feeder, LV Feeder 1, is also modelled in RSCAD, while the remainder of the PV cluster feeder is emulated in the experimental LV network. In total there are 122 customers on the PV cluster feeder. 120 customers are modelled in RSCAD and the two customers at the end of LV Feeder 1 are emulated by the PV emulator in the experimental LV network. Specifically, the PV emulator comprises of a 1.7kW programmable DC power source and an SMA Sunny Boy inverter. The DC power source is interfaced with LabVIEW from National Instruments, which allows it to model the PV generation profile. The PV generation profile modelled in LabVIEW is then used to control the DC power source to emulate the output of a PV array under varying solar irradiance. Here the PV generation profile represents the net PV

generation of two domestic PV customers at the end of LV Feeder 1, which is derived from the PV data and domestic demand data shown in Fig. 21. The laboratory EES is used to emulate the LV EES located at the end of LV Feeder 1. It consists of a 13kWh lead-acid battery bank and a 5kW SMA Sunny Island single-phase converter. This unit is controllable in terms of real and reactive power import/export via LabVIEW.

The proposed control algorithm has also been developed in RSCAD in conjunction with LabVIEW. The developed control algorithm can control the tapchanger in the model simulated in RTDS directly, and it is also able to control the import/export of real and reactive power from the laboratory EES with the help of LabVIEW.

Emulation Results

Concurrently with the voltage problems that are observed on the MV network in simulation, described in the previous section, phase B exceeds the statutory voltage limit in the laboratory at approximately 09:00 as illustrated in Fig. 23. This is due to an increase in PV generation in the model and in the laboratory. Three-phase voltages at the end of LV Feeder 1 in the laboratory are shown in Fig. 30. All the voltage control solutions are identified within the set of available solutions since the calculated %VUF and FVDF are within the threshold. The voltage control solution with the largest VCSF, which is the secondary tapchanger in this case, is selected and deployed. The tap position of the secondary tapchanger, which is realized in the RTDS network model, with respect to time is illustrated in Fig. 31. It should be noted that there are mismatches between simulation and emulation, since three-phase balanced network is modelled in IPSA but four-wire system is adopted in the PHIL emulation.

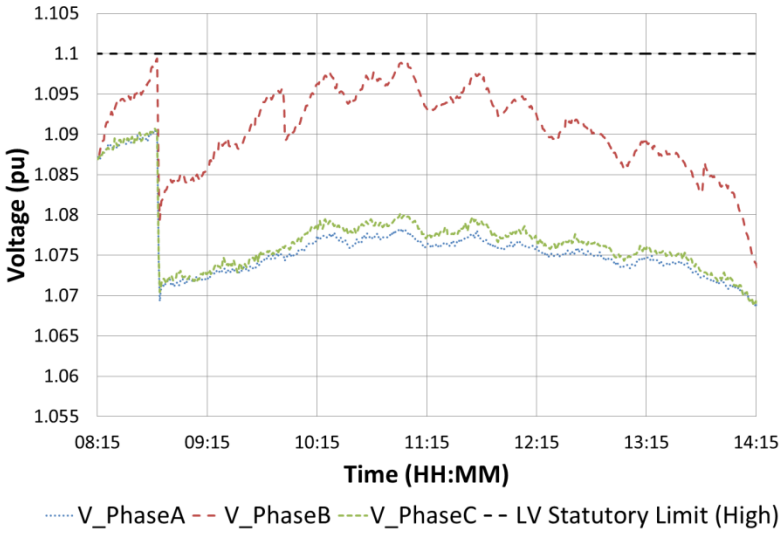

Fig. 30 Three-phase voltage profiles at the remote end of LV Feeder 1 (Laboratory LV Network)

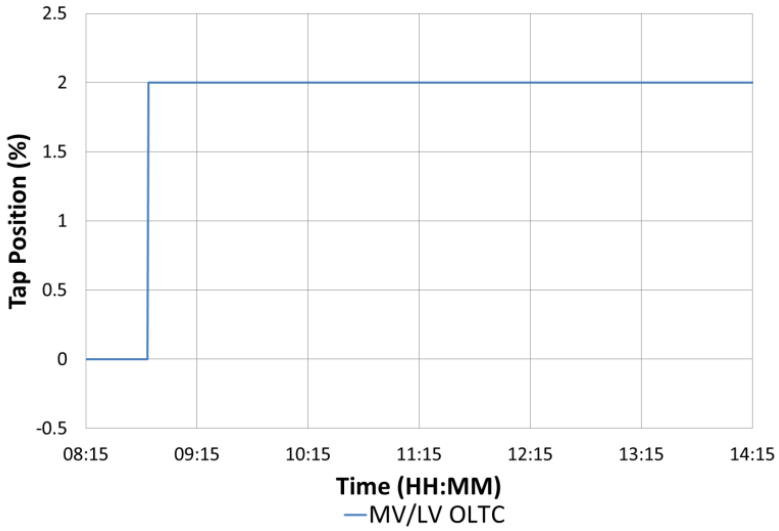

Fig. 31 Tap position of secondary tapchanger (RTDS Network Model)

It can be seen from Fig. 24 that %VUF reaches the regulatory limit at approximately 10:00 due to the uneven distribution of PV generation across the phases on the feeder. The coordinated voltage control algorithm classifies this voltage problem. Phase voltage control solutions, which enable phase voltage control, are available for deployment since the %VUF is greater than the threshold. The LV EES is selected and deployed, which has the largest VCSF among all the phase voltage control solutions. The LV EES in the laboratory begins to import real power, charging the battery, to reduce the %VUF under the limit, as shown in Fig. 32 and Fig. 33.

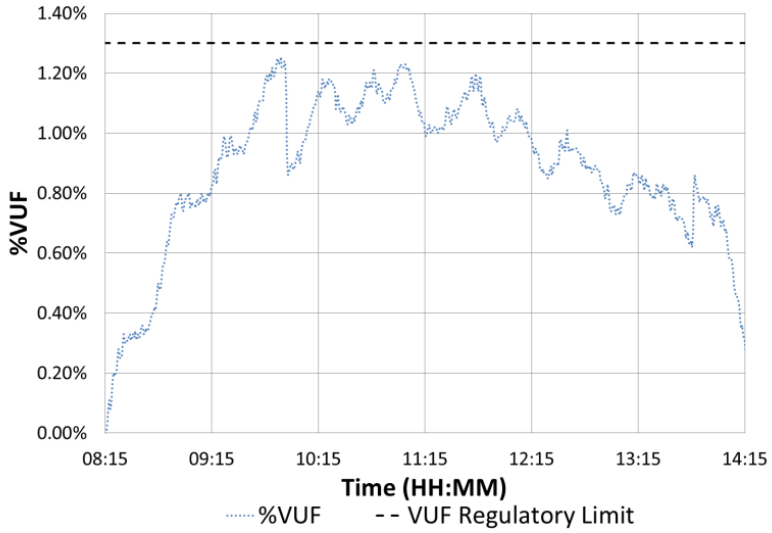

Fig. 32 %VUF at the remote end of LV Feeder 1 (Laboratory LV Network)

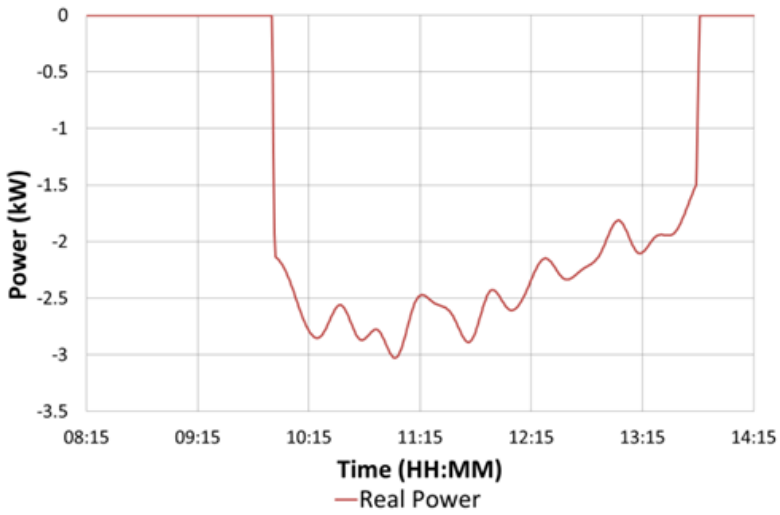

Fig. 33 Real power import of LV EES (Laboratory LV Network)

It should be noted here that in the emulation, only real power of the EES is controlled, since the effect of the reactive power is not significant in the experimental LV network and the VCSF of reactive power is relatively low for this solution. This is due to the low X/R ratio in the experimental LV network. Also, 1.2% is adopted as the %VUF limit in the emulation, instead of 1.3% (the regulatory limit). This is because the EES converter used in the emulation, the SMA Sunny Island converter, is not designed for real time remote control. There is a time delay between the EES converter and the computer, in which the control algorithm is implemented. The time delays can be over 5 minutes. To prevent the %VUF exceeding the regulatory limit, a safe margin of 0.1% is applied in this case. Of course, this is not necessary if the time delays can be reduced.

3.6 Conclusions

A rule based voltage control algorithm is proposed in this chapter for future distribution networks with large, clustered distributions of LCTs, in terms of both feeder and phase location. This proposed control algorithm can control OLTCs and EESs to solve the voltage problems caused by the large, clustered distributions of LCTs. It can determine and deploy cost optimised solutions for concurrent MV and LV voltage problems, across a range of classifications, simultaneously.

This algorithm is based on a range of network factors and metrics (VSF, VCSF, FVDF and %VUF). VCSF is derived from voltage sensitivity factors and cost functions for EES and OLTC equipped transformers. VCSF is used to select the cost-optimised voltage control solution, while VSF is utilized to determine the required response of the selected solution. FVDF is introduced in this work as a metric for the maximum voltage difference between feeders downstream of a common controlled busbar. FVDF is used in conjunction with %VUF in the proposed control algorithm to classify the voltage problems and identify available voltage control solutions.

A case study, in which a credible future network test case is proposed using a validated model of a real GB smart grid trial distribution network, equipped with multiple EES units, OLTC equipped transformers under supervisory control, is used to evaluate the algorithm. In this future network test case, clustered concentrations of load and generation LCTs, in terms of both feeder and phase location, are deployed on the case study network. Desktop simulation and laboratory based PHIL emulation are jointly conducted to evaluate the control algorithm.

The analysis and results from complementary simulation and PHIL emulation show that this VCSF based algorithm can provide cost-optimised voltage control solutions for the distribution networks with highly clustered distributions of load and generation LCTs. This control algorithm can solve steady-state voltage excursions and %VUF excursions, which are occurring concurrently at two MV nodes and a LV node in the case study network. In addition, as the algorithm is cognizant of the costs associated with deploying each network solution, it could reduce costs and increase the operating life of equipment. For example, tapchanger operations are likely to be reduced under this algorithm as the cost functions can reflect the age of the devices.

This proposed VCSF based algorithm is relatively simple and fast, and it does not have the problems of non-convergence. However, the VCSF based algorithm also has some drawbacks. It relies on voltage sensitivity factor, which is not constant but varies with the network

topology change, and the change of network voltage and load conditions. This could be solved with the application of VSF lookup tables, which can be developed via offline analysis, or real time sensitivity calculation.

The VCSF based algorithm cannot guarantee optimal solutions, although it is able to reduce the control costs. In addition, if multiple control objectives need to be considered, the rules could become too complex. Voltage optimisation algorithms, which are able to address these problems, will be discussed from next chapter.

Chapter 4 Development of Oriented Discrete Coordinate Descent Method based Voltage Control Algorithm

4.1 Introduction

In this chapter, a deterministic voltage optimisation algorithm, based on oriented discrete coordinate descent method, is introduced. ODCDM was proposed to control voltage for conventional distribution networks in [61]. However, only conventional voltage control techniques and network loss minimisation were considered before. In this PhD study, ODCDM has been extended to control voltage for future distribution networks. Specifically, both conventional and novel voltage control techniques have been considered. In addition, multiple optimisation objectives have been studied. .

In the rest of this chapter, the problem formulation for voltage optimisation is described. The implementation of the original ODCDM based voltage control algorithm is introduced, and the extensions of this algorithm to solve MINLP problems and multi-objective problems are discussed. A simple case study is presented to demonstrate the basic mechanism of the developed algorithm. The algorithm is then further validated with field trial results from the Customer-led Network Revolution Project, in which the ODCDM based control algorithm is applied in real networks. Finally, conclusions are drawn.

4.2 Problem formulation for voltage optimisation algorithms

The general problem formulation for voltage optimisation, which is shown in Chapter 2, can be specified by (29) - (32), for distribution network voltage optimisation.

$$\min_{\mathbf{u}} f(\mathbf{x},\mathbf{u}) \tag{29}$$

s.t.

$$\underline{V_i} \sum_{j=1}^{N_{busbar}} \underline{Y_{ij}}\underline{V_j} = P_i - jQ_i, i = 1,\ldots,N_{busbar} \tag{30}$$

$$u_i^{\min} \le u_i \le u_i^{\max}, i = 1,\ldots,N_u \tag{31}$$

$$V_i^{\min} < V_i < V_i^{\max}, i = 1,\ldots,N_{busbar} \tag{32}$$

where

$\underline{V_i}$ voltage at bus i

$\underline{V}_j$	voltage at bus *j*
$\underline{Y}_{ij}$	element of admittance matrix **Y**
P_i	net injected real power at busbar *i*
Q_i	net injected reactive power at busbar *i*
u_i	control variable *i*
$u_i^{\min}$	lowest value of control variable *i*
$u_i^{\max}$	highest value of control variable *i*
$V_i^{\min}$	lowest limit of busbar voltage *i*
$V_i^{\max}$	upper limit of busbar voltage *i*

The components in this problem formulation are discussed in the following.

4.2.1 Optimisation objective function

The optimisation objective function(s) is represented by (29), formulated to represent secondary control objective(s). Regarding the number of optimisation objective functions, voltage optimisation can be classified as single-objective voltage optimisation or multi-objective voltage optimisation. The optimisation objective function is a scalar function for a single-objective optimisation problem, while for a multi-objective optimisation problem, the optimisation objective function is a vector, which includes a set of scalar functions, as shown by (33).

$$f = \min f_i, i = 1, \ldots, N_{Obj} \tag{33}$$

where *fi* is the ith objective function and N_{Obj} is the number of optimisation objective functions.

4.2.2 Equality constraints

The equality constraints for voltage optimisation are the network flow equations, which are used to model the relationship between the network voltages and the net injected real and reactive powers at different busbars. Nonlinear node power equations are normally used, as represented by (30) [107].

4.2.3 Inequality constraints

The inequality constraints include the limits for control variables and state variables. Control variables are the variables which can be controlled directly, such as OLTC tap positions. The operation constraints of the control variables, which depend on specific networks, are generally represented by (31). Network voltages and their limits, are also formulated as a set of inequality constraints, as represented by (32), to represent the fundamental control objective, maintaining network voltages within their statutory limits. It should be noted that besides network voltages, some other state variables and control objectives could also be considered as inequality constraints. For example, maintaining the current flowing through network branches within the thermal limits can also be considered as a set of inequality constraints. This PhD study concentrates on voltage control, and thus only voltage constraints represented by (32) are considered.

Voltage optimisation algorithms are desired to find feasible solutions, with that all the equality and inequality constraints can be met. Also, the solutions are also expected to minimise the optimisation objective functions.

4.3 ODCDM based voltage control algorithm

4.3.1 Original ODCDM based voltage control algorithm

The original ODCDM based voltage control algorithm is introduced here. The flow chart of this algorithm is shown in Fig. 34. As per the flow chart in Fig. 34, the key procedures of the ODCDM based voltage control algorithm are discussed as follows:

- The initial value of the optimisation objective function is computed based on a starting point (SP). Normally load flow calculation is needed to calculate the state variables, which are used to formulate the objective function and constraints, such as busbar voltages. In practice, the starting point is normally the settings of the voltage control devices before the optimisation;
- An internal iteration loop is performed, to compute the partial derivatives of the objective function with respect to all n control variables individually and to find the largest partial derivative. The largest partial derivative then decides how the solution will be changed;
- Another iteration loop (outer loop) is conducted outside the internal iteration loop, to keep improving the objective function until the pre-defined stop criteria are met.

It should be noted that for ODCDM, the SP only includes control variables. This is contrast to some other algorithms, for which the SP could also include the initial values of the state

variables in the power flow equations [108]. For ODCDM, these values are not required because the load flow equations are solved with a given set of control variables, and the initial values for the state variables do not affect the optimisation progress.

It should also be noted that the partial derivative used here is different from that from calculus, which is used for continuous variables. Here the partial derivatives are calculated directly by changing the control variable by one step size and calculating the difference between the objective functions. The calculation procedure can be represented by (34):

$$\frac{\partial F^k}{\partial X_i^k} = \frac{F^{k+1} - F^k}{X_i^{k+1} - X_i^k} \tag{34}$$

where

F^k, F^{k+1} objective function values before and after the control variable change;

X_i^k, X_i^{k+1} control variable value before and after the control variable change, normally the difference between X_i^k and X_i^{k+1} is the step size of the control variable X_i.

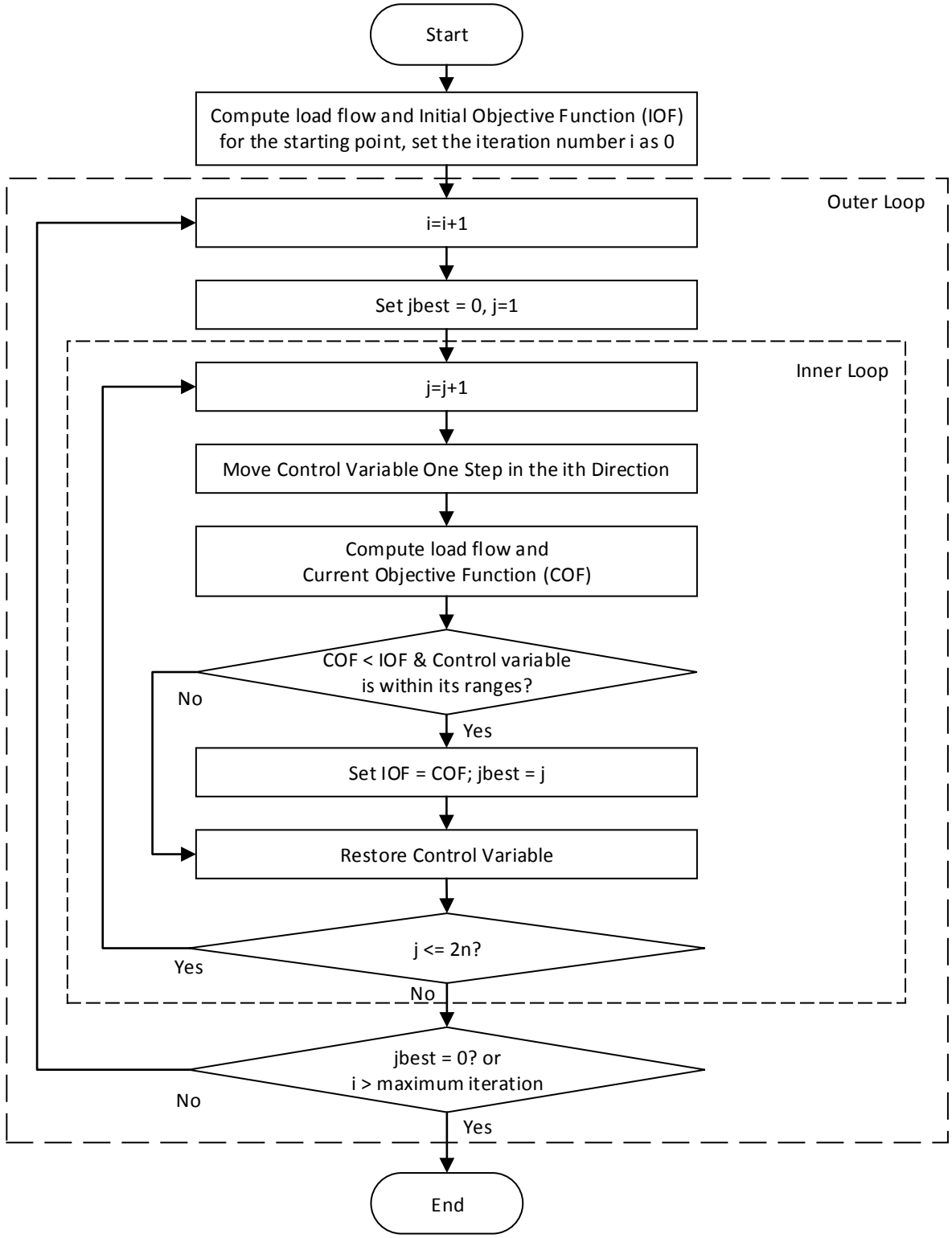

Fig. 34 Flow Chart of GUS Control

As specified in section 4.2.3, different inequality constraints need to be considered for the network safe operation, such as the statutory voltage limits. For ODCDM, the constraints are integrated into the objective function as a penalty function. Therefore, the objective function F is actually the sum of the optimisation objective function f_{obj} and the penalty function $f_{penalty}$, as demonstrated by (35):

$$F = f_{obj} + f_{penalty} \tag{35}$$

Different penalty functions can be adopted to represent the penalty caused due to the violation of the inequality constraints. The basic idea, as shown by Fig. 35, is to add a large penalty value to the objective function if the constraint of variable x is violated, while add zero penalty if the constraint is not violated.

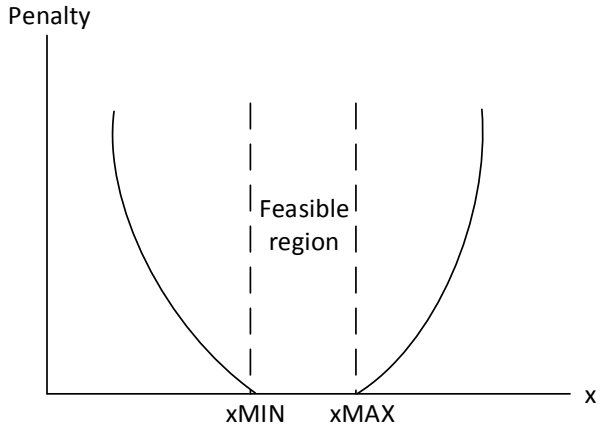

Fig. 35 Penalty Function

Here, a sum of quadratic function based step functions are used to represent the penalty, as shown by (36).

$$f_{penalty} = \sum_{i=1}^{n} \begin{cases} s_i \left(x_i - x_i^{\min} \right)^2, x_i < x_i^{\min} \\ 0, x_i^{\min} \le x_i \le x_i^{\max} \\ s_i \left(x_i^{\max} - x_i \right)^2, x_i > x_i^{\max} \end{cases} \tag{36}$$

Where x_i is a variable which needs to be kept within certain limits, $x_i^{\max}$ and $x_i^{\min}$ are the upper and lower limits for x_i, and s_i is the penalty coefficient, which reflects the importance of the constraint related to x_i. For example, x_i can be the voltage magnitude of one busbar, while $x_i^{\max}$ and $x_i^{\min}$ can be the statutory voltage limits for this busbar. The constraint can also be a function of x_i. The same idea shown by (36) and Fig. 35 can still be used.

4.3.2 Application of ODCDM to MINLP problems

As discussed before, the optimisation problem formulated for distribution network voltage control could be a MINLP problem, in which both discrete control variables and continuous control variables are involved. Normally, mathematical optimisation algorithms are designed

for problems with only continuous control variables or with only discrete control variables, and cannot be used to solve MINLP problems directly.

To apply ODCDM to MINLP problems, one possible approach is to discretize the continuous variables with certain step size, which is adopted in the CLNR project [109]. The selection of the step size may affect the partial derivative defined in (34), and in turn affect the performance of the ODCDM algorithm. This will be demonstrated and further discussed with the test results in Chapter 6.

4.3.3 *Application of ODCDM to Multi-objective optimisation problems*

Sometimes, multiple objectives need to be optimised simultaneously in distribution network voltage control. The optimisation objective functions are represented by (33). For a multi-objective optimisation problem, any two solutions x_1 and x_2 can have one of the following two possible relationships: one solution dominates the other solution or none solution dominates the other solution. Solution x_1 is said to dominate another solution x_2 if the conditions defined by (36) are satisfied, which are:

- At least one objective for x_1 is better than that for x_2;
- For all objectives, x_1 is as good as x_2.

$$\forall i \in \left[1, N_{Obj}\right], f_i(x_1) \le f_i\left(x_2\right) and \exists j, f_j(x_1) < f_j\left(x_2\right) \tag{36}$$

The solutions, which are not dominated by any other solution in the entire solution space, are Pareto optimal solutions and constitute the Pareto set. The image of the Pareto set, i.e., the image of all the Pareto optimal solutions, is called Pareto front.

Deterministic algorithms, such as ODCDM, are single objective optimisation algorithm, and they can only find a solution in a single run. As summarized in [110], different methods have been developed to facilitate deterministic algorithms to solve the multi-objective optimisation problems. One popular method, the weighted sum method, is introduced in the following. The basic idea of the weighted sum method is to convert the multiple objectives from (33) into a single objective with a linear function, as specified by (37).

$$f = \sum_{i=1}^{N_{Obj}} w_i f_i \tag{37}$$

where w_i is the weighting coefficient, representing the priority of the objective function f_i.

The weighted sum method has been adopted in many previous voltage control studies. For example, the objectives, network loss minimisation and voltage deviation minimisation, are summed together in [70], with the weighting coefficients decided by trial and error. In [111], three non-negative weighting coefficients are selected to combine three different optimisation objectives into a single objective function. In this PhD study, weighted sum method is also applied with ODCDM to solve multi-objective optimisation problems. Of course, there are some other methods, which can also be used with ODCDM to solve the multi-objective optimisation problems efficiently. For example, it is possible to minimise one of the objectives from *f*, and leave the rest of objectives as constraints. This approach has been applied to minimise the network loss and generator reactive power utilization for transmission network reactive power management [88]. Although some of them may be more efficient than weighted sum method in some applications, these methods are not studied here. This is because weighted sum method is the most widely used method for voltage control. Moreover, weighted sum method is able to represent the basic principle behind these methods, which is to convert the multi-objective optimisation problems into a single-objective optimisation problem [86]. This means to find the Pareto front, multiple runs are required.

Another issue that should be noted here is that if switching number minimisation is considered as one optimisation objective, sometimes ODCDM may be able to consider it as a constraint instead of one objective naturally. This is because for ODCDM, only one switching operation is carried out in each iteration. This will be further explained in the case study chapter.

4.4 Initial evaluation of the ODCDM based voltage control algorithm

4.4.1 Case study network

A case study network is adopted here to demonstrate the principle of the ODCDM algorithm, based on the IEEE 33 bubsar network from [112]. The network data can be found in Appendix A-1. In this case study network, one OLTC transformer and five MSCs are applied to the original network. The details of these voltage control devices are shown in Table 8. Here a standard network is used due to the following reasons. Standard networks are normally used for voltage optimisation studies, since it is easy for other researchers to duplicate the test cases and then evaluate and compare different algorithms with same test cases. Also, standard networks have multiple voltage control devices, which make it more necessary and potentially more beneficial to apply voltage optimisation algorithms.

Table 8 Voltage Control Devices in the Case Study Network

Control Device	Location	Step size	Range	Total step number
OLTC	From busbar 1 to busbar 2	1.25%	-5% - +5%	9
MSC1	Busbar 8	0.1MVAr	0-0.7MVAr	8
MSC2	Busbar 15	0.1MVAr	0-0.7MVAr	8
MSC3	Busbar 24	0.1MVAr	0-0.7MVAr	8
MSC4	Busbar 29	0.1MVAr	0-0.7MVAr	8
MSC5	Busbar 33	0.1MVAr	0-0.7MVAr	8

The network diagram is shown in Fig. 36.

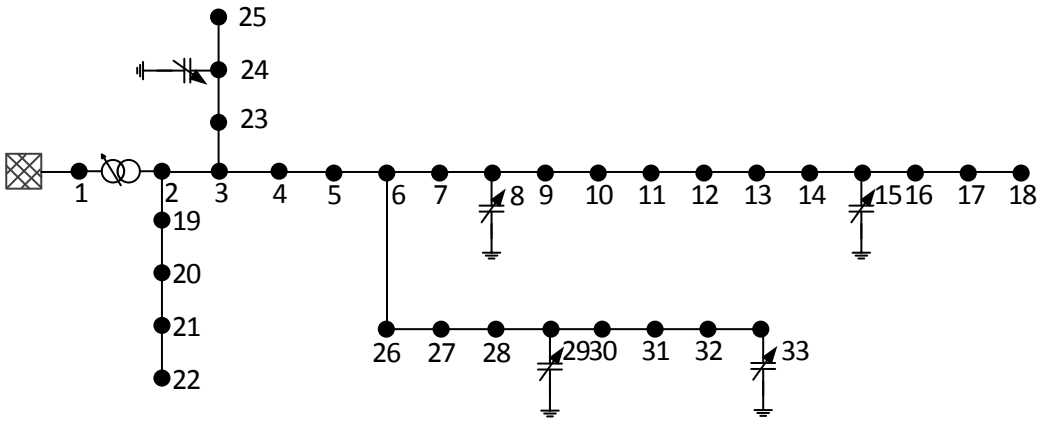

Fig. 36 Case Study Network

The case study network is modelled in IPSA2. The ODCDM algorithm is developed with Python and the load flow engine in IPSA2, based on the flow chart shown in Fig. 34.

4.4.2 Initial case study result

The original load of the case study network is used. In the initial study, network loss minimisation is selected as the optimisation objective and voltage limits, 0.94pu and 1.06pu, are adopted. Network loss minimisation is one widely used optimisation objective for voltage optimisation in conventional distribution networks [52, 56, 61, 113]. The network loss is the sum of the real power losses on all the network branches, as represented by(38).

$$f_{Loss} = \sum_{n=1}^{N_{branch}} g_{ij}(V_i^2 + V_j^2 - 2V_iV_j\cos\delta_{ij}) \tag{38}$$

where,

N_{branch} Number of network branches

g_{ij} Conductance of the branch between busbar i and j

V_i Voltage magnitude of busbar *i*

V_j Voltage magnitude of busbar *j*

δ_{ij} The phase angle between the voltages of busbar *i* and busbar *j*

As mentioned previously, a SP is needed for the ODCDM based control algorithm and different SP may lead to a different final result. Two starting points, shown in Table 9, are used to demonstrate how SP affects the algorithm performance. In practice, the SP is selected as the current positions of the voltage control devices, such as the tap position of the OLTC transformer and the stage position of the MSC.

Table 9 Starting Points used for ODCDM initial evaluation

Starting Point Index	Starting Point					
	OLTC	MSC1	MSC2	MSC3	MSC4	MSC5
	Unit: %	Unit: MVAr				
SP1	0	0	0	0	0	0
SP2	-2.5	0	0.4	0.5	0.3	0.3

For the SP1, the convergence curve of the objective function is shown in Fig. 37. As shown in Fig. 37, the sum of the objective function and penalty is decreased significantly at the first two iterations. This is because in the first two iterations, there are voltage constraints violations in the network, which add a large penalty number to the objective function.

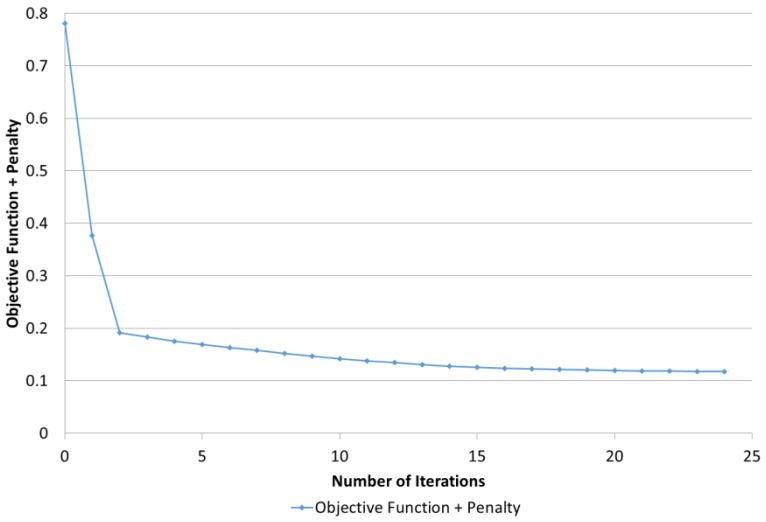

Fig. 37 Convergence curve of ODCDM – test with SP1

Table 10 Result Achieved with Two Different Starting Points

Starting Point Index	Final Solution						Network Loss
	OLTC	MSC1	MSC2	MSC3	MSC4	MSC5	
	Unit: %	Unit: MVAr					MW
SP1	-5	0.4	0.2	0.5	0.6	0.3	0.11793
SP2	-5	0.3	0.3	0.5	0.6	0.3	0.11803

The largest partial derivative, which stands for the largest objective improvement, is shown in Fig. 38, and the corresponding control variable change during the optimisation process is shown in Fig. 39.

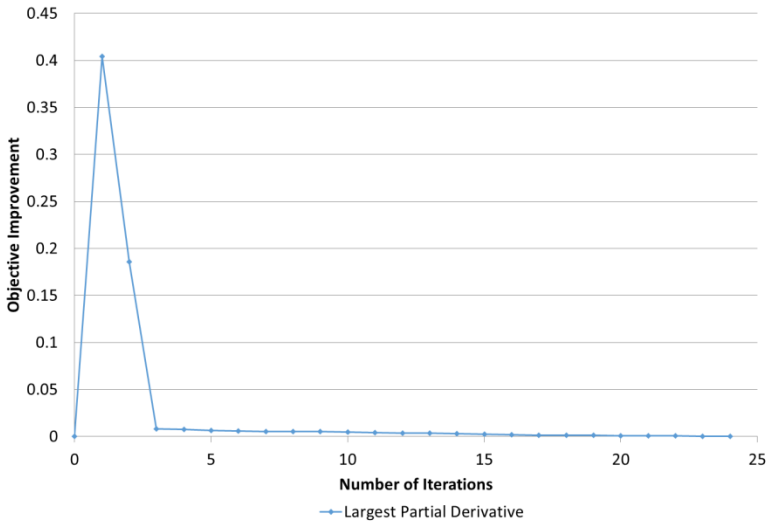

Fig. 38 Largest Partial Derivative – test with SP1

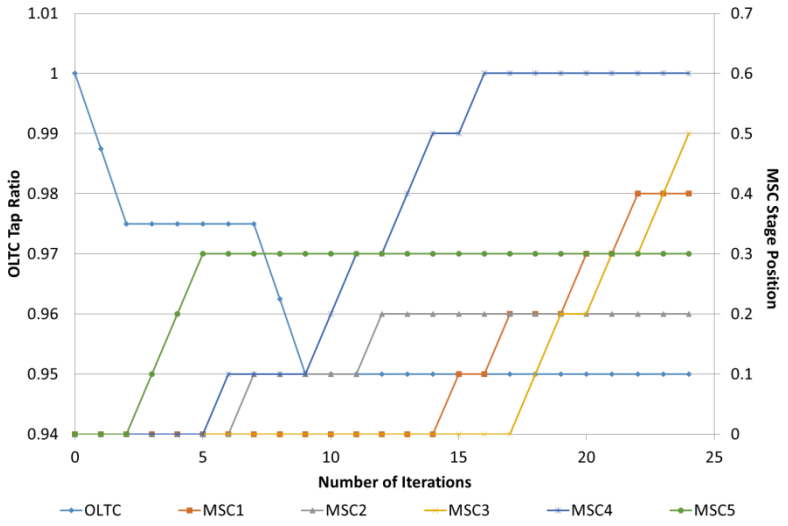

Fig. 39 Voltage control device position in the optimisation procedure – test with SP1

As shown in Fig. 39, the OLTC tap position is moved in the first two iterations. Then MSC5 is moved in the following three iterations. After 24 iterations, the optimal solution is achieved and the objective function cannot be further improved, as shown in **Fig. 37**.

SP2, which is generated randomly, is also used for test. For the SP2, the convergence curve is shown in Fig. 40. The largest partial derivative is shown in Fig. 41. The control variable change during the optimisation process is shown in Fig. 42.

The final results achieved with the ODCDM based algorithm are different for SP1 and SP2.

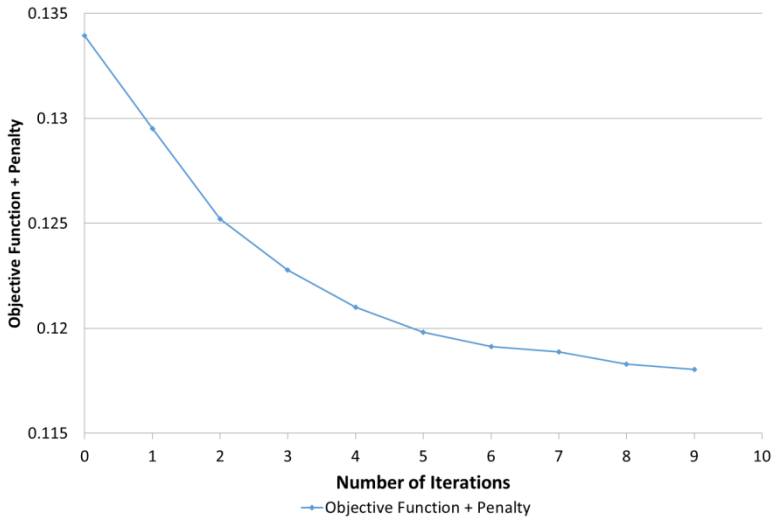

Fig. 40 Convergence Curve of ODCDM with SP2

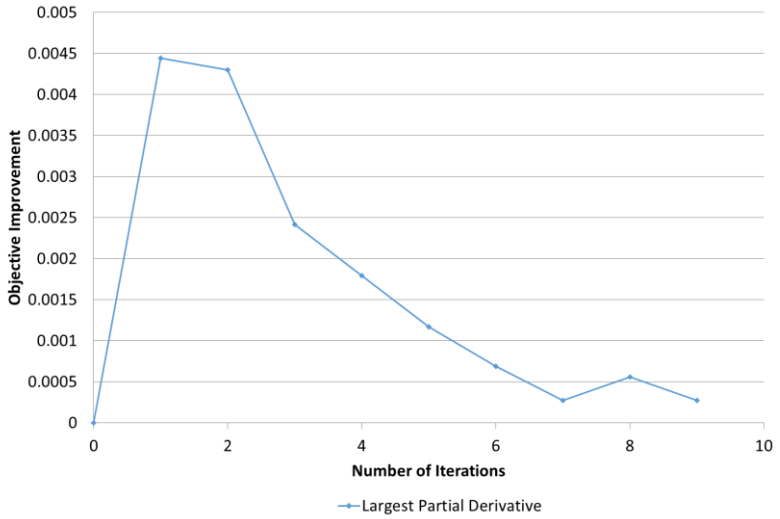

Fig. 41 Largest Partial Derivative – test with SP2

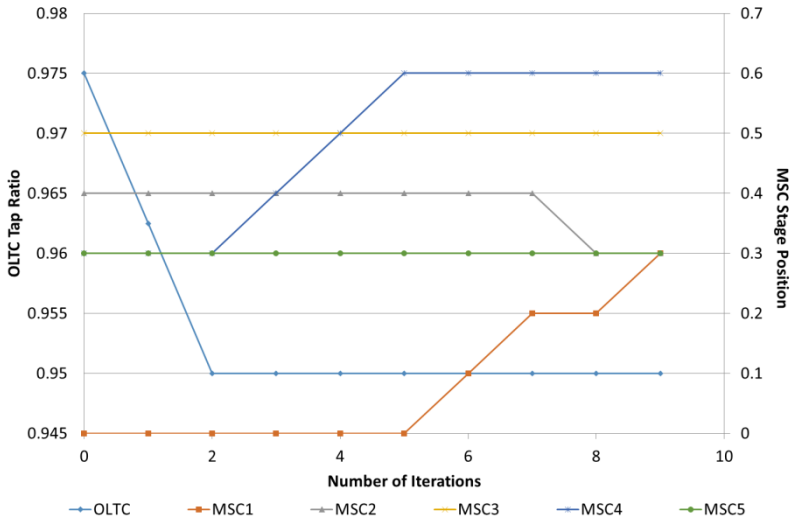

Fig. 42 The Voltage control device position in the optimisation procedure for SP2

4.5 ODCDM validation against field trials

As a robust and efficient algorithm, ODCDM has been adopted by commercial distribution management systems and applied in real distribution networks [83, 84]. In the CLNR project, ODCDM has also been applied in a distribution network control system, named as Grand Unified Scheme (GUS) [69, 109]. This GUS system has been applied and trialled in different distribution networks owned by Northern Powergrid. Some of the field trials have been used to further validate the ODCDM based algorithm developed in this PhD thesis. Here, the ODCDM based algorithm developed in this PhD thesis is named as ODCDM algorithm, while the ODCDM based algorithm implemented in the field trial is named as GUS algorithm. The validation is carried out by applying the ODCDM algorithm in the same way as the way the GUS algorithm applied in field trials, and comparing the simulation results against the measured field trial results. In the following, the method and results for a sampled validation study are presented.

4.5.1 Sampled field trial

A field trial of controlling secondary OLTC with the GUS algorithm is adopted here to demonstrate the validation process. This field trial was carried out on a low voltage network, the IPSA2 model of which is shown in Fig. 43. Here a UK network from the CLNR project, to which the GUS control system has been applied, is used for validation [69].

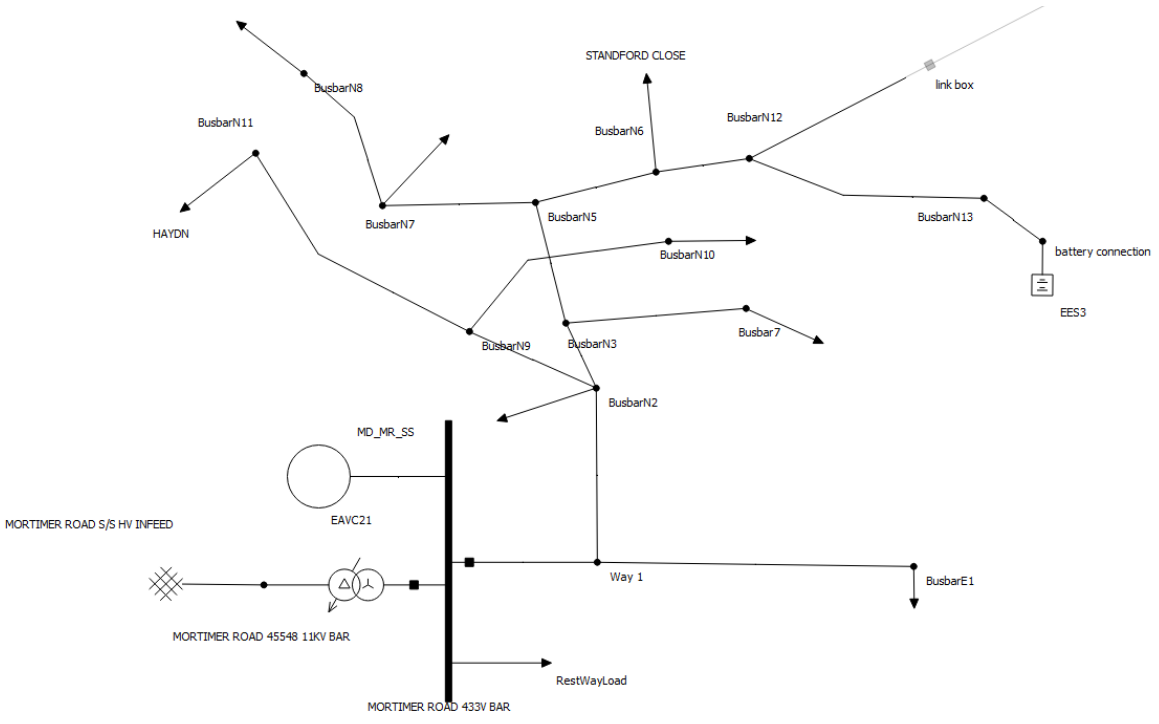

Fig. 43 Case study network model for sampled field trial

During the field trial, one electrical energy storage system, denoted by EES3 in the CLNR project, injected real power into the network, causing voltage problems in the network. The OLTC transformer at the secondary substation was controlled by the GUS algorithm to control the voltages within this LV network. The flowchart of this control system is illustrated in Fig. 44 and will be explained in section 4.5.2. The details of the field trial network and the field trial procedure can be found in [69].

4.5.2 Algorithm validation method

The application of the developed algorithm in simulation follows the flow chart of GUS system. In the CLNR project, the GUS algorithm is applied based on the requirements from NPG for different trials. Fig. 44 illustrates the flow chart of the GUS system. As per the flow chart shown in Fig. 44, the control system in GUS includes the following steps:

1) Distribution system state estimator (DSSE) takes measurement across the network, and estimates the network load condition based on the measurement and the network model within the control system. During the field trial, the state estimator is executed periodically every 5 minutes. The state estimator passes the estimated network load and generation condition, to Voltage Var Control (VVC);
2) Voltage VAr Control includes two parts. The first part is the ODCDM based voltage control algorithm, while the second part is a method adopted in the customer-led network revolution project to convert the optimal control solution to target voltage for the automatic voltage control (AVC) relay. In this field trial, no optimisation objective is defined, and the optimisation algorithm only solves voltage constraints violation;
3) The automatic voltage control relay operates the tapchanger in response to the calculated target voltage. A standard AVC algorithm is implemented here and is modelled as detailed previously, which means tap operation will be executed if the transformer secondary voltage is out of the new voltage range for over 2 minutes.

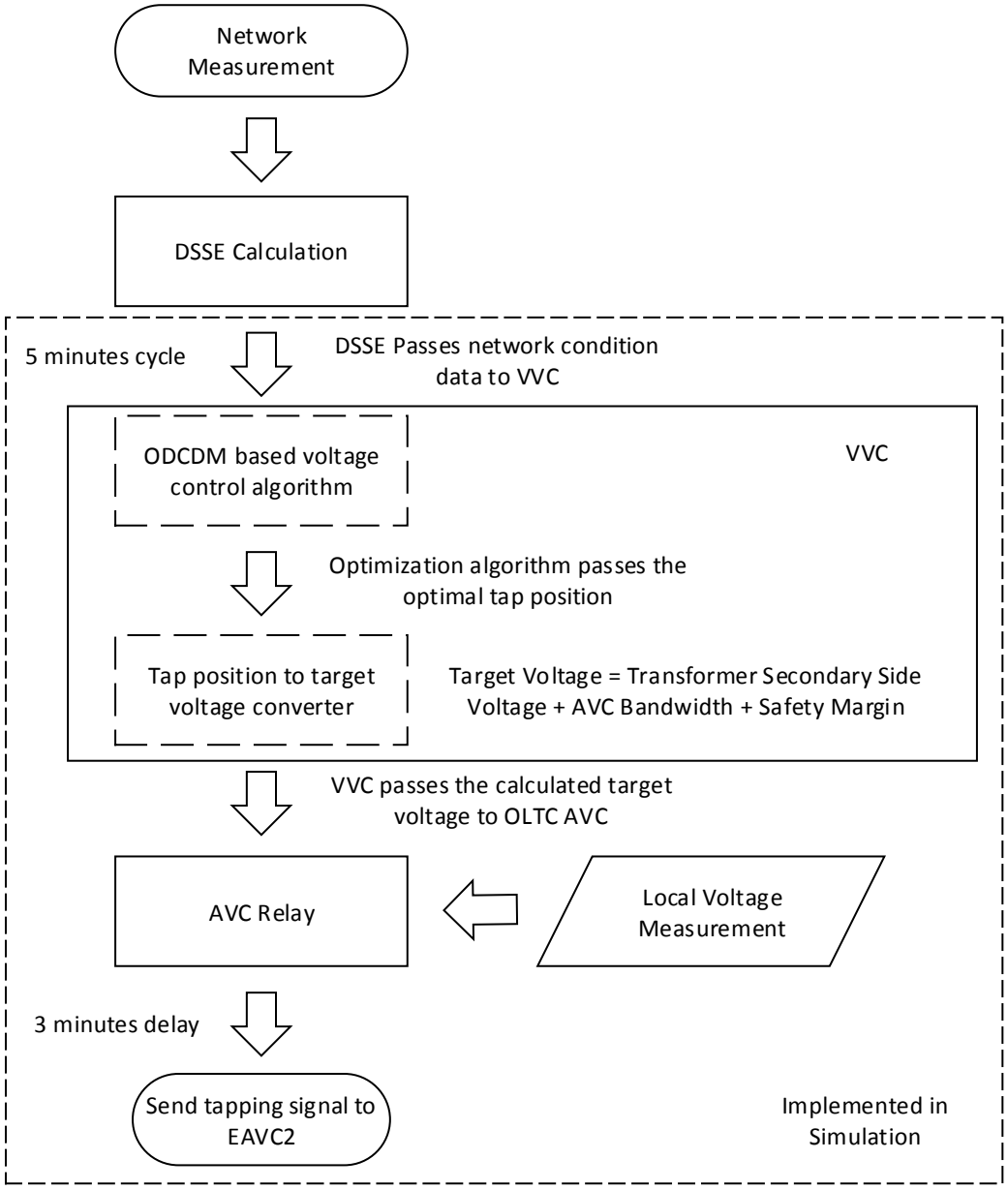

Fig. 44 Flow chart of the GUS control system in the sampled trial

It should be noted that here the network model developed in IPSA2 is used to represent both the real network and the network model in the control system for simulation. The trial results from the CLNR project demonstrated that the network model and the estimation result from DSSE are accurate enough. Therefore, the state estimator of the GUS control system is not modelled in simulation.

Then, the algorithm validation is carried out by applying the developed algorithm to the validated network model shown in Fig. 43. The load and EES3 real power injection from the field trial are used in the simulation, to create the same field trial network conditions. The details of the validation procedure can be found in [69].

4.5.3 Sampled validation results

The field trial results are shown in Fig. 45, including the voltage profiles at the secondary substation and at the EES3 connection busbar, EES3 real power output, and OLTC target voltage and tap position. It can also be seen that in this field trial, 1.04pu and 1pu are used as the upper and lower limits for network voltages.

The simulation results for the same variables are shown in Fig. 46. It can be seen that the simulation results are consistent with the trial results shown in Fig. 45. As shown in both the trial results and the simulation results, the control algorithm changes the target voltage for OLTC, responding to voltage constraints violation across the network. The EES3 connection point is the node where the lowest/highest voltages are most likely to be found due to its location deep within the LV network. This node can be seen as the remote end node for this analysis. The AVC relay changes the tap position in response to the new target voltage and the voltage measurement at the transformer secondary side. It should be noted that there is a target voltage change after 16:45, which does not lead to tap operation. This is due to a short duration voltage limits violation, which happens at other busbars.

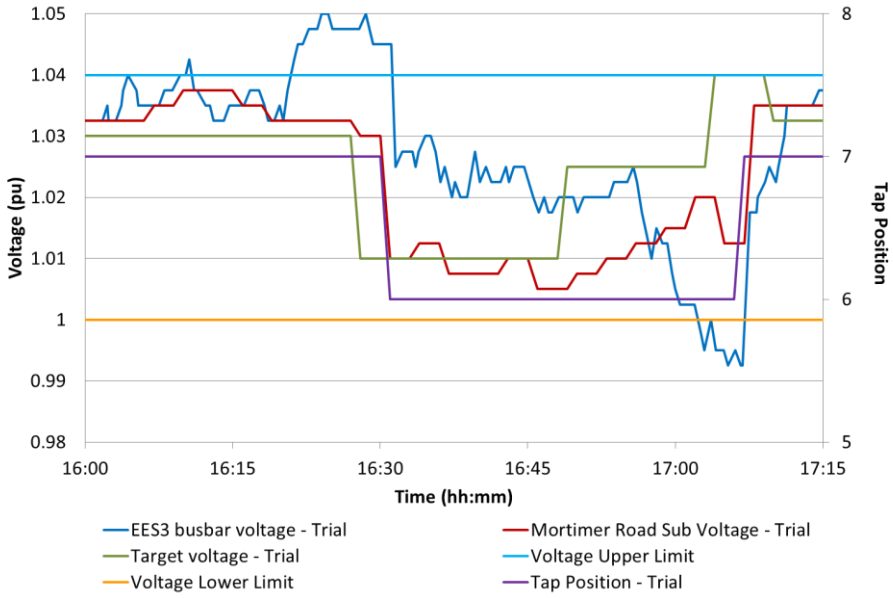

Fig. 45 Voltage profiles and tap position of Mortimer Road on 17th Sep 2014 from field trial results

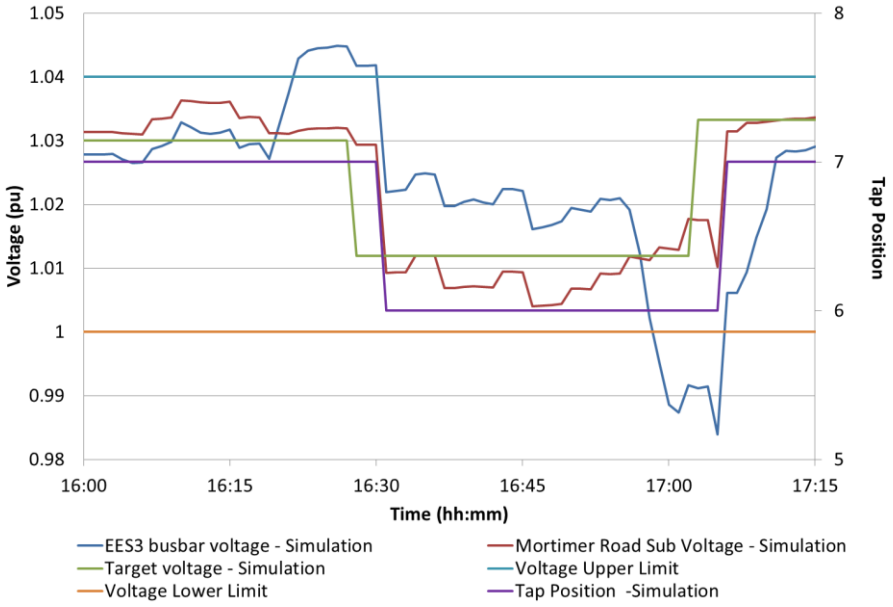

Fig. 46 Simulation results for field trial at Mortimer Road on 17th Sep 2014

It should be noted that the field trial results have a different data resolution than the simulation results. In the field trial results, different variables have different data resolution values and these values are changing from time to time, responding to the data variation. The data resolution can be less than 1 minute. For the simulation results, the data resolution is constant as 1 minute for all the variables.

The validation results shown in Fig. 45 and Fig. 46 demonstrate that the ODCDM algorithm developed in this PhD thesis is able to represent the ODCDM algorithm implemented in the GUS system, which is a state-of-the-art distribution network management system used in real distribution networks.

4.6 Conclusions

In this chapter, a voltage control algorithm based on ODCDM is introduced. The problem formulation for voltage optimisation is specified at the beginning. Then the development of an ODCDM based voltage control algorithm, as per previous study [61], is presented. The ODCDM based voltage control algorithm is extended in this PhD study to solve MINLP problems and multi-objective voltage control problems. The mechanism of the original ODCDM algorithm is demonstrated by the test results from a simple case study network. Sampled field trial results, from the CLNR project, are used to further validate the original ODCDM algorithm. It is proved with the validation results that the ODCDM algorithm developed in this PhD study is able to represent the voltage control algorithm used in a state-of-the-art distribution network management system used in real distribution networks.

Deterministic algorithms, such as ODCDM, which has been proven to be fast and effective in real distribution networks, share several common drawbacks. Specifically, they are all local solvers, and have the difficulties to deal with MINLP problems and multi-objective problems. In next chapter, metaheuristic algorithms, with the theoretical advantages in these aspects, will be applied for voltage control.

Chapter 5 Development of Cuckoo Search based Voltage Control Algorithms

5.1 Introduction

In Chapter 4, oriented discrete coordinate descent method was applied to solve the optimisation problem, which is formulated for distribution network voltage control. Initial simulation results demonstrated that this algorithm was able to minimise network losses and maintain network voltages within the limits. However, as a deterministic optimisation algorithm, ODCDM is only able to guarantee a local optimum when the optimisation problem is nonconvex. Also, it cannot be used to solve MINLP problems and multi-objective problems directly.

This chapter introduces two voltage control algorithms, based on Cuckoo Search via Lévy Flights, normally referred to as Cuckoo Search. CS was firstly proposed in 2009, inspired by the breading behaviour such as brood parasitism of certain species of cuckoos [114]. As a novel metaheuristic algorithm, CS attracts a lot of attention and has been successfully applied to solve different optimisation problems in many areas [115, 116]. Previous research demonstrated that CS outperforms many other popular meta-heuristic algorithms, such as genetic algorithm and particle swarm optimisation algorithm [116-118]. Also, CS is proved to be less sensitive to parameter tuning to some extent [114], while parameter tuning is normally seen as one of the main drawbacks of many metaheuristic algorithms. In addition, it has been proved that CS satisfies the requirements for global convergence with the development and analysis of the Markov chain model for CS in [119]. CS has also been extended to solve multi-objective optimisation problems in different areas [120-125]. In [121], a multi-objective cuckoo search algorithm was proposed and tested against a set of well-chosen test functions, as well as the design problems in structural engineering. Test results demonstrated that CS can be extended to be an efficient multi-objective optimiser. Additionally, the proposed algorithm was in comparison with other established multi-objective metaheuristic algorithms and the results showed that the proposed algorithm performed well for almost all the selected test problems [121].

CS has been applied to solve the optimisation problems from power system. For instance, CS is adopted to solve capacitor placement problem in [126] and DG allocation problem in [127]. CS is applied to solve economic dispatch problems in [128, 129], and multi-objective unit commitment problem in [120]. In this PhD study, CS has been extended to solve MINLP and

Multi-objective optimisation problems, and applied to solve voltage optimisation problems in conventional and future distribution networks.

In the rest of this chapter, the principle of CS is reviewed, followed by the development of single-objective cuckoo search algorithm (SOCS) and multi-objective cuckoo search algorithm (MOCS). Voltage optimisation algorithms, based on SOCS and MOCS, are presented. A simple test case is used to demonstrate the mechanism of the SOCS based voltage control algorithm. Two popular metaheuristic algorithms, GA and PSO, have been applied for voltage control and tested with the same test case. The results achieved by SOCS, GA and PSO are compared. Similarly, the MOCS based voltage control algorithm is tested with a simple multi-objective test case. One widely-used multi-objective metaheuristic algorithm, non-dominated sorting genetic algorithm II (NSGA-II), is applied for multi-objective voltage optimisation, and tested with the same multi-objective test case. The results achieved by MOCS and NSGA-II are compared. Finally, conclusions are drawn.

5.2 Development of Cuckoo Search algorithms

5.2.1 The principle of Cuckoo Search

CS is inspired by the obligate brood parasitism of some cuckoo species, such as the Ani and Guira Cuckoos [114]. These cuckoo species lay their eggs in the nests of the host birds from other species. Some host birds are able to discover the eggs from the intruding cuckoos with a certain possibility. Once a host bird discovers the eggs are not its own eggs, they will either throw these alien eggs away or simply abandon its nest and build a new nest elsewhere [130]. The above characteristics of the breeding process of these cuckoos and the conflict between cuckoos and host birds are adopted as the fundamental idea for CS. Three idealized rules are defined in the original CS algorithm [114]:

- Each cuckoo lays one egg at a time, and dumps this egg in a randomly chosen nest;
- Only the best nests with high quality of cuckoo eggs will carry over to the next generations;
- The number of available host nests is fixed. The egg laid by a cuckoo may be discovered by the host bird with a probability $p_a \in [0, 1]$. If the egg is discovered, this nest will be replaced with a new nest.

It should be noted that the first assumption will be changed for multi-objective cuckoo search algorithms. Multiple eggs will be laid. This will be further discussed in section 5.2.3.

The application of Lévy Flights is another important reason for the good performance of CS. A Lévy Flight is a random walk in which the step-lengths have a probability distribution that is heavy-tailed [114]. Lévy Flights have been widely observed in nature, for example, the foraging behaviour of bacteria and higher animals relies on the advantages of Lévy distributed excursion lengths [131]. Lévy Flight has been successfully applied to optimal search and the results show its promising capability [131, 132].

The Pseudo code of CS, proposed in [114], is shown in Fig. 47. The principle of CS is explained as per this pseudo code. A group of solutions (nests) are generated initially, and evaluated as per the objective function (egg). The following procedure is then repeated until the maximum generation (iteration) is reached or the predefined stop criterion is met: new solution is generated by Lévy Flights and compared with a randomly selected solution. If this new solution is better, it will replace the randomly selected one. Then a portion of worst solutions are abandoned and new solutions are generated based on the current best solution. Once maximum iteration is reached or the stop criterion is met, the iteration will stop and the best result will be returned. Different stop criterion can be defined. For example, it can be defined as when the objective cannot be further improved over a certain number of iterations, or the improved objective value is smaller than a threshold.

Cuckoo Search via Lévy Flights

```
begin
  Objective function f(x),  x = (x_1, ..., x_d)^T
  Generate initial population of
      n host nests x_i (i = 1, 2, ..., n)
  while (t <MaxGeneration) or (stop criterion)
    Get a cuckoo randomly by Lévy flights
      evaluate its quality/fitness F_i
    Choose a nest among n (say, j) randomly
    if (F_i > F_j),
      replace j by the new solution;
    end
    A fraction (p_a) of worse nests
      are abandoned and new ones are built;
    Keep the best solutions
      (or nests with quality solutions);
    Rank the solutions and find the current best
  end while
  Postprocess results and visualization
end
```

Fig. 47 Pseudo code of the Cuckoo Search[114]

As indicated in the Pseudo code, Lévy Flights play an important role in new solution generation. The specific solution generation procedure is shown by (39).

$$x_i^{t+1} = x_i^t + \alpha_0 \oplus Lévy(\lambda) \tag{39}$$

Where $\boldsymbol{x}_i^{t+1}$ is the new solution generated, while $\boldsymbol{x}_i^{t}$ is current solution. And α_0>0 is the step size scale factor which should be related to the scales of the specific problems. The product $\oplus$ represents entrywise multiplications. *Lévy (λ)* stands for the step size, which is drawn from a Lévy Flights distribution. The Lévy distribution, which has an infinite variance with an infinite mean, can be represented by (40).

$$Lévy \sim u = t^{-\lambda}, 1 < \lambda \leq 3 \tag{40}$$

Compared to normal distribution, Lévy distribution is able to generate a very large step size with a certain possibility, which allows a large space search area [131]. As indicated by (39), new solution is generated with the step size generated from Lévy Flights and the previous solutions. Some of the new solutions are generated based on the current best solution, in order to speed up the local search. Also, some new solutions should be generated, which are far enough from the current best solution. This will ensure the algorithm could escape from a local optimum.

5.2.2 Development of single-objective Cuckoo Search algorithm

The SOCS algorithm was developed in Python according to the principle stated in last section. CS is originally proposed to solve continuous-variable-only problems. Here, the developed algorithm is extended to solve mixed integer problems, by introducing discrete control variables into the algorithm. Specifically, the solution in the developed SOCS algorithm is divided into a discrete variable section and a continuous variable section, as shown by Fig. 48. Initial solution is created as a combination of discrete variable section and the continuous variable section, which are generated separately. When new solution is generated with Lévy flights, the continuous variable section of the new solution is still generated by (40). And for discrete variable section of the new solution, the step size is rounded to an integer. The discrete variables are modelled as integers for the sake of generality, and the discrete variables from the specific problems can be represented by integers. The details are shown in section 5.3.1. Combinatorial problems can also be solved with this developed algorithm, by defining the number of continuous variable as zero.

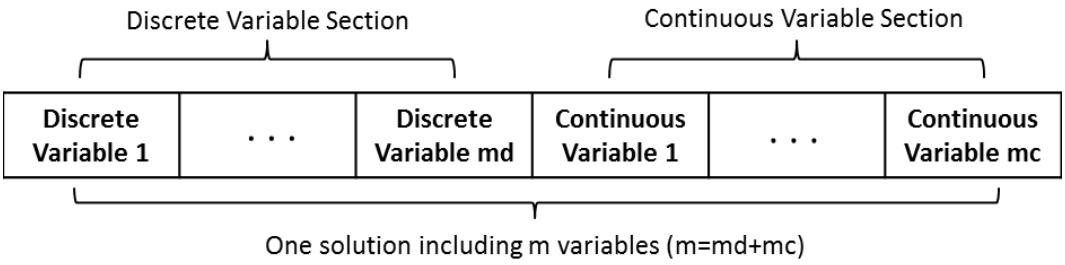

Fig. 48 Solution Structure for MINLP SOCS algorithm

The flow chart of the developed SOCS algorithm is shown in Fig. 49.

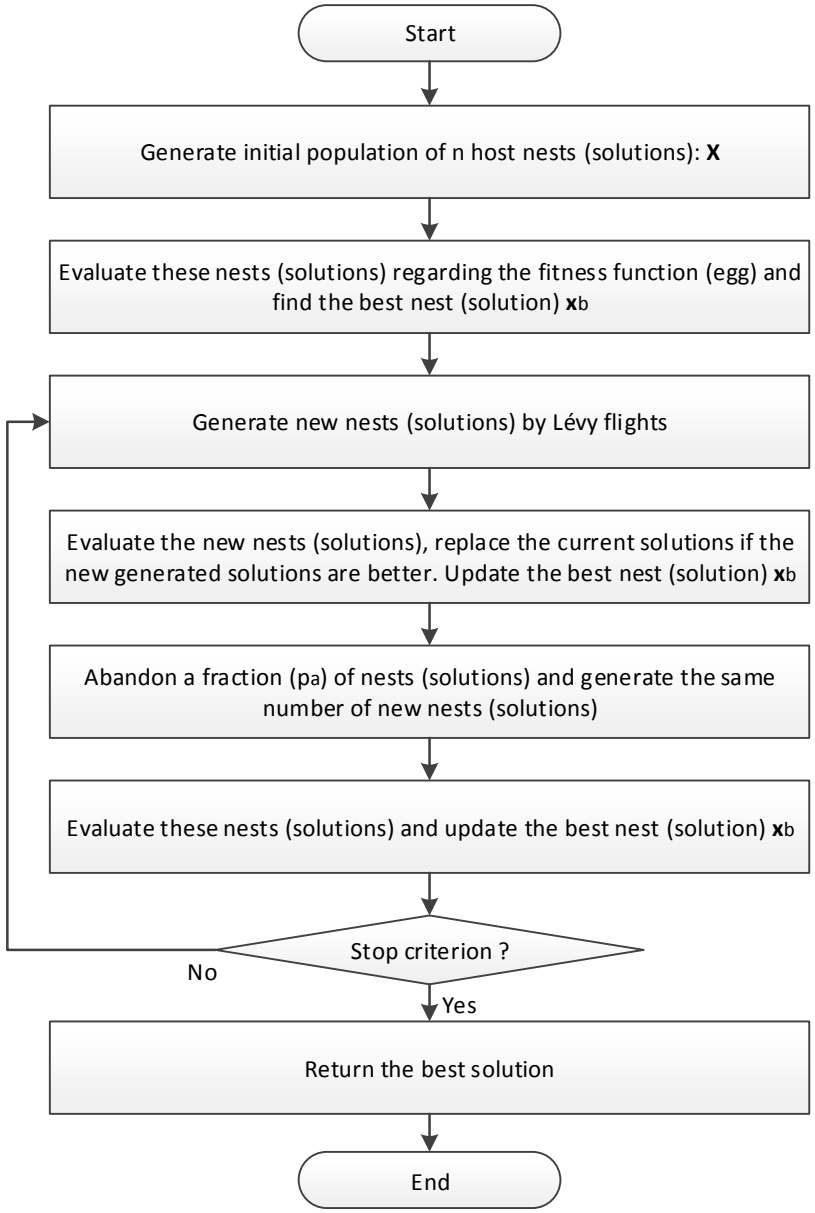

Fig. 49 Flow Chart of Single-Objective Cuckoo Search

As per the flow chart, the procedure of the developed algorithm is explained as follows:

1) Initially, a set of solutions, nominated as **X,** are generated randomly. **X** is a n×m dimension vector. The value n is the nest number, representing the number of solutions, while m is the number of variables in each solution;
2) These solutions are evaluated regarding the fitness function, and the current best solution $\mathbf{x}_b$ is found. The fitness function is normally formulated as a combination of the optimisation objective function and the penalty function defined for constraint violation;
3) New solutions are generated with Lévy flights, based on current solutions;
4) New generated solutions are evaluated and compared with current solutions. Current solutions will be replaced with new generated solutions if the new generated solutions are better. Update the current best solution $\mathbf{x}_b$;
5) A fraction of solutions, with the probability of p_a, are abandoned and the same number of new solutions are generated;
6) Evaluate the new generated solutions and update the current best solution $\mathbf{x}_b$;
7) If the stop criterion is met, return the current best solution $\mathbf{x}_b$. Otherwise go back to step 3). Here the algorithm will stop once the predefined maximum iteration number is reached or the optimal result, if known, is found.

The method of generating new solutions wth Lévy flights in step 3) is specified in the following. New solutions are generated based on current solutions by (41).

$$\mathbf{x}_i^{t+1} = \mathbf{x}_i^{t} + stepsize_i \cdot randn() \tag{41}$$

Where $\mathbf{x}_i^{t+1}$ is the new solution generated for the ith solution in (t+1)th generation (t+1), while $\mathbf{x}_i^{t}$ is solution in generation t. *randn*() is a function which generates a random scalar drawn from the standard normal distribution. $stepsize_i$ is the step size generated by Lévy flights in the ith solution, which can be calculated by (42).

$$stepsize_i = a_0 \cdot \left(\frac{u_i}{|v_i|} \right)^{\frac{1}{\beta}} \cdot (\mathbf{x}_i^{t} - \mathbf{x}_b^{t}) \tag{42}$$

Where $\mathbf{x}_b^{t}$ is the best solution found so far. α_0 is the scale factor applied to avoid the Lévy flight becoming too aggressive and makes new solutions jump out side of the design domain. β is an index used in Lévy distribution. u_i and v_i are values drawn from normal distributions, as shown by (43) and (44).

$$u_i = \phi \cdot randn() \tag{43}$$

$$v_i = randn() \tag{44}$$

ϕ is used to scale the value generated with *randn*(), and it is calculated by (45).

$$\phi = \left(\frac{\Gamma(1+\beta) \cdot \sin\left(\frac{\pi \cdot \beta}{2}\right)}{\Gamma\left(\left(\frac{1+\beta}{2}\right) \cdot \beta \cdot 2^{\frac{\beta-1}{2}}\right)} \right)^{\frac{1}{\beta}} \tag{45}$$

Γ represents gamma function and β is the scale factor indicated before.

For discrete variables in the solution, (41) is revised to make sure the new solution is feasible.

$$x_i^{t+1} = x_i^t + roundoff\,(stepsize_i \cdot randn()) \tag{46}$$

It should be noted that for CS the solutions are evaluated twice in one iteration, while for many other metaheuristic algorithms, the solutions are normally evaluated once in one iteration. Therefore, when CS is compared with other metaheuristic algorithms, the same fitness function evaluation number should be used instead of same iteration number. This is further discussed in section 5.4.2, when CS is compared with GA and PSO.

5.2.3 Development of multi-objective Cuckoo Search algorithm

When deterministic algorithms are applied to solve the multi-objective optimisation problems, multiple objectives need to be converted into a single-objective with certain methods. The same approach can also be adopted by metaheuristic algorithms. There are some drawbacks of this approach: it is sensitive to the shape of the Pareto front, and multiple runs are required to find the Pareto front. In addition, when deterministic algorithm is applied, the solutions in the achieved result may be a local optimum.

With the ability to find multiple Pareto-optimal solutions in a single run, various multi-objective metaheuristic algorithms have been developed in the last two decades [133, 134]. The following text proposes a multi-objective cuckoo search algorithm. As mentioned before, it is assumed that each nest (solution) hosts one egg (objective) in SOCS. For MOCS, each nest contains k eggs, representing k different objectives to be optimised. The solutions, which are not dominated by any other solutions, are stored and updated during the optimisation. The flow chart of MOCS is shown in Fig. 50. The procedures of MOCS are similar to that of SOCS, which are specified in section 5.2.2. For MOCS, a set of non-dominated solutions,

instead of a single best solution in SOCS, are found and used for new solution generation. As shown in section 5.2.2, a current best solution is needed for new solution generation. Here, one solution is selected randomly from the current set of non-dominated solutions every time when the current best solution is needed.

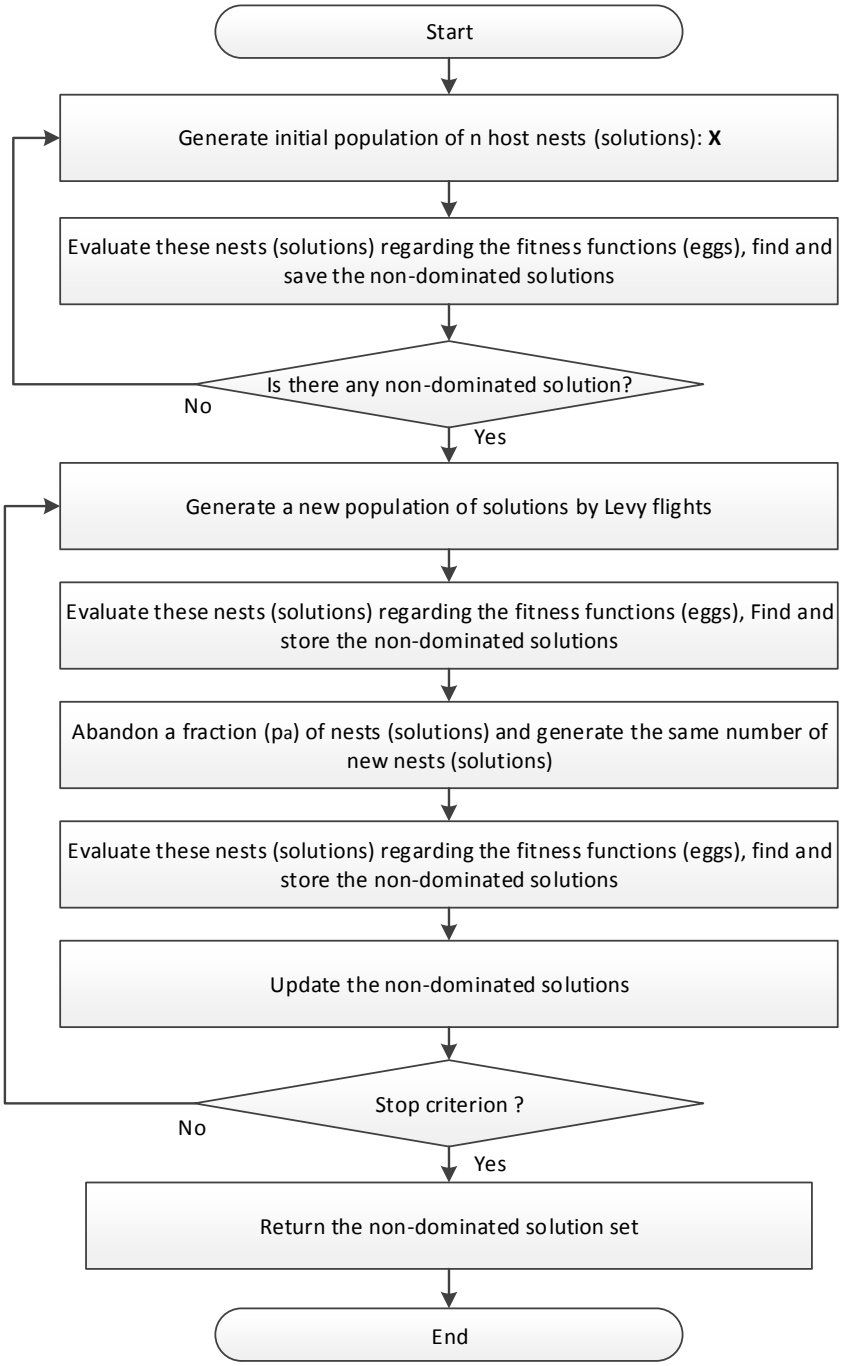

Fig. 50 Flow Chart of Multi-Objective Cuckoo Search

5.3 Development of Cuckoo Search based voltage control algorithm

5.3.1 Single-objective Cuckoo Search based voltage control algorithm

The basic idea of the CS based voltage control algorithms is to apply SOCS and MOCS to solve the optimisation problem, which is formulated for distribution network voltage control. The control variables, which are continuous values and integers, can be considered directly in the developed algorithms. However, if the control variables are non-integer discrete values, they need to be converted into integers first. For example, the tap position of on load tap changer is normally represented as a percentage value, which is normally not integer. In order to be considered in the CS based algorithms, the OLTC tap position is formulated as a function of an integer *i*, whose range is between 0 and N_{Tap}-1, as shown by (47).

$$TapPosition_{OLTC} = Tap^{min} + i \times Stepsize^{OLTC}, i = 0,1,2,...,N_{Tap} - 1 \quad (47)$$

where,

$TapPosition_{OLTC}$	The tap position of the OLTC transformer
Tap^{min}	The minimum tap position of the OLTC transformer
$Stepsize^{OLTC}$	The step size of the OLTC transformer
N_{Tap}	The total number of the tap positions

Similarly, the stage position of the mechanically switched capacitor bank (MSC) can also be represented with an integer *i* by (48).

$$StagePosition_{MSC} = i \times Stepsize^{MSC}, i = 0,1,2,...,N_{Stage} - 1 \quad (48)$$

where,

$StagePosition_{MSC}$	The stage position of MSC
$Stepsize^{MSC}$	The step size of the MSC
N_{Stage}	The total number of the MSC stage positions

The fitness function is formulated as a sum of the objective function and the penalty function. The objective function can be network loss minimisation or any other optimisation objective. The same penalty function from the ODCDM based voltage control algorithm is adopted here and added to the objective function. Load flow calculation is normally required to calculate the fitness function. In this study, load flow calculation is carried out with the load flow engine from IPSA2 and PyPower, while the rest of the algorithm is implemented in Python.

5.3.2 Multi-objective Cuckoo Search based voltage control algorithm

The same approach from last section is adopted to deal with the control variables in the MOCS based voltage control algorithm. Assuming there are N_{obj} optimisation objectives, then N_{obj} fitness functions should be formulated. These fitness functions are calculated with the corresponding objective functions and the penalty function defined for constraint violation, as represented by (49).

$$F = \begin{cases} f_1 + f_{penalty} \\ \vdots \\ f_{\mathrm{N}_{Obj}} + f_{penalty} \end{cases} \tag{49}$$

The result achieved by MOCS is normally a set of non-dominated solutions. In practice only one solution can be applied for voltage control. Therefore, a solution needs to be selected from the result achieved by MOCS manually or automatically with a decision making method. In this PhD, the ability of Pareto front search is investigated, and the solution selection therefore is not studied.

5.4 Initial evaluation of single-objective cuckoo search based voltage control algorithm

The SOCS based voltage control algorithm is evaluated with the case study network introduced in section 4.4.1. Initial evaluation results are presented in this section to demonstrate the performance of the developed SOCS based voltage control algorithm. Additionally, two popular metaheuristic algorithms, GA and PSO, are implemented for voltage control, and compared with the SOCS based voltage control algorithm.

5.4.1 Initial evaluation of SOCS based voltage control algorithm

Similarly to the initial evaluation of the ODCDM based voltage control algorithm, network loss minimisation is adopted as the optimisation objective here to evaluate the performance of the SOCS based voltage control algorithm. The fitness function is a combination of network loss and the penalty from voltage constraints violation. For this test case, the global optimum, which is founds via exhaustive search, is shown in Table 11.

Table 11 Global Optimal for This Test Case

	OLTC	MSC1	MSC2	MSC3	MSC4	MSC5	Network Loss
	Unit: %	Unit: MVAr					MW
Global Optimal	-5	0.4	0.2	0.5	0.6	0.3	0.1179

As shown in section 5.2.2, in SOCS there are several parameters, which could be tuned regarding each individual optimisation problem. As suggested by [135], it is sufficient to choose a number from 15 to 25 as the nest number, and p_a can be selected as 0.25. p_a is the possibility with which the nest (solution) will be abandoned. In addition, α_0 is recommended to be 0.01 in [136]. Here the nest number is selected as 25. The maximum iteration number can be determined by increasing the maximum iteration number gradually until a stable result can always be achieved. For this test case, the required maximum iteration number is found as 100, with the procedure specified in the following.

The SOCS based voltage control algorithm is tested with different maximum iteration numbers, increasing from 10 to 100, with the interval as 10. 100 runs are carried out for each maximum iteration number for the same test case. Due to the stochastic nature of SOCS, different results may be achieved every time the algorithm is run. Table 12 summarizes the final results for the tests with varying maximum iteration number, including the maximum, minimum, average and the standard deviation. The maximum value represents the worst result achieved with a maximum iteration number over 100 runs, while the minimum value represents the best result achieved correspondingly. The average represents the average result achieved over the 100 runs, and the standard deviation is calculated using (50).

$$\sigma = \sqrt{\frac{1}{N}\sum_{i=1}^{N}(result_i - result_{average})^2} \tag{50}$$

In (50), N standards for the number of runs conducted for each maximum iteration number, and it is found that N=100 is sufficient in this case. $result_i$ standards for the ith result achieved and $result_{average}$ standards for the average value of the results from the N runs.

It can be seen from Table 12 that sometimes, the result achieved with a small maximum iteration number may be better than that achieved with a large maximum iteration number. For example, the best result achieved with the maximum iteration number as 20 is better than

the worst result achieved with the maximum iteration number as 50. But generally the result achieved improves with increasing the maximum iteration number, as demonstrated by the average values and the standard deviations. Also, when the maximum iteration number is large enough, 100 in this case, the same result is achieved for all 100 runs. It should be noted that for the maximum iteration number of 100, the total number of fitness function evaluation, which is 25×100×2=5000, is still much smaller than the number of all the potential combinations of the control variables in this case, which is: 9×8×8×8×8×8 = 294912.

Table 12 Test results of the SOCS based voltage control algorithm for different maximum iteration number

Maximum Iteration Number	Network Loss achieved over 100 runs (MW)			
	Max	Min	Average	Standard Deviation (10e-3)
10	0.122149	0.117931	0.119111	0.772281
20	0.11994	0.117931	0.118427	0.378255
30	0.118636	0.117931	0.118078	0.135906
40	0.118185	0.117931	0.117986	0.057032
50	0.118101	0.117931	0.11796	0.036550
60	0.118033	0.117931	0.117944	0.022524
70	0.117998	0.117931	0.117934	0.012395
80	0.117989	0.117931	0.117932	0.007608
90	0.117967	0.117931	0.117931	0.005039
100	0.117931	0.117931	0.117931	0.000000

Fig. 51 shows the convergence curve for a sampled run of the CS based algorithm with the maximum iteration number as 100. The fitness function is reduced to the global optimum after around 60 iterations. It can also be seen that sometimes the fitness function cannot be improved in some iterations. Therefore, the stop criterion cannot be simply defined as when the fitness function cannot be further improved.

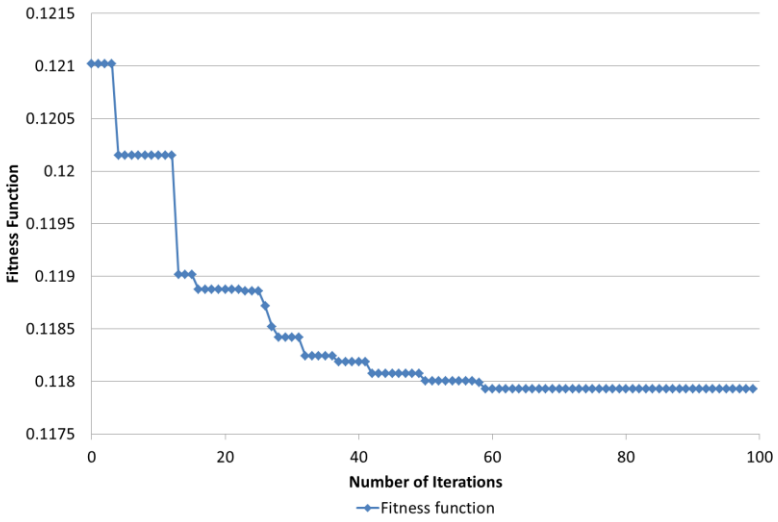

Fig. 51 Convergence curve of CS based Voltage Control Algorithm

To further demonstrate the stochastic nature of metaheuristic algorithm, the convergence curves of CS for three different runs are shown in Fig. 52.

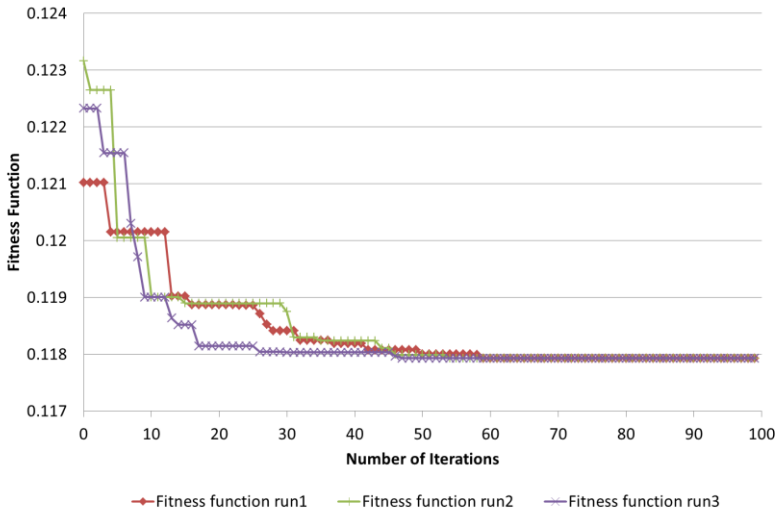

Fig. 52 Convergence Curves for Different Runs

It can be seen from Fig. 52 that for different runs, the convergence curves are not exactly the same. Although the optimisation progress is different for each run, the optimal result achieved after 100 iterations is the same for all three runs.

5.4.2 Implementation of GA and PSO based voltage control algorithms

Two popular metaheuristic algorithms, GA and PSO, are also applied here for voltage control, to facilitate the comparison between CS and other metaheuristic algorithms. Many variants have been developed for GA and PSO before. Here the GA from [137] and the PSO from [117] are utilized.

Generally metaheuristic algorithms treat the optimisation problem as a black box, which allows them to be applied with a similar approach. The GA from [137] is integer based. The same equations from (47) and (48) can be applied directly to convert the integer variables into discrete control variables. Since the basic PSO from [117] is originally developed based on continuous variables, the discrete control variables are considered as continuous variables first and the continuous values achieved are then rounded to the closest feasible discrete values after the optimisation process.

5.4.3 Comparing the voltage control algorithms based on CS, GA and PSO

These two algorithms, based on GA and PSO, are tested with the same test case from section 5.4.1. As discussed in 5.2.2, the same amount of fitness function evaluations are applied in the tests for all these three algorithms, in order to carry out a fair comparison. For CS, the number of fitness function evaluations, N_{CS}, is calculated by (51).

$$N_{CS} = 1 + 2 \times nest\ number \times maximum\ iteration\ number \tag{51}$$

The numbers of fitness function evaluations for GA (N_{GA}) and PSO (N_{PSO}), are calculated by (52) and (53).

$$N_{GA} = population\ size \times generation \tag{52}$$

$$N_{PSO} = particle\ number \times maximum\ iteration\ number \tag{53}$$

Metaheuristic algorithms have several parameters, which could affect their performance. Different metaheuristic algorithms normally have different types of parameters, which need to be determined. Here, the parameters in these three algorithms are specified in the following:

- CS: nest number = 25, maximum iteration number = 100, $p_a = 0.25$;
- GA: population size = 50, generation = 101, step = 1, mutation probability = 0.2, elite rate = 0.2;
- PSO: particle number = 25, maximum iteration number = 202, cognitive factor following personal best = 1.8, social factor following global best = 1.8, inertia weight = 0.6.

For CS, the same parameters from the study in section 5.4.1 are used. The generation number for GA and the maximum iteration number for PSO are determined, in order to ensure the similar amount of fitness function evaluations are applied in all these three algorithms. It should be noted that CS utilizes 25 less fitness function evaluations than GA and PSO, due to

the different structures of these algorithms. The rest parameters for GA and PSO, have been determined as recommended by previous studies. For GA, the rest parameters have been recommended by [137]. For PSO, the rest parameters have been recommended by [117]. Potentially, for all these three algorithms, their parameters could be tuned regarding this specific voltage optimisation problem. However, to prove the robustness of the algorithms, the parameters recommended by the references are used. Also, here the tests are for the illustrative purposes only.

The test case from 5.4.1 is solved 100 times by each of these three algorithms. The test results extracted from these 100 runs are summarized in Table 13.

Table 13 Results achieved with the algorithms based on CS, GA and PSO

	Network Loss achieved over 100 runs (MW)			
Algorithm	Maximum	Minimum	Average	Standard Deviation
CS	0.117931	0.117931	0.117931	0.000000
GA	0.119563	0.117931	0.118182	0. 000257
PSO	0.118553	0.117931	0.118018	0.000202

As shown in Table 13, all these three algorithms are able to achieve the global optimum at least once from the 100 runs. However, compared to GA and PSO, CS is able to achieve a more stable result, which can be seen from the averages and standard deviations for the results achieved by these algorithms.

5.5 Initial evaluation of multi-objective cuckoo search based voltage control algorithm

The MOCS based voltage control algorithm is also evaluated with the same test network from section 4.4.1. Besides network losses, voltage deviations are also to be minimised. Voltage deviation minimisation is another widely used optimisation objective for distribution network voltage control, in consideration of achieving better power quality [95, 127]. Voltage deviation is a measure of the differences between the magnitudes of the actual and reference values of busbar voltages. The reference voltage values could be the nominal voltage, a mean value of the operating voltage, or the declared supply voltage. The nominal voltage is used here as the reference value, without loss of generality. Different definitions have been proposed to represent the voltage deviation. Here a widely used definition, represented by (54), is adopted in this study. It is defined as the sum of the absolute values of the differences between the busbar voltages and their reference values for all network busbars.

$$f_{VoltageDeviation} = \sum_{i}^{N_{busbar}} \left| V_i - V_i^{reference} \right| \tag{54}$$

where,

$V_i^{reference}$ Reference voltage for busbar *i*

Initial evaluation results from MOCS are presented here. Moreover, MOCS is compared with NSGA-II, which is one widely used multi-objective metaheuristic algorithm. The open source python algorithm of real-coded NSGA-II from [138] is applied for multi-objective voltage control. In this real-coded NSGA-II python algorithm, the control variables are required to be the values within the range of [0, 1]. Therefore, the tap position of OLTC and the stage position of MSC are represented by the control variables of this NSGA-II python algorithm using (55) and (56).

$$TapPosition_{OLTC} = Tap^{min} + \text{Round}\left[i \times (N_{Tap} - 1) \right] \times Stepsize^{OLTC}, i \in [0,1] \tag{55}$$

$$StagePosition_{MSC} = \text{Round}[i \times \left(N_{Stage} - 1 \right)] \times Stepsize^{MSC}, i \in [0,1] \tag{56}$$

5.5.1 Initial evaluation of MOCS based voltage control algorithm

For multi-objective optimisation algorithms, the result evaluation is substantially more complex than that for single-objective optimisation. This is because the result normally includes a set of solutions, which normally need to be measured by some performance metrics, before the result can be evaluated. Many performance metrics have been developed before, to evaluate the results achieved by multi-objective optimisation algorithms. Here, the Ratio of the Reference Point Found (RRPF) is used to evaluate the results in this initial evaluation. RRPF, as its name suggests, is the ratio of found solutions against the ideal or reference Pareto set. It is seen as the most natural quality measure if a reference set composed of all the efficient solutions is known in previous researches. The ratio of the reference point found can be defined by (57).

$$C_R(A) = \frac{|A \cap R|}{|R|} \tag{57}$$

where *A* is the solution set, while *R* is the reference set. The voltage optimisation problem in this test case is a combinatorial problem. The Pareto set can be achieved by exhaustive search and used as the reference set *R*.

As shown in section 5.2, MOCS has several parameters, which could affect the performance of MOCS. Potentially, these parameters could be tuned for each individual multi-objective optimisation problem and parameter tuning can be seen as an optimisation problem itself. However, the parameter tuning for multi-objective metaheuristic algorithms, such as MOCS, is very difficult and time consuming. It is not practical to tune all the parameters for each individual problem. Here, the parameters are determined as per the literature and with some experiments.

As per [121], the ranges of the parameters in MOCS are suggested as: nest number = 25 to 50, p_a = 0.25 to 0.5 and β =1 or 1.5. In addition, α_0 is recommended to be 0.1, as suggested by [121]. p_a and β are determined experimentally. MOCS was tested with β = 1, 1.5 and p_a = 0.25, 0.3,…, 0.5. For each set of parameters, 20 runs were carried out for MOCS, with the nest number set as 50 and the maximum iteration number set as 200. The results are evaluated with the ratio of the reference point found. The results are shown in Table 14.

Table 14 Ratios of the Reference Point found with different β *and* p_a

p_a	Average RRPF over 20 runs	
	β=1	β=1.5
0.25	6.02%	6.63%
0.3	6.33%	5.96%
0.35	5.78%	5.84%
0.4	4.88%	5.24%
0.45	5.60%	5.24%
0.5	4.16%	4.28%

Based on the results shown in Table 14, the following parameters are selected for MOCS in this study: p_a = 0.25 and β = 1.5. With this set of values for p_a and β, the largest average RRPF of the results over 20 runs were achieved.

Besides the parameters discussed above, the nest and maximum iteration numbers also need to be decided. More solutions can be achieved with larger nest and maximum iteration numbers, or by multiple runs. To show the impacts of the nest and maximum iteration numbers, MOCS was tested with different nest and maximum iteration numbers. Specifically, both the nest and the maximum iteration numbers are varied from 25 to 200, with the step size

as 25. For each combination of the number and maximum iteration numbers, MOCS was run 20 times. The results were evaluated with RRPF. The average RRPF and the average computation time are shown in Fig. 53 and Fig. 54. It can be seen from Fig. 53 and Fig. 54 that generally better results can be achieved with the larger nest and maximum iteration numbers. However, the computation time is also expected to be longer, if larger nest number and maximum iteration number are used.

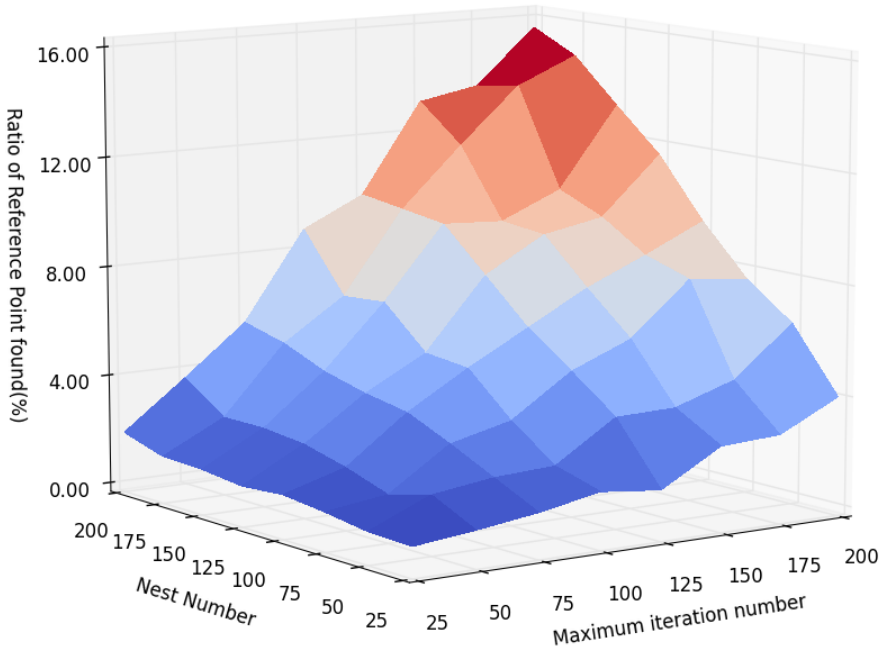

Fig. 53 RRPF for the tests with different nest and maximum iteration numbers

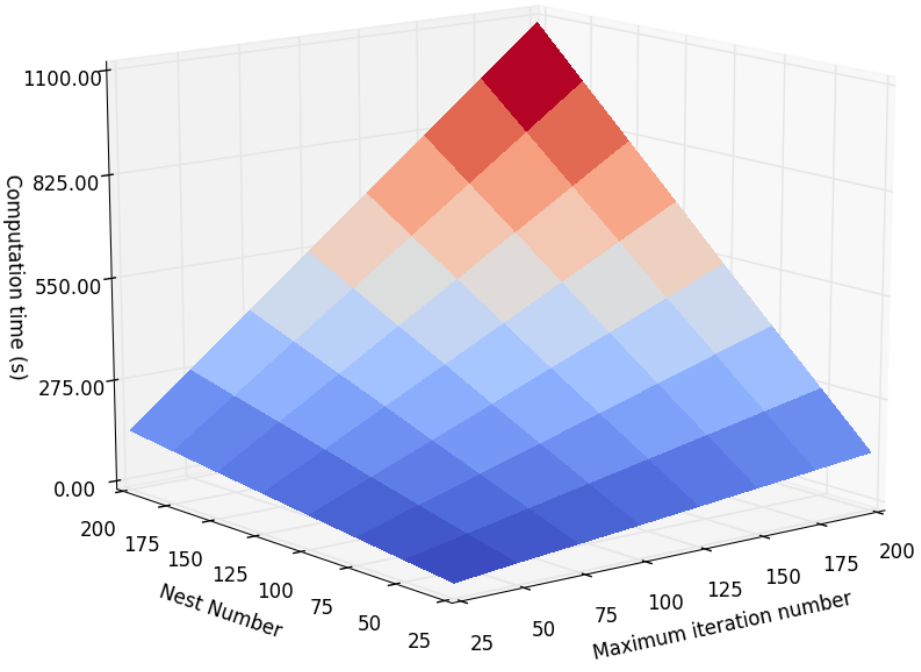

Fig. 54 Computation times of the tests with different nest and maximum iteration numbers

Theoretically, an optimal set of nest and maximum iteration numbers could be found for each optimisation problem. However, tuning the population size (nest number for MOCS) and maximum iteration number for multi-objective metaheuristic algorithms is a difficult task and there is no specific rule for guiding the selection of these numbers. In many previous studies, the population size and maximum iteration number were just given by the authors without specifying how these values were decided. In this study, the nest number is increased with the number of objectives and control variables. The maximum iteration number is determined experimentally. Specifically, the maximum iteration number is being increased, until the result cannot be further improved, as shown in Fig. 55.

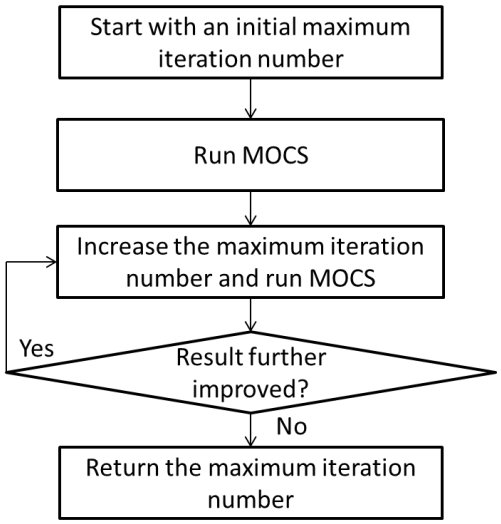

Fig. 55 MOCS maximum iteration number determination

It is not always straightforward to judge if the result is further improved or not for multi-objective optimisation problems. As discussed at the beginning of this section, normally the results for multi-objective voltage optimisation need to be measured by certain performance metrics, such as RRPF, before they can be compared. However, RRPF requires the information of Pareto front, which is normally unknown in practice. Another performance metric, coverage metric, is introduced here, to facilitate the comparison between two different sets of results. The coverage metric C(*A, B*) is defined as the ratio of the number of points in the solution set *B* dominated by the points from the solution set *A,* over the total number of points in the solution set *B* [139]. If all the points in *B* are dominated by the points in *A*, C(*A, B*) equals 1, while if none of the points in solution set *B* are dominated by the points in *A*, C(*A, B*) equals zero. Here, it is seen that the result can be further improved as long as the condition represented by (58) can be met.

$$C\left(SolutionSet^{before}, SolutionSet^{after}\right) > C\left(SolutionSet^{after}, SolutionSet^{before}\right) \qquad (58)$$

where $SolutionSet^{before}$ is the solution set achieved before increasing the maximum iteration number, while $SolutionSet^{after}$ is the solution set achieved after increasing the maximum iteration number. To mitigate the influence of the stochastic nature of metaheuristic algorithms, a large step size can be used to increase of the maximum iteration number. For this test case, the nest was set as 50 and the iteration number was determined as 300.

5.5.2 Comparison the voltage control algorithms based on MOCS and NSGA-II

The parameters for MOCS are shown in the section. The parameters of NSGA-II are set as recommended in [138]: population size = 100, generation = 301, crossover distribution = 20, mutation distribution = 20, crossover probability = 0.9, mutation probability = 0.1. Both algorithms are tested with 20 runs and the results are evaluated with RRPF, which are summarized in Table 15.

Table 15 Ratios of the reference point found of the results achieved with the multi-objective voltage optimisation algorithms based on MOCS and NSGA-II

	RRPF over 20 runs		
	Max	Min	Average
MOCS	10.24%	4.82%	6.75%
NSGA-II	3.98%	2.41%	3.45%

It can be seen from Table 15 that better results can be achieved with MOCS in terms of the performance metric, ratio of reference point found. Also, visual presentations of the results are also used to evaluate and compare the results achieved by MOCS and NSGA-II. The Pareto front found by exhaustive search and the best results achieved by MOCS and NSGA-II over 20 runs are shown in Fig. 56.

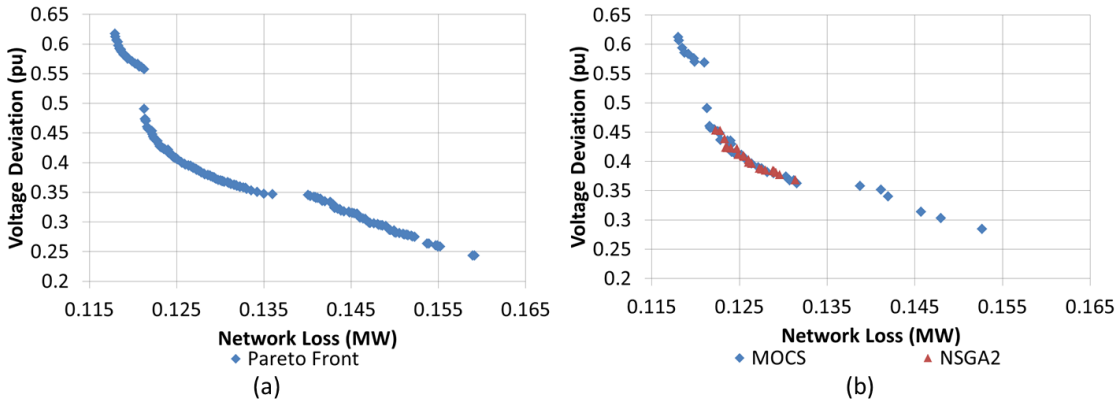

Fig. 56 Pareto front and test results for the initial multi-objective test case (a) Pareto front found by exhaustive search, (b) Results achieved by ODCDM and MOCS

As demonstrated by the results in Fig. 56, it can also be found that MOCS can reach to the space where NSGA-II cannot reach. It should be noted that potentially, better results could be achieved by NSGA-II, by tuning its parameters. However, instead of comparing MOCS and NSGA-II, here the purpose is just to illustrate the performance of MOCS.

Due to the stochastic nature of MOCS, the results achieved by different runs may not be the same, as shown by Fig. 57. However, it can be seen from Fig. 57 that the results achieved in both runs can reflect the Pareto front shown in Fig. 56–(a).

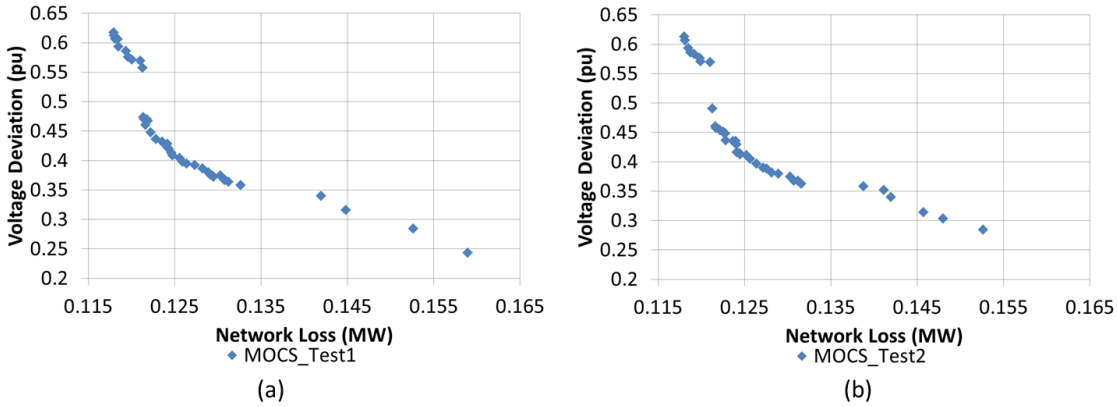

Fig. 57 Results for different runs of MOCS (a) Test 1 (b) Test 2

5.6 Conclusions

In this chapter, the CS based voltage control algorithms were introduced. CS, as a novel metaheuristic algorithm, has been extended to solve mixed integer and multi-objective optimisation problems and implemented here. These developed CS algorithms are then applied for distribution network voltage control. Initial test is conducted to illustrate the basic mechanism of the CS based voltage control algorithm. The developed CS algorithm is also compared with two popular algorithms, GA and PSO. Test results demonstrated that the CS

based voltage control algorithm is able to achieve a more stable result for the given test case, compared to the algorithms based on GA and PSO. And the MOCS based voltage control algorithm is compared with the NSGA-II based voltage control algorithm. The comparison results also demonstrate that MOCS achieved a more comprehensive set of Pareto-optimal solutions in comparison with NSGA-II.

As summarized in the last two chapters, deterministic algorithms and heuristic algorithms have their own characteristics. Although the theoretical differences between these two types of algorithms were discussed in previous studies, these two types of algorithms haven't been compared regarding the voltage control problems in future smart distribution networks before. In the following chapter, a methodology is proposed to compare these two algorithms and these two algorithms are evaluated and contrasted with different test cases.

Chapter 6 Evaluation of Single-objective Voltage Optimisation Algorithms

6.1 Introduction

In Chapter 4 and Chapter 5, the development and initial evaluation of two single-objective voltage optimisation algorithms, based on ODCDM and SOCS, were described. This chapter describes the further evaluation and comparison of these two algorithms, regarding various voltage control problems in conventional and future distribution networks. Specifically, a number of test cases have been generated, based on different test networks, optimisation objectives and load and generation conditions. The voltage optimisation algorithms were applied to solve the test cases, and their performance was evaluated and compared to predetermined performance metrics. For the remainder of this chapter, the ODCDM based voltage optimisation algorithm will be referred to as ODCDM, while the SOCS based voltage optimisation algorithm will be referred to as SOCS.

In the rest of this chapter, the evaluation method is introduced. The voltage optimisation problem formulated for conventional distribution networks is analysed. Test cases are then generated based on the analysis of the problem formulation, followed by the test results achieved by ODCDM and SOCS. The changes in the voltage optimisation problem for future distribution networks are then discussed, followed by the generation of test cases and the corresponding test results. Finally, conclusions are drawn.

6.2 Voltage optimisation algorithm evaluation method

As shown in Chapter 4 and Chapter 5, voltage control problems can be formulated as optimisation problems, which consist of optimisation objective(s), equality and inequality constraints. These components are determined according to the specific issues related to the voltage control problems, such as the network under control and control preferences. Various test cases are generated based on the potential variations of the components of the voltage optimisation problem. Voltage optimisation algorithms are then applied to solve these test cases and their performance is evaluated.

As discussed in Chapter 4, voltage optimisation algorithms are required to find a feasible solution, with which network voltages can be maintained with their statutory limits. Also, voltage optimisation algorithms are expected to minimise the optimisation objective functions, which are defined to represent secondary control objectives. In this chapter, single-objective voltage optimisation is considered, which means voltage optimisation algorithms can be assessed and compared, regarding the values they achieved for the optimisation objective

function. In addition, voltage optimisation algorithms must meet the computation time requirement for real time control, which is related to different issues in practice, such as the computation power of the controller and the computational burden of the algorithm itself. Here the algorithms are evaluated and compared regarding the computation time they required for each test case. Therefore, the following performance metrics are used to evaluate the performance of single-objective voltage optimisation algorithms:

- The ability to find a feasible solution;
- The value achieved for the optimisation objective function;
- The computation time.

6.3 Problem formulation and analysis for conventional distribution networks

The following assumptions were made regarding the voltage control problems in conventional distribution networks, as per the discussion in Chapter 2:

- Only load is connected to distribution networks;
- Conventional voltage control techniques are used for voltage control. Here, OLTC and MSC are considered as voltage control techniques in conventional distribution networks.

Regarding these two assumptions, the specific problem formulation for voltage control in conventional distribution networks is introduced, with regards to the optimisation objective functions, equality constraints and inequality constraints.

6.3.1 Optimisation objective functions

Network loss minimisation and voltage deviation minimisation, as defined in Chapter 4 and Chapter 5, are used to create test cases. In addition, minimising the numbers of OLTC and MSC switching operations is also considered as an optimisation objective. By reducing the numbers of switching operations of the OLTCs and MSCs, the lifetime of these voltage control devices can be extended. Also, this can reduce the likelihood of affecting the operation of other network components and customers [140]. The switching operations could also be formulated as a set of constraints [76, 78, 141], which are normally adopted in the control scheduling problems. This PhD thesis concentrates on real time control, for which the number of switching operations is normally considered as one optimisation objective, as represented by (59). In the rest of this chapter, this optimisation objective is simply referred to as switching operation minimisation.

$$N_{Switching}^{Total} = \sum_{i}^{N_{OLTC}} SwitchingNumber_i^{OLTC} + \sum_{i}^{N_{MSC}} SwitchingNumber_i^{MSC} \quad (59)$$

where $N_{Switching}^{Total}$ is the total number of switching operations for all OLTCs and MSCs. $SwitchingNumber_i^{OLTC}$ and $SwitchingNumber_i^{MSC}$ are the numbers of the switching operations for OLTC i and MSC i. For an OLTC, the number of switching operation can be calculated by (60).

$$SwitchingNumber = \frac{\left| Position - Position^0 \right|}{StepSize} \quad (60)$$

where,

Position	Position of the voltage control device after control
$Position^0$	Position of the voltage control device before control
StepSize	Step size of the voltage control device

As shown by (60), the switching operation is affected by the positions of the voltage control devices before a control action is applied.

The number of switching operations for a MSC can also be calculated by (60), if the MSC only has one stage (one capacitor bank), or the MSC has multiple stages and the capacitor banks of this multi-stage MSC have the same size. However, if the capacitor banks in a multi-stage MSC have different sizes, the number of switching operations for this multi-stage MSC may not be simply calculated by (60). Instead, more complicated relationships between the number of switching operation and the MSC stage positions need to be considered. This is illustrated with the MSCs in the case study network used for the initial algorithm evaluation in Chapter 4. The relationship between the MSC stage positions and the CB status can be defined by a look up table as shown in Table 16. In this case, the number of switching operation of CBs needs to be calculated regarding the CB status changes, when the MSC is switched between different stage positions.

Table 16 Relationship between MSC stage position and CB status

MSC Stage Position	Total MVAr	Capacitor Bank Switch		
		0.1MVAr	0.2MVAr	0.4MVAr
1	0	Off	Off	Off
2	0.1	On	Off	Off
3	0.2	Off	On	Off
4	0.3	On	On	Off
5	0.4	Off	Off	On
6	0.5	On	Off	On
7	0.6	Off	On	On
8	0.7	On	On	On

The optimisation objective function can also be formulated as a combination of more than one of the control objectives described above. However, in this chapter, these objectives are evaluated individually, to investigate the relationships between the optimisation objectives and the algorithms' performance.

6.3.2 Equality constraints

As discussed in Chapter 4, the equality constraints for voltage optimisation are the power flow equations of the network under control. Node power equations are normally used, as represented by (30). The power flow equations model the relationship between the network voltages and the net injected real and reactive powers at different busbars. The admittance matrix is determined by the network topology, as well as the OLTC tap positions and the shunt connected components, such as capacitor banks [107]. In simple terms, power flow calculations are considered as the problem of solving the node voltage magnitude and phasor of each busbar when the injected complex power is specified [107, 142]. As assumed at the beginning of section 6.3, only load is connected in conventional distribution networks. Therefore, the net injected complex powers are solely determined by the variations of load.

6.3.3 Inequality constraints

Maintaining network voltages within their statutory limits, is defined as a set of inequality voltage constraints, as represented by (32). As the fundamental control objective, this set of inequality voltage constraints is always considered.

As shown in Chapter 4, inequality constraints also include the operation ranges of the control variables. Based on the assumptions given at the beginning of section 6.3, the control variables include the tap positions of OLTCs and stage positions of MSCs for conventional distribution networks. The inequality constraints for the control variables of OLTCs and MSCs, are represented by (61) and (62).

$$Tap_i^{\min} \le Tap_i \le Tap_i^{\max}, i = 1, \ldots, N_{OLTC} \tag{61}$$

$$Cap_i^{\min} \le Cap_i \le Cap_i^{\max}, i = 1, \ldots, N_{MSC} \tag{62}$$

where,

Tap_i	tap position of OLTC *i*
Tap_i^{min}	lowest tap position of OLTC *i*
Tap_i^{max}	highest tap position of OLTC *i*
N_{OLTC}	number of OLTCs
Cap_i	stage position of MSC *i*
Cap_i^{min}	lowest stage position of MSC *i*
Cap_i^{max}	highest stage position of MSC *i*
N_{MSC}	number of MSCs

6.4 Test case development and algorithm implementation for conventional distribution networks

Based on the discussion in section 6.3, it can be seen that the problem formulation is determined based on various factors, as summarized in Fig. 58. Different test cases, regarding the variation of these factors, are developed to systematically evaluate voltage optimisation algorithms.

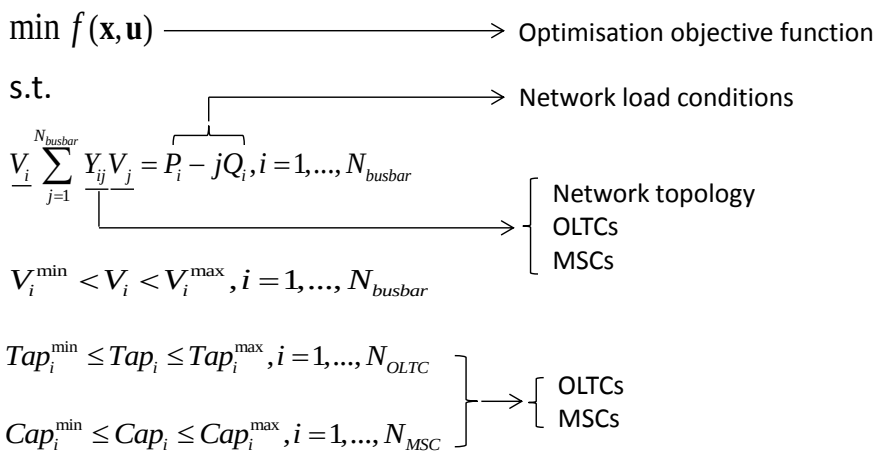

Fig. 58 Voltage optimisation problem determination for conventional distribution networks

6.4.1 Case study networks

Three case study networks are used for the single-objective voltage optimisation evaluation. Two of them are based on the IEEE 33 busbar network [143], while the other one is based on the IEEE 69 busbar network [144]. The network data for these networks is given in Appendix A-2. There are no voltage control devices in the original networks. In previous studies, different voltage control devices were connected to create case study networks [51, 76, 145-148]. In this work, one case study network was developed by defining voltage control techniques, while the other two case study networks were developed based on previous studies [51, 76].

The case study network, which was used for initial study in Chapter 4 and Chapter 5, is used here and designated as Network A. The details of Network A can be found in section 4.5.1.

The second case study network, designated as Network B, is also based on the IEEE 33 busbar network. The OLTC and MSCs placement from [51] is used. Specifically, one OLTC at the primary substation and four MSCS are connected into the network [51]. The details of these voltage control devices are summarized in Table 17.

Table 17 Voltage Control Devices in the Case Study Network B

Control Device	Location	Step size	Range	Total step number
OLTC	From busbar 1 to busbar 2	1.25%	-5% - +5%	9
MSC1	Busbar 8	0.05MVAr	0-0.3MVAr	7
MSC2	Busbar 12	0.05MVAr	0-0.3MVAr	7
MSC3	Busbar 15	0.05MVAr	0-0.3MVAr	7
MSC4	Busbar 29	0.05MVAr	0-0.3MVAr	7

The single line diagram of Network B is shown in Fig. 59.

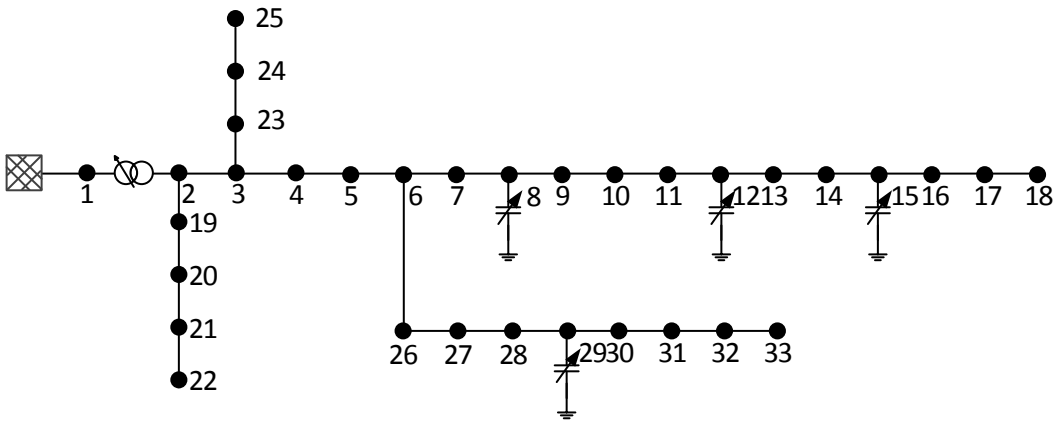

Fig. 59 Case study Network B

The third case study network, designated as Network C, is based on the IEEE 69 busbar network. The capacitor bank placement from [76] is used here. Ten capacitor banks are connected to this network. In addition, one OLTC is connected to create a more realistic case study network. The details of the control actions are listed in Table 18.

Table 18 Voltage Control Devices in the Case Study Network C

Control Device	Location	Step size	Range	Total step number
OLTC	From busbar 1 to busbar 2	1.25%	-5% - +5%	9
MSC1	Busbar 9	0.3MVAr	0-0.6MVAr	3
MSC2	Busbar 19	0.3MVAr	0-0.6MVAr	3
MSC3	Busbar 31	0.3MVAr	0-0.6MVAr	3
MSC4	Busbar 48	0.3MVAr	0-0.9MVAr	4
MSC5	Busbar 51	0.3MVAr	0-0.6MVAr	3
MSC6	Busbar 58	0.3MVAr	0-0.6MVAr	3
MSC7	Busbar 63	0.3MVAr	0-1.2MVAr	5
MSC8	Busbar 66	0.3MVAr	0-0.6MVAr	3
MSC9	Busbar 68	0.3MVAr	0-0.6MVAr	3
MSC10	Busbar 42	0.3MVAr	0-0.6MVAr	3

The single line diagram of Network C is shown in Fig. 60.

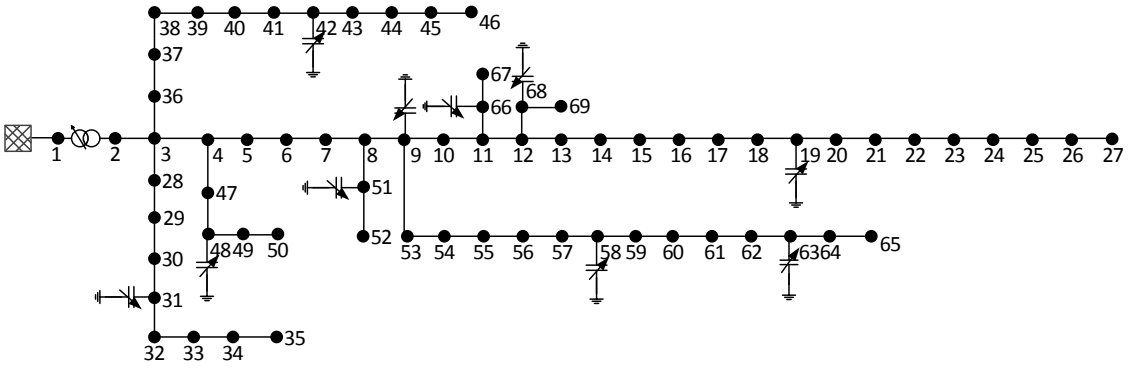

Fig. 60 Case study Network C

The original load is used as the maximum load condition, while the minimum load condition is defined to be 25% of the original load condition.

6.4.2 Test cases for conventional distribution networks

Once the network topology and the details of the voltage control devices are defined, the optimisation problem mainly changes with the optimisation objectives, and network load conditions. Here, the following three optimisation objectives, as discussed in section 6.3.1, are used:

1. Network loss minimisation;
2. Voltage deviation minimisation;
3. Switching operation minimisation.

Different load conditions are used to develop the test cases for each of these optimisation objectives. These load conditions are selected with two different approaches:

- ***Snapshot***: The network load conditions are generated by scaling all the loads in the network with a load scale index, which is varied from 25% to 100% with a step size of 5% (16 load conditions).
- ***Profile***: The network load conditions are generated by scaling all the loads based on a load profile. Here, a generic 24-hour load profile, as shown in Fig. 61, is used to develop the profile test cases. This profile is from the CLNR project, with the step size equal to one hour [101].

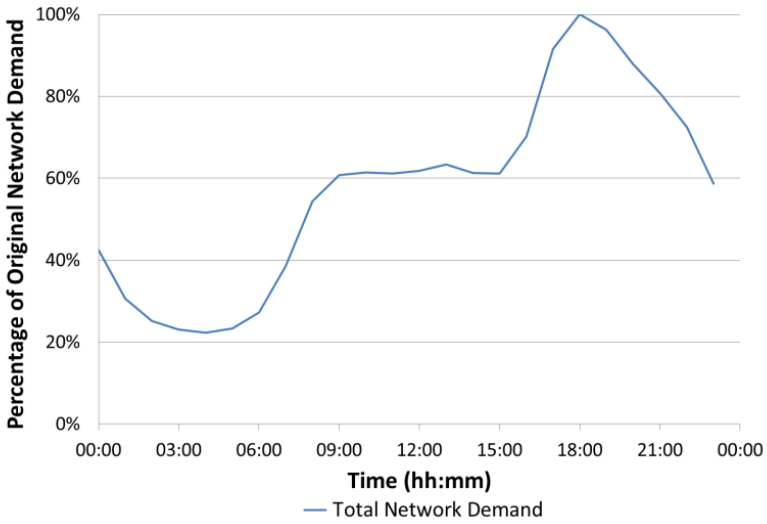

Fig. 61 Generic load profile from the CLNR project

For the first two optimisation objectives, the test case can be determined when the network and the load condition are decided. For the switching operation minimisation, the positions of the OLTCs and MSCs before control are also required, to develop the test cases. As shown by (60), the switching operation calculation depends on the positions of the OLTCs and MSCs before optimisation. Here, the nominal position (0%) is used for the OLTC tap positions before optimisation, and 0MVAr is used for the MSCs stage positions before optimisation, which means no reactive power is injected into the network.

In total, 360 test cases have been generated, by combining different test networks, optimisation objectives and load conditions, as summarized in Table 19.

Table 19 Summary of test cases for conventional distribution networks

	Variants
Network	3
Optimisation objective	3
Load condition	40 (16 snapshot + 24 profile)
Total test case number	360 (3×3×40=360)

It is assumed that the capacitor banks in MSCs have the same sizes in the test cases shown in Table 19, which means the number of switching operation of MSCs can be calculated by (60). Ten additional snapshot test cases have been developed for switching operation minimisation, with the assumption that the capacitor banks in MSCs have different sizes, as shown in Table 16. The details of these ten test cases will be shown with the test results in section 6.5.3.

6.4.3 Algorithm application

The optimisation problems in the test cases developed for conventional distribution networks are combinatorial problems, since only discrete control variables, the tap positions of OLTCs and the stage positions of MSCs, are considered. ODCDM, as a combinatorial algorithm, can be applied directly to solve the optimisation problems in these test cases. As shown in Chapter 4, a SP, consisting of the initial values of all the control variables, is required by ODCDM and the result achieved by ODCDM may be affected by the SP. Nominal values of the control variables are normally used to test deterministic optimisation algorithms [85, 108] and are also used here for ODCDM.

As shown in Chapter 5, there are some parameters in SOCS, which could be tuned, such as the nest number and the maximum iteration number. Potentially, these parameters could be tuned to improve the performance of SOCS regarding each individual problem. However, parameter tuning is time consuming and it is not practical to tune all the parameters for each individual problem. Here, the majority of the parameters are fixed as per previous studies [130, 135], in order to demonstrate that the algorithm can be applied without large efforts in parameter tuning. Specifically, the nest number is selected as 25, the step size scale factor and nest abandon probability p_a are selected as 0.01 and 0.25. For a given network, the maximum iteration number required for the test cases with each optimisation objective function is determined as per the procedure described in section 5.4.1. The maximum iteration number for SOCS is determined under maximum load condition, which is seen as the worst case scenario [8]. The maximum iteration numbers of SOCS for the conventional test cases are

summarized in Appendix B-1. SOCS will stop once the maximum iteration number is reached, or the expected value of the optimisation objective function is found.

In Chapter 4 and Chapter 5, it was demonstrated that the penalty function is used within both SOCS and ODCDM, to deal with violation of voltage constraints. A large penalty factor (10^6) is adopted here for both algorithms, to avoid any voltage violations.

6.5 Case study results – test cases for conventional distribution networks

In this study, PYPOWER is used as the platform for load flow analysis. PYPOWER is the Python version of MATPOWER [149]. A constant power load model is used to model the loads in the case study networks. Both algorithms, SOCS and ODCDM, are implemented in Python and can be used with different PYPOWER network models. The tests are run on an Intel i5, 3.20GHz computer (8GB) in the Spyder (Scientific PYthon Development EnviRonment) [150].

For all the test cases for conventional distribution networks, both ODCDM and CS always found a feasible solution, which means there was no voltage violation observed during these tests. The other two performance metrics are presented in the following.

6.5.1 Network loss minimisation

Snapshot Analysis

For each case study network, both ODCDM and SOCS are evaluated with 16 snapshot test cases, which are created with different load conditions. The test results for illustrative sample test cases, in which load scale is set as 1, are shown in Table 20. The full test results are detailed in Appendix B-2.

Table 20 Snapshot test results comparison – Network loss minimisation

Case study network	Network loss (MW)			Computation time (s)	
	ODCDM	SOCS	Reduction	ODCDM	SOCS
A	0.1179	0.1179	0.0%	4.01	48.77
B	0.1343	0.1343	0.0%	3.28	22.75
C	0.1309	0.1306	0.2%	3.63	86.12

It can be seen that there are no significant differences between the results achieved by both algorithms, in terms of network loss minimisation. However, the computation time required for ODCDM is much shorter than that required for SOCS.

Profile Analysis

The results for the profile test analysis are shown in Fig. 62.

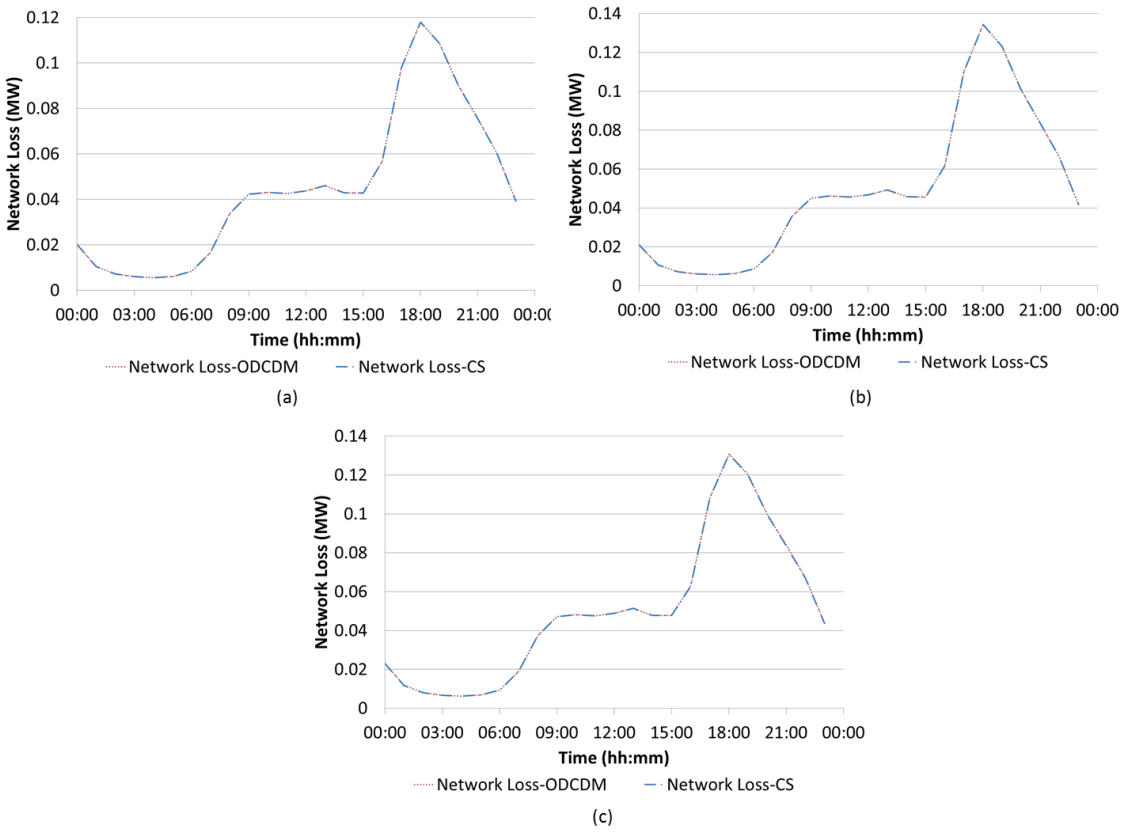

Fig. 62 Profile test results - Network loss minimisation (a) Network A (b) Network B (c) Network C

The computation times for profile test cases are summarized in Appendix B-2. Again, it can be seen that there are no significant differences between the results achieved by both algorithms, in terms of network loss minimisation, and the computation time of ODCDM is much shorter than that of SOCS.

6.5.2 Voltage deviation minimisation

Snapshot Analysis

For each case study network, both ODCDM and SOCS are evaluated with 16 snapshot test cases, which are created with different load conditions. The test results for illustrative sample test cases, in which load scale is set as 1, are shown in Table 21. The full test results are listed in Appendix B-3.

Table 21 Snapshot test results – Voltage deviation minimisation

Case study network	Voltage deviation (pu)			Computation time (s)	
	ODCDM	SOCS	Reduction	ODCDM	SOCS
A	0.35	0.24	29.9%	4.22	42.08
B	0.57	0.53	7.6%	2.52	47.39
C	0.76	0.76	0.0%	5.36	65.48

As shown by the test results in Table 21 and Appendix B-3, for some of the test cases, SOCS could achieve a significantly better result in terms of the value achieved for voltage deviation in comparison with ODCDM. However, the computation times required by ODCDM are still much shorter than that required by SOCS.

Profile Analysis

The algorithms are also tested with the load profile shown in Fig. 61, for voltage deviation minimisation. The results are shown in Fig. 63.

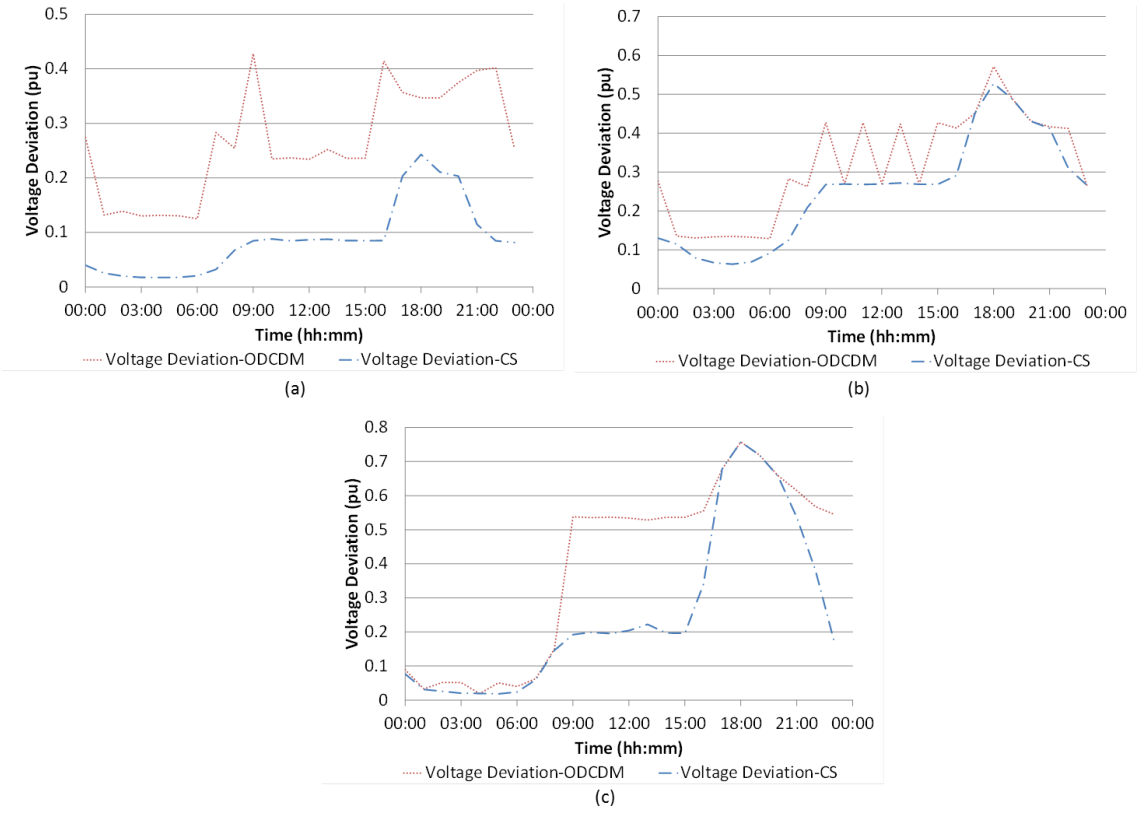

Fig. 63 Profile test results – Voltage deviation minimisation (a) Network A (b) Network B (c) Network C

The computation times for profile test cases are summarized in Appendix B-3. The results from the profile analysis are consistent with the snapshot analysis and indicate that SOCS could reduce the voltage deviation observed compared to ODCDM for some test cases. Also, the computation times required for ODCDM are much shorter than that required for SOCS.

6.5.3 Switching operation minimisation

Snapshot Analysis

For each case study network, both ODCDM and SOCS are evaluated with 16 snapshot test cases, which are created with different load conditions. The test results for four illustrative sample test cases, in which load scale is set as 1, are shown in Table 22. The full test results are listed in Appendix B-4.

Table 22 Snapshot test results – Switching operation minimisation

Case study network	Switching operation			Computation time (s)	
	ODCDM	SOCS	Reduction	ODCDM	SOCS
A	2	2	0.0%	0.55	31.87
B	2	2	0.0%	0.32	31.70
C	3	3	0.0%	1.09	63.90

From the results shown in **Table 22** and Appendix B-4, it can be seen that both ODCDM and SOCS can achieve the same switching operation. Again, SOCS needs a much longer computation time than ODCDM.

Profile Analysis

The profile test results for switching operation minimisation are shown in Fig. 64.

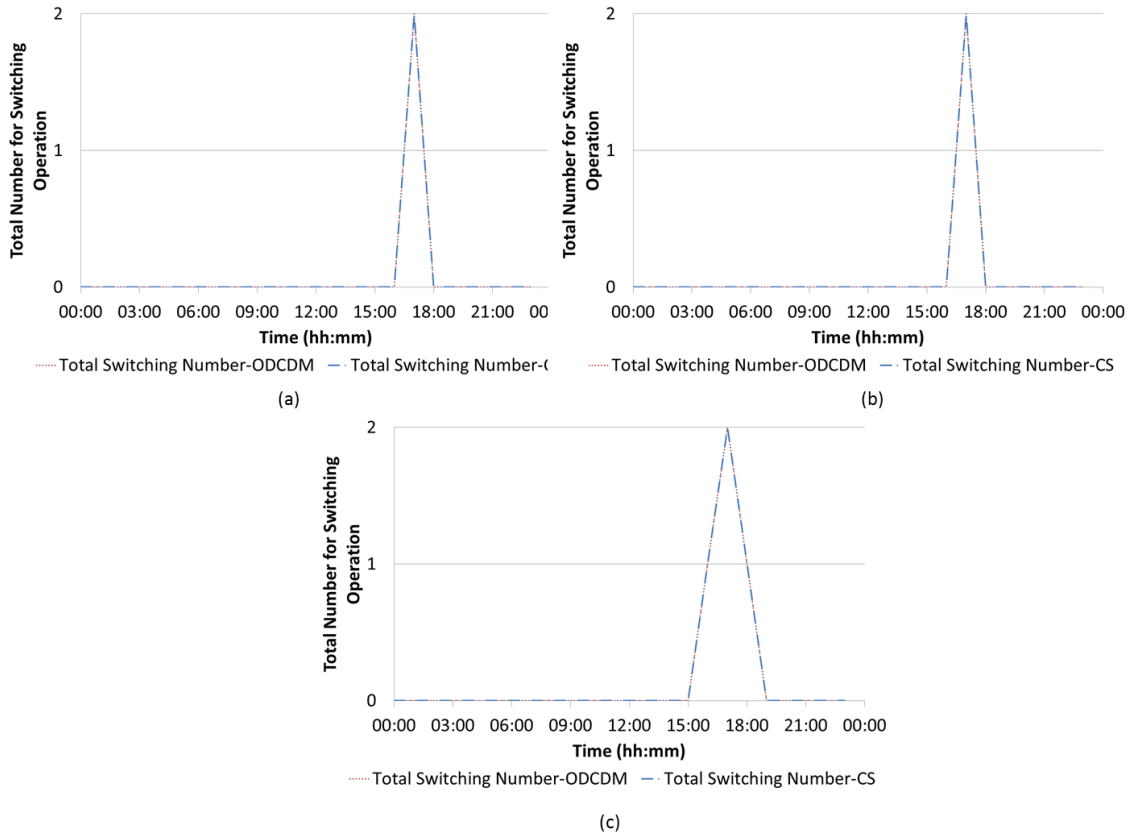

Fig. 64 Profile test results – Switching number minimisation (a) Network A (b) Network B (c) Network C

The computation times for profile test cases are summarized in Appendix B-4. The results from the profile analysis are consistent with the snapshot analysis and indicate that same

results are achieved by both algorithms. Also, the computation times required for ODCDM are much shorter than that required for SOCS.

The mechanism of ODCDM allows it to achieve a feasible solution with the minimum switching operation, if it is assumed that the movement of each control variable will lead to one switching operation with equivalent value [61].

Snapshot Analysis - MSCs with different capacitor bank sizes

MSCs have capacitor banks of different sizes in Network A, making the decisions on which capacitor bank to switch in/out more complex. To emphasize the effect of MSCs on switching operation, the OLTC is locked. Ten test cases are developed with random values used as the MSC positions before optimisation. The network load scale is set as 1 in these test cases. The test results are shown in Table 23.

Table 23 Test results – Switching operation minimisation (MSCs with different capacitor bank sizes)

Test case index	**Switching operation**			**Computation time (s)**	
	ODCDM	**SOCS**	**Reduction**	**ODCDM**	**SOCS**
RandomSP1	4	2	50.0%	2.34	31.94
RandomSP2	4	2	50.0%	2.82	31.87
RandomSP3	3	3	0.0%	1.73	32.13
RandomSP4	2	2	0.0%	1.57	31.26
RandomSP5	3	3	0.0%	1.91	31.41
RandomSP6	2	2	0.0%	1.65	31.25
RandomSP7	3	3	0.0%	1.96	31.52
RandomSP8	4	2	50.0%	2.61	31.79
RandomSP9	5	2	60.0%	2.38	31.47
RandomSP10	1	1	0.0%	0.57	31.82

From the results in Table 23, it can be seen that when the relationship specified in Table 16 is used, SOCS is able to achieve a better result than ODCDM. This is because the relationship between the number of switching operation and the capacitor bank stage position is non-convex. Similar results could be expected when the switching actions of different control variables are not equivalent to each other. For example, there may be some preference to avoid switching specified control devices, which are nearing end of life or end of maintenance cycles [27].

6.6 Problem formulation and analysis for future distribution networks

In future distribution networks, the following assumptions are made:

- Besides load, DGs are connected to distribution networks;
- Maximum load is increased due to the connection of load LCTs;
- Besides conventional voltage control techniques (OLTC, etc.), DG real and reactive powers are used for voltage control, as novel voltage control techniques.

Controlling DG real and reactive powers directly is used here to represent the novel voltage control techniques in future distribution networks, since many novel voltage control techniques, such as EES and D-STATCOM, also control the real and reactive power import/export of the connected busbars [68]. The controllable DG real and reactive powers introduce additional control variables for the voltage control problems. Since the DG real and reactive powers are continuous control variables, the problems formulated for the voltage control problems become a MINLP problem. In addition, the other components of the formulated optimisation problem are also affected by the DG connection, as specified in the following.

6.6.1 Optimisation objective functions

Besides the optimisation objectives considered for conventional distribution networks, additional optimisation objectives may also need to be considered in future. DG real power curtailment has also been previously demonstrated to enable voltage support [42, 151]. Where DG real power curtailment is integrated into a voltage control algorithm, DG curtailment minimisation is usually considered as an optimisation objective [100, 151-153]. Total DG real power curtailment is calculated as the sum of the differences between available outputs and the real outputs of all DGs with real power control, as represented by (63).

$$f_{DGCurtailment} = \sum_{i}^{N_{DG}^{PControl}} (P_{DGi}^{available} - P_{DGi}^{output}) \tag{63}$$

where,

$N_{DG}^{PControl}$ total number of DGs with real power control

$P_{DGi}^{available}$ available real power output of DG *i*

P_{DGi}^{output} real power output of DG *i*

DG reactive power control has been previously demonstrated to enable voltage support regarding the conventional optimisation objectives [51, 151, 154]. There are occasions when DG reactive power usage minimisation, as represented by (64), is also considered as an optimisation objective [151, 152, 154, 155].

$$f_{DGQUsage} = \sum_{i}^{N_{DG}^{QControl}} \left| Q_i^{reference} - Q_i^{output} \right| \tag{64}$$

where,

$N_{DG}^{QControl}$ total number of DGs with reactive power control

$Q_{DGi}^{reference}$ reference value for the reactive power from DG *i*

Q_{DGi}^{output} reactive power output of DG *i*

The reference value for the reactive power from DG can be determined by the DG owners and the distribution network operators [156]. Here, the reference value is selected to be zero, as per previous studies [51, 151, 154].

6.6.2 Equality constraints

In this study, it is assumed that DGs and load LCTs are connected to the existing busbars directly. The real and reactive powers of DGs and load LCTs could affect the net import/export of real and reactive powers from the busbars where the DGs and load LCTs are connected, and then affect the power flow equations, represented by (30).

6.6.3 Inequality constraints

In this study, the DG real power and reactive powers are controlled directly. The box constraints, which are commonly used in previous studies [151, 157], can be represented by(65) and (66).

$$P_{DGi}^{\min} \le P_{DGi}^{output} \le P_{DGi}^{\max}, i = 1, \ldots, N_{DG}^{PControl} \tag{65}$$

$$Q_{DGi}^{\min} \le Q_{DGi}^{output} \le Q_{DGi}^{\max}, i = 1, \ldots, N_{DG}^{QControl} \tag{66}$$

where,

P_{DGi}^{min} lower limit of the real power output of DG *i*;

P_{DGi}^{max} upper limit of the real power output of DG *i*;

Q_{DGi}^{min} lower limit of the reactive power output of DG *i*;

Q_{DGi}^{max} upper limit of the reactive power output of DG *i*;

Normally, the lower limit of the DG real power export is zero, while the upper limit of the DG real power is the available DG real power output. The limits of the DG reactive power are defined by (67) and (68).

$$Q_{DGi}^{\min} = -P_{DGi}^{Capacity} \cdot \tan(\arccos(\varphi)) \tag{67}$$

$$Q_{DGi}^{\max} = P_{DGi}^{Capacity} \cdot \tan(\arccos(\varphi)) \tag{68}$$

where $P_{DGi}^{Capacity}$ is the installed capacity of DG *i*, and φ is the power factor limit of DG output, when DG real power is at its installed capacity. φ is selected as 0.95 in this study based on previous studies [8, 53]. The maximum reactive power import/export that can be controlled is equal to the reactive power import/export at rated real power at a power factor of 0.95.

6.7 Test case development and algorithm implementation for future distribution networks

As shown in section 6.6, it can be seen that the problem formulation is determined based on various factors, as summarized in Fig. 65. New optimisation objectives may need to be considered in future distribution networks. The connection of DGs affects the power flow equations and additional inequality constraints need to be considered. As previously a set of test cases for systematic evaluation of the performance of the ODCDM and SOCS algorithms are developed.

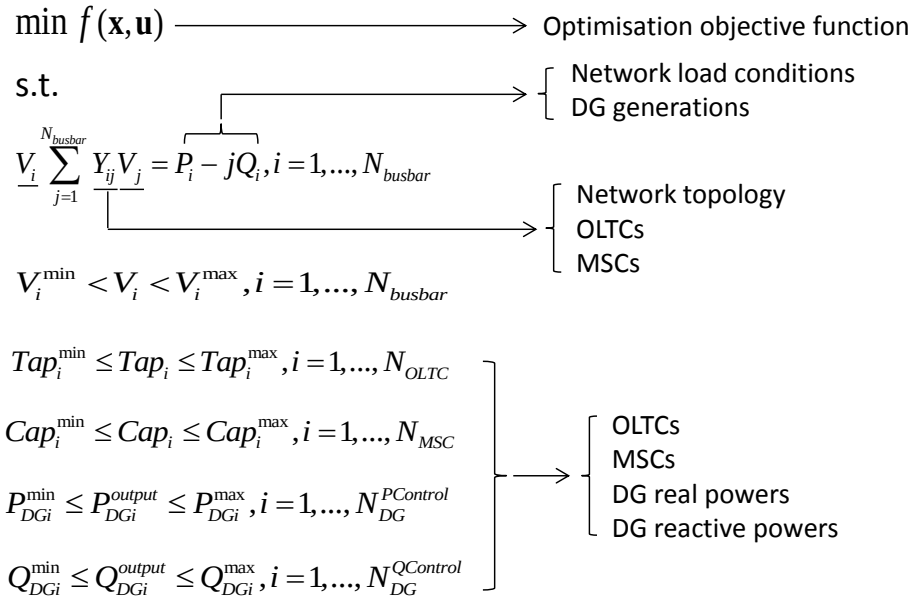

Fig. 65 Voltage optimisation problem determination for future distribution networks

6.7.1 Case study networks for algorithm evaluation

Two future case study networks are utilized here. These case study networks are developed by connecting DG(s) to conventional case study networks introduced in section 6.4.1. A negative load is used here to model DG. A single-DG case study network, designated as Network D, is created based on Network B. As shown in Fig. 66, one DG is connected to busbar 18 in Network B. The installed capacity of this DG is assumed to be 4MW.

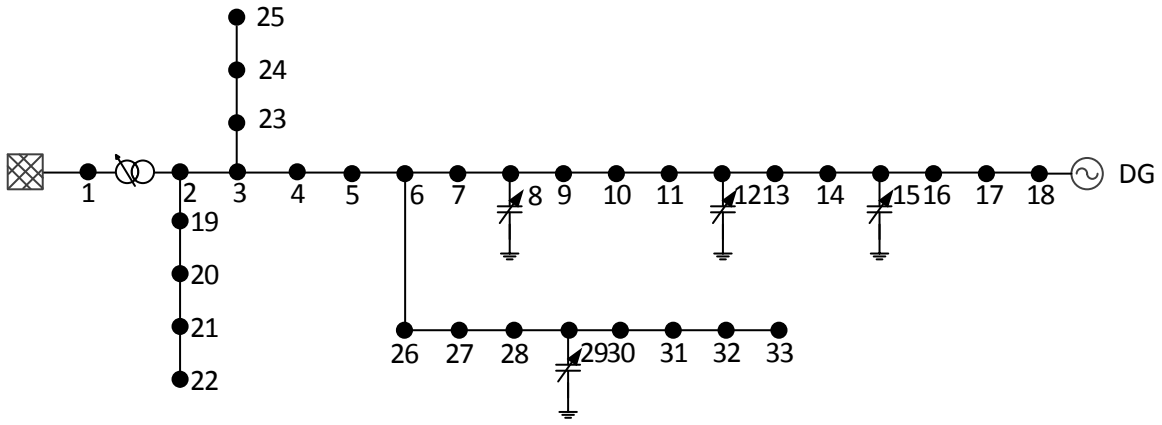

Fig. 66 Single-DG case study network – Network D

A multi-DG case study network, designated as Network E, is created by connecting three DGs to Network C, as shown in Fig. 67. The installed capacities of these three DGs are assumed to be 2.5MW.

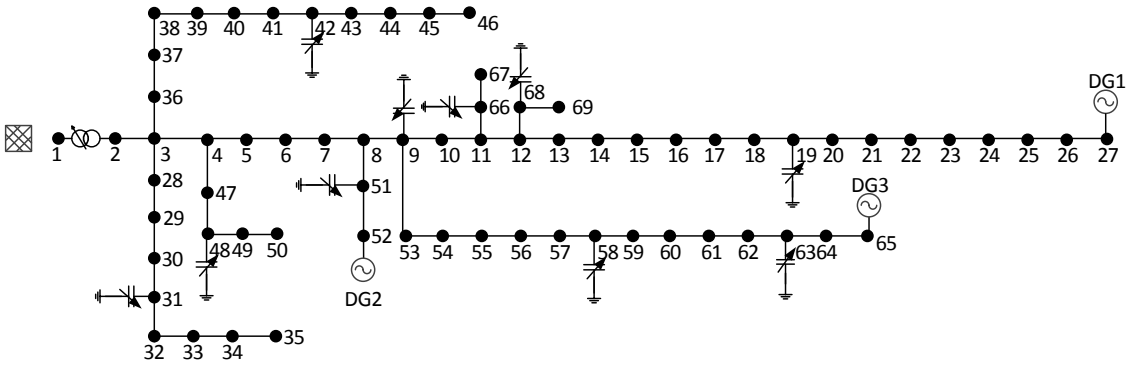

Fig. 67 Multi-DG case study network – Network E

It is assumed that the maximum network load is increased from the original value by a factor of 1.1, to represent the effect of the connection of load LCTs. For both case study networks, DG real and reactive powers are controlled with the existing OLTC and the MSCS in the networks.

6.7.2 Test cases for future distribution networks

The optimisation objectives from section 6.3.1 and two optimisation objectives defined in section 6.6.1 are considered for future distribution networks, as shown below:

1. Network loss minimisation;
2. Voltage deviation minimisation;
3. Switching operation minimisation;
4. DG real power curtailment minimisation;
5. DG reactive power usage minimisation.

These objectives are used individually to generate different test cases. For each optimisation objective, different load and generation conditions are used to develop the test cases for future distribution networks. Similar to the test case development for conventional distribution networks, snapshot and profile test cases are developed based on the case study networks from section 6.7.1.

- ***Snapshot:*** Load is varied from 25% to 110% with the step size of 5% (18 load conditions). Also, the generation is varied from 0.25MW to the maximum generation with the step size as 0.25MW.
- ***Profile***: As in the case of the conventional network case, a generic 24-hour load profile, shown in Fig. 61, is used to develop the profile test cases. A constant value is used to represent the available DG real power export.

For the test cases with switching operation minimisation as the optimisation objective, the nominal position (0%) is used for the OLTC tap positions before optimisation, and 0MVAr is used for the MSC stage positions before optimisation, which means no reactive power is injected into the network.

In total, test cases have been generated, by combining optimisation objectives and load conditions, as summarized in Table 24 and Table 25.

Table 24 Summary of test cases for Network D

	Variants
Optimisation objective	5
Load condition	312 (288 snapshot + 24 profile)
Total test case number	1560 (5×312=1560)

Table 25 Summary of test cases for Network E

	Variants
Optimisation objective	5
Load condition	204 (180 snapshot + 24 profile)
Total test case number	1020 (5×204=1020)

6.7.3 Algorithm application

The involvement of continuous control variables changes the optimisation problem from a combinatorial problem to a MINLP problem. For ODCDM, continuous control variables in the MINLP problems need to be discretised, as discussed in Chapter 4. Different step sizes, which are used to discretize continuous control variables, could create different optimisation problems. The performance of ODCDM is affected by the step size used, as illustrated by an example shown in Appendix B-5. Generally speaking, a better result could be achieved by using smaller step sizes, but a longer computation time is required when small step size is used. Here, 0.01MW/MVAr is used as the step size to discretize DG real and reactive powers for ODCDM. Starting points still affect the results achieved by ODCDM. The DG real power is set to the available DG real power output, and the DG reactive power is set to zero in the SPs. According to the discussion in section 6.4.3, nominal values of the control variables for OLTCs and MSCs are used in the SPs.

SOCS can be applied directly to solve the MINLP problems. Similar to the SOCS application for the test cases in conventional distribution networks, only the maximum iteration number is determined based on the 'worst case scenarios'. Here, the worst case scenarios are defined as the following, as per previous research [8]:

- Maximum load and no generation;
- Maximum load and maximum generation;
- Minimum load and maximum generation.

These network load and generation conditions are used to determine the maximum iteration number for SOCS. The largest value for the maximum iteration number determined is used, as summarized in Appendix B-6.

6.8 Case study results – test cases for future distribution networks

6.8.1 Test results for Network D

Snapshot Analysis

For each optimisation objective, both ODCDM and SOCS are evaluated with 288 snapshot test cases, which are based on different load and generation conditions. More test results are shown in Appendix B-7. Here, the results for the test cases with the minimum load and maximum generation are summarized in Table 26, while the results for the test cases with the maximum load and maximum generation are summarized in Table 27.

Table 26 Snapshot test results of Network D – minimum load and maximum generation

Network loss minimisation						
Network loss (MW)			Number of voltage violation busbars		Computation time (s)	
ODCDM	SOCS	Reduction	ODCDM	SOCS	ODCDM	SOCS
0.0045	0.0044	1.0%	0	0	188.44	76.45
Voltage deviation minimisation						
Voltage deviation (pu)			Number of voltage violation busbars		Computation time (s)	
ODCDM	SOCS	Reduction	ODCDM	SOCS	ODCDM	SOCS
0.08	0.07	10.4%	0	0	70.93	86.36
Switching number minimisation						
Switching operation			Number of voltage violation busbars		Computation time (s)	

ODCDM	SOCS	Reduction	ODCDM	SOCS	ODCDM	SOCS
4	0	100.0%	0	0	27.53	20.60
DG real power curtailment minimisation						
DG P Curtailment (MW)			Number of voltage violation busbars		Computation time (s)	
ODCDM	SOCS	Reduction	ODCDM	SOCS	ODCDM	SOCS
0.32	0.31	3.3%	0	0	36.67	403.60
DG reactive power usage minimisation						
DG Q usage (MVAr)			Number of voltage violation busbars		Computation time (s)	
ODCDM	SOCS	Reduction	ODCDM	SOCS	ODCDM	SOCS
1.31	0.00	100.0%	0	0	27.65	31.27

Table 27 Snapshot test results of Network D – maximum load and maximum generation

Network Loss minimisation						
Network Loss (MW)			Number of voltage violation busbars		Computation time (s)	
ODCDM	SOCS	Reduction	ODCDM	SOCS	ODCDM	SOCS
0.87	0.10	88.0%	3	0	48.15	88.11
Voltage deviation minimisation						
Voltage Deviation (pu)			Number of voltage violation busbars		Computation time (s)	
ODCDM	SOCS	Reduction	ODCDM	SOCS	ODCDM	SOCS
0.99	0.41	58.9%	3	0	30.44	92.38
Switching number minimisation						
Switching Number			Number of voltage violation busbars		Computation time (s)	
ODCDM	SOCS	Reduction	ODCDM	SOCS	ODCDM	SOCS
19	1	94.7%	3	0	28.81	58.53
DG real power curtailment minimisation						
DG P Curtailment (MW)			Number of voltage violation busbars		Computation time (s)	
ODCDM	SOCS	Reduction	ODCDM	SOCS	ODCDM	SOCS

0.12	0.06	46.4%	3	0	43.99	390.97
DG reactive power usage minimisation						
DG Q usage (MVAr)			Number of voltage violation busbars		Computation time (s)	
ODCDM	SOCS	Reduction	ODCDM	SOCS	ODCDM	SOCS
1.31	0.00	100.0%	3	0	30.21	32.92

As shown in Table 26 and Table 27, for most of the test cases, SOCS achieved a smaller value, regarding the optimisation objective, in comparison with ODCDM. The computation times required by ODCDM are still shorter than that required by SOCS for most of the test cases. However, there are a few test cases, such as the network loss minimisation test case shown in Table 26, where the computation time of ODCDM is longer than that of SOCS. This is because DG real and reactive powers, with a step size of 0.01MW/MVAr, introduce control variables with a large number of step sizes to the problem. ODCDM may need a large number of iterations to achieve the final result, depending on the starting point. The computation time of ODCDM could be reduced if large step sizes are used to discretize the continuous DG real and reactive powers. However, the results achieved with large step sizes may not be as good as that achieved with small step sizes, as shown by the example in Appendix B-5.

Also, as shown in Table 27 and Appendix B-7, ODCDM failed to find a feasible solution in some of the test cases, but SOCS could always find a feasible solution. For example, when DG curtailment minimisation was used as the optimisation objective, SOCS found a feasible solution for all the 288 test cases, but ODCDM failed to find a feasible solution for 56 out of 288 test cases. One of the 56 test cases is used here to demonstrate the failure of ODCDM. In this test case, load scaling factor is set as 0.7 and DG real power output is set as 4MW. In Fig. 68, the highest and lowest voltages observed by the algorithm during each iteration of the algorithm are presented.

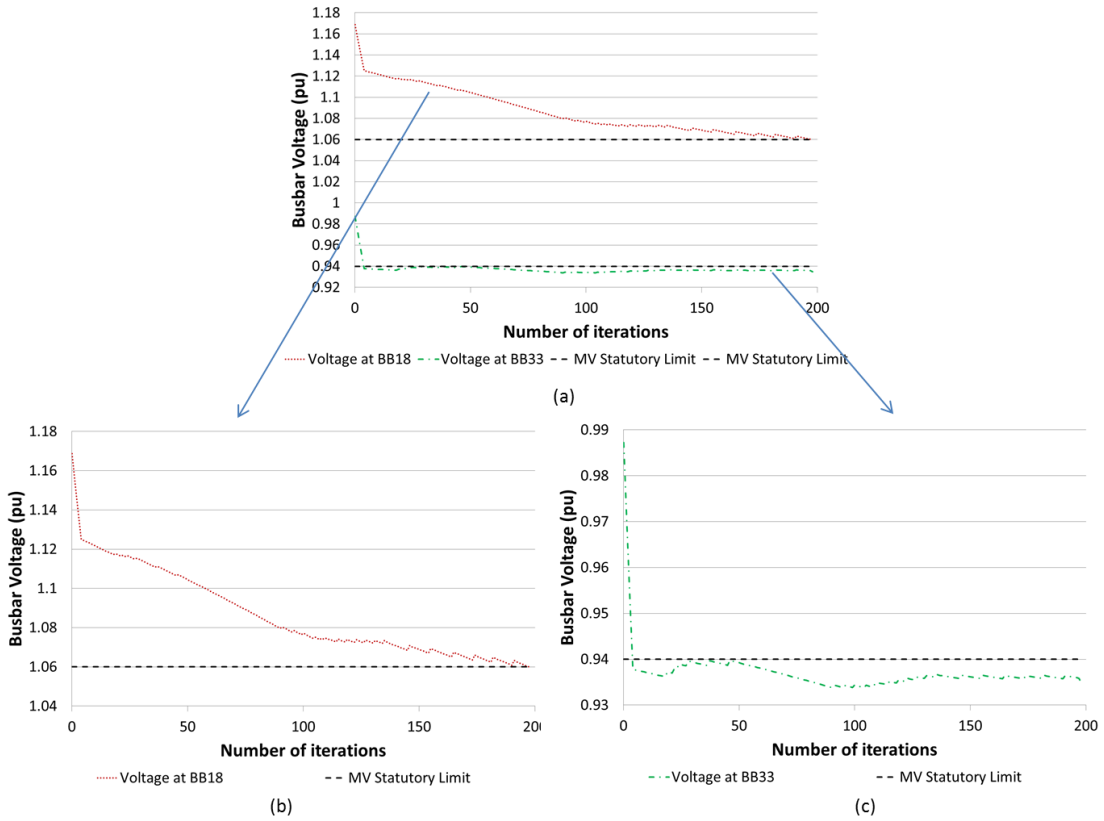

Fig. 68 Voltage change during the optimisation progress of ODCDM – Sampled ODCDM failure test case (a) highest and lowest voltages (b) highest voltage only (c) lowest voltage only

As shown in Fig. 68, the highest voltage was found at busbar 18, where DG is connected, and the lowest voltage was found at busbar 33, which is another feeder end. It can be seen that the total voltage violation was decreased gradually by ODCDM. However, ODCDM was trapped at a point, in which ODCDM cannot further reduce the voltage violation. The infeasible solution could be avoided by choosing a different SP. For example, the DG real power could be set as zero in the SP. ODCDM was able to find a feasible solution with this SP. However, the result achieved regarding the optimisation objective, DG curtailment minimisation, was 2.24MW, while the result achieved by SOCS was 0MW. The results are summarized in Table 28.

Table 28 Sampled test case for ODCDM SP study

	DG Curtailment (MW)	**Number of voltage violation busbars**
CS	0	0
ODCDM – Test1	0.61	5
ODCDM – Test2	2.24	0

The improvements achieved by SOCS are due to the following reasons. The connection of DG could create a network condition, in which there are both over voltage and undervoltage problems in the network. ODCDM may be trapped at a point because of the existence of both over and under voltages. Sometimes, ODCDM may fail to find a feasible solution. In addition, the values achieved by ODCDM, regarding the optimisation objective functions, may be restricted by the step size used to discretize continuous control variables.

Profile Analysis

In the profile analysis, ODCDM failed to find a feasible solution in some test cases, which SOCS could always find a feasible solution. The numbers of voltage violation busbars in the results achieved by ODCDM for network loss minimisation profile analysis are shown in Table 29. The numbers of voltage violation busbars for the rest profile test cases are shown in Appendix B-7.

Table 29 Number of voltage violation busbars in profile test cases for ODCDM

Time	00:00	01:00	02:00	03:00	04:00	05:00	06:00	07:00
Number of voltage violation busbars	0	0	0	0	0	0	0	0
Time	08:00	09:00	10:00	11:00	12:00	13:00	14:00	15:00
Number of voltage violation busbars	0	0	3	2	3	4	3	2
Time	16:00	17:00	18:00	19:00	20:00	21:00	22:00	23:00
Number of voltage violation busbars	0	2	0	1	0	4	0	3

The values achieved by both ODCDM and SOCS, regarding the optimisation objective functions are shown in Fig. 69.

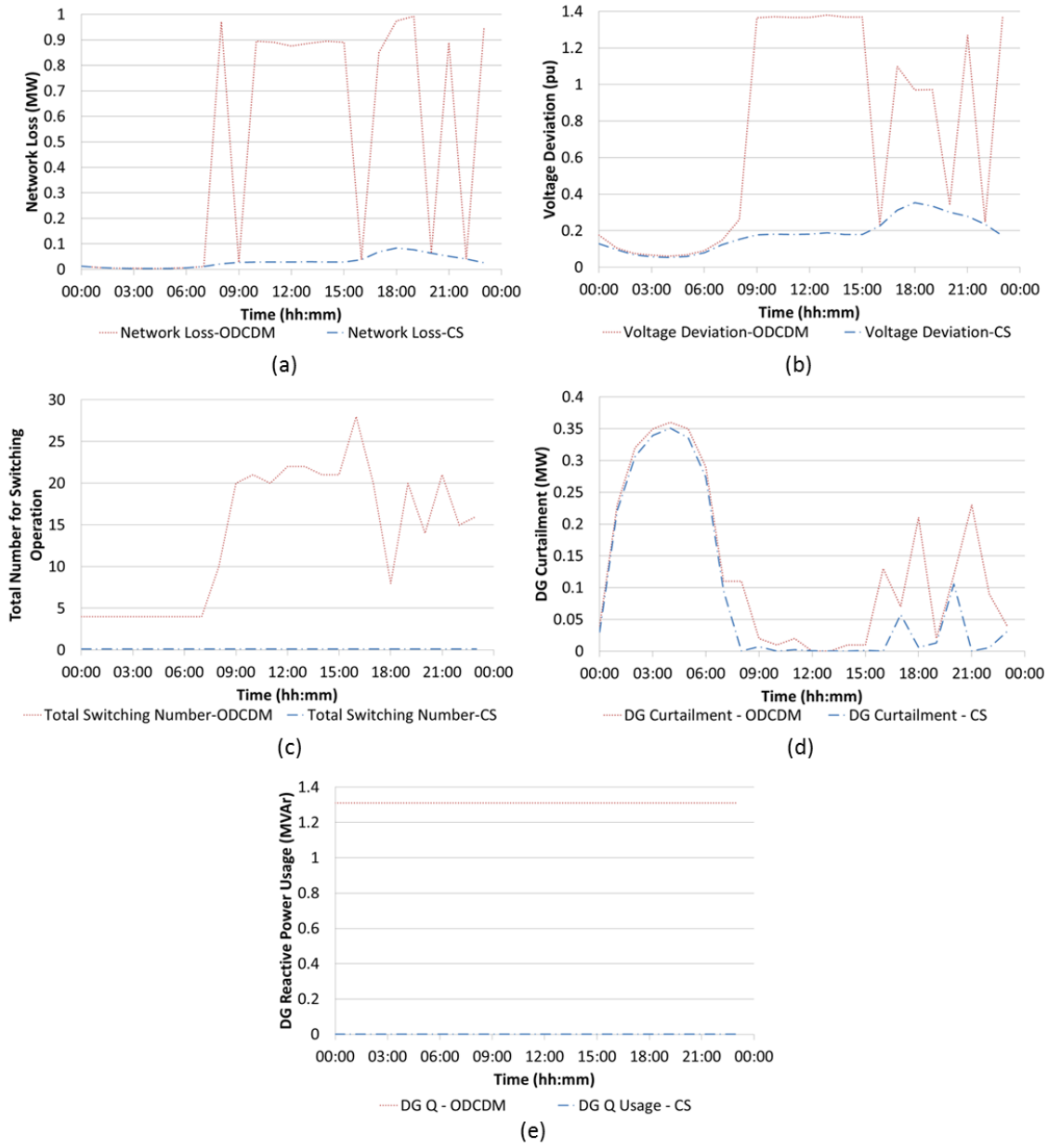

Fig. 69 Profile test results – Network D (a) Network loss minimisation (b) Voltage deviation minimisation (c) Switching operation minimisation (d) DG real power curtailment minimisation (e) DG reactive power usage minimisation

The computation times for profile test cases are summarized in Appendix B-7. The results from the profile analysis are consistent with the snapshot analysis and it can be seen that the values achieved by SOCS regarding the optimisation objective functions are smaller than that achieved by ODCDM for many test cases. For example, regarding DG curtailment, in total, 3.14MWh DG curtailment is required when ODCDM is used, while 2.18MWh DG curtailment is required when SOCS is used. 0.96MWh more DG generation is allowed.

6.8.2 Test results for Network E

Snapshot Analysis

In total, 180 snapshot test cases are generated for each optimisation objective. For all the test cases, both ODCDM and SOCS could always find a feasible solution, since the network load and generation are more even distributed in this test case. More test results are shown in Appendix B-8. Here, the results for the test cases with the minimum load and maximum generation are summarized in Table 30, while the results for the test cases with the maximum load and maximum generation are summarized in Table 31.

Table 30 Snapshot test results of Network E – minimum load and maximum generation

Network Loss minimisation						
Network Loss (MW)			Number of voltage violation busbars		Computation time (s)	
ODCDM	SOCS	Reduction	ODCDM	SOCS	ODCDM	SOCS
0.0021	0.0017	16.3%	0	0	656.15	344.93
Voltage deviation minimisation						
Voltage Deviation (pu)			Number of voltage violation busbars		Computation time (s)	
ODCDM	SOCS	Reduction	ODCDM	SOCS	ODCDM	SOCS
0.33	0.02	94.4%	0	0	229.13	245.40
Switching number minimisation						
Switching Number			Number of voltage violation busbars		Computation time (s)	
ODCDM	SOCS	Reduction	ODCDM	SOCS	ODCDM	SOCS
4	0	100.0%	0	0	38.34	33.77
DG real power curtailment minimisation						
DG P Curtailment (MW)			Number of voltage violation busbars		Computation time (s)	
ODCDM	SOCS	Reduction	ODCDM	SOCS	ODCDM	SOCS
0.86	0.31	63.7%	0	0	36.64	267.47
DG reactive power utilization minimisation						
DG Q Utilization (MVAr)			Number of voltage violation busbars		Computation time (s)	
ODCDM	SOCS	Reduction	ODCDM	SOCS	ODCDM	SOCS
0.00	0.00	0.00	0	0	38.58	121.25

Table 31 Snapshot test results of Network E – maximum load and maximum generation

Network Loss minimisation						
Network Loss (MW)			Number of voltage violation busbars		Computation time (s)	
ODCDM	SOCS	Reduction	ODCDM	SOCS	ODCDM	SOCS
0.03	0.03	0.8%	0	0	342.23	239.57
Voltage deviation minimisation						
Voltage Deviation (pu)			Number of voltage violation busbars		Computation time (s)	
ODCDM	SOCS	Reduction	ODCDM	SOCS	ODCDM	SOCS
0.41	0.07	83.1%	0	0	143.91	235.28
Switching number minimisation						
Switching Number			Number of voltage violation busbars		Computation time (s)	
ODCDM	SOCS	Reduction	ODCDM	SOCS	ODCDM	SOCS
0	0	0.0%	0	0	7.10	37.62
DG reactive power utilization minimisation						
DG P Curtailment (MW)			Number of voltage violation busbars		Computation time (s)	
ODCDM	SOCS	Reduction	ODCDM	SOCS	ODCDM	SOCS
0.13	0.00	100.0%	0	0	7.18	25.12
DG reactive power utilization minimisation						
DG Q Utilization (MVAr)			Number of voltage violation busbars		Computation time (s)	
ODCDM	SOCS	Reduction	ODCDM	SOCS	ODCDM	SOCS
0.00	0.00	0.0%	0	0	7.11	117.23

As shown by the test results, SOCS could achieve a smaller value, regarding the optimisation objective, in comparison with ODCDM for most of the test cases. The computation times required by ODCDM are still shorter than that required by SOCS for most of the test cases. However, there are a few test cases, such as the network loss minimisation test case shown in Table 30, the computation time of ODCDM is significantly longer than that of SOCS.

Profile Analysis

For all the profile test cases, both ODCDM and CS always found a feasible solution, which means there was no voltage violation observed during these tests. The profile test cases results for DG curtailment minimisation is shown in Fig. 70. The computation times for profile test cases are shown in Appendix B-8.

The results from the profile analysis are consistent with the snapshot analysis and it can be seen from Fig. 70 that the values achieved by SOCS regarding the optimisation objective functions are smaller than that achieved by ODCDM for many test cases. For example, DG curtailment was reduced when using SOCS in comparison with ODCDM. In total, 12.52MWh DG curtailment is required when ODCDM is used, while 2.56MWh DG curtailment is required when SOCS is used. 9.96MWh more DG generation is allowed.

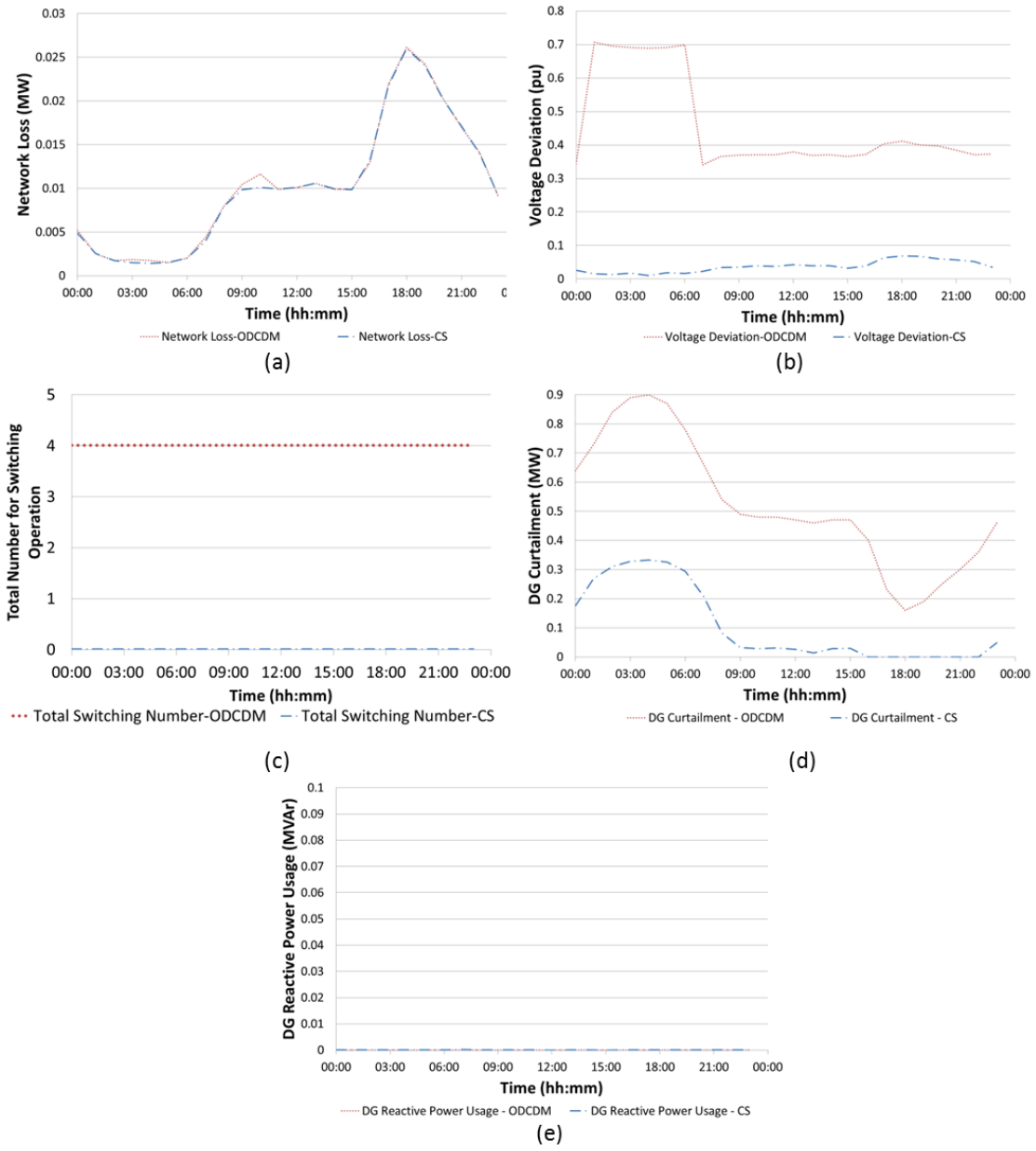

Fig. 70 Profile test results – Network E (a) Network loss minimisation (b) Voltage deviation minimisation (c) Switching operation minimisation (d) DG real power curtailment minimisation (e) DG reactive power usage minimisation

6.9 Discussions

As shown by the test results in this chapter, the differences between the results achieved by ODCDM and SOCS varied from case to case. The voltage optimisation problem is nonlinear and nonconvex [74, 75], which theoretically has many local optimal solutions. ODCDM may only be able to find a local optimal solution, depending on the starting point. As per previous literature and the test results in this chapter, it can be seen that SOCS could achieve the global optimal solution when the allowed number of iteration is large enough. It is assumed that SOCS always achieved global optimal solutions, then these differences generally depend on the voltage optimisation problem itself and the results achieved by ODCDM.

The optimisation objective is one important aspect for voltage optimisation. For the conventional test cases generated in this study, the differences between the results achieved by ODCDM and SOCS, regarding the objective, network loss minimisation, are not significant. ODCDM could provide a sufficient solution for these test cases. However, regarding the objective, voltage deviation minimisation, significant differences between the results achieved by ODCDM and SOCS were observed. For switching operation minimisation, the differences depend on how the switching operation is counted, as specified in section 6.5.3.

For future distribution networks, more significant improvement can be achieved by SOCS, in terms of the optimisation objective. SOCS could easily escape from infeasible local optimal solutions, while ODCDM may be trapped at an infeasible local optimal solution, when the network busbar voltages are close to both the upper and lower voltage limits. The values achieved by SOCS regarding the optimisation objective functions, could be significantly less than that achieved by ODCDM. This can be explained with the recent non-convexity studies regarding the general OPF problems [74, 158-160]:

- Nonlinear load flow equations represented by (30) [74, 158];
- Mixed integer problem [159];
- The non-convexity of the feasible voltage region [160].

The nonlinearity of the load flow equations is due to the nonlinear relationship between the voltages and the powers injected at different busbars [161]. The integration of DG and additional LCT loads could make the load flow equations more nonlinear [161]. The MINLP problem needs to be changed to a combinatorial problem, which can then be solved by ODCDM. The nonconvex feasible region of voltage magnitudes is also a reason of the OPF non-convexity [160]. As shown in Fig. 71, the feasible region of voltage is like a donut, which is nonconvex. When the load and generation are not evenly distributed, it is possible that there are voltages being close to both limits and the impact of this nonconvex feasible region may be more significant. It should be noted that the actual differences between the results achieved by the algorithms for specific test cases, also depend on the results achieved by ODCDM, which are affected by some other issues, such as the SP of ODCDM.

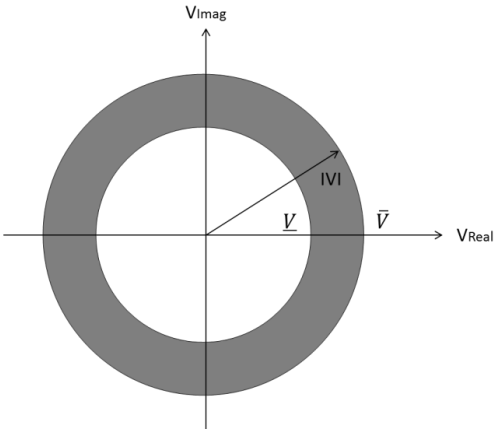

Fig. 71 Feasible region of voltage magnitudes

6.10 Conclusions

In this chapter, ODCDM and SOCS have been comparatively evaluated regarding single-objective voltage optimisation for conventional and future distribution networks. A method has been proposed for systematically evaluating the performance of single objective optimisation algorithms. In this method various test cases are developed based on the analysis of the formulated voltage optimisation problem. Voltage optimisation algorithms, which are applied to solve the test cases, are evaluated regarding their abilities to find a feasible solution, the values achieved for the objective functions and the computation times.

Using this method, both ODCDM and SOCS have been evaluated for single-objective voltage optimisation in conventional distribution networks. A number of test cases were developed using three different case study networks, three different optimisation objectives and various network load conditions. The performance of ODCDM and SOCS were compared regarding these test cases. Generally, for the test cases created for conventional distribution networks, ODCDM and SOCS were always able to find a feasible solution. The algorithms were also compared regarding the values achieved for the optimisation objective functions. When network loss minimisation was used as the optimisation objective, there was no significant difference between the results achieved by both algorithms. When voltage deviation minimisation was used as the optimisation objective, SOCS was able to reduce voltage deviation in comparison with ODCDM for some test cases. When switching operation minimisation was adopted as the optimisation objective, it was found that the structure of MSCs had large impact on the performance of the algorithms. Similar performance was observed using ODCDM and SOCS, if the capacitor banks of the MSCS have the same size. However it was shown that SOCS was able to reduce switching operations for some test cases, if the capacitor banks of the MSCs have different sizes and the MSC stage positions are

achieved with the different combinations of these capacitor banks. For all these test cases, SOCS requires a much longer computation time than ODCDM.

ODCDM and SOCS were then evaluated for the single-objective voltage optimisation in future distribution networks. Additional control variables and objectives are expected for voltage optimisation. The connections of DGs and load LCTs could create additional network load and generation conditions. A single-DG case study network and one multiple-DG case study network were developed from the conventional case study networks. Test cases have been developed based on these two future test networks. For some test cases, ODCDM failed to find a feasible solution. In addition, as shown by the test results, the differences between the values achieved by ODCDM and SOCS regarding the optimisation objective functions could be significant. Although for most of the test cases, the computation times of ODCDM were still shorter than that of SOCS, there are a few test cases, SOCS required shorter computation time in comparison with ODCDM.

As shown in this chapter, both ODCDM and SOCS are able to find optimal solutions when different optimisation objectives are used. Theoretically, ODCDM is only able to provide a local optimal solution, while SOCS is able to provide a global optimal solution if a large enough iteration number is allowed. As shown in this chapter, the actual difference between the optimal solutions found by ODCDM and SOCS depend on the specific test case and some other issues, such as the starting point used by ODCDM. Generally speaking, ODCDM could provide a sufficient solution for conventional distribution networks, and the computation time of ODCDM is much shorter than that of SOCS. For future distribution networks, SOCS could be more preferable in comparison with ODCDM. SOCS could easily escape from infeasible local optimal solutions, while ODCDM may be trapped at an infeasible local optimal solution, when the network busbar voltages are close to both the upper and lower voltage limits. The values achieved by SOCS regarding the optimisation objective functions, could be significantly less than that achieved by ODCDM. In addition, the computation time of SOCS could be shorter than ODCDM sometimes.

Chapter 7 Evaluation of Multi-objective Voltage Optimisation Algorithms

7.1 Introduction

In Chapter 6, different voltage optimisation objectives have been studied separately for distribution networks. Frequently, more than one optimisation objective, which are often non-commensurable, needs to be considered simultaneously. As shown in Chapter 4, for multi-objective optimisation problems, the concept of Pareto optimality has to be introduced. A solution is said to be a Pareto-optimal solution for a multi-objective optimisation problem, if and only if it is not dominated by any other solutions of this multi-objective optimisation problem. The image of all the Pareto-optimal solutions is called Pareto front. The multi-objective voltage optimisation algorithms are expected to find a set of solutions, the image of which is as close as possible to the Pareto front [162].

Two different approaches have been adopted by multi-objective optimisation algorithms. The first approach uses single-objective optimisation algorithms, by reformulating the problem to address multi-objectives with the consideration of the preferences between different objectives. This approach is simple and widely used. However, this approach requires multiple runs to find a set of solutions, and normally it is sensitive to the shape of the Pareto front [134]. The second approach integrates the concept of Pareto optimality into the population-based metaheuristic algorithms. A set of non-dominated solutions can be found in a single run. This first approach can be used by both deterministic and metaheuristic optimisation algorithms, while the second approach can only be used by metaheuristic algorithms.

Two multi-objective voltage optimisation algorithms have been proposed in Chapter 4 and Chapter 5. In Chapter 4, the oriented discrete coordinate descent method was extended with the weighted sum method, while in Chapter 5, multi-objective cuckoo search algorithm was developed. In this chapter, these two multi-objective voltage optimisation algorithms are evaluated and compared, for conventional and future distribution networks.

In the rest of this chapter, the evaluation method is introduced. Conventional distribution network test cases are generated, followed by the test case results. The test cases and corresponding results for future distribution networks are then presented. At the end, the conclusion is drawn. For the remainder of this chapter, the ODCDM with the weighted sum method will be referred to as ODCDM, while the MOCS bases voltage optimisation algorithm will be referred to as MOCS.

7.2 Evaluation method of multi-objective voltage optimisation algorithms

The method used for multi-objective voltage optimisation algorithm evaluation includes the following three steps:

- Generating the test cases;
- Solving the optimisation problems from the generated test cases;
- Evaluating the results regarding the performance metrics.

The problem formulation defined in Chapter 6, can also be used for multi-objective voltage optimisation, except that the single optimisation objective function is replaced with a set of optimisation functions, represented by (69).

$$f = \min\left[f_1, f_2, ..., f_n \right] \tag{69}$$

As specified in Chapter 6, the formulated optimisation problem is not fixed, but varies with the changes of the components in the problem formulation, such as the definition of the optimisation objective function, and the network load and generation conditions. The test cases are generated to reflect the problem variation. This chapter focused on the problem variation caused by the different combinations of various optimisation objective functions.

Similar to single-objective voltage optimisation algorithms, multi-objective voltage optimisation algorithms should always find at least one feasible solution in a reasonable computation time. Therefore, the following two performance criteria adopted for single-objective voltage optimisation algorithm evaluation are also used here:

- The number of voltage violation busbars, which is desired to be zero;
- The computation time to find the result.

As discussed in Chapter 5, for multi-objective voltage optimisation, the result evaluation is substantially more complex than that for single-objective optimisation [163]. This is because the result normally includes a set of solutions, which need to be measured by some performance metrics, before they can be evaluated and compared. Many performance metrics have been developed before to evaluate the results achieved by multi-objective optimisation algorithms [86, 139, 162, 164]. Here, the ratio of the reference point found, which has been introduced in Chapter 5, is used to evaluate and compare the results achieved for conventional distribution networks, while the coverage metric is used to compare the results achieved for future distribution networks.

The voltage optimisation problem in conventional distribution networks is a combinatorial problem, based on the assumptions made in Chapter 6. The Pareto front can be achieved by exhaustive search and used as the reference set for the performance metric, ratio of the reference point found. The voltage optimisation problem becomes a mixed integer nonlinear programming problem in future distribution networks, because of the integration of continuous control variables. It is very difficult to determine the Pareto front and thus the reference set *R*. Therefore the ratio of the reference point found could not be used. Instead, the results achieved by MOCS and ODCDM are compared with the coverage metric, as explained in Chapter 5 [139, 162, 164].

Beside these two performance metrics, visual presentations of the results are also used to evaluate and compare the results for 2-objective and 3-objective test cases.

7.3 Test case design and algorithm application for conventional distribution networks

7.3.1 Test case design

To generate the test cases for conventional distribution networks, the Case Study Network B from Chapter 6 with its original load is used, as well as the following three optimisation objectives:

- Network loss minimisation
- Voltage deviation minimisation
- OLTC and MSC switching operation minimisation

Four test cases, as shown in Table 32, are generated by combining these three optimisation objectives in different ways. As shown in Table 32, three 2-objective test cases and one 3-objective test case are generated. ‘Yes’ indicates the objective is considered in the test case, while ‘No’ indicates not. The indexes, CTC1-4 (CTC, conventional test case), are assigned to each test case.

Table 32 Multi-objective voltage optimisation test cases - conventional distribution networks

Test case Index	Number of Objectives	Optimisation objective		
		Network loss minimisation	Voltage Deviation minimisation	Switching operation minimisation
CTC1	2	Yes	Yes	No
CTC2	2	Yes	No	Yes
CTC3	2	No	Yes	Yes
CTC4	3	Yes	Yes	Yes

As shown in Chapter 6, the positions of OLTCs and MSCs before optimisation, affect the optimisation function for switching number minimisation. In addition, the structure of MSC also affects the switching number calculation. Here, for the test cases including switching number minimisation, the nominal position (0%) is used for the OLTC tap positions, and 0MVAr is used for the MSCs stage positions before optimisation. Also, it is assumed that for all the MSCs, the simple structure is used, which means all the capacitors in the MSC have the same size.

7.3.2 Algorithm application

For the test cases with two optimisation objectives, the optimisation objective for ODCDM should be formulated as (70).

$$f = w_1 f_1 + w_2 f_2 \tag{70}$$

Where w_1 and w_2 are the weighting coefficients adopted for the two optimisation objectives. Potentially, by varying the weighting coefficients, different solutions could be achieved. Normally, the weighting coefficients are being varied linearly, to find the solutions for the multi-objective optimisation problems [88, 165]. Here, w_1 is being varied in the range [0, 1] with a given step size, as shown in [165]. Then w_2 is calculated by (71).

$$w_2 = 1 - w_1 \tag{71}$$

If a smaller step size is used to vary w_1, potentially more solutions could be generated, but more runs of ODCDM are also required. For example, if 0.01 is used as the step size for the weighting coefficient variation, ODCDM needs to be run 101 times. The impact of the step size used for weighting coefficient variation is studied in section 7.4.1. The weighting

coefficients can be varied with different strategies. For example, in [88], a 2-objective optimisation problem was solved with weighted sum method. One weighting coefficient was kept constant, while the other one was varied from 0 to 2000 in steps of 100. The basic ideas of these two approaches are the same, which is assigning various priorities to the optimisation objectives. Also, the range of w_1 could be adjusted based on the result achieved. However, this should be carried out based on the analysis of the specific optimisation problem. Therefore, it is not used in this study.

Similarly, for the test cases with three optimisation objectives, the optimisation objective is represented by (72).

$$f = w_1 f_1 + w_2 f_2 + w_3 f_3 \tag{72}$$

Where w_1, w_2 *and* w_3 are the weighting coefficients adopted for the three optimisation objectives. Different solutions can be found with various combinations of w_1, w_2, and w_3, and the relationship of these weighting coefficients should follow that defined by (73).

$$w_1 + w_2 + w_3 = 1 \tag{73}$$

It should be noted that there will be more combinations for three weighting coefficients, if the same step size is used. For example, if the step size is 0.01, then there are 5151 combinations in total.

ODCDM also requires a starting point and the SP may affect the result achieved by ODCDM. The impact of the SP is also shown with a simple example in section 7.4.1.

As shown in Chapter 5, MOCS has several parameters, which could affect the performance of MOCS. Theoretically, these parameters could be tuned for each individual multi-objective optimisation problem. However, the parameter tuning for multi-objective metaheuristic algorithms, such as MOCS, is very difficult and time consuming. It is not practical to tune all the parameters for each individual problem. Here, the parameters are determined as per the literature and experimentally, as the approach adopted in many previous studies [163, 166, 167]. As shown in [163], several parameters were fixed for all the test problems as per the literature, and the remaining parameters were chosen regarding each test problem. The algorithm was run five times, each time using a different parameter. The parameter value which achieved the best results for the measure was chosen. The nest number and maximum iteration number are determined as per the procedures specified in Chapter 5.

In this chapter, the following parameters are set for MOCS as per the literature and the initial studies in Chapter 5: discovery probability p_a= 0.25, Lévy exponent β = 1.5 and step size scale factor α_0 as 0.1. The nest number and the maximum iteration number are determined with the method introduced in Chapter 5. For CTC1-3, the nest number is set as 50 while the maximum iteration number is determined as 100. For CTC4, the nest number is increased to 100, since the more solutions are expected in the Pareto front. The maximum iteration number is determined as 150. Theoretically, an optimal set of nest number and maximum iteration number could be found for each optimisation problem. However, this is not within the scope of this PhD study.

As informed by previous research, such as [139, 167], and the initial test results in Chapter 5, normally the exact same result cannot be achieved by MOCS, because of its stochastic nature. Therefore, for each test case, MOCS is run 20 times, and the result, which has the closest performance metric to the average value for these 20 runs, is used in the comparative study.

7.4 Results of conventional distribution network test cases

For all conventional distribution network test cases, the solutions achieved by both algorithms are always feasible.

7.4.1 Impact of the step size used for the weighting coefficient variation and the starting point for ODCDM

The Pareto front of CTC1, found by exhaustive search, is shown in Fig. 72.

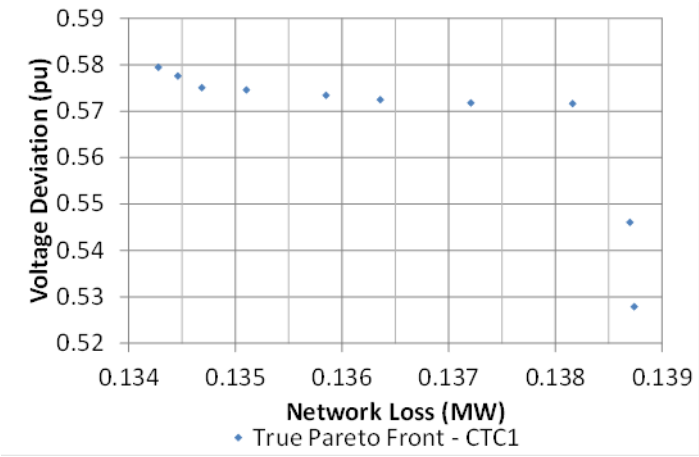

Fig. 72 Pareto front for CTC1 achieved by exhaustive search

As discussed in section 7.3.2, the step size used for the weighting coefficient variation may affect the result achieved and the number of runs required for ODCDM. Here, ODCDM is

tested with three different step sizes, which are 0.1, 0.01 and 0.001. In addition, the impact from the SP is also studied, with the two SPs shown in Table 9.

Table 33 Starting Points used by ODCDM for CTC1

Starting Point Index	Starting Point				
	OLTC	MSC1	MSC2	MSC3	MSC4
	Unit: %	Unit: MVAr			
SP1	100	0	0	0	0
SP2	100	0.2	0.05	0.15	0.1

With these three different step sizes and SPs, four different ODCDM test were carried out. The settings for these four ODCDM tests are listed in Table 34 and the results for these four tests are shown in Fig. 73.

Table 34 Settings for ODCDM Tests – CTC1

ODCDM Test	SP	Step size for w1
ODCDM Test 1	SP1	0.1
ODCDM Test 2	SP1	0.01
ODCDM Test 3	SP1	0.001
ODCDM Test 4	SP2	0.01

The test results of ODCDM with different settings are shown in Fig. 73.

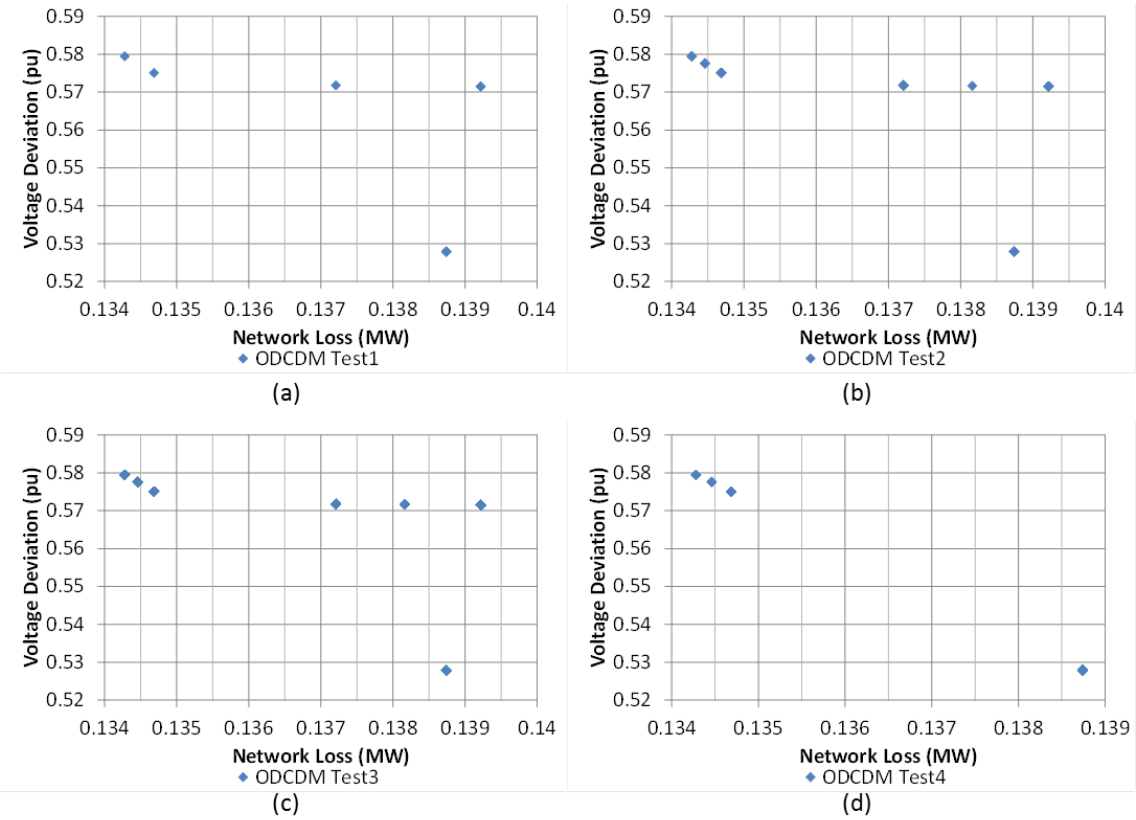

Fig. 73 ODCDM test results for CTC1 (a) Test1, (b) Test2, (c) Test3, (d) Test4.

As shown in Fig. 73, the results achieved with ODCDM are affected by the step size selection for the weighting coefficient variation and the SP used by ODCDM. As shown by Fig. 73-(a) and Fig. 73-(b), better results can be achieved if a smaller step size is used for the weighting coefficients variation. However, as indicated by Fig. 73-(b), a better result may not necessarily be obtained if the step size is further reduced. Also, the result achieved also depends on the SP adopted by ODCDM. As shown by Fig. 73-(b) and Fig. 73-(d), different results are achieved for SP1 and SP2. The performance metrics and the computation times for these tests are summarized in Table 35. The total computation times for Test 2 and Test 4 are different, since the computation time of ODCDM is affected by the starting point used in these two tests.

Table 35 Ratio of the reference point founds and computation times of ODCDM tests for CTC1

	Test1	Test2	Test3	Test4
Ratio of the reference point found	40%	60%	60%	40%
Computation time (s)	33.12	313.54	3022.43	214.12

In the following test, SP1 is used as the starting point, in which the OLTC tap position is set as 0%, while the stage positions of MSCs are set as zero. 0.01 is used as the step size for the weighting coefficient variation.

7.4.2 Test results of 2-objective voltage optimisation test cases

The results achieved by ODCDM and MOCS for CTC1-3, are shown in Fig. 74, against the Pareto fronts found via exhaustive search.

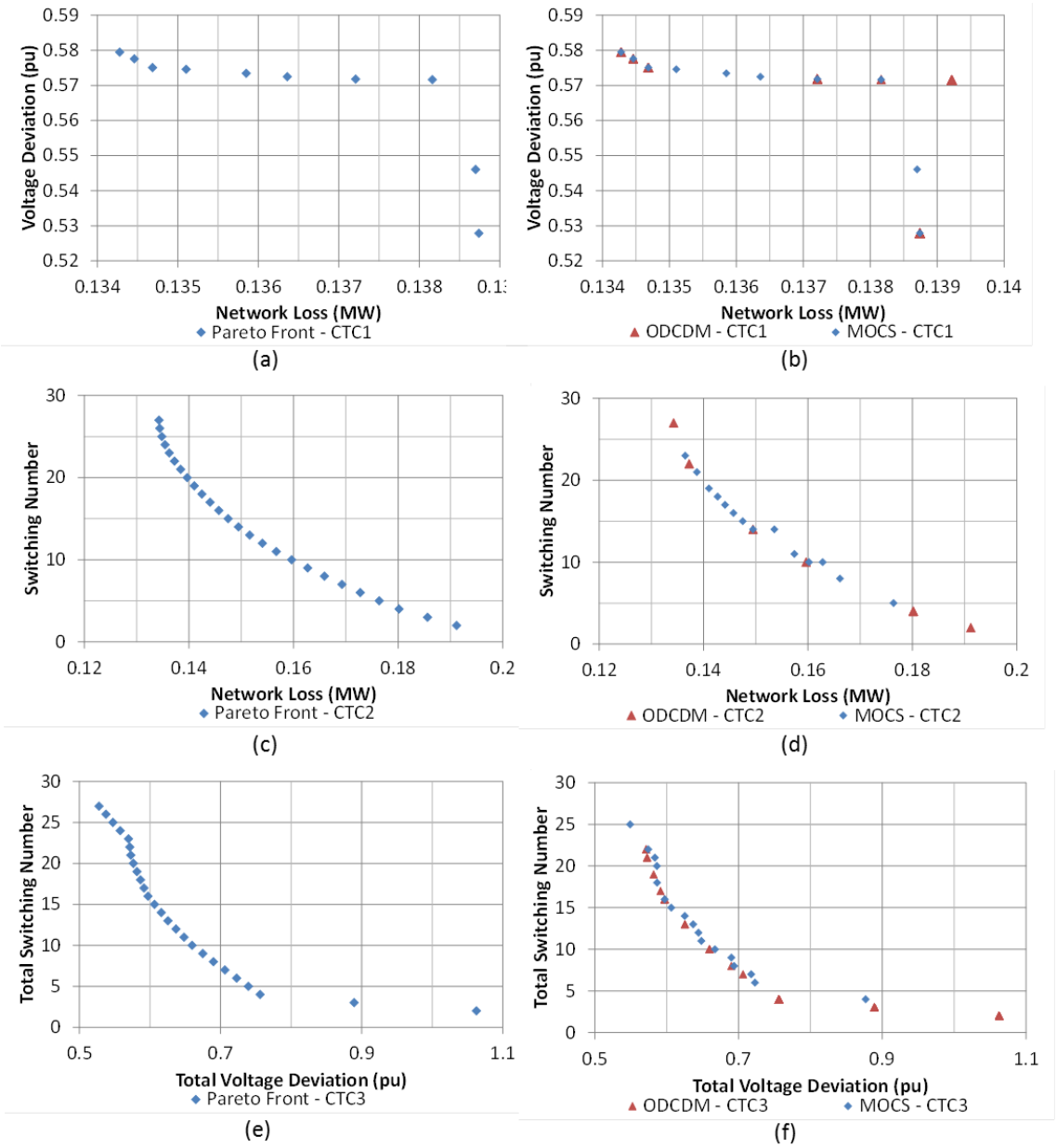

Fig. 74 Pareto front and test results for the conventional distribution network test cases with 2 optimisation objectives. (a) Pareto front for CTC1, (b) Results achieved by ODCDM and MOCS for CTC1, (c) Pareto front for CTC2, (d) Results achieved by ODCDM and MOCS for CTC2, (e) Pareto front for CTC3, (f) Results achieved by ODCDM and MOCS for CTC3.

As shown in Fig. 74, MOCS could achieve a better result than ODCDM for CTC1. The Pareto front, show in Fig. 74 – (a), is nonconvex, which may cause problems to the weighted sum method [168]. For CTC2, more solutions are achieved by MOCS. For CTC3, ODCDM could achieve a better result, although it cannot reach the upper section of the Pareto front. This is because ODCDM can only find the local optimal with the SP1.

The ratios of the reference point found and computation times of both algorithms for CTC1 – CTC3 are shown in Table 36.

Table 36 Ratio of the reference point found and computation time for CTC1 – CTC3

Test Case	Ratio of the reference point found		Computation time (s)	
	ODCDM	MOCS (average value over 20 runs)	ODCDM	MOCS (average value over 20 runs)
CTC1	60%	96%	313.54	100.18
CTC2	23%	23%	342.22	103.05
CTC3	42%	19%	390.63	102.85

For CTC2 and CTC3, MOCS did not achieve a better result than ODCDM, in terms of RRPF. This is because of the mechanism of ODCDM, as introduced in Chapter 4. It can be seen from Table 36 that multiple runs of ODCDM may require a longer computation time than MOCS, if a small step size is used as the step size for the weighting coefficient variation.

7.4.3 Test results of 3-objective voltage optimisation test cases

The Pareto front and the results achieved by ODCDM and MOCS for CTC4 are shown in Fig. 75. It can be seen from Fig. 75–(a) that the Pareto front in this test case has a larger number of solutions, compared to the Pareto fronts for the test cases with two optimisation objectives. This is because all the Pareto-optimal solutions from the three 2-objective test cases are still the Pareto-optimal solutions in this test case, and new Pareto-optimal solutions may also be introduced when three optimisation objectives are considered at the same time. As shown in Fig. 75–(b), more solutions are achieved by MOCS.

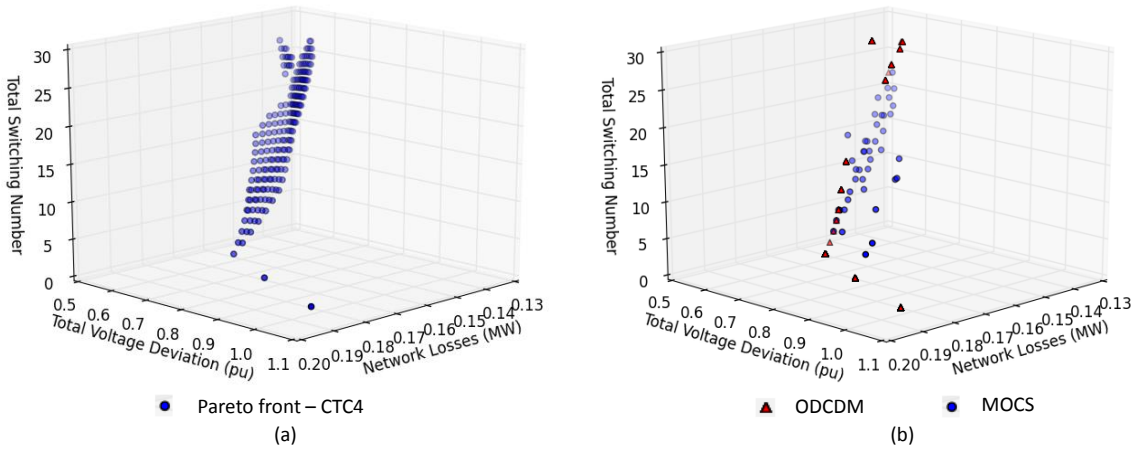

Fig. 75 Pareto front and test results for CTC4. (a) Pareto front for CTC4, (b) Results achieved by ODCDM and MOCS for CTC4.

The ratios of the reference point found and the computation times for CTC4 are shown in Table 37.

Table 37 Ratio of the reference point found and computation time for CTC4

Ratio of the reference point found		Computation time (s)	
ODCDM	MOCS (average value over 20 runs)	ODCDM	MOCS
7%	9%	2532.46	307.20

For CTC4, the result achieved by MOCS is better than that achieved by ODCDM, according to the ratio of the reference point founds. Also, the computation time of MOCS is much shorter than that of ODCDM. For ODCDM, the required number of runs increases significantly with the increase of the optimisation objective, if the same step size is used for the weighting coefficient variation.

7.5 Test case design and algorithm application for future smart distribution networks

For all future distribution network test cases, the solutions achieved by both algorithms are always feasible.

7.5.1 Test case design

A future case study network is created, by connecting two 3MW DGs to Case Study Network B. As shown in Fig. 76, the DGs are connected to the feeder ends. DG real and reactive power controls are integrated, with the control ranges specified in Chapter 6.

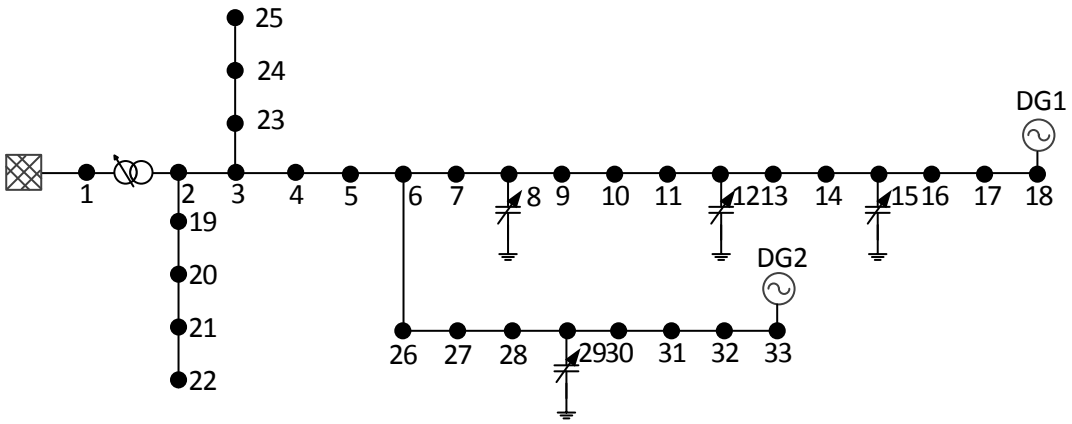

Fig. 76 Case study network for future distribution network test case generation

The following four optimisation objectives are considered for voltage optimisation in future distribution networks:

- Voltage deviation minimisation
- DG real power curtailment minimisation
- DG reactive power usage minimisation
- OLTC and MSC switching operation minimisation

With these four optimisation objectives, ten test cases are created, as summarized in Table 38. The test case indexes (FTC, future test case) are also assigned to the test cases, as shown in Table 38. It should be noted that the number of optimisation objectives is limited to three in this study. This is because if there are more than three objectives to be optimised simultaneously, the problem could be too complicated and it will be difficult to evaluate the results achieved, since the results cannot be visualized.

Table 38 Multi-objective test cases – Future distribution network

Test case Index	Number of Objectives	Voltage Deviation	DG real power curtailment	DG reactive power usage	Switching operation
FTC1	2	Yes	Yes	No	No
FTC2	2	No	Yes	Yes	No
FTC3	2	No	Yes	No	Yes
FTC4	2	Yes	No	Yes	No
FTC5	2	Yes	No	No	Yes
FTC6	2	No	No	Yes	Yes
FTC7	3	Yes	Yes	Yes	No
FTC8	3	No	Yes	Yes	Yes
FTC9	3	Yes	Yes	No	Yes
FTC10	3	Yes	No	Yes	Yes

The minimum load and maximum generation is adopted to generate the test cases.

7.5.2 Algorithm application

For future distribution networks, continuous control variables will be integrated into voltage optimisation. The continuous control variables need to be discretized before ODCDM can be applied. As shown in Chapter 6, the step size used for continuous control variable discretization affects the result achieved by ODCDM and the computation time. The impact of the step size for multi-objective voltage optimisation will be shown in section 7.6.1. For 2-objective test cases, 0.01 is used for both the weighting coefficient variation and the continuous control variable discretisation.

For 3-objective test cases, as informed by initial test, the total computation time may exceed 48 hours if 0.01 is used for both the weighting coefficient variation and the continuous control variable discretisation. Therefore, the step size for continuous control variable discretisation is kept as 0.01 to obtain an accurate result, while 0.1 is used for weighting coefficient variation.

For all the test cases, the DG rated powers are used for DG real power outputs, and zero is used for the DG reactive power outputs in the SP for ODCDM.

As shown in Chapter 6, cuckoo search based algorithm requires more iterations to achieve a stable result, when continuous control variables are integrated. Also, the Pareto front could

include infinite solutions, when continuous control variables are integrated. Therefore, both the nest number and the maximum iteration number are expected to be increased. As per the method introduced in section 5.5.1, the nest number is set as 100 and the maximum iteration number is determined as 400 for FCT1-6. The nest number is increased to 150 for FCT7-10. The maximum iteration number is determined as 500. Potentially, optimal values for the nest number and maximum iteration number should exist regarding each individual test case. However, so far there is no standard procedure to find these optimal values.

7.6 Results of conventional distribution network test cases

7.6.1 Impact of continuous control variables on ODCDM

The impact of continuous control variable on ODCDM regarding multi-objective optimisation is shown here. Two different step sizes are used to discretize the DG real and reactive powers, which are 0.01MW/MVAr and 0.05MW/MVAr. ODCDM is tested with these two step sizes, and the results shown in Fig. 77.

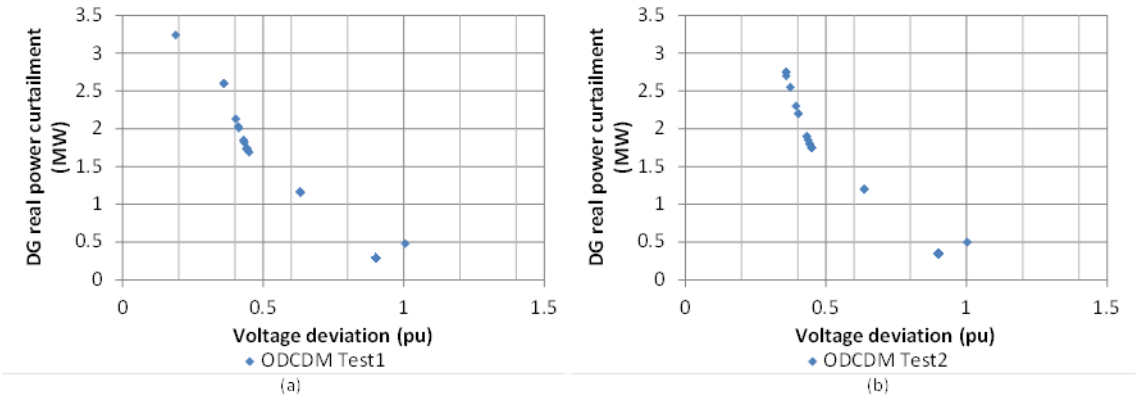

Fig. 77 ODCDM test results for FTC1. (a) Test 1 - step size as 0.01MW/MVAr (b) Test 2 - step size as 0.05MW/MVAr

As shown in Fig. 77, it can be seen that the results achieved by ODCDM are affected by the step size used for continuous variable discretization. The coverage relationships of the two sets of results are shown in Table 39. It can be seen that a better result is achieved when a smaller step size is used for continuous variable discretization. However, a longer computation time is also required for the smaller step size. For this test case, ODCDM requires around 5847 seconds if 0.01 is used, while it requires around 1218 seconds if 0.05 is used.

Table 39 Coverage metric C of the results achieved by ODCDM with different step size adopted for continuous variable discretisation

Result set *A*	Result set *B*	Coverage metric (*A*, *B*)
ODCDM Test 1	ODCDM Test 2	0.15
ODCDM Test 2	ODCDM Test 1	0.01

7.6.2 *Test results of 2-objective voltage optimisation test cases*

The results achieved by ODCDM and MOCS for the six 2-objective test cases, FTC 1-6, are shown in Fig. 78. For FTC1 and FTC2, as shown by Fig. 78 – (a) and Fig. 78 – (b), more solutions are achieved by MOCS and the solutions are better distributed. For FTC3 and FTC4, as shown by Fig. 78 – (c) and Fig. 78 – (d), the results achieved by ODCDM, are all dominated by one or some of the results achieved by MOCS. For FTC5, as shown by Fig. 78 – (e), ODCDM found a solution which was also found by MOCS. However, the rest of the solutions achieved by ODCDM are dominated by one or some of the solutions achieved by MOCS. For FTC6, as shown by Fig. 78 – (f), the Pareto front of the optimisation problem is a single point, and both ODCDM and MOCS could achieve this solution.

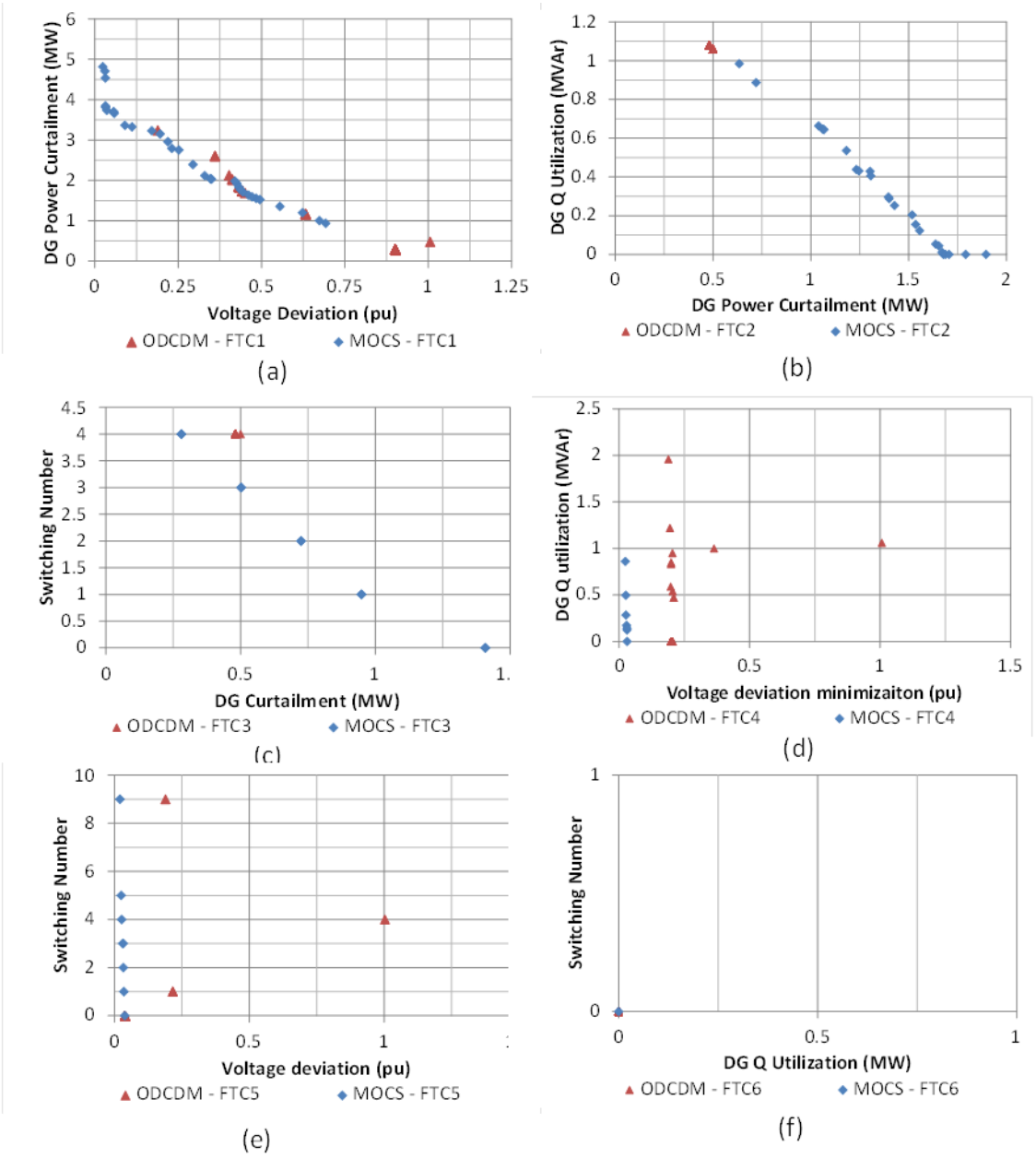

Fig. 78 Results achieved for future distribution network 2-objective voltage optimisation test cases. (a) FTC1, (b) FTC2, (c) FTC3, (d) FTC4, (e)FTC5, (d) FTC6.

The coverage metrics and computation time of the results achieved for FTC1-6 are shown in Table 40. It can be seen that for FTC1 and FTC5, although some of the solutions achieved by MOCS are dominated by that achieved by ODCDM, more solutions achieved by ODCDM are dominated by that achieved by MOCS. For FTC2, none of the results achieved by ODCDM is dominated by that achieved by MOCS, and vice versa. However, as shown in Fig. 78, the results achieved by MOCS covered a larger range than that achieved by ODCDM. For FTC3 and FTC4, the results achieved by ODCDM are all dominated by that achieved by MOCS. For FTC6, same result is achieved by both algorithms.

Table 40 Coverage metrics of test results and computation for Future Test Case 1-6

Test Case Number	Average value over 20 runs		Computation time (s)	
	Coverage metric (ODCDM, MOCS)	Coverage metric (MOCS, ODCDM)	ODCDM	MOCS (average)
FTC1	0.01	0.3	5911.35	825.12
FTC2	0	0	3314.09	823.26
FTC3	0	1	3152.58	827.11
FTC4	0	1	14533.75	821.74
FTC5	0	0.68	12520.82	819.33
FTC6	0	0	0.18	808.08

7.6.3 Test results of 3-objective voltage optimisation test cases

The results achieved for the 3-objective voltage optimisation test cases, FTC7-10, are shown in Fig. 79. It can be seen that, much more solutions are achieved by MOCS for all these four test cases. The coverage metrics and the computation time for Future Test Case 7-10 are shown in Table 41.

Table 41 Coverage metrics of test results and computation for Future Test Case 7-10

Test Case Number	Average value over 20 runs		Computation time (s)	
	Coverage metric (ODCDM, MOCS)	Coverage metric (MOCS, ODCDM)	ODCDM	MOCS (average)
FTC7	0	0	4060.91	1553.66
FTC8	0	0	2340.71	1560.11
FTC9	0.02	0.1	4669.22	1586.11
FTC10	0.03	0.6	8816.15	1470.23

In Table 41, it can be seen that for FTC7, none of the solutions achieved by ODCDM is dominated by the solutions achieved by MOCS, and vice versa. For FTC8 and FTC9, ODCDM achieved the solutions which dominate some of the solutions achieved by MOCS. However, in FTC9, coverage metric of MOCS over ODCDM is larger. For FTC10, nearly

half of the solutions achieved by ODCDM are dominated by at least one of the solutions achieved by MOCS.

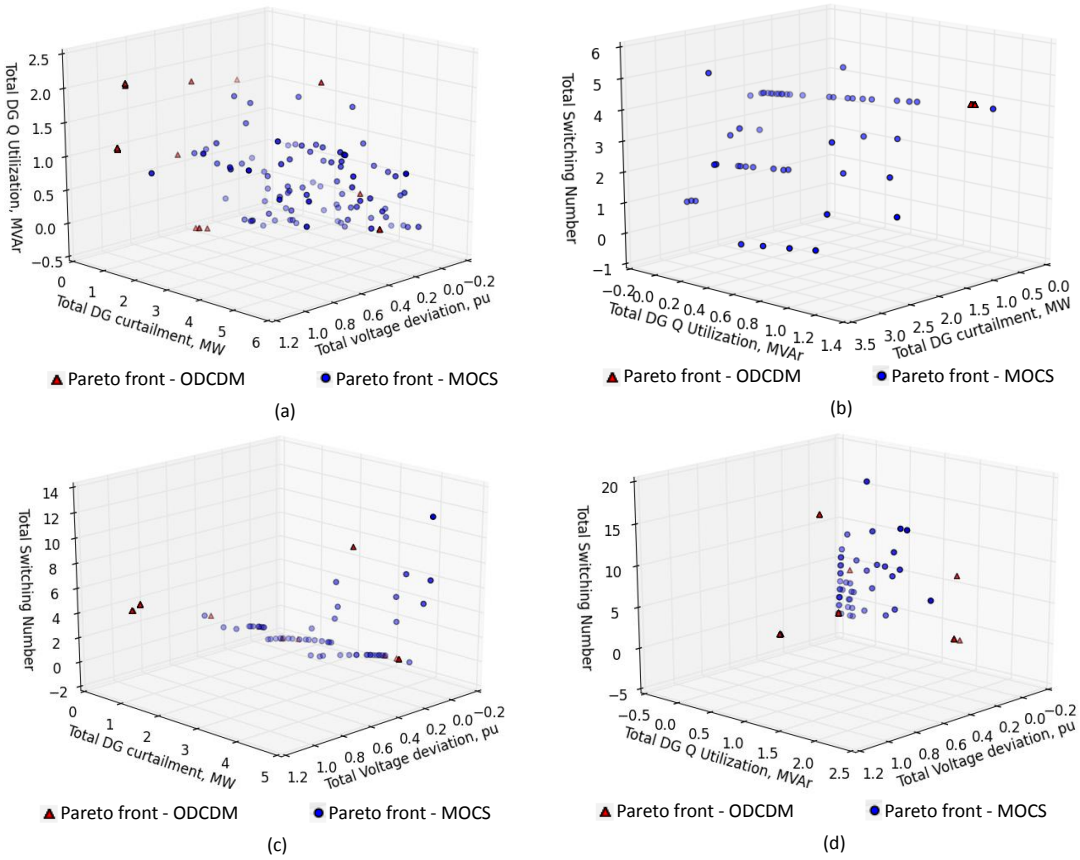

Fig. 79 Pareto front achieved for 3-objective voltage optimisation for future distribution network test cases. (a) FTC7, (b) FTC8, (c) FTC9, (d) FTC10.

7.7 Conclusions

In this chapter, ODCDM with the weighted sum method and MOCS, are evaluated and compared, regarding multi-objective voltage optimisation for conventional and future distribution networks. A method is proposed to evaluate the multi-objective voltage optimisation algorithms. Test cases are generated regarding different combinations of various optimisation objective functions. Two performance metrics, ratio of the reference point found and coverage metric, have been adopted to evaluate the results.

For conventional distribution networks, the performance of ODCDM is affected by the starting point and the step size selected for the weighting coefficient variation. As per the results of conventional distribution network test cases, MOCS could achieve a better result compared to ODCDM, when the Pareto front of the multi-objective voltage optimisation is nonconvex. For future distribution networks, more control variables and optimisation objectives are expected. The performance of ODCDM is also affected by the step size used

for the continuous control variable discretization. Generally speaking, better results could be achieved by MOCS, in terms of the number of non-dominated solutions achieved and the coverage metric. For example, the coverage metrics (MOCS, ODCDM) are significantly larger than the coverage metrics (ODCDM, MOCS), as shown in section 7.6.2, which means many solutions from the results found by ODCDM are dominated by the solutions found by MOCS.

For multi-objective voltage optimisation, the computation of ODCDM is generally longer than MOCS, since ODCDM requires multiple runs to find a set of solutions.

Chapter 8 Discussion

8.1 Introduction

In this work, three different types of centralized voltage control algorithms have been developed and evaluated for future smart distribution networks. Specifically, a rule-based voltage control algorithm has been proposed and evaluated in Chapter 3. In Chapter 4 and Chapter 5, the development and initial evaluation of voltage optimisation algorithms, based on ODCDM and CS, were described. These voltage optimisation algorithms have been further evaluated in Chapter 6 and Chapter 7, with respect to single-objective and multi-objective voltage optimisation in conventional and future distribution networks. In this chapter, these three types of voltage control algorithms are comparatively evaluated. Guidelines are provided for voltage control algorithm selection for future smart distribution networks.

8.2 Comparative algorithm evaluation

The algorithms are evaluated under the following criteria:

- Algorithm development, application and implementation
- Ability to maintain network voltages within their statutory limits
- Integration of novel voltage control techniques
- Secondary control objectives
- Solution optimality
- Computation time

8.2.1 Algorithm development, application and implementation

The VCSF based algorithm is developed based on the potential scenarios of voltage control problems. Rules are defined to represent the relationships between the voltage problems and the control devices under these scenarios. The operational costs and the voltage change capabilities of different voltage control devices are related via the voltage cost sensitivity factor. The algorithm development is relatively easy, when there are only a few potential voltage control scenarios. However, the number of scenarios could increase dramatically with the number of control devices.

The VCSF based algorithm requires offline load flow analysis, to determine potential voltage problems and possible control solutions. The parameters in the VCSF based algorithm, such as voltage sensitivity factor, need to be calculated for each individual network and may need to be recalculated, if the network topology is reconfigured. State estimators and online load flow are not required for the application of the VCSF based algorithm. However, state

estimators and online load flow could potentially be used to update the voltage sensitivity factors or/and to verify the control solution.

For both ODCDM and CS, the voltage control problem is formulated and solved as an optimisation problem. ODCDM follows a deterministic optimisation path, based on the classic optimisation theory. Like all the other metaheuristic algorithms, CS uses a combination of local search and global search, and the optimisation path is non-deterministic.

ODCDM and CS both require state estimators and online load flow, which bring the full visibility of the entire network under control. Both ODCDM and CS can be easily applied to different networks and adapted to network topology change by changing the network models. However, changing and validating the network models used by state estimators and online load flow engines is non-trivial. This is necessary after any network topology change. Potentially, the application of ODCDM and CS may lead to higher requirement regarding network measurement, in comparison with the application of VCSF. This is because only the voltages of critical busbars need to be monitored for VCSF, while for ODCDM and CS, much more busbars may need to be monitored to achieve an accurate state estimation.

VCSF and ODCDM based algorithms give deterministic and repeatable results. In contrast, CS, as a stochastic algorithm, may not do this. SOCS has been shown to be able to provide a stable result if a large maximum iteration number is allowed, as shown in Chapter 5 and Chapter 6. Here a stable result means that the difference between the results achieved by SOCS over different runs is negligible. It should be noted that even though a stable result can be achieved by SOCS, the optimisation path for each run may be different, as shown in Chapter 5. For MOCS, it is more difficult to achieve repeatable results, especially when the number of Pareto-optimal solutions is large or infinite. Although the results achieved by MOCS over different runs may not be exactly the same, these results are all acceptable, as shown in Chapter 5. This stochastic nature of CS makes it difficult to trace and analyse the optimisation path.

Parameter tuning is seen as one of the key issues in the application of metaheuristic algorithms. It is possible to spend many effects to tune the parameters for each individual problem. But the results suggested that acceptable performance can be achieved even without too much effect on parameter tuning. The test results in Chapter 6 indicate that SOCS could achieve acceptable results when the majority of the parameters are fixed, and only the maximum iteration number is determined regarding specific test network and optimisation objective. For MOCS, it is more difficult to tune the parameters, due to the difficulty of

evaluating the results for multi-objective optimisation problems. Also, both the nest number and the maximum iteration number may need to be tuned, as shown in Chapter 5. Again, the test results in Chapter 7 indicate that MOCS could achieve acceptable results when the parameters are determined as per the literature and with simple experiments.

Distribution system can be divided into electrically subnetworks and the voltage control is applied to a subnetwork. The number of control variables in the subnetwork is normally less than transmission networks. It can be seen that both ODCDM and SOCS could deal with the test cases with various numbers of control variables. It should be noted that the complexity of the voltage optimisation problems is not only decided by the number of control variables, but also decided by many other issues, such as the type of control variables and the network load and generation conditions.

The VCSF based algorithm does not have any convergence problem, while for optimisation algorithms, there is a risk that no solution will be found if the algorithm does not converge to a feasible solution.

8.2.2 Ability to maintain network voltages within their statutory limits

Based on the evaluation results from Chapter 3, Chapter 6 and Chapter 7, it can be seen that these algorithms are capable of maintaining network voltages within their statutory limits.

For VCSF, the critical busbars, at which the voltage problems are more likely to occur, are found by offline analysis. These critical busbars require monitoring in order to detect voltage issues within the network. A limitation of this approach is that some voltage problems, caused by unexpected network conditions, may not be found by at the offline analysis stage. In this case, VCSF based algorithm may not be able to detect and solve these problems.

Voltage optimisation based algorithms such ODCDM and CS require state estimators and therefore are not as susceptible to this. However, as the algorithms use model data from the state estimator and online load flow, it is possible that errors from state estimation and online load flow could reduce this capability. Therefore, having a well maintained state estimator network model and adequate network measurement is essential to ensuring that voltages are maintained within limits.

As shown in Chapter 6, the result achieved by ODCDM is affected by the SP. Moreover, it is possible that ODCDM could be trapped at an infeasible solution from which further mitigation of voltage violations would not be possible. This may happen when there is a large

divergence between the network voltages. This could be avoided by choosing the SP with certain predefined rules. An example of this would be to set the DG real power output to zero where ODCDM could then always find a feasible solution. However, a larger DG curtailment may be required, as shown in section 6.8.1.

For CS, the voltage problems can always be mitigated if CS can be run with a large enough number of iterations. Due to its stochastic nature, CS could escape from the infeasible local optima easily.

8.2.3 Integration of novel voltage control techniques

Novel voltage control techniques could be integrated into all of these three algorithms. Specifically, electrical energy storage was shown to be integrated in the VCSF based algorithm, with both the real and reactive power from EES controlled. Although only OLTCs and EESs are considered by the VCSF based algorithm in Chapter 3, other voltage control techniques can also be integrated into this proposed voltage control algorithm, such as Flexible AC transmission system (FACTS) devices. EES can be considered to be a FACTS device with a large real power storage capability. Therefore, it can be seen that the integration of other FACTS devices, such as D-STATCOM, into VCSF, is straightforward by treating them as an EES without a real power import/export capability. In both ODCDM and CS, DG control is integrated, by controlling the DG real and reactive powers directly. Other novel voltage control techniques, such as EES and controllable load, can also be integrated in the same way. DG real and reactive power control can also be considered within a VCSF based algorithm.

It should be noted that the classic voltage control techniques in distribution networks are normally discrete control variables, while many novel voltage control techniques are continuous control variables. For VCSF, the discrete nature of the classic voltage control techniques is not explicitly considered. Potentially, this could lead to solutions where the cost is unnecessarily high.

For ODCDM and CS, the integration of continuous control variables changes the voltage optimisation problem from a combinatorial problem to a MINLP problem. ODCDM does not deal with MINLP problems directly and instead continuous control variables are discretized. In Chapter 6 it was shown that the performance of ODCDM is affected by the step size used for continuous control variable discretization. If the step size is too large, the capability of the continuous control variables may not be fully used. If the step size is too small, the

computation time of ODCDM can increase dramatically, especially when the number of continuous control variables is large. In contrast, CS based algorithms can solve MINLP problems directly. However, this work shows that CS generally requires more iterations and therefore longer computation time, to solve MINLP problems.

In this PhD study, box real/reactive power constraints are adopted for EES and DG. In practice however, sometimes more sophisticated constraints may need to be considered. For example, the apparent power limit of EES may need to be considered, as represented by (74):

$$\sqrt{P_{\mathrm{EES}}^2 + Q_{\mathrm{EES}}^2} \leq S_{EES}^{Max} \tag{74}$$

where S_{EES}^{Max} is the limit of the EES apparent power, while P_{EES} and Q_{EES} are the EES real and reactive power outputs.

This relationship between EES real and reactive powers cannot be easily addressed by the VCSF based algorithm but it can be easily considered by the optimisation algorithms.

The relationship between the DG real and reactive powers can be more complicated than the box constraints adopted in this study. These more complex relationships can be adopted by both ODCDM and CS. However, in this case the voltage optimisation problem may become more nonconvex. This could result in ODCDM getting trapped at a local optimal point rather than a global optimal point more easily.

Some of the novel voltage control techniques that are expected to be used in future smart distribution networks could be used to provide multiple network services, besides voltage control. For example, EES has been shown to be able to mitigate overvoltage problems and voltage unbalance problems. Therefore, the application of EES for multiple network services should be considered. The VCSF based algorithm considers voltage unbalance control and voltage control as they can be controlled simultaneously. For voltage optimisation algorithms, unbalance can also be considered by using three-phase load flow equations in the problem formulation. Also, power flow management could be easily considered by voltage optimisation algorithms, by including a set of inequality constraints, which represent the thermal limits of network components, into the problem formulation. For example, the thermal limit of the branch between busbar i and j can be considered by (75).

$$I_{ij} \leq I_{ij}^{\max} \tag{75}$$

where I_{ij} is the current flow for the branch between busbar i and busbar j, and $I_{ij}^{\max}$ is the capacity of this branch.

8.2.4 Secondary control objectives

Besides maintaining network voltages within their statutory limits, secondary control objectives have been considered by these voltage control algorithms. For the VCSF based algorithm, control cost reduction is also considered along with maintaining voltages within statutory limits. However, it is difficult to consider complicated control objectives. For example, the network loss minimisation cannot be easily considered with a VCSF based algorithm. Moreover, the objectives cannot be easily changed, and it is difficult to consider multiple secondary control objectives.

For voltage optimisation algorithms, it is far easier to integrate and change secondary control objectives. As shown in Chapter 6, different control objectives can be formulated as optimisation objective functions and be optimised by both ODCDM and SOCS. SOCS was shown to be more flexible in terms of the form of the optimisation objective function.

Multiple secondary objectives can be considered by voltage optimisation algorithms in two different ways. The first one would be to reformulate all the objectives as one single objective function. However, the objectives may not always be comparable. The other way is to find a set of non-dominated solutions, which are expected to be as close as possible to the Pareto front of the multi-objective voltage optimisation problem. Then a solution can be selected with the information of these solutions. Two different approaches can be applied to find a set of solutions. The first approach uses single-objective optimisation algorithms, by reformulating the problem to address multi-objectives with the consideration of the preferences between different objectives. This approach is simple and widely used. However, this approach requires multiple run to find a set of solutions, and normally it is sensitive to the shape of the Pareto front. The second approach integrates the concept of Pareto optimality into the population-based metaheuristic algorithms. A set of non-dominated solutions can be found in a single run. This first approach can be used by both deterministic and metaheuristic algorithms, such as ODCDM and SOCS, while the second approach can only be used by metaheuristic algorithms, such as MOCS. As per the results shown in Chapter 7, the result achieved by ODCDM with the weighted sum method is affected by the step size used for weighting coefficient variation, and the starting point. ODCDM with the weighted sum method may have the difficulties if the Pareto front is nonconvex. Additionally, with the number of optimisation objectives increasing, it becomes more and more impractical to solve

the multi-objective voltage optimisation problems with ODCDM. The result achieved by MOCS may be different for each run, due to the stochastic nature of MOCS.

8.2.5 Solution optimality

The solution optimality is normally considered with regard to secondary control objectives.

The VCSF based algorithm is able to provide a solution, which could reduce the control cost, by selecting the most cost effective voltage control devices. However, the solution achieved may not be an optimal solution. Even if the solution is an optimal solution by coincidence, the VCSF based algorithm is not aware of that.

ODCDM is able to find an optimal solution. However, it cannot be guaranteed that this optimal solution is a global optimal solution. As shown in Chapter 4 and Chapter 6, SP affects the solution achieved by ODCDM. Distribution network voltage optimisation problems are typically nonlinear and nonconvex, and theoretically the voltage optimisation problems could have many local optima. Also, when ODCDM is applied to solve a MINLP problem, the continuous control variables in the problem need to be discretized. The MINLP problem is then converted to a combinatorial problem, which could be solved by ODCDM. The solution achieved by ODCDM for the converted combinatorial problem, may not be the optimal solution for the original MINLP problem.

SOCS can theoretically achieve a global optimal, if a long computation time is allowed. It was shown in Chapter 6 that SOCS was at least able to find the same results as ODCDM. For many test cases, SOCS was able to find a better solution than ODCDM, regarding the optimisation objective function. It is difficult to estimate the difference between the results achieved by ODCDM and SOCS, which is affected by different factors, for example, the voltage optimisation problem itself and the starting point used by ODCDM. As shown in Chapter 6, for most of the conventional distribution network test cases, generally there is no significant difference between the results achieved by both ODCDM and SOCS. This is not the case when the capacitor bank sizes are not the same in a MSC where the differences between the results found by ODCDM and SOCS could be significant. This is because the objective function itself is nonconvex in this case. In future distribution networks, the differences between the results achieved by both ODCDM and SOCS could be more significant. The solutions achieved by ODCDM are affected by the step size used for continuous control variable discretization. More importantly, the integration of DG can create

network conditions, in which ODCDM may be trapped at an infeasible solution, if the SP is not appropriately selected. The reasons were discussed in Chapter 6.

8.2.6 Computation time

The VCSF based algorithm requires simple calculations and is therefore not particularly computationally intensive. The VCSF based algorithm is verified by the real-time PHIL emulation platform, and the results demonstrated that this algorithm could be used for real time control. Voltage optimisation algorithms are slower than VCSF, since large numbers of load flow calculations are typically required. Moreover, additional time is required for the state estimation calculation. In the CLNR project, it is found that for the largest case study network, in which there are around 2,000 busbars, it took approximately 10 minutes to complete the state estimation computation.

ODCDM is generally much faster than CS, especially for the test cases in existing distribution networks. Like all the metaheuristic algorithms, CS typically requires a longer computation time than deterministic algorithms. However, ODCDM can also require a long computation time to solve the MINLP problems, if the number of continuous control variables is large and the step size used for continuous control variable discretization is small. It should be noted that some other deterministic optimisation algorithms, could be faster than ODCDM, in terms of solving MINLP problems, such as the primal-dual interior point algorithm. However, these algorithms have some other practical limitations in comparison with ODCDM. For example, discrete variables are modelled as continuous variables in PDIP, and this approach may not be valid when the step sizes of the discrete control variables in distribution networks are relatively large. Also, convergence problem needs to be considered for PDIP.

If the expected value of optimal result is known, SOCS could be stopped once this expected value is found, before the maximum iteration number is reached. In this case, the computation time of SOCS could be shortened. For example, when DG curtailment minimisation is used as the optimisation objective, the DG curtailment value is expected to be zero. SOCS could stop once the DG curtailment is reduced to zero.

The results in Chapter 7 demonstrated that, for multi-objective voltage optimisation, typically MOCS requires less computation time, compared to ODCDM with weighted sum method, to find a set of non-dominated solutions. This is because MOCS, as a population based algorithm, is able to find a set of non-dominated solutions in a single run, while ODCDM with weighted sum method needs multiple runs.

Although the computation time is an important assessment criterion, it may become less of critical factor in algorithm selection with the advancement in computing capability both locally and within the cloud.

8.3 Algorithm selection suggestions

The centralised voltage control algorithms evaluated in the previous section have been shown to have capabilities for voltage control in future distribution networks. However, it has been shown that the adoption of a single algorithm for all scenarios is not likely to be the best approach. In summary the following recommendations could be made for the algorithm selection in the context of future distribution network voltage control.

The VCSF based algorithm should be used, when:

- There are only several voltage control variables;
- The number of potential voltage control problem scenarios is small;
- The functions of state estimation and online load flow are not available;
- A deterministic result is required;
- The relationship between the secondary voltage control objective and the control variables is simple, and it is not required to consider multiple secondary control objectives;
- Optimal solutions are not required;
- The algorithm should not be computationally intensive.

Voltage optimisation algorithms should be used, when:

- It is difficult to determine all the potential voltage control problem scenarios by offline analysis, or the scenario number is large;
- A state estimator and online load flow are available;
- The relationship between the secondary voltage control objective and the control variables is complicated;
- Multiple secondary control objectives need to be considered;
- Optimal solutions are required;
- There are not many constraints on computing power.

Within voltage optimisation algorithms, ODCDM should be used, when:

- The control variables are mainly discrete variables;
- The load and generation are evenly distributed across the network;

- The function formulated for the secondary control objective is convex;
- The multiple secondary control objectives are comparable.

Within voltage optimisation algorithms, CS could be used, when:

- The objective function is non-convex;
- The control variables are mixed with discrete control variables and continuous control variables;
- The load and distributed generation are unevenly distributed in the network;
- The multiple objectives are not easily comparable.

It should be noted that this work focused on the characteristics of the algorithms themselves. If these algorithms are deployed and implemented in real distribution networks, the cost and benefits of the control algorithms need to be assessed with the long-term evaluation, regarding the specific network load and generation conditions.

Chapter 9 Conclusions and Future Work

9.1 Introduction

The research presented in this thesis investigated the capabilities of advanced voltage control algorithms for future smart distribution networks using a combination of simulation, field trial results, laboratory demonstrations and literature. In the following sections, conclusions have been drawn as a result of this research and future work is proposed.

9.2 Conclusions

It was shown previously that the control of voltages in distribution networks will become more challenging in the future. The anticipated widespread, customer driven, adoption of LCTs, such as wind and PV generation, EVs and heat pumps, is likely to cause complex voltage problems. These complex voltage problems may require novel control techniques, such as DG and EES, to be controlled cooperatively with centralized voltage control techniques, to mitigate voltage problems and also achieve secondary control objectives. Centralized control techniques were categorized into three different groups: rule-based control algorithms, deterministic optimisation algorithms and metaheuristic optimisation algorithms. To enable evaluation of the most appropriate voltage control solutions for future distribution networks, three centralized voltage control algorithms from each category have been developed and evaluated in this work.

A rule-based voltage control algorithm has been developed, which could be used to mitigate the voltage problems and voltage unbalance problems, caused by the clustered distributions of LCTs in terms of both feeder and phase location. With this algorithm, EES is integrated into voltage control and the control cost is reduced by introducing the concept of voltage cost sensitivity factor. This algorithm was evaluated using a combination of steady-state simulation and PHIL emulation.

A deterministic voltage optimisation algorithm, based on ODCDM, has been developed. This algorithm was compared with and validated using the field trial results from the CLNR project, where a sophisticated centralised voltage control system using the same algorithm was deployed on distribution networks in the north east of England. This ODCDM based algorithm has been proposed previously [1]. In this study, it has been extended to solve MINLP problems and multi-objective problems.

A metaheuristic algorithm, cuckoo search via Lévy flight, has been extended to solve single-objective and multi-objective MINLP problems. Single-objective cuckoo search algorithm

was compared with a genetic algorithm and a particle swarm optimisation algorithm. Multi-objective cuckoo search algorithm was compared with a non-dominated sorting genetic algorithm-II. It has been found that SOCS and MOCS outperform these three widely used metaheuristic algorithms regarding the voltage optimisation test cases in this study. The voltage optimisation algorithms, based on ODCDM and CSs have been further evaluated and compared, with respect to single-objective and multi-objective voltage optimisation in conventional and future distribution networks.

These three types of centralized voltage control algorithms are comparatively evaluated, regarding various criteria. In Chapter 8, all these three types of voltage control algorithms have been shown to have capabilities for voltage control in future distribution networks. However, it has been shown that the adoption of a single type of algorithm for all scenarios is not likely to be the best approach. In summary the following recommendations could be made for the algorithm selection in the context of future smart distribution network voltage control.

The VCSF based algorithm should be used, when:

- There are only several voltage control variables;
- The number of potential voltage control problem scenarios is small;
- The functions of state estimation and online load flow are not available;
- A deterministic result is required;
- The relationship between the secondary voltage control objective and the control variables is simple, and it is not required to consider multiple secondary control objectives;
- Optimal solutions are not required;
- The algorithm should not be computationally intensive.

Voltage optimisation algorithms should be used, when:

- It is difficult to determine all the potential voltage control problem scenarios by offline analysis, or the scenario number is large;
- A state estimator and online load flow are available;
- The relationship between the secondary voltage control objective and the control variables is complicated;
- Multiple secondary control objectives need to be considered;
- Optimal solutions are required;
- There are not many constraints on computing power.

Within voltage optimisation algorithms, ODCDM should be used, when:

- The control variables are mainly discrete variables;
- The load and generation are evenly distributed across the network;
- The function formulated for the secondary control objective is convex;
- The multiple secondary control objectives are comparable.

Within voltage optimisation algorithms, CS could be used, when:

- The objective function is non-convex;
- The control variables are mixed with discrete control variables and continuous control variables;
- The load and distributed generation are unevenly distributed in the network;
- The multiple objectives are not easily comparable.

In future distribution networks, it is expected that novel voltage control techniques will be integrated and large quantities of unplanned, clustered LCT may be connected. Potentially, more control objectives, which may not be comparable to each other, need to be considered for voltage control. Therefore, metaheuristic algorithms could become more preferable in future distribution networks.

The following contributions to knowledge have been made in this thesis:

- A novel rule-based voltage control algorithm has been proposed to solve voltage problems and voltage unbalanced problems in future distribution networks. Voltage cost sensitivity factor has been defined to represent the cost-effectiveness of network interventions in terms of voltage control. Feeder voltage divergence factor has been introduced as a network voltage metric for networks with large, clustered distributions of LCTs;
- Representing two different types of optimisation algorithms, ODCDM and CS algorithms have been extended and applied to solve mixed integer and multi-objective voltage optimisation problems in future smart distribution networks. A novel test methodology has been proposed to test, evaluate and compare two different types of voltage optimisation algorithms, regarding voltage control problems in conventional and future smart distribution networks;
- The rule-based voltage control algorithm and the two different voltage optimisation algorithms have been comparatively evaluated, regarding various aspects of potential voltage control problems in future smart distribution networks. The salient

characteristics of these three algorithms have been summarized and guidelines have been proposed to distribution network management product manufactures and DNOs, regarding voltage control algorithm selection for future smart distribution networks.

The algorithms and findings from this study could provide useful information for practical distribution network voltage control algorithm design, and the voltage optimisation theoretical studies. This study has some limitations. Although the algorithms can be used to represent three different types of algorithms, there are many other algorithms, which may have different characteristics of the developed algorithms in this study. For example, ODCDM is based on discrete control variables, while some other deterministic optimisation algorithms are based on continuous control variables. This study concentrates on the snapshot study. However, control scheduling could provide some additional benefits in some conditions, for example, when EES is considered. It should be also noted that although the characteristics of the algorithms have been studied, the cost and benefits of the control algorithms should be assessed with a longer term evaluation, using appropriate network load and generation data to make a comprehensive assessment.

9.3 Future work

In this study, three different types of advanced voltage control algorithms have been evaluated and compared. Useful conclusions have been drawn and could be used for voltage control algorithm design in future distribution networks. The following work could be carried out in future to augment the research presented in this thesis.

These algorithms have their own advantages and disadvantages. Potentially, a hybrid approach could be developed, by combing the advantages of different algorithms. One simple way is to implement two algorithms, and use the most suitable one based on the current network conditions using simple rules. Another approach would be to combine multiple algorithms. For example, ODCDM could be used for local search while CS could be used for a global search of the solution space.

In this study, real-time control is studied. With the integration of energy storage, and the conventional consideration of the switching number daily limit, the control scheduling could provide additional benefits, compared to real-time control. However, the computation burden is much heavier than real-time control and the uncertainty of forecasting may also need to be considered. It is valuable to compare the benefits from control scheduling, and moreover, to integrate real-time control and control scheduling.

This study focuses on the algorithm evaluation from the algorithm development aspect. Long-term evaluation could be conducted, to select the most appropriate approach. Annual load and generation data should be considered in the long-term evaluation in the context of multiple control objectives.

Reference

[1] "Reducing the UK's greenhouse gas emissions by 80% by 2050," D. o. E. C. Change, Ed., ed. London, 2013.

[2] "Electricity system: assessment of future challenges - Summary," D. o. E. C. Change, Ed., ed, 2012.

[3] Ofgem. (5 Dec 2015). *The GB electricity distribution network*. Available: https://www.ofgem.gov.uk/electricity/distribution-networks/gb-electricity-distribution-network

[4] M. Fila, "Modelling, evaluation and demonstration of novel active voltage control schemes to accomodate distributed generation in distribution networks," PhD, School of Engineering and Design Theses Electronic and Computer Engineering, Brunel University, 2010.

[5] *The Electricity Safety, Quality and Continuity Regulations 2002, S. I. 2002 No. 2665*, 2002.

[6] Nick Jenkins, Ron Allan, Peter Crossley, Daniel Kirschen, and G. Strbac, *Embedded Generation*. London: The Institution of Electrical Engineers, 2000.

[7] J. A. P. Lopes, N. Hatziargyriou, J. Mutale, P. Djapic, and N. Jenkins, "Integrating distributed generation into electric power systems: A review of drivers, challenges and opportunities," *Electric Power Systems Research,* vol. 77, pp. 1189-1203, 7// 2007.

[8] C. L. Masters, "Voltage rise: the big issue when connecting embedded generation to long 11 kV overhead lines," *Power Engineering Journal,* vol. 16, pp. 5-12, 2002.

[9] T. H. Bradley and A. A. Frank, "Design, demonstrations and sustainability impact assessments for plug-in hybrid electric vehicles," *Renewable and Sustainable Energy Reviews,* vol. 13, pp. 115-128, 1// 2009.

[10] J. Yi, P. Wang, P. C. Taylor, P. J. Davison, P. F. Lyons, D. Liang*, et al.*, "Distribution network voltage control using energy storage and demand side response," in *Innovative Smart Grid Technologies (ISGT Europe), 2012 3rd IEEE PES International Conference and Exhibition on*, 2012, pp. 1-8.

[11] P. Mancarella, G. Chin Kim, and G. Strbac, "Evaluation of the impact of electric heat pumps and distributed CHP on LV networks," in *PowerTech, 2011 IEEE Trondheim*, 2011, pp. 1-7.

[12] P. F. Lyons, "Experimental Investigation and Evaluation of Future Active Distribution Networks," PhD, School of Engineering and Computing Science, Durham University, Durham, 2009.

[13] A. Kulmala, "Active Voltage Control in Distribution Networks Including Distributed Energy Resources," PhD, Faculty of Computing and Electrical Engineering, Tampere University of Technology, Tampere, 2014.

[14] C. M. Hird, H. Leite, N. Jenkins, and H. Li, "Network voltage controller for distributed generation," *Generation, Transmission and Distribution, IEE Proceedings-,* vol. 151, pp. 150-156, 2004.

[15] R. C. Dugan, M. F. McGranaghan, S. Surya, and H. W. Beaty, *Electrical Power Systems Quality*, 2nd ed.: The McGraw-Hill Companies, Inc., 2003.

[16] T. E. Council, "Engineering recommendation P29 - Planning limits for voltage unbalance in the united kingdom," ed: The Electricity Council, 1990.

[17] "EN 50160: Voltage characteristics of electricity supplied by public distribution systems," ed. Brussels, Belgium: CENELEC, 1999.

[18] A. von Jouanne and B. Banerjee, "Assessment of voltage unbalance," *Power Delivery, IEEE Transactions on,* vol. 16, pp. 782-790, 2001.

[19] P. Trichakis, P. C. Taylor, L. M. Cipcigan, P. F. Lyons, R. Hair, and T. Ma, "An Investigation of Voltage Unbalance in Low Voltage Distribution Networks with High Levels of SSEG," in *Universities Power Engineering Conference, 2006. UPEC '06. Proceedings of the 41st International*, 2006, pp. 182-186.

[20] P. Trichakis, P. C. Taylor, P. F. Lyons, and R. Hair, "Predicting the technical impacts of high levels of small-scale embedded generators on low-voltage networks," *Renewable Power Generation, IET,* vol. 2, pp. 249-262, 2008.

[21] B. Werther, J. Schmiesing, A. Becker, and E.-A. Wehrmann, "Voltage control in low voltage systems with controlled low voltage transformer (CLVT)," in *Integration of Renewables into the Distribution Grid, CIRED 2012 Workshop*, 2012, pp. 1-4.
[22] F. A. Viawan, "Voltage Control and Voltage Stability of Power Distribution Systems in the Presence of Distributed Generation," PhD, Department of Energy and Environment, Chalmers University of Technology, Goeteborg Sweden, 2008.
[23] X. Liu, A. Aichhorn, L. Liu, and H. Li, "Coordinated Control of Distributed Energy Storage System With Tap Changer Transformers for Voltage Rise Mitigation Under High Photovoltaic Penetration," *Smart Grid, IEEE Transactions on,* vol. 3, pp. 897-906, 2012.
[24] H. Farhangi, "The path of the smart grid," *Power and Energy Magazine, IEEE,* vol. 8, pp. 18-28, 2010.
[25] Y. Xinghuo, C. Cecati, T. Dillon, Simo, x, and M. G. es, "The New Frontier of Smart Grids," *Industrial Electronics Magazine, IEEE,* vol. 5, pp. 49-63, 2011.
[26] P. Järventausta, S. Repo, A. Rautiainen, and J. Partanen, "Smart grid power system control in distributed generation environment," *Annual Reviews in Control,* vol. 34, pp. 277-286, 12// 2010.
[27] R. W. Uluski, "VVC in the Smart Grid era," in *Power and Energy Society General Meeting, 2010 IEEE*, 2010, pp. 1-7.
[28] B. P. Roberts and C. Sandberg, "The Role of Energy Storage in Development of Smart Grids," *Proceedings of the IEEE,* vol. 99, pp. 1139-1144, 2011.
[29] N. S. Wade, P. C. Taylor, P. D. Lang, and P. R. Jones, "Evaluating the benefits of an electrical energy storage system in a future smart grid," *Energy Policy,* vol. 38, pp. 7180-7188, 2010.
[30] T. Strasser, F. Andren, J. Kathan, C. Cecati, C. Buccella, P. Siano*, et al.*, "A Review of Architectures and Concepts for Intelligence in Future Electric Energy Systems," *Industrial Electronics, IEEE Transactions on,* vol. PP, pp. 1-1, 2014.
[31] X. Fang, S. Misra, G. Xue, and D. Yang, "Smart Grid — The New and Improved Power Grid: A Survey," *Communications Surveys & Tutorials, IEEE,* vol. 14, pp. 944-980, 2012.
[32] J. Momoh, *Smart Grid: Fundamentals of Design and Analysis (IEEE Press Series on Power Engineering)*, 1st ed.: Wiley-Blackwell, 2012.
[33] S. Rahimi, M. Marinelli, and F. Silvestro, "Evaluation of requirements for Volt/Var control and optimization function in distribution management systems," in *Energy Conference and Exhibition (ENERGYCON), 2012 IEEE International*, 2012, pp. 331-336.
[34] R. E. Brown, "Impact of Smart Grid on distribution system design," in *Power and Energy Society General Meeting - Conversion and Delivery of Electrical Energy in the 21st Century, 2008 IEEE*, 2008, pp. 1-4.
[35] N. Powergrid. (2014, 01/12/2015). *Customer-Led Network Revolution*. Available: http://www.networkrevolution.co.uk/
[36] E. Northwest. (2015, 01/12/2015). *Customer Load Active System Services*. Available: http://www.enwl.co.uk/CLASS#
[37] W. Pengfei, Y. Jialiang, P. Lyons, D. Liang, P. Taylor, D. Miller*, et al.*, "Customer Led Network Revolution — Integrating renewable energy into LV networks using energy storage," in *Integration of Renewables into the Distribution Grid, CIRED 2012 Workshop*, 2012, pp. 1-4.
[38] M. A. Kashem and G. Ledwich, "Energy requirement for distributed energy resources with battery energy storage for voltage support in three-phase distribution lines," *Electric Power Systems Research,* vol. 77, pp. 10-23, 2007.
[39] L. H. Macedo, J. F. Franco, M. J. Rider, and R. Romero, "Optimal Operation of Distribution Networks Considering Energy Storage Devices," *Smart Grid, IEEE Transactions on,* vol. 6, pp. 2825-2836, 2015.
[40] W. Lei, D. H. Liang, A. F. Crossland, P. C. Taylor, D. Jones, and N. S. Wade, "Coordination of Multiple Energy Storage Units in a Low-Voltage Distribution Network," *Smart Grid, IEEE Transactions on,* vol. 6, pp. 2906-2918, 2015.

[41] V. Calderaro, V. Galdi, F. Lamberti, and A. Piccolo, "A Smart Strategy for Voltage Control Ancillary Service in Distribution Networks," *Power Systems, IEEE Transactions on,* vol. 30, pp. 494-502, 2015.
[42] Q. Zhou and J. W. Bialek, "Generation curtailment to manage voltage constraints in distribution networks," *Generation, Transmission & Distribution, IET,* vol. 1, pp. 492-498, 2007.
[43] N. Yorino, Y. Zoka, M. Watanabe, and T. Kurushima, "An Optimal Autonomous Decentralized Control Method for Voltage Control Devices by Using a Multi-Agent System," *Power Systems, IEEE Transactions on,* vol. 30, pp. 2225-2233, 2015.
[44] N. J. M. Hird, P. C. Taylor, "An active 11kv voltage controller: Practical considerations," presented at the CIRED 17th International Conference on Electricity Distribution, 2003.
[45] L. H. Alan Collinson, Peter Thomas, Eric Paalman, "Modelling The Interaction between An In-line Voltage Regulator and A Doubly-Fed Introduction Generator," 2003.
[46] A. Gabash and L. Pu, "Active-Reactive Optimal Power Flow in Distribution Networks With Embedded Generation and Battery Storage," *Power Systems, IEEE Transactions on,* vol. 27, pp. 2026-2035, 2012.
[47] Allan Collinson, Fangtao Dai, A. Beddoes, and J. Crabtree, "Solutions for the connection and operation of distributed generation," 2003.
[48] X. Tao, P. C. Taylor, "Voltage Control Techniques for Electrical Distribution Networks Including Distributed Generation," in *The International Federation of Automatic Control*, Seoul, Korea, 2008, pp. 11967-11971.
[49] G. Strbac, N. Jenkins, M. Hird, P. Djapic, and G. Nicholson, "Integration of operation of embedded generation and distribution networks," Manchester Centre for Electrical Energy, Manchester2002.
[50] M. H. J. Bollen and A. Sannino, "Voltage control with inverter-based distributed generation," *Power Delivery, IEEE Transactions on,* vol. 20, pp. 519-520, 2005.
[51] J. Zhihan, C. Jinfu, L. Naihu, Y. Meiqi, and L. Huijie, "Dynamic optimization of reactive power and voltage control in distribution network considering the connection of DFIG," in *Power Engineering and Automation Conference (PEAM), 2011 IEEE*, 2011, pp. 30-34.
[52] S. Toma, T. Senjyu, Y. Miyazato, A. Yona, T. Funabashi, A. Y. Saber*, et al.*, "Optimal coordinated voltage control in distribution system," in *Power and Energy Society General Meeting - Conversion and Delivery of Electrical Energy in the 21st Century, 2008 IEEE*, 2008, pp. 1-7.
[53] K. Nara, S. Ishizu, and Y. Mishima, "Voltage control availability of distributed generators in power distribution system," in *Power Tech, 2005 IEEE Russia*, 2005, pp. 1-6.
[54] L. F. Ochoa and G. P. Harrison, "Minimizing Energy Losses: Optimal Accommodation and Smart Operation of Renewable Distributed Generation," *Power Systems, IEEE Transactions on,* vol. 26, pp. 198-205, 2011.
[55] H. Ying-Yi and L. Yi-Feng, "Optimal VAR Control Considering Wind Farms Using Probabilistic Load-Flow and Gray-Based Genetic Algorithms," *Power Delivery, IEEE Transactions on,* vol. 24, pp. 1441-1449, 2009.
[56] K. Young-Jin, A. Seon-Ju, H. Pyeong-Ik, P. Gi-Chan, and M. Seung-Il, "Coordinated Control of a DG and Voltage Control Devices Using a Dynamic Programming Algorithm," *Power Systems, IEEE Transactions on,* vol. 28, pp. 42-51, 2013.
[57] F. H. Math Bollen, *Integration of Distributed Generation in the Power System*, 2010.
[58] L. Kuang, L. Jinjun, W. Zhaoan, and W. Biao, "Strategies and Operating Point Optimization of STATCOM Control for Voltage Unbalance Mitigation in Three-Phase Three-Wire Systems," *Power Delivery, IEEE Transactions on,* vol. 22, pp. 413-422, 2007.
[59] J. Wong, Y. S. Lim, and E. Morris, "Distributed Energy Storage Systems with an Improved Fuzzy Controller for Mitigating Voltage Unbalance on Low-Voltage Networks," *Journal of Energy Engineering,* vol. 0, 2014.

[60] K. H. Chua, L. Yun Seng, P. Taylor, S. Morris, and W. Jianhui, "Energy Storage System for Mitigating Voltage Unbalance on Low-Voltage Networks With Photovoltaic Systems," *Power Delivery, IEEE Transactions on,* vol. 27, pp. 1783-1790, 2012.
[61] I. Roytelman, B. K. Wee, and R. L. Lugtu, "Volt/var control algorithm for modern distribution management system," *Power Systems, IEEE Transactions on,* vol. 10, pp. 1454-1460, 1995.
[62] (30th Nov 2015). *Voltage Control - SuperTAPP n+*. Available: http://www.fundamentalsltd.co.uk/voltage-control-relays/supertapp-n
[63] M. Fila, D. Reid, G. A. Taylor, P. Lang, and M. R. Irving, "Coordinated voltage control for active network management of distributed generation," in *Power & Energy Society General Meeting, 2009. PES '09. IEEE*, 2009, pp. 1-8.
[64] F. Bouhafs, M. Mackay, and M. Merabti, *Communication Challenges and Solutions in the Smart Grid*. London: Springer, 2014.
[65] S. Qiuye, H. Renke, Z. Huaguang, Z. Jianguo, and J. M. Guerrero, "A Multiagent-Based Consensus Algorithm for Distributed Coordinated Control of Distributed Generators in the Energy Internet," *Smart Grid, IEEE Transactions on,* vol. 6, pp. 3006-3019, 2015.
[66] S. N. Liew and G. Strbac, "Maximising penetration of wind generation in existing distribution networks," *Generation, Transmission and Distribution, IEE Proceedings-,* vol. 149, pp. 256-262, 2002.
[67] P. Trichakis, "Multi Agent Systems for the Active Management of Electrical Distribution Networks," PhD, School of Engineering and Computing Science, Durham University, Durham, 2009.
[68] A. Kulmala, S. Repo, and P. Jarventausta, "Coordinated Voltage Control in Distribution Networks Including Several Distributed Energy Resources," *Smart Grid, IEEE Transactions on,* vol. 5, pp. 2010-2020, 2014.
[69] P. Wang, T. Jiang, P. Lyons, and J. Yi, "Tapchanging Secondary Transformer Autonomous and GUS Voltage Control," L-126, 2014.
[70] T. Senjyu, Y. Miyazato, A. Yona, N. Urasaki, and T. Funabashi, "Optimal Distribution Voltage Control and Coordination With Distributed Generation," *Power Delivery, IEEE Transactions on,* vol. 23, pp. 1236-1242, 2008.
[71] A. Kulmala, A. Mutanen, A. Koto, S. Repo, Ja, x*, et al.*, "RTDS verification of a coordinated voltage control implementation for distribution networks with distributed generation," in *Innovative Smart Grid Technologies Conference Europe (ISGT Europe), 2010 IEEE PES*, pp. 1-8.
[72] A. Gomez Exposito, J. L. Martinez Ramos, J. L. Ruiz Macias, and Y. Cuellar Salinas, "Sensitivity-based reactive power control for voltage profile improvement," *Power Systems, IEEE Transactions on,* vol. 8, pp. 937-945, 1993.
[73] X. Tao, P. Taylor, M. Prodanovic, T. Green, E. Davidson, and S. McArthur, "Case based reasoning for distributed voltage control," in *Electricity Distribution - Part 1, 2009. CIRED 2009. 20th International Conference and Exhibition on*, 2009, pp. 1-4.
[74] S. Frank, I. Steponavice, and S. Rebennack, "Optimal power flow: a bibliographic survey I," *Energy Systems,* vol. 3, pp. 221-258, 2012/09/01 2012.
[75] M. Liu, S. K. Tso, and Y. Cheng, "An extended nonlinear primal-dual interior-point algorithm for reactive-power optimization of large-scale power systems with discrete control variables," *Power Systems, IEEE Transactions on,* vol. 17, pp. 982-991, 2002.
[76] M. B. Liu, C. A. Canizares, and W. Huang, "Reactive Power and Voltage Control in Distribution Systems With Limited Switching Operations," *Power Systems, IEEE Transactions on,* vol. 24, pp. 889-899, 2009.
[77] Z. Hu, X. Wang, H. Chen, and G. A. Taylor, "Volt/VAr control in distribution systems using a time-interval based approach," *Generation, Transmission and Distribution, IEE Proceedings-,* vol. 150, pp. 548-554, 2003.
[78] Z. H. Bie, Y. H. Song, X. F. Wang, G. A. Taylor, and M. R. Irving, "Integration of algorithmic and heuristic techniques for transition-optimised voltage and reactive power control," *IEE Proceedings - Generation, Transmission and Distribution,* vol. 153, p. 205, 2006.

[79] H. W. Dommel and W. F. Tinney, "Optimal Power Flow Solutions," *Power Apparatus and Systems, IEEE Transactions on,* vol. PAS-87, pp. 1866-1876, 1968.
[80] M. Huneault and F. D. Galiana, "A survey of the optimal power flow literature," *Power Systems, IEEE Transactions on,* vol. 6, pp. 762-770, 1991.
[81] M. R. Irving and Y.-H. Song. (2000, Optimisation techniques for electrical power systems. Part 1: Mathematical optimisation methods. *Power Engineering Journal 14(5),* 245-254. Available: http://digital-library.theiet.org/content/journals/10.1049/pe_20000509
[82] K. R. C. Mamandur and R. D. Chenoweth, "Optimal Control of Reactive Power flow for Improvements in Voltage Profiles and for Real Power Loss Minimization," *Power Apparatus and Systems, IEEE Transactions on,* vol. PAS-100, pp. 3185-3194, 1981.
[83] I. Roytelman, B. K. Wee, R. L. Lugtu, T. M. Kulas, and T. Brossart, "Pilot project to estimate the centralized volt/VAr control effectiveness," in *Power Industry Computer Applications., 1997. 20th International Conference on*, 1997, pp. 340-345.
[84] J. Martí, "Southern Scenario Results and Evaluation Lessons Learned and Demo Conclusions," Iberdrola Distribución Eléctrica, Bilbao, Spain26/10/2009 2009.
[85] P. J. Macfie, G. A. Taylor, M. R. Irving, P. Hurlock, and W. Hai-Bin, "Proposed Shunt Rounding Technique for Large-Scale Security Constrained Loss Minimization," *Power Systems, IEEE Transactions on,* vol. 25, pp. 1478-1485, 2010.
[86] K. Deb, A. Pratap, S. Agarwal, and T. Meyarivan, "A fast and elitist multiobjective genetic algorithm: NSGA-II," *Evolutionary Computation, IEEE Transactions on,* vol. 6, pp. 182-197, 2002.
[87] A. Shafiu, V. Thornley, N. Jenkins, G. Strbac, and A. Maloyd, "Control of active networks," in *Electricity Distribution, 2005. CIRED 2005. 18th International Conference and Exhibition on*, 2005, pp. 1-4.
[88] P. Macfie, "Large-scale security constrained optimal reactive power flow for operational loss management on the GB electricity transmission network," PhD, Department of Electronic and Computer Engineering, Brunel University, 2010.
[89] I. Osman and G. Laporte, "Metaheuristics: A bibliography," *Annals of Operations Research,* vol. 63, pp. 511-623, 1996/10/01 1996.
[90] S. Frank, I. Steponavice, and S. Rebennack, "Optimal power flow: a bibliographic survey II," *Energy Systems,* vol. 3, pp. 259-289, 2012/09/01 2012.
[91] X.-S. Yang, *Nature-Inspired Metaheuristic Algorithms*, 2nd ed. Frome, UK: Luniver Press, 2010.
[92] S. Voß, "Meta-heuristics: The State of the Art," in *Local Search for Planning and Scheduling*. vol. 2148, A. Nareyek, Ed., ed: Springer Berlin Heidelberg, 2001, pp. 1-23.
[93] A. G. Madureira and J. A. Pecas Lopes, "Coordinated voltage support in distribution networks with distributed generation and microgrids," *Renewable Power Generation, IET,* vol. 3, pp. 439-454, 2009.
[94] F. G. Montoya, R. Baños, C. Gil, A. Espín, A. Alcayde, and J. Gómez, "Minimization of voltage deviation and power losses in power networks using Pareto optimization methods," *Engineering Applications of Artificial Intelligence,* vol. 23, pp. 695-703, 8// 2010.
[95] T. Niknam, M. R. Narimani, R. Azizipanah-Abarghooee, and B. Bahmani-Firouzi, "Multiobjective Optimal Reactive Power Dispatch and Voltage Control: A New Opposition-Based Self-Adaptive Modified Gravitational Search Algorithm," *Systems Journal, IEEE,* vol. 7, pp. 742-753, 2013.
[96] L. Fang, C. Y. Chung, K. P. Wong, Y. Wei, and X. Guoyu, "Hybrid Immune Genetic Method for Dynamic Reactive Power Optimization," in *Power System Technology, 2006. PowerCon 2006. International Conference on*, 2006, pp. 1-6.
[97] P. N. Biskas, N. P. Ziogos, A. Tellidou, C. E. Zoumas, A. G. Bakirtzis, and V. Petridis, "Comparison of two metaheuristics with mathematical programming methods for the solution of OPF," *Generation, Transmission and Distribution, IEE Proceedings-,* vol. 153, pp. 16-24, 2006.
[98] "International Electrotechnical Vocabulary - Part 601: Generation, transmission and distribution of electricity - General - Medium Voltage," in *IEC 60050* vol. 601-01-28, ed, 2009.

[99] "International Electrotechnical Vocabulary - Part 601: Generation, transmission and distribution of electricity - General - Low Voltage," in *IEC 60050* vol. 601-01-26, ed, 2009.
[100] A. Keane, Q. Zhou, J. W. Bialek, and M. O'Malley, "Planning and operating non-firm distributed generation," *Renewable Power Generation, IET,* vol. 3, pp. 455-464, 2009.
[101] R. Wardle, Christian, Barteczko-Hibbert., Miller, David and Sidebotham, Liz, "Initial Load Profiles form CLNR Intervention Trials," 2013.
[102] S. Abu-Sharkh, R. J. Arnold, J. Kohler, R. Li, T. Markvart, J. N. Ross*, et al.*, "Can microgrids make a major contribution to UK energy supply?," *Renewable and Sustainable Energy Reviews,* vol. 10, pp. 78-127, 4// 2006.
[103] A. A. Sousa, G. L. Torres, and C. A. Canizares, "Robust Optimal Power Flow Solution Using Trust Region and Interior-Point Methods," *Power Systems, IEEE Transactions on,* vol. 26, pp. 487-499, 2011.
[104] E. Veldman, M. Gibescu, H. Slootweg, and W. L. Kling, "Impact of electrification of residential heating on loading of distribution networks," in *PowerTech, 2011 IEEE Trondheim*, 2011, pp. 1-7.
[105] (3rd Dec 2015). *Smart Grid Forum*. Available: https://www.ofgem.gov.uk/publications-and-updates/assessing-impact-low-carbon-technologies-great-britains-power-distribution-networks
[106] M. A. Kashem and G. Ledwich, "Multiple Distributed Generators for Distribution Feeder Voltage Support," *Energy Conversion, IEEE Transactions on,* vol. 20, pp. 676-684, 2005.
[107] X.-F. Wang, Song, Yonghua, Irving, Malcolm, *Modern Power Systems Analysis*: Springer, 2009.
[108] R. P. O'Neill, A. Castillo, and M. B. Cain, "The Computational Testing of AC Optimal Power Flow Using the Current Voltage (IV) Formulations," 2012.
[109] J. Tianxiang, B. Simon, L. Pádraig, W. Pengfei, and Y. jialiang, "CLNR Post Trial Analysis EES2 and EES3 GUS Powerflow Management," Newcastle University2014.
[110] E. K. P. Chong and S. H. Zak, *An Introduction to Optimization*: John Wiley & Sons, 2011.
[111] N. Daratha, B. Das, and J. Sharma, "Coordination Between OLTC and SVC for Voltage Regulation in Unbalanced Distribution System Distributed Generation," *Power Systems, IEEE Transactions on,* vol. 29, pp. 289-299, 2014.
[112] S. K. Goswami and S. K. Basu, "A new algorithm for the reconfiguration of distribution feeders for loss minimization," *Power Delivery, IEEE Transactions on,* vol. 7, pp. 1484-1491, 1992.
[113] T. Niknam, M. Zare, and J. Aghaei, "Scenario-Based Multiobjective Volt/Var Control in Distribution Networks Including Renewable Energy Sources," *Power Delivery, IEEE Transactions on,* vol. 27, pp. 2004-2019, 2012.
[114] S. D. X.-S. Yang, "Cuckoo Search via Levy Flights," in *World Congress on Nature \& Biologically Inspired Computing (NaBIC 2009)*, India, 2009, pp. 210-214.
[115] I. Fister, Jr., X.-S. Yang, D. Fister, and I. Fister, "Cuckoo Search: A Brief Literature Review," in *Cuckoo Search and Firefly Algorithm*. vol. 516, X.-S. Yang, Ed., ed: Springer International Publishing, 2014, pp. 49-62.
[116] X.-S. Yang and S. Deb, "Cuckoo search: recent advances and applications," *Neural Computing and Applications,* pp. 1-6, 2013/03/09 2013.
[117] P. Civicioglu and E. Besdok, "A conceptual comparison of the Cuckoo-search, particle swarm optimization, differential evolution and artificial bee colony algorithms," *Artificial Intelligence Review,* vol. 39, pp. 315-346, 2013/04/01 2013.
[118] M. Basu and A. Chowdhury, "Cuckoo search algorithm for economic dispatch," *Energy,* vol. 60, pp. 99-108, 10/1/ 2013.
[119] H. E. X.-S. W. Y. Y. S.-M. Wang Fan, "Markov Model and Convergence Analysis Based on Cuckoo Search Algorithm," *Computer Engineering,* vol. 38, pp. 180-182,185, 2012-06-05 2012.
[120] K. Chandrasekaran and S. P. Simon, "Multi-objective scheduling problem: Hybrid approach using fuzzy assisted cuckoo search algorithm," *Swarm and Evolutionary Computation,* vol. 5, pp. 1-16, 8// 2012.

[121] X.-S. Yang and S. Deb, "Multiobjective cuckoo search for design optimization," *Computers & Operations Research,* vol. 40, pp. 1616-1624, 6// 2013.
[122] K. C. a. S. P. Simon, "Multi-objective unit commitment problem using Cuckoo search Lagrangian method," *International Journal of Engineering, Science and Technology,* vol. 4, pp. 89-105, 2012.
[123] Y. Zhang, L. Wang, and Q. Wu, "Modified Adaptive Cuckoo Search (MACS) algorithm and formal description for global optimisation," *International Journal of Computer Applications in Technology,* vol. 44, pp. 73-79, 01/01/ 2012.
[124] K. N. A. Rani, M. F. A. Malek, N. Siew Chin, F. Jamlos, N. A. M. Affendi, L. Mohamed*, et al.*, "Hybrid multiobjective optimization using modified cuckoo search algorithm in linear array synthesis," in *Antennas and Propagation Conference (LAPC), 2012 Loughborough*, 2012, pp. 1-4.
[125] "Multi-Objective Cuckoo Search for the Optimal Design of Water Distribution Systems," in *Civil Engineering and Urban Planning 2012*, ed, pp. 402-405.
[126] D. N. Arcanjo, J. L. R. Pereira, E. J. Oliveira, W. Peres, L. W. de Oliveira, and I. C. da Silva Junior, "Cuckoo Search Optimization technique applied to capacitor placement on distribution system problem," in *Industry Applications (INDUSCON), 2012 10th IEEE/IAS International Conference on*, 2012, pp. 1-6.
[127] Z. Moravej and A. Akhlaghi, "A novel approach based on cuckoo search for DG allocation in distribution network," *International Journal of Electrical Power & Energy Systems,* vol. 44, pp. 672-679, 1// 2013.
[128] M. H. Sulaiman and M. R. Mohamed, "Solving economic dispatch problems utilizing Cuckoo Search algorithm," in *Power Engineering and Optimization Conference (PEOCO), 2014 IEEE 8th International*, 2014, pp. 89-93.
[129] E. Afzalan and M. Joorabian, "An improved cuckoo search algorithm for power economic load dispatch," *International Transactions on Electrical Energy Systems,* pp. n/a-n/a, 2014.
[130] A. Gandomi, X.-S. Yang, and A. Alavi, "Cuckoo search algorithm: a metaheuristic approach to solve structural optimization problems," *Engineering with Computers,* vol. 29, pp. 17-35, 2013/01/01 2013.
[131] I. Pavlyukevich, "Lévy flights, non-local search and simulated annealing," *Journal of Computational Physics,* vol. 226, pp. 1830-1844, 10/1/ 2007.
[132] M. F. Shlesinger, "Mathematical physics: Search research," *Nature,* vol. 443, pp. 281-282, 09/21/print 2006.
[133] R. T. Marler and J. S. Arora, "Survey of multi-objective optimization methods for engineering," *Structural and Multidisciplinary Optimization,* vol. 26, pp. 369-395, 2004/04/01 2004.
[134] N. M. Pindoriya, S. N. Singh, and K. Y. Lee, "A comprehensive survey on multi-objective evolutionary optimization in power system applications," in *Power and Energy Society General Meeting, 2010 IEEE*, 2010, pp. 1-8.
[135] X.-S. Yang and S. Deb, "Engineering Optimisation by Cuckoo Search," *Int. J. Mathematical Modelling and Numerical Optimisation,* vol. 1, pp. 330-343, 2010.
[136] Y. Zhou and H. Zheng, "A Novel Complex Valued Cuckoo Search Algorithm," *The Scientific World Journal,* vol. 2013, p. 6, 2013.
[137] T. Segaran, *Programming Collective Intelligence: Building Smart Web 2.0 Applications*: O'Reilly Media, Inc, 2007.
[138] P. AGH University of Science and Technology in Krakow, "Implementation of "Non-dominated Sorting Genetic Algorithm II" in Python," ed, 2007.
[139] H. Lu, M. Zhang, Z. Fei, and K. Mao, "Multi-Objective Energy Consumption Scheduling in Smart Grid Based on Tchebycheff Decomposition," *Smart Grid, IEEE Transactions on,* vol. PP, pp. 1-1, 2015.
[140] M. Gitizadeh and H. Karampour, "Multi-objective fuzzy based reactive power and voltage control in a distribution system using SA," in *Hybrid Intelligent Systems (HIS), 2011 11th International Conference on*, 2011, pp. 334-339.

[141] F. Capitanescu and L. Wehenkel, "Redispatching Active and Reactive Powers Using a Limited Number of Control Actions," *Power Systems, IEEE Transactions on,* vol. 26, pp. 1221-1230, 2011.
[142] J. Zhu, *Optimization of Power System Operation*. Hoboken, New Jersey: John Wiley & Sons, Inc, 2009.
[143] M. E. Baran and F. F. Wu, "Network reconfiguration in distribution systems for loss reduction and load balancing," *Power Delivery, IEEE Transactions on,* vol. 4, pp. 1401-1407, 1989.
[144] M. E. Baran and F. F. Wu, "Optimal capacitor placement on radial distribution systems," *Power Delivery, IEEE Transactions on,* vol. 4, pp. 725-734, 1989.
[145] W. Yang, Z. Peng, L. Wenyuan, X. Weidong, and A. Abdollahi, "Online Overvoltage Prevention Control of Photovoltaic Generators in Microgrids," *Smart Grid, IEEE Transactions on,* vol. 3, pp. 2071-2078, 2012.
[146] T. Sousa, H. Morais, Z. Vale, and R. Castro, "A multi-objective optimization of the active and reactive resource scheduling at a distribution level in a smart grid context," *Energy,* vol. 85, pp. 236-250, 6/1/ 2015.
[147] R. S. Rao, K. Ravindra, K. Satish, and S. V. L. Narasimham, "Power Loss Minimization in Distribution System Using Network Reconfiguration in the Presence of Distributed Generation," *Power Systems, IEEE Transactions on,* vol. 28, pp. 317-325, 2013.
[148] M. Zare, T. Niknam, R. Azizipanah-Abarghooee, and B. Amiri, "Multi-objective probabilistic reactive power and voltage control with wind site correlations," *Energy,* vol. 66, pp. 810-822, 3/1/ 2014.
[149] R. D. Zimmerman, S. Murillo, x, C. E. nchez, and R. J. Thomas, "MATPOWER: Steady-State Operations, Planning, and Analysis Tools for Power Systems Research and Education," *Power Systems, IEEE Transactions on,* vol. 26, pp. 12-19, 2011.
[150] (29 Nov 2015). *Spyder*. Available: https://pythonhosted.org/spyder/#
[151] F. Capitanescu, I. Bilibin, and E. Romero Ramos, "A Comprehensive Centralized Approach for Voltage Constraints Management in Active Distribution Grid," *Power Systems, IEEE Transactions on,* vol. 29, pp. 933-942, 2014.
[152] Q. Zhifeng, G. Deconinck, and R. Belmans, "A literature survey of Optimal Power Flow problems in the electricity market context," in *Power Systems Conference and Exposition, 2009. PSCE '09. IEEE/PES*, 2009, pp. 1-6.
[153] S. Carr, G. C. Premier, A. J. Guwy, R. M. Dinsdale, and J. Maddy, "Energy storage for active network management on electricity distribution networks with wind power," *Renewable Power Generation, IET,* vol. 8, pp. 249-259, 2014.
[154] S. Deshmukh, B. Natarajan, and A. Pahwa, "State Estimation and Voltage/VAR Control in Distribution Network With Intermittent Measurements," *Smart Grid, IEEE Transactions on,* vol. 5, pp. 200-209, 2014.
[155] S. Deshmukh, B. Natarajan, and A. Pahwa, "Voltage/VAR Control in Distribution Networks via Reactive Power Injection Through Distributed Generators," *Smart Grid, IEEE Transactions on,* vol. 3, pp. 1226-1234, 2012.
[156] A. V. Chechkin, R. Metzler, J. Klafter, and V. Y. Gonchar, "Introduction to the Theory of Lévy Flights," in *Anomalous Transport*, ed: Wiley-VCH Verlag GmbH & Co. KGaA, 2008, pp. 129-162.
[157] W. Rosehart, C. Roman, and A. Schellenberg, "Optimal power flow with complementarity constraints," *Power Systems, IEEE Transactions on,* vol. 20, pp. 813-822, 2005.
[158] J. Lavaei and S. H. Low, "Zero Duality Gap in Optimal Power Flow Problem," *Power Systems, IEEE Transactions on,* vol. 27, pp. 92-107, 2012.
[159] J. Lavaei, "Zero duality gap for classical opf problem convexifies fundamental nonlinear power problems," in *American Control Conference (ACC), 2011*, 2011, pp. 4566-4573.
[160] X. Xia and A. M. Elaiw, "Optimal dynamic economic dispatch of generation: A review," *Electric Power Systems Research,* vol. 80, pp. 975-986, 8// 2010.
[161] "Load Flow Analysis," in *Modern Power Systems Analysis*, ed: Springer US, 2008, pp. 71-128.
[162] Z. Eckart, D. Kalyanmoy, and T. Lothar, "Comparison of Multiobjective Evolutionary Algorithms: Empirical Results," *Evol. Comput.,* vol. 8, pp. 173-195, 2000.

[163] E. Zitzler, "Evolutionary Algorithms for Multiobjective Optimization: Methods and Applications," Doctor of Technical Sciences, Swiss Federal Institute of Technology Zurich, Zurich, 1999.
[164] T. Okabe, Y. Jin, and B. Sendhoff, "A critical survey of performance indices for multi-objective optimisation," in *Evolutionary Computation, 2003. CEC '03. The 2003 Congress on*, 2003, pp. 878-885 Vol.2.
[165] M. Varadarajan and K. S. Swarup, "Solving multi-objective optimal power flow using differential evolution," *Generation, Transmission & Distribution, IET,* vol. 2, pp. 720-730, 2008.
[166] S. Jeyadevi, S. Baskar, C. K. Babulal, and M. Willjuice Iruthayarajan, "Solving multiobjective optimal reactive power dispatch using modified NSGA-II," *International Journal of Electrical Power & Energy Systems,* vol. 33, pp. 219-228, 2// 2011.
[167] L. Yan-Fu, N. Pedroni, and E. Zio, "A Memetic Evolutionary Multi-Objective Optimization Method for Environmental Power Unit Commitment," *Power Systems, IEEE Transactions on,* vol. 28, pp. 2660-2669, 2013.
[168] I. Das and J. E. Dennis, "A closer look at drawbacks of minimizing weighted sums of objectives for Pareto set generation in multicriteria optimization problems," *Structural optimization,* vol. 14, pp. 63-69, 1997/08/01 1997.

Appendix A Case Study Network Data

Appendix A-1 Network Data of IEEE 33 busbar network

The diagram of IEEE 33 busbar network is shown in Fig. A - 1.

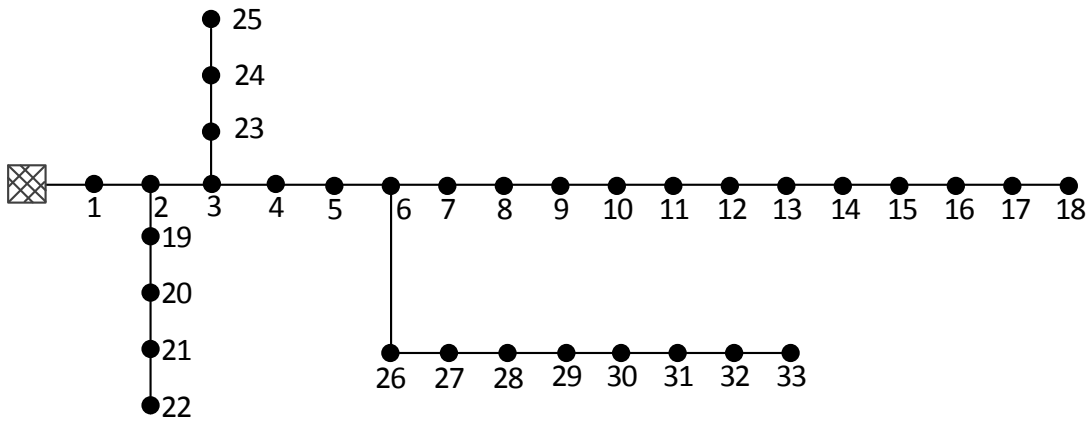

Fig. A - 1 Diagram of IEEE 33 Busbar Network

The network load and branch impedance data are listed in Table A - 1 and Table A - 2.

Table A - 1 Network Load Data of IEEE 33 Busbar Network

Busbar	P, MW	Q, MVAr	Busbar	P, MW	Q, MVAr
1	0.000	0.000	18	0.090	0.040
2	0.100	0.060	19	0.090	0.040
3	0.090	0.040	20	0.090	0.040
4	0.120	0.080	21	0.090	0.040
5	0.060	0.030	22	0.090	0.040
6	0.060	0.020	23	0.090	0.050
7	0.200	0.100	24	0.420	0.200
8	0.200	0.100	25	0.420	0.200
9	0.060	0.020	26	0.060	0.025
10	0.060	0.020	27	0.060	0.025
11	0.045	0.030	28	0.060	0.020
12	0.060	0.035	29	0.120	0.070
13	0.060	0.035	30	0.200	0.600
14	0.120	0.080	31	0.150	0.070
15	0.060	0.010	32	0.210	0.100
16	0.060	0.020	33	0.060	0.040
17	0.060	0.020			

Table A - 2 Branch data of IEEE 33 Busbar Network

Branch No.	Starting busbar	Ending busbar	R(Ω)	X(Ω)	R(pu)	X(pu)
1	1	2	0.0922	0.047	0.0575	0.0293
2	2	3	0.493	0.2511	0.3076	0.1567
3	3	4	0.366	0.1864	0.2284	0.1163
4	4	5	0.3811	0.1941	0.2378	0.1211
5	5	6	0.819	0.707	0.5110	0.4411
6	6	7	0.1872	0.6188	0.1168	0.3861
7	7	8	0.7114	0.2351	0.4439	0.1467
8	8	9	1.03	0.74	0.6426	0.4617
9	9	10	1.044	0.74	0.6514	0.4617
10	10	11	0.1966	0.065	0.1227	0.0406
11	11	12	0.3744	0.1238	0.2336	0.0772
12	12	13	1.468	1.155	0.9159	0.7206
13	13	14	0.5416	0.7129	0.3379	0.4448
14	14	15	0.591	0.526	0.3687	0.3282
15	15	16	0.7463	0.545	0.4656	0.3400
16	16	17	1.289	1.721	0.8042	1.0738
17	17	18	0.732	0.574	0.4567	0.3581
18	2	19	0.164	0.1565	0.1023	0.0976
19	19	20	1.5042	1.3554	0.9385	0.8457
20	20	21	0.4095	0.4784	0.2555	0.2985
21	21	22	0.7089	0.9373	0.4423	0.5848
22	3	23	0.4512	0.3083	0.2815	0.1924
23	23	24	0.898	0.7091	0.5603	0.4424
24	24	25	0.896	0.7011	0.5590	0.4374
25	6	26	0.203	0.1034	0.1267	0.0645
26	26	27	0.2842	0.1447	0.1773	0.0903
27	27	28	1.059	0.9337	0.6607	0.5826
28	28	29	0.8042	0.7006	0.5018	0.4371
29	29	30	0.5075	0.2585	0.3166	0.1613
30	30	31	0.9744	0.963	0.6080	0.6008
31	31	32	0.3105	0.3619	0.1937	0.2258
32	32	33	0.341	0.5302	0.2128	0.3308

The load flow results, including the busbar voltages and the power flow are shown in Table A - 3 and Table A - 4.

Table A - 3 IEEE 33 Busbar Network load flow results - voltage magnitudes

Busbar	|V|, pu	Busbar	|V|, pu	Busbar	|V|, pu
1	1.000	12	0.927	23	0.979
2	0.997	13	0.921	24	0.973
3	0.983	14	0.919	25	0.969
4	0.975	15	0.917	26	0.948
5	0.968	16	0.916	27	0.945
6	0.950	17	0.914	28	0.934
7	0.946	18	0.913	29	0.926
8	0.941	19	0.997	30	0.922
9	0.935	20	0.993	31	0.918
10	0.929	21	0.992	32	0.917
11	0.928	22	0.992	33	0.917

Table A - 4 IEEE 33 Busbar Network load flow results – real and reactive power flows

Branch No.	Starting busbar	Ending busbar	P, MW	Q, MVAr
1	1	2	3.9178	2.4351
2	2	3	3.4444	2.2078
3	3	4	2.3630	1.6842
4	4	5	2.2231	1.5941
5	5	6	2.1061	1.5215
6	6	7	1.0953	0.5279
7	7	8	0.8934	0.4216
8	8	9	0.6885	0.3200
9	9	10	0.6243	0.2970
10	10	11	0.5608	0.2744
11	11	12	0.5144	0.2440
12	12	13	0.4543	0.2090
13	13	14	0.3917	0.1719
14	14	15	0.2709	0.0909
15	15	16	0.2106	0.0806
16	16	17	0.1503	0.0604
17	17	18	0.0901	0.0400
18	2	19	0.3611	0.1611
19	19	20	0.2701	0.1202
20	20	21	0.1801	0.0802
21	21	22	0.0900	0.0401
22	3	23	0.9396	0.4572
23	23	24	0.8464	0.4051
24	24	25	0.4213	0.2010
25	6	26	0.9509	0.9736

26	26	27	0.8849	0.9456
27	27	28	0.8249	0.9206
28	28	29	0.7536	0.8906
29	29	30	0.6258	0.8138
30	30	31	0.4202	0.2103
31	31	32	0.2700	0.1400
32	32	33	0.0600	0.0400

Appendix A-2 Network Data of IEEE 69 busbar network

The diagram of IEEE 69 busbar network is shown in Fig. A - 2.

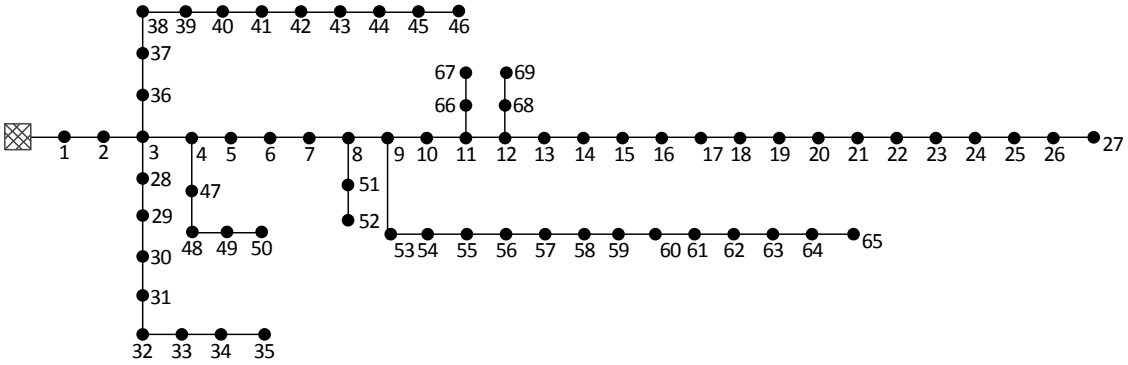

Fig. A - 2 Diagram of IEEE 69 Busbar Network

The network load and branch impedance data are listed in Table A - 5 and Table A - 6.

Table A - 5 Network Load Data of IEEE 69 Busbar Network

Busbar	P, MW	Q, MVAr	Busbar	P, MW	Q, MVAr
1	0	0	36	0.026	0.01855
2	0	0	37	0.026	0.01855
3	0	0	38	0	0
4	0	0	39	0.024	0.017
5	0	0	40	0.024	0.017
6	0.0026	0.0022	41	0.0012	0.001
7	0.0404	0.03	42	0	0
8	0.075	0.054	43	0.006	0.0043
9	0.03	0.022	44	0	0
10	0.028	0.019	45	0.03922	0.0263
11	0.145	0.104	46	0.03922	0.0263
12	0.145	0.104	47	0	0
13	0.008	0.0055	48	0.079	0.0564
14	0.008	0.0055	49	0.3847	0.2745
15	0	0	50	0.384	0.2745
16	0.0455	0.03	51	0.0405	0.0283
17	0.06	0.035	52	0.0036	0.0027
18	0.06	0.035	53	0.00435	0.0035
19	0	0	54	0.0264	0.019
20	0.001	0.0006	55	0.024	0.0172
21	0.114	0.081	56	0	0
22	0.0053	0.0035	57	0	0
23	0	0	58	0	0
24	0.028	0.02	59	0.1	0.072
25	0	0	60	0	0
26	0.014	0.01	61	1.244	0.888
27	0.014	0.01	62	0.032	0.023

28	0.026	0.0186	63	0	0
29	0.026	0.0186	64	0.227	0.162
30	0	0	65	0.059	0.042
31	0	0	66	0.018	0.013
32	0	0	67	0.018	0.013
33	0.014	0.01	68	0.028	0.02
34	0.0195	0.014	69	0.028	0.02
35	0.006	0.004	36	0.026	0.01855

Table A - 6 Branch data of IEEE 69 Busbar Network

Branch No.	Starting busbar	Ending busbar	R(Ω)	X(Ω)	R(pu)	X(pu)
1	1	2	0.0005	0.0012	0.0003	0.0007
2	2	3	0.0005	0.0012	0.0003	0.0007
3	3	4	0.0015	0.0036	0.0009	0.0022
4	4	5	0.0251	0.0294	0.0157	0.0183
5	5	6	0.366	0.1864	0.2284	0.1163
6	6	7	0.3811	0.1941	0.2378	0.1211
7	7	8	0.0922	0.047	0.0575	0.0293
8	8	9	0.0493	0.0251	0.0308	0.0157
9	9	10	0.819	0.2707	0.5110	0.1689
10	10	11	0.1872	0.0691	0.1168	0.0431
11	11	12	0.7114	0.2351	0.4439	0.1467
12	12	13	1.03	0.34	0.6426	0.2121
13	13	14	1.044	0.345	0.6514	0.2153
14	14	15	1.058	0.3496	0.6601	0.2181
15	15	16	0.1966	0.065	0.1227	0.0406
16	16	17	0.3744	0.1238	0.2336	0.0772
17	17	18	0.0047	0.0016	0.0029	0.0010
18	18	19	0.3276	0.1083	0.2044	0.0676
19	19	20	0.2106	0.069	0.1314	0.0431
20	20	21	0.3416	0.1129	0.2131	0.0704
21	21	22	0.014	0.0046	0.0087	0.0029
22	22	23	0.1591	0.0526	0.0993	0.0328
23	23	24	0.3463	0.1145	0.2161	0.0714
24	24	25	0.7488	0.2745	0.4672	0.1713
25	25	26	0.3089	0.1021	0.1927	0.0637
26	26	27	0.1732	0.0572	0.1081	0.0357
27	3	28	0.0044	0.0108	0.0027	0.0067
28	28	29	0.064	0.1565	0.0399	0.0976
29	29	30	0.3978	0.1315	0.2482	0.0820
30	30	31	0.0702	0.0232	0.0438	0.0145
31	31	32	0.351	0.116	0.2190	0.0724
32	32	33	0.839	0.2816	0.5235	0.1757
33	33	34	1.708	0.5646	1.0657	0.3523
34	34	35	1.474	0.4673	0.9197	0.2916

35	3	36	0.0044	0.0108	0.0027	0.0067
36	36	37	0.064	0.1565	0.0399	0.0976
37	37	38	0.1053	0.123	0.0657	0.0767
38	38	39	0.0304	0.0355	0.0190	0.0221
39	39	40	0.0018	0.0021	0.0011	0.0013
40	40	41	0.7283	0.8509	0.4544	0.5309
41	41	42	0.31	0.3623	0.1934	0.2260
42	42	43	0.041	0.0478	0.0256	0.0298
43	43	44	0.0092	0.0116	0.0057	0.0072
44	44	45	0.1089	0.1373	0.0679	0.0857
45	45	46	0.0009	0.0012	0.0006	0.0007
46	4	47	0.0034	0.0084	0.0021	0.0052
47	47	48	0.0851	0.2083	0.0531	0.1300
48	48	49	0.2898	0.7091	0.1808	0.4424
49	49	50	0.0822	0.2011	0.0513	0.1255
50	8	51	0.0928	0.0473	0.0579	0.0295
51	51	52	0.3319	0.1114	0.2071	0.0695
52	9	53	0.174	0.0886	0.1086	0.0553
53	53	54	0.203	0.1034	0.1267	0.0645
54	54	55	0.2842	0.1447	0.1773	0.0903
55	55	56	0.2813	0.1433	0.1755	0.0894
56	56	57	1.59	0.5337	0.9920	0.3330
57	57	58	0.7837	0.263	0.4890	0.1641
58	58	59	0.3042	0.1006	0.1898	0.0628
59	59	60	0.3861	0.1172	0.2409	0.0731
60	60	61	0.5075	0.2585	0.3166	0.1613
61	61	62	0.0974	0.0496	0.0608	0.0309
62	62	63	0.145	0.0738	0.0905	0.0460
63	63	64	0.7105	0.3619	0.4433	0.2258
64	64	65	1.041	0.5302	0.6495	0.3308
65	11	66	0.2012	0.0611	0.1255	0.0381
66	66	67	0.0047	0.0014	0.0029	0.0009
67	12	68	0.7394	0.2444	0.4613	0.1525
68	68	69	0.0047	0.0016	0.0029	0.0010

The load flow results, including the busbar voltages and the power flow are shown in Table A - 7 and Table A - 8.

Table A - 7 IEEE 69 Busbar Network load flow results - voltage magnitudes

Busbar	|V|, pu	Busbar	|V|, pu	Busbar	|V|, pu
1	1.000	24	0.957	47	1.000
2	1.000	25	0.956	48	0.999
3	1.000	26	0.956	49	0.995
4	1.000	27	0.956	50	0.994
5	0.999	28	1.000	51	0.979
6	0.990	29	1.000	52	0.979

7	0.981	30	1.000	53	0.975
8	0.979	31	1.000	54	0.971
9	0.977	32	1.000	55	0.967
10	0.972	33	0.999	56	0.963
11	0.971	34	0.999	57	0.940
12	0.968	35	0.999	58	0.929
13	0.965	36	1.000	59	0.925
14	0.962	37	1.000	60	0.920
15	0.959	38	1.000	61	0.912
16	0.959	39	1.000	62	0.912
17	0.958	40	1.000	63	0.912
18	0.958	41	0.999	64	0.910
19	0.958	42	0.999	65	0.909
20	0.957	43	0.999	66	0.971
21	0.957	44	0.999	67	0.971
22	0.957	45	0.998	68	0.968
23	0.957	46	0.998	69	0.968

Table A - 8 IEEE 69 Busbar Network load flow results – real and reactive power flows

Branch No.	Starting busbar	Ending busbar	P, MW	Q, MVAr
1	1	2	4.0266	2.7968
2	2	3	4.0265	2.7966
3	3	4	3.7493	2.6021
4	4	5	2.8988	1.9904
5	5	6	2.8970	1.9882
6	6	7	2.8661	1.9716
7	7	8	2.7964	1.9266
8	8	9	2.6705	1.8381
9	9	10	0.7804	0.5333
10	10	11	0.7476	0.5127
11	11	12	0.5656	0.3824
12	12	13	0.3624	0.2376
13	13	14	0.3531	0.2317
14	14	15	0.3439	0.2258
15	15	16	0.3427	0.2254
16	16	17	0.2969	0.1953
17	17	18	0.2375	0.1602
18	18	19	0.1766	0.1252
19	19	20	0.1765	0.1252
20	20	21	0.1754	0.1245
21	21	22	0.0612	0.0435
22	22	23	0.0561	0.0400
23	23	24	0.0560	0.0400
24	24	25	0.0280	0.0200
25	25	26	0.0280	0.0200

26	26	27	0.0140	0.0100
27	3	28	0.0915	0.0652
28	28	29	0.0655	0.0466
29	29	30	0.0395	0.0280
30	30	31	0.0395	0.0280
31	31	32	0.0396	0.0280
32	32	33	0.0395	0.0280
33	33	34	0.0255	0.0180
34	34	35	0.0060	0.0040
35	3	36	0.1856	0.1292
36	36	37	0.1598	0.1106
37	37	38	0.1337	0.0920
38	38	39	0.1338	0.0920
39	39	40	0.1101	0.0750
40	40	41	0.0857	0.0580
41	41	42	0.0845	0.0569
42	42	43	0.0845	0.0569
43	43	44	0.0787	0.0526
44	44	45	0.0784	0.0526
45	45	46	0.0393	0.0263
46	4	47	0.8501	0.6112
47	47	48	0.8500	0.6111
48	48	49	0.7704	0.5533
49	49	50	0.3841	0.2748
50	8	51	0.0442	0.0310
51	51	52	0.0036	0.0027
52	9	53	1.8566	1.2811
53	53	54	1.8465	1.2747
54	54	55	1.8134	1.2522
55	55	56	1.7802	1.2304
56	56	57	1.7716	1.2259
57	57	58	1.7219	1.2092
58	58	59	1.6975	1.2010
59	59	60	1.5880	1.1259
60	60	61	1.5772	1.1226
61	61	62	0.3189	0.2275
62	62	63	0.2869	0.2044
63	63	64	0.2867	0.2044
64	64	65	0.0590	0.0420
65	11	66	0.0360	0.0260
66	66	67	0.0182	0.0130
67	12	68	0.0560	0.0400
68	68	69	0.0275	0.0200

Appendix B Test Results for Single-objective Voltage Optimisation

Appendix B-1: Maximum iteration number of SOCS – Conventional Test Cases

The maximum iteration number determined for SOCS, regarding different case study networks and optimisation objectives are shown in Table B - 1.

Table B - 1 Maximum iteration number determined for SOCS

Optimisation Objective	Case study network	Maximum iteration number determined for SOCS
Network loss minimisation	Network A	100
	Network B	40
	Network C	151
Voltage deviation minimisation	Network A	85
	Network B	87
	Network C	108
Switching number minimisation	Network A	62
	Network B	53
	Network C	109

Appendix B-2: Test results for network loss minimisation – Conventional Test Cases

Test results for network loss minimisation are shown in Table B - 2, Table B - 3 and Table B - 4.

Table B - 2 Network loss minimisation – Conventional test cases for Network A

Load scale index	Network loss (MW)			Computation time (s)	
	ODCDM	SOCS	difference	ODCDM	SOCS
0.25	0.0071	0.0071	0.0%	1.59	47.72
0.3	0.0101	0.0101	0.0%	1.65	47.09
0.35	0.0137	0.0137	0.0%	1.99	47.10
0.4	0.0180	0.0180	0.0%	2.16	47.07
0.45	0.0228	0.0228	0.0%	2.14	47.17
0.5	0.0284	0.0283	0.0%	2.19	47.36
0.55	0.0344	0.0344	0.0%	2.36	47.59
0.6	0.0411	0.0411	0.0%	2.69	47.82
0.65	0.0485	0.0485	0.0%	2.85	48.13
0.7	0.0564	0.0564	0.0%	2.84	48.33
0.75	0.0650	0.0650	0.1%	3.03	48.19
0.8	0.0742	0.0742	0.0%	3.34	48.23
0.85	0.0841	0.0841	0.0%	3.50	48.36
0.9	0.0947	0.0947	0.0%	3.67	48.34
0.95	0.1059	0.1059	0.0%	3.85	48.60
1	0.1179	0.1179	0.0%	4.01	48.77

Table B - 3 Network loss minimisation – Conventional test cases for Network B

Load scale index	Network loss (MW)			Computation time (s)	
	ODCDM	SOCS	difference	ODCDM	SOCS
0.25	0.0072	0.0072	0.0%	1.27	20.16
0.3	0.0103	0.0103	0.0%	1.47	20.03
0.35	0.0141	0.0141	0.0%	1.56	19.98
0.4	0.0186	0.0186	0.0%	1.78	20.12
0.45	0.0238	0.0238	0.0%	1.90	20.26
0.5	0.0297	0.0297	0.0%	1.99	20.39
0.55	0.0364	0.0364	0.0%	2.12	20.43
0.6	0.0438	0.0438	0.0%	2.24	20.77
0.65	0.0521	0.0521	0.0%	2.38	21.11
0.7	0.0612	0.0612	0.0%	2.55	21.34
0.75	0.0712	0.0712	0.0%	2.60	21.60
0.8	0.0820	0.0820	0.0%	2.75	21.20
0.85	0.0937	0.0937	0.0%	2.94	22.48
0.9	0.1063	0.1063	0.0%	3.12	22.42
0.95	0.1198	0.1198	0.0%	3.12	22.68
1	0.1343	0.1343	0.0%	3.28	22.75

Table B - 4 Network loss minimisation – Conventional test cases for Network C

Load scale index	Network loss (MW)			Computation time (s)	
	ODCDM	SOCS	difference	ODCDM	SOCS
0.25	0.0079	0.0079	0.0%	1.47	81.65
0.3	0.0112	0.0112	0.0%	1.97	81.89
0.35	0.0155	0.0154	0.3%	1.95	82.23
0.4	0.0206	0.0206	0.0%	2.03	82.47
0.45	0.0258	0.0256	0.7%	2.24	82.61
0.5	0.0315	0.0315	0.0%	2.25	82.85
0.55	0.0382	0.0382	0.0%	2.27	83.67
0.6	0.0459	0.0458	0.4%	2.51	84.31
0.65	0.0540	0.0540	0.0%	2.54	84.56
0.7	0.0629	0.0625	0.7%	2.53	83.88
0.75	0.0720	0.0719	0.2%	2.81	84.20
0.8	0.0821	0.0821	0.0%	2.80	84.80
0.85	0.0934	0.0934	0.0%	3.05	84.87
0.9	0.1048	0.1048	0.0%	3.34	85.57
0.95	0.1172	0.1172	0.0%	3.36	85.86
1	0.1309	0.1306	0.2%	3.63	86.12

The computation time for network loss minimisation profile studies are shown in Table B - 5.

Table B - 5 Computation time – Network loss minimisation profile study

Time	Computation time (s)					
	Network A		Network B		Network C	
	ODCDM	SOCS	ODCDM	SOCS	ODCDM	SOCS
00:00	2.25	51.18	1.76	51.18	2.33	84.63
01:00	1.76	51.77	1.48	51.77	2.13	83.25
02:00	1.53	52.12	1.38	52.12	1.51	82.24
03:00	1.54	52.15	1.22	52.15	1.48	82.35
04:00	1.55	51.93	1.24	51.93	1.50	82.18
05:00	1.54	52.12	1.23	52.12	1.49	82.31
06:00	1.69	52.28	1.34	52.28	1.75	82.32
07:00	2.42	52.37	1.70	52.37	2.01	84.84
08:00	2.59	51.76	2.13	51.76	2.29	84.62
09:00	2.93	51.43	2.41	51.43	2.57	85.43
10:00	2.96	51.59	2.38	51.59	2.57	85.50
11:00	2.93	52.04	2.25	52.04	2.58	87.03
12:00	2.94	51.70	2.35	51.70	2.56	85.41
13:00	2.93	51.79	2.35	51.79	2.58	85.92
14:00	2.94	51.64	2.25	51.64	2.56	85.41
15:00	2.93	51.56	2.25	51.56	2.58	85.35
16:00	3.13	51.83	2.48	51.83	2.60	85.83
17:00	4.01	52.26	2.93	52.26	3.42	87.89

18:00	4.38	52.48	3.04	52.48	3.64	89.97
19:00	4.20	52.27	2.95	52.27	3.39	90.24
20:00	3.81	51.94	2.81	51.94	3.37	87.22
21:00	3.63	51.75	2.70	51.75	3.10	86.60
22:00	3.30	51.68	2.46	51.68	2.83	85.54
23:00	2.75	51.39	2.24	51.39	2.51	84.56

Appendix B-3: Test results for voltage deviation minimisation – Conventional Test Cases

Test results for voltage deviation minimisation are shown in Table B - 6, Table B - 7 and Table B - 8.

Table B - 6 Voltage deviation minimisation – Conventional test cases for Network A

Load scale index	Voltage deviation (pu)			Computation time (s)	
	ODCDM	SOCS	Difference	ODCDM	SOCS
0.25	0.13	0.02	84.8%	0.96	41.84
0.3	0.12	0.02	80.7%	1.56	41.38
0.35	0.11	0.03	74.8%	1.83	42.28
0.4	0.28	0.04	86.4%	0.85	41.55
0.45	0.27	0.05	81.4%	1.18	41.51
0.5	0.26	0.06	78.5%	1.53	41.50
0.55	0.25	0.07	70.9%	1.67	41.64
0.6	0.24	0.09	64.9%	2.23	41.96
0.65	0.22	0.08	62.4%	3.02	41.99
0.7	0.42	0.08	79.7%	1.45	42.11
0.75	0.41	0.08	79.3%	1.75	42.21
0.8	0.38	0.11	72.3%	2.56	42.10
0.85	0.37	0.17	52.8%	3.27	42.01
0.9	0.36	0.20	43.6%	3.23	42.10
0.95	0.35	0.20	41.6%	3.74	42.15
1	0.35	0.24	29.9%	4.22	42.08

Table B - 7 Voltage deviation minimisation – Conventional test cases for Network B

Load scale index	Voltage deviation (pu)			Computation time (s)	
	ODCDM	SOCS	Difference	ODCDM	SOCS
0.25	0.13	0.08	40.4%	0.76	45.68
0.3	0.13	0.11	16.3%	1.01	45.81
0.35	0.14	0.12	13.6%	1.34	46.02
0.4	0.28	0.13	55.0%	0.66	45.54
0.45	0.27	0.13	50.8%	1.08	46.18
0.5	0.27	0.15	43.8%	1.61	44.43
0.55	0.26	0.22	17.6%	2.31	44.04
0.6	0.27	0.27	0.0%	2.62	44.38
0.65	0.42	0.27	34.6%	1.29	44.98
0.7	0.41	0.29	30.1%	1.75	45.20
0.75	0.41	0.34	18.4%	2.35	45.88
0.8	0.42	0.40	3.1%	2.49	47.43
0.85	0.42	0.42	0.0%	3.29	47.17
0.9	0.44	0.44	0.0%	3.29	48.24
0.95	0.48	0.48	0.0%	3.29	47.63
1	0.57	0.53	7.6%	2.52	47.39

Table B - 8 Voltage deviation minimisation – Conventional test cases for Network C

Load scale index	Voltage deviation (pu)			Computation time (s)	
	ODCDM	SOCS	Difference	ODCDM	SOCS
0.25	0.05	0.03	46.1%	2.53	61.45
0.3	0.04	0.03	23.5%	3.67	64.39
0.35	0.05	0.04	20.9%	3.45	62.34
0.4	0.08	0.06	22.1%	4.35	64.76
0.45	0.10	0.09	8.4%	4.68	66.88
0.5	0.13	0.12	10.4%	4.90	65.62
0.55	0.49	0.15	69.7%	3.03	65.97
0.6	0.54	0.18	66.0%	2.45	66.27
0.65	0.53	0.25	53.5%	2.73	65.67
0.7	0.55	0.34	39.3%	3.04	65.97
0.75	0.58	0.43	26.2%	3.34	66.10
0.8	0.61	0.52	14.7%	3.90	65.90
0.85	0.64	0.64	0.3%	4.19	66.70
0.9	0.67	0.67	0.0%	5.43	67.20
0.95	0.71	0.71	0.0%	5.65	66.66
1	0.76	0.76	0.0%	5.36	65.48

The computation time for network loss minimisation profile studies are shown in Table B - 9.

Table B - 9 Computation time – Voltage deviation minimisation profile study

Time	Computation time (s)					
	Network A		Network B		Network C	
	ODCDM	SOCS	ODCDM	SOCS	ODCDM	SOCS
00:00	1.06	44.46	0.87	34.39	4.32	67.24
01:00	1.24	44.66	1.10	34.21	3.25	66.83
02:00	0.70	44.61	0.86	34.35	2.67	65.94
03:00	0.72	44.96	0.63	34.31	2.39	65.88
04:00	0.71	44.61	0.62	34.37	2.94	66.43
05:00	0.69	44.63	0.74	34.36	2.37	66.16
06:00	1.07	44.61	0.93	34.35	2.93	67.04
07:00	0.69	44.85	0.52	34.19	4.25	68.07
08:00	1.78	45.07	2.02	34.53	5.32	67.69
09:00	1.06	45.10	0.86	34.55	2.39	67.84
10:00	3.03	44.26	2.48	34.63	2.35	67.49
11:00	2.64	44.43	0.88	34.52	2.29	67.70
12:00	3.03	44.21	2.61	34.64	2.30	67.72
13:00	2.69	44.42	0.99	34.74	2.57	67.43
14:00	3.03	44.17	2.50	34.68	2.29	67.47
15:00	2.67	44.33	0.86	34.60	2.29	67.65
16:00	1.61	44.71	1.75	34.94	2.82	67.41
17:00	3.79	44.53	3.33	35.48	5.25	68.79

18:00	4.63	44.60	2.54	35.54	5.30	70.02
19:00	4.26	44.72	3.35	35.47	5.30	69.60
20:00	3.38	44.70	3.34	35.37	4.98	69.50
21:00	2.32	44.63	2.64	35.00	3.62	67.84
22:00	1.94	44.60	1.99	34.89	3.11	67.67
23:00	1.93	44.27	2.84	34.58	2.04	67.87

Appendix B-4 Test results for switching operation minimisation – Conventional Test Cases

Test results for switching operation minimisation are shown in Table B - 10, Table B - 11 and Table B - 12.

Table B - 10 Switching operation minimisation – Conventional test cases for Network A

Load scale index	Switching number			Computation time (s)	
	ODCDM	SOCS	Difference	ODCDM	SOCS
0.25	0	0	0.0%	0.19	16.52
0.3	0	0	0.0%	0.22	13.51
0.35	0	0	0.0%	0.17	15.06
0.4	0	0	0.0%	0.18	17.64
0.45	0	0	0.0%	0.17	30.71
0.5	0	0	0.0%	0.20	22.82
0.55	0	0	0.0%	0.18	14.81
0.6	0	0	0.0%	0.17	16.92
0.65	0	0	0.0%	0.20	15.45
0.7	0	0	0.0%	0.18	17.54
0.75	1	1	0.0%	0.35	31.79
0.8	1	1	0.0%	0.35	31.86
0.85	1	1	0.0%	0.36	31.74
0.9	2	2	0.0%	0.56	31.64
0.95	2	2	0.0%	0.53	31.82
1	2	2	0.0%	0.55	31.87

Table B - 11 Switching operation minimisation – Conventional test cases for Network B

Load scale index	Switching number			Computation time (s)	
	ODCDM	SOCS	Difference	ODCDM	SOCS
0.25	0	0	0.0%	0.10	5.03
0.3	0	0	0.0%	0.10	7.46
0.35	0	0	0.0%	0.10	20.92
0.4	0	0	0.0%	0.10	10.40
0.45	0	0	0.0%	0.11	9.03
0.5	0	0	0.0%	0.10	9.03
0.55	0	0	0.0%	0.11	6.13
0.6	0	0	0.0%	0.10	12.06
0.65	0	0	0.0%	0.10	7.66
0.7	0	0	0.0%	0.11	9.71
0.75	1	1	0.0%	0.21	26.68
0.8	1	1	0.0%	0.21	26.94
0.85	1	1	0.0%	0.21	27.15
0.9	2	2	0.0%	0.31	27.14
0.95	2	2	0.0%	0.32	29.57
1	2	2	0.0%	0.32	31.70

Table B - 12 Switching operation minimisation – Conventional test cases for Network C

Load scale index	Switching number			Computation time (s)	
	ODCDM	SOCS	Difference	ODCDM	SOCS
0.25	0	0	0.0%	0.26	35.61
0.3	0	0	0.0%	0.25	39.45
0.35	0	0	0.0%	0.27	32.73
0.4	0	0	0.0%	0.26	26.93
0.45	0	0	0.0%	0.26	30.11
0.5	0	0	0.0%	0.27	18.45
0.55	0	0	0.0%	0.26	50.09
0.6	0	0	0.0%	0.25	29.04
0.65	0	0	0.0%	0.26	32.08
0.7	1	1	0.0%	0.51	62.35
0.75	1	1	0.0%	0.52	62.63
0.8	1	1	0.0%	0.52	62.74
0.85	2	2	0.0%	0.77	62.86
0.9	2	2	0.0%	0.79	63.34
0.95	2	2	0.0%	0.80	63.61
1	3	3	0.0%	1.09	63.90

The computation time for network loss minimisation profile studies are shown in Table B - 13.

Table B - 13 Computation time – Switching operation minimisation profile study

Time	Computation time (s)					
	Network A		Network B		Network C	
	ODCDM	SOCS	ODCDM	SOCS	ODCDM	SOCS
00:00	0.11	16.52	0.10	9.44	0.25	33.12
01:00	0.11	13.51	0.10	2.17	0.25	43.78
02:00	0.11	15.06	0.10	6.01	0.27	23.72
03:00	0.11	17.64	0.10	13.19	0.25	25.37
04:00	0.12	30.71	0.10	13.28	0.25	30.10
05:00	0.11	22.82	0.10	9.96	0.25	40.06
06:00	0.11	14.81	0.10	13.41	0.25	28.57
07:00	0.13	16.92	0.12	14.46	0.25	39.16
08:00	0.12	15.45	0.10	8.70	0.25	34.45
09:00	0.11	17.54	0.10	13.72	0.25	41.96
10:00	0.11	31.79	0.10	18.84	0.25	30.61
11:00	0.11	31.86	0.11	19.42	0.25	43.07
12:00	0.11	31.74	0.10	6.82	0.27	34.62
13:00	0.11	31.64	0.10	9.87	0.25	46.59
14:00	0.12	31.82	0.10	7.83	0.27	38.00
15:00	0.11	31.87	0.10	14.39	0.25	35.69
16:00	0.11	16.52	0.11	11.43	0.53	62.90
17:00	0.37	31.96	0.34	27.35	0.79	64.06
18:00	0.11	31.70	0.11	14.76	0.26	64.41

19:00	0.11	31.52	0.11	17.25	0.26	35.70
20:00	0.11	22.75	0.13	12.06	0.26	35.38
21:00	0.12	16.33	0.10	9.47	0.25	40.46
22:00	0.11	16.46	0.10	14.02	0.25	12.45
23:00	0.11	17.53	0.10	12.11	0.27	22.69

Appendix B-5: Impact of step size used for continuous variable discretization – Future Test Cases

The impact of the step size selection on the performance of ODCDM is illustrated with an initial test case. Network D, with the maximum generation and minimum load condition, is used in this test case. DG curtailment minimisation is used as the optimisation objective. Real and reactive powers of the DG are discretised with different step sizes. The test results are shown in Table B - 14.

Table B - 14 Impact of step size used for continuous variable discretization for ODCDM

Step size used for continuous control variable discretization (MW/MVAr)	0.001	0.01	0.02	0.03	0.04	0.05
DG curtailment (MW)	0.311	0.32	0.34	0.36	0.4	0.35
Computation time (s)	338.77	34.88	18.03	12.44	9.72	7.85

It can be seen from Table B - 14. that smaller step sizes result in greater computation time and generally reduced the DG curtailment. Sometimes ODCDM does not achieve a better result when a smaller step size is selected. For example, the result achieved when the step size is selected as 0.05 MW/MVAr is better than that achieved when the step size is selected as 0.04 MW/MVAr. The minimum step size evaluated in this study is 0.01 MW/MVAr which results in a computation time that is still much shorter than that required for SOCS.

Appendix B-6 Maximum iteration number of SOCS – Future Test Cases

The maximum iteration number determined for SOCS, regarding different case study networks and optimisation objectives are shown in Table B - 15 and Table B - 16.

Table B - 15 Maximum iteration number determined for SOCS - Network D

Optimisation Objective	Maximum iteration number
DG real power curtailment minimisation	741
DG reactive power utilization minimisation	60
Network Loss minimisation	95
Voltage deviation minimisation	162
Switching operation minimisation	110

Table B - 16 Maximum iteration number determined for SOCS - Network E

Optimisation Objective	Maximum iteration number
DG real power curtailment minimisation	425
DG reactive power utilization minimisation	138
Network Loss minimisation	262
Voltage deviation minimisation	290
Switching operation minimisation	145

Appendix B-7 Test results for Network D - Future Test Cases

Since the number of test cases is too large, sampled snapshot test results are shown here. Test results of these sampled test cases for different optimisation objectives are shown in Table B - 17, Table B - 18, Table B - 19, Table B - 20 and Table B - 21. For all the test cases, SOCS was able to find a feasible solution and the voltage violation number is always zero.

Table B - 17 Sampled test cases for network loss minimisation – snapshot test cases for Network D

Load scale factor	DG (MW)	Network loss (MW)			Voltage violation	Computation time (s)	
		ODCDM	SOCS	Reduction	ODCDM	ODCDM	SOCS
0.25	0.25	0.0044	0.0044	0.0%	0	5.08	73.70
0.25	2	0.0044	0.0044	0.0%	0	52.91	74.21
0.25	4	0.0045	0.0044	1.0%	0	188.44	76.45
0.3	0.25	0.0064	0.0064	0.1%	0	4.87	77.35
0.3	2	0.0064	0.0064	0.1%	0	48.77	63.89
0.3	4	0.0065	0.0064	1.9%	0	171.05	64.77
0.35	0.25	0.0087	0.0087	0.0%	0	3.61	63.63
0.35	2	0.0087	0.0087	0.3%	0	47.93	63.94
0.35	4	0.0088	0.0087	1.0%	0	171.42	65.59
0.4	0.25	0.0116	0.0116	0.0%	0	3.88	65.77
0.4	2	0.0114	0.0114	0.0%	0	49.03	66.65
0.4	4	0.0116	0.0115	0.9%	0	176.32	67.27
0.45	0.25	0.0151	0.0151	0.0%	0	4.60	66.14
0.45	2	0.0147	0.0146	0.1%	0	46.33	64.53
0.45	4	0.0148	0.0146	0.9%	0	177.93	65.44
0.5	0.25	0.0193	0.0193	0.0%	0	5.08	67.20
0.5	2	0.0183	0.0183	0.1%	0	48.29	67.29
0.5	4	0.0184	0.0183	0.6%	0	174.15	67.18
0.55	0.25	0.0242	0.0242	0.0%	0	5.13	67.71
0.55	2	0.0225	0.0224	0.0%	0	47.00	68.54
0.55	4	0.9692	0.0226	97.7%	2	36.69	67.80
0.6	0.25	0.0297	0.0297	0.0%	0	5.71	66.63
0.6	2	0.0271	0.0271	0.1%	0	45.98	66.67
0.6	4	0.9167	0.0271	97.0%	2	41.59	67.46
0.65	0.25	0.0360	0.0360	0.0%	0	5.61	66.84
0.65	2	0.0324	0.0323	0.2%	0	42.79	64.68
0.65	4	0.8987	0.0324	96.4%	4	40.05	65.17
0.7	0.25	0.0431	0.0431	0.0%	0	5.58	64.62
0.7	2	0.0381	0.0380	0.1%	0	45.88	77.02
0.7	4	0.5925	0.0381	93.6%	5	53.55	76.59
0.75	0.25	0.0509	0.0509	0.0%	0	6.11	77.31
0.75	2	0.0444	0.0443	0.1%	0	42.71	78.13
0.75	4	0.9120	0.0444	95.1%	3	45.31	77.07
0.8	0.25	0.0595	0.0595	0.0%	0	6.39	76.57

0.8	2	0.0512	0.0511	0.0%	0	42.77	76.66
0.8	4	0.8852	0.0512	94.2%	4	46.54	76.73
0.85	0.25	0.0689	0.0689	0.0%	0	7.01	76.55
0.85	2	0.0586	0.0585	0.1%	0	41.72	76.50
0.85	4	0.9677	0.0586	93.9%	2	38.53	77.74
0.9	0.25	0.0790	0.0790	0.0%	0	7.01	76.56
0.9	2	0.0665	0.0665	0.0%	0	40.24	75.84
0.9	4	0.8806	0.0665	92.5%	2	45.23	77.78
0.95	0.25	0.0900	0.0900	0.0%	0	6.98	77.06
0.95	2	0.0750	0.0750	0.0%	0	39.20	76.26
0.95	4	0.8758	0.0750	91.4%	4	49.08	83.00
1	0.25	0.1019	0.1019	0.0%	0	7.20	76.52
1	2	0.0842	0.0842	0.0%	0	38.33	76.64
1	4	0.0843	0.0842	0.0%	0	160.91	77.12
1.05	0.25	0.1146	0.1146	0.0%	0	14.23	85.84
1.05	2	0.0939	0.0940	0.0%	0	66.70	97.81
1.05	4	0.9183	0.0940	89.8%	2	42.65	68.74
1.1	0.25	0.1283	0.1283	0.0%	0	7.19	66.46
1.1	2	0.1043	0.1044	0.0%	0	67.92	102.08
1.1	4	0.8706	0.1044	88.0%	3	48.15	88.11

Table B - 18 Sampled test cases for voltage deviation minimisation – snapshot test cases for Network D

Load scale factor	DG (MW)	Voltage deviation (pu)			Voltage violation	Computation time (s)	
		ODCDM	SOCS	Reduction	ODCDM	ODCDM	SOCS
0.25	0.25	0.08	0.07	12.0%	0	4.16	83.60
0.25	2	0.07	0.07	7.0%	0	37.23	84.12
0.25	4	0.08	0.07	10.4%	0	70.93	86.36
0.3	0.25	0.12	0.11	15.1%	0	3.11	82.46
0.3	2	0.10	0.09	6.6%	0	35.92	81.99
0.3	4	0.10	0.10	5.8%	0	68.59	83.11
0.35	0.25	0.13	0.12	4.5%	0	2.19	80.46
0.35	2	0.13	0.12	2.6%	0	36.88	83.42
0.35	4	0.13	0.12	3.4%	0	71.31	85.52
0.4	0.25	0.13	0.12	6.2%	0	2.71	82.28
0.4	2	0.16	0.12	22.2%	0	35.28	83.49
0.4	4	0.16	0.13	19.9%	0	71.95	86.80
0.45	0.25	0.14	0.13	4.2%	0	4.21	82.62
0.45	2	0.20	0.13	33.3%	0	33.94	83.96
0.45	4	0.19	0.13	32.3%	0	70.96	85.99
0.5	0.25	0.15	0.14	5.9%	0	4.22	84.78
0.5	2	0.23	0.14	40.2%	0	30.44	83.00
0.5	4	0.23	0.14	39.5%	0	67.98	84.83
0.55	0.25	0.26	0.16	40.0%	0	2.40	82.84

0.55	2	0.27	0.15	42.8%	0	28.20	84.19
0.55	4	1.39	0.16	88.6%	2	22.26	85.17
0.6	0.25	0.26	0.18	30.7%	0	2.40	82.48
0.6	2	0.18	0.17	3.9%	0	33.93	83.98
0.6	4	1.37	0.17	87.3%	2	25.31	84.26
0.65	0.25	0.27	0.21	21.7%	0	2.69	82.99
0.65	2	0.20	0.20	3.1%	0	34.23	84.64
0.65	4	1.39	0.20	85.8%	4	25.79	85.24
0.7	0.25	0.27	0.24	10.3%	0	4.36	83.14
0.7	2	0.23	0.22	3.1%	0	32.46	83.68
0.7	4	1.40	0.22	84.2%	5	32.82	86.05
0.75	0.25	0.40	0.27	33.1%	0	2.41	83.85
0.75	2	0.26	0.25	2.2%	0	29.54	84.40
0.75	4	1.24	0.25	79.8%	3	27.66	86.21
0.8	0.25	0.40	0.28	30.7%	0	2.72	84.03
0.8	2	0.29	0.28	4.4%	0	28.43	84.14
0.8	4	1.26	0.28	78.0%	4	28.39	86.47
0.85	0.25	0.40	0.29	26.8%	0	3.20	89.06
0.85	2	0.32	0.29	10.3%	0	27.26	83.92
0.85	4	1.12	0.29	74.1%	2	23.60	85.54
0.9	0.25	0.41	0.32	21.2%	0	3.41	84.70
0.9	2	0.35	0.31	13.0%	0	22.64	84.75
0.9	4	1.10	0.31	72.3%	2	27.21	83.93
0.95	0.25	0.41	0.35	14.1%	0	3.92	83.04
0.95	2	0.38	0.33	13.9%	0	22.08	82.94
0.95	4	1.13	0.33	70.9%	4	27.99	83.42
1	0.25	0.55	0.41	25.4%	0	2.10	82.77
1	2	0.42	0.35	15.5%	0	20.37	83.02
1	4	0.41	0.35	13.3%	0	64.33	83.52
1.05	0.25	0.55	0.42	23.9%	0	3.21	91.65
1.05	2	0.45	0.38	15.9%	0	21.98	89.82
1.05	4	0.97	0.38	61.1%	2	25.70	85.76
1.1	0.25	0.55	0.43	21.7%	0	3.42	84.91
1.1	2	0.41	0.41	2.1%	0	25.44	89.20
1.1	4	0.99	0.41	58.9%	3	30.44	92.38

Table B - 19 Sampled test cases for switching operation minimisation – snapshot test cases for Network D

Load Scale factor	DG (MW)	Switching operation			Voltage violation	Computation time (s)	
		ODCDM	SOCS	Reduction	ODCDM	ODCDM	SOCS
0.25	0.25	0	0	0.0%	0	0.15	4.37
0.25	2	4	0	100.0%	0	0.81	13.86
0.25	4	4	0	100.0%	0	27.53	20.60
0.3	0.25	0	0	0.0%	0	0.15	9.40

0.3	2	4	0	100.0%	0	0.76	8.51
0.3	4	4	0	100.0%	0	26.24	7.32
0.35	0.25	0	0	0.0%	0	0.16	10.37
0.35	2	4	0	100.0%	0	0.76	8.03
0.35	4	4	0	100.0%	0	24.88	13.68
0.4	0.25	0	0	0.0%	0	0.17	15.90
0.4	2	3	0	100.0%	0	0.63	15.82
0.4	4	4	0	100.0%	0	23.63	24.60
0.45	0.25	0	0	0.0%	0	0.15	6.35
0.45	2	3	0	100.0%	0	0.61	15.24
0.45	4	4	0	100.0%	0	22.31	24.28
0.5	0.25	0	0	0.0%	0	0.15	20.05
0.5	2	3	0	100.0%	0	0.62	12.67
0.5	4	7	0	100.0%	0	22.36	11.05
0.55	0.25	0	0	0.0%	0	0.15	6.39
0.55	2	2	0	100.0%	0	0.63	10.65
0.55	4	10	0	100.0%	2	22.58	18.37
0.6	0.25	0	0	0.0%	0	0.15	8.12
0.6	2	2	0	100.0%	0	0.46	18.98
0.6	4	19	0	100.0%	2	25.31	13.66
0.65	0.25	0	0	0.0%	0	0.15	11.50
0.65	2	2	0	100.0%	0	0.46	14.43
0.65	4	22	0	100.0%	4	26.59	15.35
0.7	0.25	0	0	0.0%	0	0.17	13.69
0.7	2	2	0	100.0%	0	0.46	9.58
0.7	4	28	0	100.0%	5	32.94	15.97
0.75	0.25	0	0	0.0%	0	0.15	20.14
0.75	2	1	0	100.0%	0	0.31	11.23
0.75	4	18	0	100.0%	3	28.39	11.87
0.8	0.25	1	0	100.0%	0	0.32	9.10
0.8	2	1	0	100.0%	0	0.37	14.80
0.8	4	21	0	100.0%	4	28.39	18.11
0.85	0.25	1	1	0.0%	0	0.30	56.84
0.85	2	1	0	100.0%	0	0.33	10.12
0.85	4	9	0	100.0%	2	23.38	4.14
0.9	0.25	1	1	0.0%	0	0.31	57.06
0.9	2	0	0	0.0%	0	0.15	12.29
0.9	4	17	0	100.0%	2	26.78	32.02
0.95	0.25	1	1	0.0%	0	0.30	57.31
0.95	2	0	0	0.0%	0	0.15	23.30
0.95	4	20	0	100.0%	4	28.63	23.52
1	0.25	2	2	0.0%	0	0.46	57.25
1	2	0	0	0.0%	0	0.17	34.92
1	4	9	0	100.0%	0	27.76	41.62
1.05	0.25	2	2	0.0%	0	0.46	60.62
1.05	2	0	0	0.0%	0	0.16	50.24

1.05	4	15	1	93.3%	2	27.10	62.53
1.1	0.25	2	2	0.0%	0	0.47	60.84
1.1	2	1	1	0.0%	0	0.30	58.27
1.1	4	19	1	94.7%	3	28.81	58.53

Table B - 20 Sampled test cases for DG curtailment minimisation – snapshot test cases for Network D

Load scale factor	DG (MW)	DG P Curtailment (MW)			Voltage violation	Computation time (s)	
		ODCDM	SOCS	Reduction	ODCDM	ODCDM	SOCS
0.25	0.25	0.00	0.00	0.0%	0	0.20	0.73
0.25	2	0.00	0.00	0.0%	0	1.03	2.29
0.25	4	0.32	0.31	3.3%	0	36.67	403.60
0.3	0.25	0.00	0.00	0.0%	0	0.19	0.73
0.3	2	0.00	0.00	0.0%	0	1.04	3.26
0.3	4	0.24	0.23	3.7%	0	35.21	404.88
0.35	0.25	0.00	0.00	0.0%	0	0.20	3.45
0.35	2	0.00	0.00	0.0%	0	1.04	2.31
0.35	4	0.16	0.15	5.2%	0	31.91	397.08
0.4	0.25	0.00	0.00	0.0%	0	0.19	0.70
0.4	2	0.00	0.00	0.0%	0	0.78	2.64
0.4	4	0.08	0.07	10.7%	0	30.20	391.60
0.45	0.25	0.00	0.00	0.0%	0	0.19	0.72
0.45	2	0.00	0.00	0.0%	0	0.80	1.19
0.45	4	0.00	0.00	0.0%	0	28.58	72.59
0.5	0.25	0.00	0.00	0.0%	0	0.19	1.17
0.5	2	0.00	0.00	0.0%	0	0.81	0.72
0.5	4	0.00	0.00	0.0%	0	28.66	52.33
0.55	0.25	0.00	0.00	0.0%	0	0.20	0.73
0.55	2	0.00	0.00	0.0%	0	0.79	3.15
0.55	4	0.01	0.00	100.0%	2	28.58	108.79
0.6	0.25	0.00	0.00	0.0%	0	0.19	0.71
0.6	2	0.00	0.00	0.0%	0	0.61	6.03
0.6	4	0.04	0.01	75.1%	2	32.46	390.80
0.65	0.25	0.00	0.00	0.0%	0	0.19	0.71
0.65	2	0.00	0.00	0.0%	0	0.61	1.20
0.65	4	0.03	0.00	100.0%	4	33.09	65.42
0.7	0.25	0.00	0.00	0.0%	0	0.19	0.71
0.7	2	0.00	0.00	0.0%	0	0.59	0.72
0.7	4	0.61	0.00	100.0%	5	41.67	80.09
0.75	0.25	0.00	0.00	0.0%	0	0.19	0.71
0.75	2	0.00	0.00	0.0%	0	0.39	0.72
0.75	4	0.04	0.04	7.5%	3	35.45	390.67
0.8	0.25	0.00	0.00	0.0%	0	0.39	1.21
0.8	2	0.00	0.00	0.0%	0	0.41	1.71
0.8	4	0.05	0.00	100.0%	4	36.34	102.30

0.85	0.25	0.00	0.00	0.0%	0	0.39	1.22
0.85	2	0.00	0.00	0.0%	0	0.39	2.18
0.85	4	0.01	0.00	100.0%	2	30.14	87.45
0.9	0.25	0.00	0.00	0.0%	0	0.39	1.21
0.9	2	0.00	0.00	0.0%	0	0.20	1.71
0.9	4	0.10	0.07	28.5%	2	35.52	390.32
0.95	0.25	0.00	0.00	0.0%	0	0.39	1.20
0.95	2	0.00	0.00	0.0%	0	0.20	1.20
0.95	4	0.08	0.03	59.4%	4	36.69	389.81
1	0.25	0.00	0.00	0.0%	0	0.59	0.72
1	2	0.00	0.00	0.0%	0	0.22	2.22
1	4	0.24	0.01	97.4%	0	37.75	389.80
1.05	0.25	0.00	0.00	0.0%	0	0.84	1.31
1.05	2	0.00	0.00	0.0%	0	0.25	6.34
1.05	4	0.07	0.11	-62.3%	2	39.11	393.41
1.1	0.25	0.00	0.00	0.0%	0	0.71	1.72
1.1	2	0.00	0.00	0.0%	0	0.48	1.27
1.1	4	0.12	0.06	46.4%	3	43.99	390.97

Table B - 21 Sampled test cases for DG reactive power usage minimisation – snapshot test cases for Network D

Load scale factor	DG (MW)	DG Q usage (MVAr)			Voltage violation	Computation time (s)	
		ODCDM	SOCS	Reduction	ODCDM	ODCDM	SOCS
0.25	0.25	0.00	0.00	0.0%	0	0.14	30.87
0.25	2	0.00	0.00	0.0%	0	0.78	31.04
0.25	4	1.31	0.00	100.0%	0	27.65	31.27
0.3	0.25	0.00	0.00	0.0%	0	0.14	30.30
0.3	2	0.00	0.00	0.0%	0	0.77	30.52
0.3	4	1.31	0.00	100.0%	0	26.75	31.79
0.35	0.25	0.00	0.00	0.0%	0	0.14	30.21
0.35	2	0.00	0.00	0.0%	0	0.75	30.44
0.35	4	1.31	0.00	100.0%	0	24.88	31.44
0.4	0.25	0.00	0.00	0.0%	0	0.14	30.58
0.4	2	0.00	0.00	0.0%	0	0.62	30.90
0.4	4	1.31	0.00	100.0%	0	23.41	31.21
0.45	0.25	0.00	0.00	0.0%	0	0.14	30.30
0.45	2	0.00	0.00	0.0%	0	0.61	30.58
0.45	4	1.31	0.00	100.0%	0	21.56	30.70
0.5	0.25	0.00	0.00	0.0%	0	0.14	29.55
0.5	2	0.00	0.00	0.0%	0	0.59	30.42
0.5	4	1.28	0.00	100.0%	0	21.75	30.40
0.55	0.25	0.00	0.00	0.0%	0	0.14	29.83
0.55	2	0.00	0.00	0.0%	0	0.59	29.90
0.55	4	1.24	0.00	100.0%	2	21.81	30.49

0.6	0.25	0.00	0.00	0.0%	0	0.15	29.92
0.6	2	0.00	0.00	0.0%	0	0.44	30.13
0.6	4	1.30	0.00	100.0%	2	24.58	30.27
0.65	0.25	0.00	0.00	0.0%	0	0.14	29.87
0.65	2	0.00	0.00	0.0%	0	0.45	29.99
0.65	4	1.31	0.00	100.0%	4	25.05	30.55
0.7	0.25	0.00	0.00	0.0%	0	0.15	29.76
0.7	2	0.00	0.00	0.0%	0	0.47	29.88
0.7	4	1.08	0.00	100.0%	5	31.77	30.98
0.75	0.25	0.00	0.00	0.0%	0	0.15	30.08
0.75	2	0.00	0.00	0.0%	0	0.30	30.34
0.75	4	1.31	0.00	100.0%	3	27.01	30.54
0.8	0.25	0.00	0.00	0.0%	0	0.29	30.18
0.8	2	0.00	0.00	0.0%	0	0.30	30.23
0.8	4	1.31	0.00	100.0%	4	28.27	31.66
0.85	0.25	0.00	0.00	0.0%	0	0.30	30.84
0.85	2	0.00	0.00	0.0%	0	0.31	31.52
0.85	4	1.28	0.00	100.0%	2	23.47	31.57
0.9	0.25	0.00	0.00	0.0%	0	0.31	31.04
0.9	2	0.00	0.00	0.0%	0	0.15	30.97
0.9	4	1.31	0.00	100.0%	2	27.72	31.46
0.95	0.25	0.00	0.00	0.0%	0	0.30	31.19
0.95	2	0.00	0.00	0.0%	0	0.15	31.30
0.95	4	1.31	0.00	99.9%	4	28.32	31.76
1	0.25	0.00	0.00	0.0%	0	0.45	31.02
1	2	0.00	0.00	0.0%	0	0.15	31.18
1	4	1.17	0.00	100.0%	0	29.20	31.65
1.05	0.25	0.00	0.00	0.0%	0	0.46	30.95
1.05	2	0.00	0.00	0.0%	0	0.15	32.93
1.05	4	1.31	0.00	100.0%	2	26.34	32.85
1.1	0.25	0.00	0.00	0.0%	0	0.48	35.14
1.1	2	0.00	0.00	0.0%	0	0.31	32.16
1.1	4	1.31	0.00	100.0%	3	30.21	32.92

The number of voltage violation busbar are shown in Table B - 22.

Table B - 22 Number of voltage violation busbars in profile test cases for ODCDM

Time	Network loss minimisation	Voltage deviation minimisation	Switching operation minimisation	DG real power curtailment minimisation	DG reactive power usage minimisation
00:00	0	0	0	0	0
01:00	0	0	0	0	0
02:00	0	0	0	0	0
03:00	0	0	0	0	0
04:00	0	0	0	0	0
05:00	0	0	0	0	0

06:00	0	0	0	0	0
07:00	0	0	0	0	0
08:00	0	0	0	0	0
09:00	0	2	0	0	0
10:00	3	3	0	0	0
11:00	2	2	0	0	0
12:00	3	3	1	1	1
13:00	4	4	1	2	0
14:00	3	3	0	3	0
15:00	2	2	0	2	0
16:00	0	0	0	0	0
17:00	2	2	0	0	0
18:00	0	0	0	0	0
19:00	1	1	1	1	1
20:00	0	0	0	0	0
21:00	4	4	0	0	0
22:00	0	0	0	0	0
23:00	3	1	0	0	0

The computation time for profile studies are shown in Table B - 23 and Table B - 24.

Table B - 23 Computation time –profile study for Network D part 1

	Computation time (s)					
Time	Network loss minimisation		Voltage deviation minimisation		Switching operation minimisation	
	ODCDM	SOCS	ODCDM	SOCS	ODCDM	SOCS
00:00	144.16	67.70	95.50	85.82	31.21	29.78
01:00	148.68	67.28	67.00	86.75	4.91	12.82
02:00	148.60	67.04	67.32	85.81	6.81	7.27
03:00	146.27	65.07	67.13	86.51	7.30	9.77
04:00	149.87	67.43	67.34	86.20	7.39	18.15
05:00	149.74	68.14	66.01	85.73	7.19	23.18
06:00	148.61	68.10	65.70	85.89	6.02	13.32
07:00	146.71	69.53	68.06	84.89	2.40	9.84
08:00	29.61	68.92	56.03	85.19	2.59	14.49
09:00	113.66	69.50	3.16	85.54	0.79	10.77
10:00	35.80	68.51	1.49	85.22	0.40	12.42
11:00	1.78	67.73	1.71	84.71	0.62	14.37
12:00	2.45	67.87	2.35	85.07	0.20	18.91
13:00	1.55	67.43	1.50	85.64	0.59	13.93
14:00	1.79	67.08	1.70	84.84	0.79	19.36
15:00	1.78	67.22	1.72	84.94	0.60	13.92
16:00	107.78	67.27	59.06	85.36	3.38	15.41
17:00	38.44	67.41	4.26	85.71	2.00	4.27
18:00	3.11	67.65	3.02	85.22	4.98	21.62

19:00	1.57	67.61	1.48	85.49	1.19	23.99
20:00	106.14	68.00	49.35	86.31	3.38	17.93
21:00	36.88	67.05	2.15	85.13	0.40	10.92
22:00	108.12	67.17	55.46	82.07	2.79	16.40
23:00	33.23	66.99	2.22	81.46	2.20	9.82

Table B - 24 Computation time –profile study for Network D part 2

	Computation time (s)			
Time	DG real power curtailment minimisation		DG reactive power usage minimisation	
	ODCDM	SOCS	ODCDM	SOCS
00:00	39.61	409.91	22.17	31.06
01:00	6.29	400.86	3.88	30.55
02:00	8.61	395.56	5.32	30.74
03:00	9.40	396.51	5.88	30.64
04:00	9.66	396.09	5.98	30.31
05:00	9.21	393.39	5.96	31.47
06:00	7.67	392.34	4.98	31.50
07:00	3.06	394.40	2.00	31.28
08:00	3.30	23.63	2.22	31.51
09:00	1.01	394.03	0.67	31.54
10:00	0.53	89.72	0.33	31.78
11:00	0.75	393.33	0.52	31.33
12:00	0.25	393.99	0.16	31.50
13:00	0.76	39.85	0.50	31.42
14:00	1.03	394.54	0.66	31.28
15:00	0.50	394.67	0.33	31.30
16:00	4.07	18.16	2.66	31.22
17:00	2.55	393.78	1.66	31.59
18:00	6.10	391.59	3.95	31.20
19:00	2.04	392.91	1.32	31.45
20:00	4.36	392.91	2.81	31.26
21:00	6.08	42.40	3.97	31.14
22:00	2.92	393.96	1.83	31.59
23:00	1.50	394.33	1.02	31.24

Appendix B-8 Test results for Network E - Future Test Cases

Since the number of test cases is too large, sampled snapshot test results are shown here. Test results of these sampled test cases for different optimisation objectives are shown in Table B - 25, Table B - 26, Table B - 27, Table B - 28 and Table B - 29. For all the test cases, SOCS was able to find a feasible solution and the voltage violation number is always zero.

Table B - 25 Sampled test cases for network loss minimisation – snapshot test cases for Network E

Load scale factor	DG (MW)	Network loss (MW)			Computation time (s)	
		ODCDM	SOCS	Reduction	ODCDM	SOCS
0.25	0.25	0.0018	0.0018	0.0%	40.07	234.59
0.25	1.25	0.0017	0.0018	0.0%	318.41	235.51
0.25	2.5	0.0021	0.0017	16.3%	656.15	235.24
0.3	0.25	0.0029	0.0029	0.8%	33.86	234.32
0.3	1.25	0.0024	0.0025	0.0%	311.71	233.39
0.3	2.5	0.0024	0.0025	0.0%	453.22	238.01
0.35	0.25	0.0047	0.0045	5.3%	19.55	233.52
0.35	1.25	0.0035	0.0033	6.9%	199.81	239.64
0.35	2.5	0.0033	0.0033	0.0%	434.19	233.75
0.4	0.25	0.0069	0.0066	5.5%	22.04	232.60
0.4	1.25	0.0045	0.0043	3.3%	188.77	233.29
0.4	2.5	0.0043	0.0043	0.0%	428.81	234.09
0.45	0.25	0.0096	0.0094	1.8%	18.99	232.71
0.45	1.25	0.0059	0.0055	6.7%	186.64	233.14
0.45	2.5	0.0057	0.0057	0.0%	426.79	235.24
0.5	0.25	0.0124	0.0124	0.5%	15.93	234.32
0.5	1.25	0.0068	0.0069	0.0%	176.03	234.17
0.5	2.5	0.0068	0.0068	0.9%	412.15	234.68
0.55	0.25	0.0159	0.0159	0.0%	11.81	235.20
0.55	1.25	0.0081	0.0081	0.0%	174.54	246.29
0.55	2.5	0.0081	0.0082	0.0%	423.90	248.22
0.6	0.25	0.0200	0.0200	0.0%	15.04	246.87
0.6	1.25	0.0098	0.0095	2.8%	167.35	247.18
0.6	2.5	0.0098	0.0097	1.3%	419.04	248.48
0.65	0.25	0.0250	0.0248	0.5%	20.24	247.74
0.65	1.25	0.0115	0.0113	1.6%	171.31	248.50
0.65	2.5	0.0112	0.0113	0.0%	421.26	248.34
0.7	0.25	0.0305	0.0304	0.4%	19.86	250.17
0.7	1.25	0.0132	0.0131	1.0%	165.02	248.51
0.7	2.5	0.0131	0.0132	0.0%	412.58	250.87
0.75	0.25	0.0366	0.0363	0.7%	19.05	250.41
0.75	1.25	0.0150	0.0151	0.0%	154.01	251.89
0.75	2.5	0.0151	0.0150	0.2%	400.83	242.53
0.8	0.25	0.0432	0.0430	0.4%	13.52	243.95

0.8	1.25	0.0170	0.0168	1.4%	140.37	243.30
0.8	2.5	0.0169	0.0169	0.5%	405.60	250.73
0.85	0.25	0.0505	0.0503	0.3%	15.41	251.97
0.85	1.25	0.0190	0.0188	1.1%	131.67	260.13
0.85	2.5	0.0190	0.0189	0.5%	385.51	252.35
0.9	0.25	0.0586	0.0584	0.3%	19.39	252.41
0.9	1.25	0.0212	0.0211	0.6%	127.80	250.99
0.9	2.5	0.0212	0.0213	0.0%	381.11	252.43
0.95	0.25	0.0671	0.0670	0.2%	13.30	252.47
0.95	1.25	0.0239	0.0235	1.7%	125.70	252.12
0.95	2.5	0.0236	0.0236	0.0%	368.91	245.10
1	0.25	0.0762	0.0762	0.0%	16.86	246.39
1	1.25	0.0260	0.0262	0.0%	111.65	246.17
1	2.5	0.0271	0.0263	2.9%	359.55	247.82
1.05	0.25	0.0867	0.0861	0.7%	31.11	248.07
1.05	1.25	0.0287	0.0288	0.0%	95.92	247.84
1.05	2.5	0.0290	0.0286	1.3%	350.93	239.38
1.1	0.25	0.0973	0.0969	0.5%	15.27	241.67
1.1	1.25	0.0320	0.0315	1.3%	99.02	241.03
1.1	2.5	0.0317	0.0314	0.8%	342.23	239.57

Table B - 26 Sampled test cases for voltage deviation minimisation – snapshot test cases for Network E

Load scale factor	DG (MW)	Voltage deviation (pu)			Computation time (s)	
		ODCDM	SOCS	Reduction	ODCDM	SOCS
0.25	0.25	0.02	0.01	40.3%	11.16	239.81
0.25	1.25	0.34	0.02	95.5%	96.23	240.34
0.25	2.5	0.33	0.02	94.4%	229.13	245.40
0.3	0.25	0.03	0.02	42.9%	9.39	240.89
0.3	1.25	0.33	0.01	95.8%	93.30	239.95
0.3	2.5	0.33	0.02	94.8%	238.06	243.71
0.35	0.25	0.03	0.02	37.4%	7.04	242.22
0.35	1.25	0.34	0.02	94.2%	87.06	242.11
0.35	2.5	0.34	0.02	92.9%	215.35	244.59
0.4	0.25	0.04	0.02	44.9%	6.74	243.44
0.4	1.25	0.35	0.02	93.9%	82.17	241.44
0.4	2.5	0.34	0.02	94.0%	224.67	248.33
0.45	0.25	0.04	0.02	45.4%	8.07	245.99
0.45	1.25	0.36	0.03	91.9%	75.91	242.48
0.45	2.5	0.35	0.03	91.8%	215.18	247.75
0.5	0.25	0.05	0.03	34.8%	13.64	247.76
0.5	1.25	0.37	0.03	92.3%	69.83	241.69
0.5	2.5	0.35	0.03	90.8%	199.27	240.81
0.55	0.25	0.07	0.06	15.4%	17.50	240.71

0.55	1.25	0.36	0.03	92.2%	65.90	235.89
0.55	2.5	0.35	0.04	89.7%	201.05	241.04
0.6	0.25	0.09	0.08	12.3%	18.34	242.03
0.6	1.25	0.36	0.03	91.1%	66.74	242.88
0.6	2.5	0.36	0.04	87.9%	170.31	247.61
0.65	0.25	0.11	0.11	-0.2%	22.43	245.50
0.65	1.25	0.07	0.04	47.6%	43.82	244.74
0.65	2.5	0.36	0.04	88.7%	172.58	246.82
0.7	0.25	0.47	0.14	71.3%	27.97	245.41
0.7	1.25	0.08	0.04	47.5%	42.00	245.38
0.7	2.5	0.36	0.04	87.7%	168.05	245.26
0.75	0.25	0.49	0.16	66.5%	24.96	244.70
0.75	1.25	0.08	0.04	52.0%	50.09	245.29
0.75	2.5	0.37	0.05	86.7%	161.30	240.13
0.8	0.25	0.51	0.19	61.7%	25.28	238.54
0.8	1.25	0.09	0.05	44.1%	46.83	239.06
0.8	2.5	0.38	0.05	87.8%	166.67	241.78
0.85	0.25	0.52	0.23	57.1%	17.78	238.15
0.85	1.25	0.09	0.05	49.2%	43.99	240.36
0.85	2.5	0.38	0.06	85.5%	155.99	233.32
0.9	0.25	0.55	0.27	51.2%	8.86	231.46
0.9	1.25	0.10	0.05	42.6%	41.39	233.07
0.9	2.5	0.39	0.06	83.8%	160.50	235.46
0.95	0.25	0.57	0.32	44.4%	8.91	233.79
0.95	1.25	0.10	0.06	43.0%	42.56	231.93
0.95	2.5	0.39	0.06	84.5%	152.62	247.20
1	0.25	0.60	0.37	38.0%	9.79	246.82
1	1.25	0.10	0.06	37.3%	42.38	244.56
1	2.5	0.40	0.07	83.4%	160.72	249.23
1.05	0.25	0.63	0.45	28.1%	11.13	246.91
1.05	1.25	0.11	0.07	36.4%	49.44	234.22
1.05	2.5	0.40	0.08	80.5%	146.74	235.20
1.1	0.25	0.65	0.54	17.3%	13.55	237.05
1.1	1.25	0.11	0.08	28.1%	58.81	232.82
1.1	2.5	0.41	0.07	83.1%	143.91	235.28

Table B - 27 Sampled test cases for switching operation minimisation – snapshot test cases for Network E

Load Scale factor	DG (MW)	Switching operation			Computation time (s)	
		ODCDM	SOCS	Reduction	ODCDM	SOCS
0.25	0.25	0	0	0.0%	0.39	40.70
0.25	1.25	1	0	100.0%	0.81	29.78
0.25	2.5	4	0	100.0%	38.34	33.77
0.3	0.25	0	0	0.0%	0.39	35.38

0.3	1.25	1	0	100.0%	0.83	37.29
0.3	2.5	4	0	100.0%	32.74	55.29
0.35	0.25	0	0	0.0%	0.39	38.60
0.35	1.25	1	0	100.0%	0.80	32.84
0.35	2.5	4	0	100.0%	32.39	39.47
0.4	0.25	0	0	0.0%	0.40	47.28
0.4	1.25	1	0	100.0%	0.80	43.32
0.4	2.5	4	0	100.0%	29.38	41.62
0.45	0.25	0	0	0.0%	0.41	26.54
0.45	1.25	1	0	100.0%	0.81	21.50
0.45	2.5	4	0	100.0%	28.18	36.14
0.5	0.25	0	0	0.0%	0.40	29.12
0.5	1.25	0	0	0.0%	0.40	43.99
0.5	2.5	4	0	100.0%	27.00	46.40
0.55	0.25	0	0	0.0%	0.40	55.94
0.55	1.25	0	0	0.0%	0.40	41.47
0.55	2.5	4	0	100.0%	24.83	31.44
0.6	0.25	0	0	0.0%	0.42	45.72
0.6	1.25	0	0	0.0%	0.40	15.71
0.6	2.5	4	0	100.0%	23.21	38.83
0.65	0.25	0	0	0.0%	0.40	26.81
0.65	1.25	0	0	0.0%	0.40	37.56
0.65	2.5	4	0	100.0%	21.99	41.78
0.7	0.25	0	0	0.0%	0.40	19.28
0.7	1.25	0	0	0.0%	0.41	45.30
0.7	2.5	4	0	100.0%	20.26	48.76
0.75	0.25	0	0	0.0%	0.40	36.57
0.75	1.25	0	0	0.0%	0.42	24.04
0.75	2.5	4	0	100.0%	18.67	53.12
0.8	0.25	0	0	0.0%	0.42	59.46
0.8	1.25	0	0	0.0%	0.40	43.99
0.8	2.5	4	0	100.0%	16.97	29.34
0.85	0.25	0	0	0.0%	0.43	65.96
0.85	1.25	0	0	0.0%	0.40	31.59
0.85	2.5	4	0	100.0%	15.34	42.79
0.9	0.25	1	1	0.0%	0.82	86.73
0.9	1.25	0	0	0.0%	0.40	21.16
0.9	2.5	4	0	100.0%	14.12	30.97
0.95	0.25	1	1	0.0%	0.82	87.55
0.95	1.25	0	0	0.0%	0.42	20.77
0.95	2.5	4	0	100.0%	12.50	9.85
1	0.25	1	1	0.0%	0.86	88.05
1	1.25	0	0	0.0%	0.43	23.64
1	2.5	4	0	100.0%	11.11	39.72
1.05	0.25	2	2	0.0%	1.23	92.70
1.05	1.25	0	0	0.0%	0.40	43.80

1.05	2.5	4	0	100.0%	8.71	41.27
1.1	0.25	2	2	0.0%	1.22	92.75
1.1	1.25	0	0	0.0%	0.41	35.27
1.1	2.5	4	0	100.0%	7.10	37.62

Table B - 28 Sampled test cases for DG curtailment minimisation – snapshot test cases for Network E

Load scale factor	DG (MW)	DG P Curtailment (MW)			Computation time (s)	
		ODCDM	SOCS	Reduction	ODCDM	SOCS
0.25	0.25	0.00	0.00	0.0%	0.39	9.18
0.25	1.25	0.00	0.00	0.0%	0.79	6.80
0.25	2.5	0.86	0.31	63.7%	36.64	267.47
0.3	0.25	0.00	0.00	0.0%	0.41	9.73
0.3	1.25	0.00	0.00	0.0%	0.77	9.10
0.3	2.5	0.73	0.27	62.6%	32.09	262.86
0.35	0.25	0.00	0.00	0.0%	0.39	5.06
0.35	1.25	0.00	0.00	0.0%	0.80	5.00
0.35	2.5	0.70	0.23	66.5%	30.25	265.27
0.4	0.25	0.00	0.00	0.0%	0.38	4.91
0.4	1.25	0.00	0.00	0.0%	0.80	5.58
0.4	2.5	0.66	0.20	70.4%	28.90	267.68
0.45	0.25	0.00	0.00	0.0%	0.41	6.76
0.45	1.25	0.00	0.00	0.0%	0.78	2.69
0.45	2.5	0.62	0.16	74.7%	27.53	267.28
0.5	0.25	0.00	0.00	0.0%	0.42	10.78
0.5	1.25	0.00	0.00	0.0%	0.42	1.45
0.5	2.5	0.59	0.12	80.1%	27.87	271.18
0.55	0.25	0.00	0.00	0.0%	0.44	8.00
0.55	1.25	0.00	0.00	0.0%	0.40	8.74
0.55	2.5	0.55	0.08	85.9%	24.17	267.60
0.6	0.25	0.00	0.00	0.0%	0.41	15.60
0.6	1.25	0.00	0.00	0.0%	0.41	5.56
0.6	2.5	0.51	0.04	92.3%	22.58	264.75
0.65	0.25	0.00	0.00	0.0%	0.39	9.69
0.65	1.25	0.00	0.00	0.0%	0.42	6.17
0.65	2.5	0.47	0.00	100.0%	21.38	170.31
0.7	0.25	0.00	0.00	0.0%	0.39	4.39
0.7	1.25	0.00	0.00	0.0%	0.39	3.26
0.7	2.5	0.43	0.00	100.0%	19.89	69.51
0.75	0.25	0.00	0.00	0.0%	0.40	9.77
0.75	1.25	0.00	0.00	0.0%	0.40	12.41
0.75	2.5	0.40	0.00	100.0%	18.27	84.46
0.8	0.25	0.00	0.00	0.0%	0.40	5.70
0.8	1.25	0.00	0.00	0.0%	0.42	6.24
0.8	2.5	0.36	0.00	100.0%	16.62	70.54

0.85	0.25	0.00	0.00	0.0%	0.41	2.70
0.85	1.25	0.00	0.00	0.0%	0.42	15.84
0.85	2.5	0.32	0.00	100.0%	15.31	49.33
0.9	0.25	0.00	0.00	0.0%	0.84	4.67
0.9	1.25	0.00	0.00	0.0%	0.41	12.50
0.9	2.5	0.28	0.00	100.0%	13.94	17.14
0.95	0.25	0.00	0.00	0.0%	0.81	11.74
0.95	1.25	0.00	0.00	0.0%	0.41	7.64
0.95	2.5	0.24	0.00	100.0%	12.56	58.90
1	0.25	0.00	0.00	0.0%	0.83	5.83
1	1.25	0.00	0.00	0.0%	0.41	4.01
1	2.5	0.20	0.00	100.0%	10.85	25.84
1.05	0.25	0.00	0.00	0.0%	1.22	7.41
1.05	1.25	0.00	0.00	0.0%	0.39	9.21
1.05	2.5	0.16	0.00	100.0%	8.75	16.51
1.1	0.25	0.00	0.00	0.0%	1.21	8.68
1.1	1.25	0.00	0.00	0.0%	0.42	13.38
1.1	2.5	0.13	0.00	100.0%	7.18	25.12

Table B - 29 Sampled test cases for DG reactive power usage minimisation – snapshot test cases for Network E

Load scale factor	DG (MW)	DG Q usage (MVAr)			Computation time (s)	
		ODCDM	SOCS	Reduction	ODCDM	SOCS
0.25	0.25	0	0	0.0%	0.39	61.10
0.25	1.25	0	0	0.0%	0.82	77.88
0.25	2.5	0	0	0.0%	38.58	106.80
0.3	0.25	0	0	0.0%	0.40	47.63
0.3	1.25	0	0	0.0%	0.82	93.97
0.3	2.5	0	0	0.0%	33.11	118.91
0.35	0.25	0	0	0.0%	0.41	58.79
0.35	1.25	0	0	0.0%	0.82	98.01
0.35	2.5	0	0	0.0%	31.31	84.65
0.4	0.25	0	0	0.0%	0.40	63.73
0.4	1.25	0	0	0.0%	0.80	89.60
0.4	2.5	0	0	0.0%	29.43	95.65
0.45	0.25	0	0	0.0%	0.39	53.41
0.45	1.25	0	0	0.0%	0.82	53.71
0.45	2.5	0	0	0.0%	28.11	115.08
0.5	0.25	0	0	0.0%	0.40	64.79
0.5	1.25	0	0	0.0%	0.41	81.92
0.5	2.5	0	0	0.0%	26.45	105.40
0.55	0.25	0	0	0.0%	0.40	53.88
0.55	1.25	0	0	0.0%	0.40	90.73
0.55	2.5	0	0	0.0%	24.79	105.09

0.6	0.25	0	0	0.0%	0.40	60.91
0.6	1.25	0	0	0.0%	0.40	85.42
0.6	2.5	0	0	0.0%	23.18	113.94
0.65	0.25	0	0	0.0%	0.40	54.12
0.65	1.25	0	0	0.0%	0.40	79.09
0.65	2.5	0	0	0.0%	23.40	102.75
0.7	0.25	0	0	0.0%	0.40	60.88
0.7	1.25	0	0	0.0%	0.42	105.08
0.7	2.5	0	0	0.0%	20.27	119.02
0.75	0.25	0	0	0.0%	0.41	61.52
0.75	1.25	0	0	0.0%	0.40	86.82
0.75	2.5	0	0	0.0%	18.61	119.08
0.8	0.25	0	0	0.0%	0.40	61.30
0.8	1.25	0	0	0.0%	0.40	80.41
0.8	2.5	0	0	0.0%	17.09	119.21
0.85	0.25	0	0	0.0%	0.41	76.97
0.85	1.25	0	0	0.0%	0.40	76.90
0.85	2.5	0	0	0.0%	15.26	116.44
0.9	0.25	0	0	0.0%	0.82	81.71
0.9	1.25	0	0	0.0%	0.40	83.00
0.9	2.5	0	0	0.0%	14.50	110.41
0.95	0.25	0	0	0.0%	0.85	60.57
0.95	1.25	0	0	0.0%	0.42	100.29
0.95	2.5	0	0	0.0%	12.63	108.27
1	0.25	0	0	0.0%	0.83	61.79
1	1.25	0	0	0.0%	0.40	97.34
1	2.5	0	0	0.0%	10.87	117.16
1.05	0.25	0	0	0.0%	1.22	69.42
1.05	1.25	0	0	0.0%	0.41	93.06
1.05	2.5	0	0	0.0%	8.70	122.12
1.1	0.25	0	0	0.0%	1.20	82.37
1.1	1.25	0	0	0.0%	0.41	108.67
1.1	2.5	0	0	0.0%	7.11	117.23

No voltage violation was seen in the profile studies for both ODCDM and SOCS. The computation time for profile studies are shown in Table B - 30 and Table B - 31.

Table B - 30 Computation time – Switching operation minimisation profile study

	Computation time (s)					
Time	Network loss minimisation		Voltage deviation minimisation		Switching operation minimisation	
	ODCDM	SOCS	ODCDM	SOCS	ODCDM	SOCS
00:00	84.17	245.01	28.78	176.82	0.41	41.89
01:00	60.66	253.66	10.49	175.24	0.39	57.12
02:00	50.57	244.78	14.07	174.67	0.40	43.79

03:00	46.93	242.89	7.43	173.66	0.39	25.68
04:00	46.11	238.55	5.44	175.03	0.40	56.57
05:00	46.21	236.44	6.62	175.27	0.41	39.59
06:00	54.30	230.53	11.66	175.45	0.39	17.16
07:00	73.22	242.16	17.69	178.55	0.40	54.88
08:00	91.18	239.72	62.06	179.95	0.42	55.65
09:00	107.67	240.72	70.98	178.03	0.43	44.34
10:00	107.48	240.54	71.25	180.50	0.43	43.95
11:00	108.69	247.41	69.44	179.45	0.40	61.12
12:00	110.84	246.17	69.22	175.29	0.40	27.77
13:00	113.75	250.20	74.47	175.90	0.40	39.54
14:00	107.13	239.95	69.51	174.73	0.40	34.19
15:00	106.43	240.52	68.69	174.95	0.40	38.84
16:00	122.55	240.56	67.18	174.11	0.40	56.42
17:00	161.10	241.89	98.86	177.12	1.25	56.09
18:00	165.03	243.39	111.18	176.24	1.28	45.52
19:00	161.71	242.45	129.10	176.19	1.26	32.80
20:00	142.29	242.39	124.27	175.49	1.24	28.66
21:00	135.36	240.79	89.30	175.24	0.99	39.89
22:00	122.22	239.14	70.74	174.68	0.81	56.13
23:00	93.07	232.80	62.96	175.07	0.40	21.38

Table B - 31 Computation time – Switching operation minimisation profile study

	Computation time (s)			
Time	DG real power curtailment minimisation		DG reactive power usage minimisation	
	ODCDM	SOCS	ODCDM	SOCS
00:00	29.03	269.20	29.43	83.32
01:00	30.61	265.26	31.02	83.68
02:00	35.73	265.54	36.09	85.22
03:00	37.62	267.71	36.53	81.85
04:00	38.06	299.32	37.73	80.48
05:00	36.91	283.39	36.15	80.33
06:00	32.75	267.18	32.60	80.66
07:00	28.23	266.82	27.03	80.38
08:00	23.34	267.32	22.60	79.66
09:00	20.69	269.92	20.61	80.06
10:00	20.72	268.48	20.42	79.84
11:00	20.65	268.34	20.96	79.55
12:00	20.32	269.27	21.09	83.50
13:00	19.56	269.98	20.76	84.16
14:00	20.32	278.31	21.25	83.95
15:00	19.92	288.11	21.53	83.46
16:00	17.48	104.76	18.62	83.78

17:00	10.40	53.28	11.69	84.74
18:00	7.47	33.38	9.24	84.81
19:00	8.31	20.01	10.66	84.78
20:00	11.23	51.26	12.89	84.53
21:00	13.28	75.92	15.30	84.10
22:00	15.84	66.06	17.83	83.97
23:00	20.01	281.87	22.00	83.77